A COMBINED GENETIC AND CHIMERIC ANALYSIS OF THE FLAVIVIRAL NON-STRUCTURAL PROTEINS
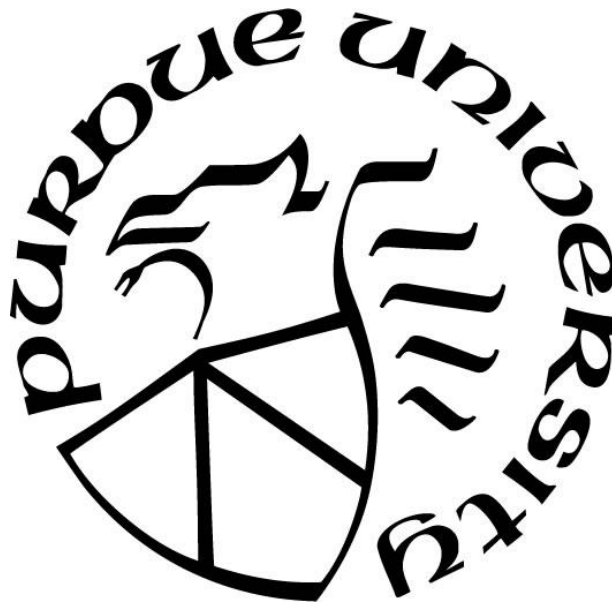
by

Shishir Poudyal

A Dissertation

Submitted to the Faculty of Purdue University

In Partial Fulfillment of the Requirements for the degree of

Doctor of Philosophy

Department of Biological Sciences

West Lafayette, Indiana

May 2020

THE PURDUE UNIVERSITY GRADUATE SCHOOL
STATEMENT OF COMMITTEE APPROVAL

Dr. Richard J. Kuhn, Chair

Department of Biological Sciences

Dr. Andrew D. Mesecar

Department of Biochemistry

Dr. Douglas J. LaCount

Department of Medicinal Chemistry and Molecular Pharmacology

Dr. Steven S. Broyles

Department of Biochemistry

Approved by:

Dr. Janice P. Evans

Dedicated to Shyam Sir (my father/my first teacher) and Nirvan (my kiddo). I hope I could be the same to Nir.

ACKNOWLEDGMENTS

Nirvan is growing up very fast. Keeps Geeta and me on our toes. He has many bumps and boo-boos, nothing we can do. I hope he will learn from all these things. I tried showing him the bacteriophage T4 structure, and before I could say anything, he said it looks like a pineapple and I have accepted it as a pineapple, just the sour one. During summer and fall (if there is one, it is either winter or summer here), we go to Farmer's Market. They sell pretty good stuff, but man, are they expensive? I cannot buy two tomatoes for $5. I am sorry wife; I must think about our future, monthly payment of car is due in two days. But remember, I love you guys.

When I see Nirvan running around all the time, I picture my mom, except for, we were two. Now I feel for her. She was and is one heck of women; soft as cotton, hard like those spankings I got. My goodness mom how could you be so hard on me? I always thought I was your favorite one. But you know what, graduate school happened, and you were just introducing me to the tough roads ahead. Father O Father! You were my first teacher and the best teacher one could ask for. I could have praised you more, had you allowed me to play more when I was a kid. These days I don't like to go outside much. There are Netfilx and Twitter and other random stuffs. I am stuck. I miss those days when you dragged me from playground to finish my homework. I would never be here without you.

And to all those innocent *E. coli s* that I sacrificed to please the science God! To those cells/viruses that I drowned in bleach! To all those coffee runs! To failure and to a sliver of success! To friends I earned, to science I learned! Boiler up! Jaya Nepal!

TABLE OF CONTENTS

LIST OF TABLES

LIST OF FIGURES

13

14

15

17

amino acid residues, respectively, the changes in the hydrophobic faces of the TMDs of the chimeric viruses are depicted in the bottom panel.

LIST OF ABBREVIATIONS

BHK	Baby hamster kidney cells
C	Capsid Protein
Ca	Capsid anchor
DC	Dendritic cells
DENV	Dengue virus
DHF	Dengue hemorrhagic fever
DSS	Dengue shock syndrome
DPE	Days post electroporation
E	Envelope Protein
EMC	Endoplasmic reticulum membrane protein complex
ER	Endoplasmic reticulum
HCV	Hepatitis c virus
HPE	Hours post electroporation
HPT	hours post transfection
IFN	Interferon
JEV	Japanese Encephalitis virus
Kb	kilobase pair
kDa	kilodalton
KUNV	Kunjin virus
LIV	Louping ill virus
MHC	Major histocompatibility complex
MOI	Multiplicity of infection
MVEV	Murray valley encephalitis virus

MTase	Methyltransferase
NS	Non-structural protein
PFU	Plaque forming unit
ORF	Open reading frame
PCR	Polymerase chain reaction
POWV	Powassan Virus
RDRP	RNA dependent RNA polymerase
RLU	Relative light unit
ssRNA	Single stranded ribonucleic acid
SAM	S-adenosyl methionine
SRP	Signal recognition particle
SPC	Signal peptidase complex
TBEV	Tick-borne encephalitis virus
TMD	Transmembrane domain
UTR	Untranslated region
µl	microliter
µm	micrometer
WNV	West Nile virus
YFV	Yellow fever virus

ABSTRACT

A successful flaviviral life cycle involves several coordinated events between viral proteins and host factors. The polyprotein processing at the surface of the ER membrane results in the formation of several replication proteins that bring about changes in the ER membrane making it permissive for viral genome amplification. Non-structural proteins 4A (NS4A) and non-structural protein 4B (NS4B) are two of the most important integral membrane proteins of DENV that are essential part of the viral replicase complex. The cleavage at NS4A-2K-NS4B is temporally and spatially regulated. The cleavage at the N-terminal of 2K is carried out by viral NS2B/3 protease while host signalase cleaves on the C-terminal side at the ER lumen to give rise to a mature NS4B protein. This thesis primarily focuses on demonstrating the function of 2K as an independent peptide rather than simply a signal sequence, and the role 2K plays, when present as 2K-NS4B vs NS4B. Moreover, this thesis has attempted to explore the function of transmembrane domains (TMDs) in replication separating them from their membrane anchor function. This thesis will also describe the development of a ZIKV replicon and its use in screening small molecule inhibitors in the last chapter.

In Chapter 2 of the thesis, we established 2K as an independent, information carrying peptide rather than just a signal peptide. A strategy involving chimeric virus generation and mutational analysis supported the notion that 2K is rather unique and important for viral replication and infectious particle production. Using an interserotypic 2K chimeric virus, it was established that the 2Ks of DENV are serotype specific, however, they are interchangeable with a huge fitness cost in infectious particle production. We further showed that individual amino acid residues towards then end of h-region and C-terminus of the 2K peptide affect viral replication and infectious particle production. Moreover, it was shown that the 2K peptide consists of a highly conserved 'DNQL' region at its N-terminal that plays an important role in viral replication.

Chapter 3 details the mechanistic aspect of the effects observed in interserotypic 2K chimeric viruses. The interserotypic chimeric viruses were comparable to wild type in replication, however, they were deficient in infectious particle production early in the life cycle. The major change to be noted in the chimeric viruses was the absence of signalase cleavage at the 2K-NS4B junction.

We demonstrated that in a virus infected system, 2K-NS4B and NS4B populations are always present which led us to look for any specific functions of the cleaved vs uncleaved 2K-NS4B protein. Using a transcomplementation system where NS4B was presented in the absence of 2K, we showed that particle production can be rescued in the interserotypic 2K chimeric viruses. It was further concluded using NS4B truncations that the property of NS4B to rescue particle production was concentrated in the ER luminal loop. Further, alanine scanning mutagenesis of the conserved residues of ER loop resulted in pinpointing T198 and its involvement in the early stages of viral packaging.

Chapter 4 examined the role of TMDs of NS4A and NS4B and attempted to define their roles separately from their membrane anchoring functions. Several interserotypic TMD chimeric viruses were generated to address the function of these domains. We concluded that TMD1 and TMD3 of NS4A could be replaced with partial success across the DENV serotypes, whereas, TMD2 was serotype specific. The specificity of TMD2 of NS4A is not contributed by a single amino acid and should be a function of the secondary structure formed by TMD2 as it sits on the inner leaflet of the ER membrane. We demonstrated the variable roles different TMDs of NS4B play in viral replication using a similar strategy of reverse genetics of chimeric viruses. TMD1 of NS4B was replaceable with no to minimal effect, whereas, the remaining four showed variable effect upon substitution. More importantly, we demonstrated how the reorientation of TMD5 of NS4B post NS2B/3 cleavage might vary in different serotypes of DENV using revertant virus obtained from the TMD5 interserotypic chimera. Analysis of interserotypic cytosolic and ER luminal loop chimeras of NS4B pointed to functional conservation of the cytosolic loop between DENV-2 and DENV-3, whereas, the remaining cytosolic loops and the ER loops showed variable level of defects upon substitution, suggesting their functions in serotype-dependent manner.

Chapter 5 describes the construction and characterization of a ZIKV replicon system and use of it to screen several small molecule inhibitors of the flaviviruses MTase. Several small molecule inhibitors of flavivirus N-7-MTase were designed/synthesized in Dr. Arun K Ghosh's lab which would target the extra pocket unique to the flavivirus SAM-binding site. We analyzed the docking of a set of these compounds into MTase domain of NS5 of ZIKV, DENV and YFV and screened them for their ability to inhibit replication of ZIKV, DENV and YFV. A huge variation in the activity profile of these compounds were observed against different flaviviruses even though these

compounds were targeted against the highly conserved MTase domain of flavivirus NS5. GRL-002- and GRL-004-16-MT specifically inhibited ZIKV replication with low micromolar IC_{50} value, while these compounds showed little to no effect on DENV and YFV. On the other hand, compounds GRL-007-, GRL-0012- and GRL-0015-16-MT demonstrated a dual inhibitory effect against DENV and YFV albeit the CC_{50} values of the GRL-012 and GRL-015 were concerning. Compounds GRL-007-16-MT showed broad spectrum activity against ZIKV, DENV and YFV even though it was slightly cytotoxic to Vero cells. Moreover, GRL-002-16 was inhibitory to YFV while ineffective against DENV, whereas, GRL-016-16 had the opposite effect. Our results reveal the differential efficacies of the small molecule inhibitors targeting N-7-MTase. The experimental data suggests these compounds have different cytotoxicities in different cell lines and the compounds act in a virus-specific way. Nonetheless, we were able to shortlist some potent compounds for future modifications.

CHAPTER 1. *FLAVIVIRIDAE* FAMILY AND THE FLAVIVIRUSES

1.1 Chapter summary

Flaviviridae comprises a family of several medically important viruses that has been consistently reported since 17th century. The story of recent outbreak of yellow fever virus (YFV) tells how significant these groups of pathogens are even when there are effective vaccines available for some of these viruses. The diseases caused by members of this family ranges from mild flu-like symptoms to more severe encephalitis, hemorrhagic fever, microcephaly in newborns, Gullian-Barre syndrome and death in many cases. Of the most common flaviviruses circulating around the world, dengue (DENV) and Zika (ZIKV) viruses are more prominent. DENV has been estimated to infect about 390 million people with 96 million apparent infections each year and is endemically circulating in the Americas and Southeast Asia. The 2015-2016 ZIKV outbreak added more enigmas to the already existing vast array of diseases a flavivirus could cause in addition to the added routes of vertical and sexual transmission. With no approved therapeutics and a limited scope of vaccines, these viruses are here to stay, underlining the need for detailed study of the viral life cycle. The integral membrane proteins non-structural proteins 4A (NS4A) and 4B (NS4B) of the flaviviruses are the least studied proteins. A two kilo Dalton signal peptide called 2K connects these proteins whose nonconventional functions have been frequently underestimated during the viral life cycle. In the wake of emerging and reemerging flaviviral infections, a comprehensive understanding of all the viral components and their functions will equip us with novel therapeutic agents and ways to tackle the unprecedented threat the flaviviruses possess.

1.2 Introduction

The members of the flavivirus genus are simply intriguing. The members of chiefly arthropod-borne viruses can cause myriads of human diseases ranging from asymptomatic flu-like infection, acute febrile illness to serum sickness, hemorrhagic fever, encephalitis or microcephaly. The flavivirus genome has a single open reading frame that encodes ten proteins that orchestrate the hijacking of the host machinery and interference of the immune system resulting in successful replication and assembly of progeny virions. An infection is established after a bite from infected mosquitoes or ticks. Resident dendritic cells (DCs), keratinocytes, fibroblasts and monocytes are

infected by the virus, which are then carried to draining lymph nodes where they multiply and get disseminated (1). The ensuing host immune response, organs targeted by virus, virus virulence, and genetic factors of the host determine the outcome of an infection (2). Some flaviviral infections provide lifelong homotypic immunity. For example, infection with any serotype of DENV will make the host immune to that particular serotype, however, secondary infection with any other serotypes can result into more debilitating form of disease like dengue hemorrhagic fever (DHF) or dengue shock syndrome (DSS) (3).

The *Flaviviridae* family consists of four genera, Flavivirus, Pestivirus, Hepacivirus, and Pegivirus. These viruses mainly infect birds and animals with some being host specific and pathogenic (4). Even though most of the flaviviruses are transmitted by arthropods (mosquito or ticks), there are flaviviruses without known vectors and those infecting insects only. The current phylogenetics classifies flaviviruses into four different groups tick-borne, mosquito-borne, no known-vector flaviviruses and insect-specific flaviviruses (5, 6). Several medically important flaviviruses are members of either the tick-borne group i.e. Tick-borne encephalitis virus (TBEV), Powassan virus (POWV), louping ill virus (LIV) or the mosquito-borne group i.e DENV, WNV, ZIKV, YFV and Japanese encephalitis virus (JEV) (5). Among these, infections caused by DENV are the most widespread and can be caused by any of the four antigenically unique serotypes of DENV. It has been estimated that DENV alone are responsible for 390 million infections per year with half of the world population living in the area where dengue is prevalent. DENV infection often leads to no apparent signs and symptoms and resolves on itself, however, it can lead to diseases ranging from mild flu-like syndrome to DHF and DSS (7). ZIKV came into prominence as a major reemerging flavivirus after the recent outbreak in the Americas and the Pacific islands. The disease outcomes like congenital microcephaly, Guillain-Barre syndrome as well as the mode of transmission i.e. sexual and vertical in addition to mosquito transmission added more challenges and questions than answers (8).

As members of the flaviviruses can reemerge as a potentially threatening public health pathogen, a thorough understanding of viral biology is warranted. Despite great strides taken in that direction, there are some gaping holes in understanding their life cycle and pathogenesis. The availability of limited scope vaccines for DENV or lack of any therapeutics or vaccines to combat ZIKV can have a severe socioeconomic burden in the tropics and subtropics where these diseases

circulate in endemic and epidemic transmission cycles. This underscores a need for a multifaceted approach in combatting the challenges posed by these viruses.

1.3   Genome organization and life cycle of flaviviruses

Flaviviruses are enveloped viruses encasing a single strand of positive sense RNA genome. The RNA genome is ~10.7kb in size and is capped at 5′ end with no 3′ poly A tail (9). The 5′ UTR precedes the single open reading frame that codes for ten viral proteins followed by the 3′ UTR (Fig 1.1 A). The structural elements of the 5′ and 3′ UTR are essential for viral RNA replication, immune evasion and translation (10). Once the single strand RNA genome of positive polarity is released in the cytoplasm, the fate of particle formation relies on the pathway it follows. The intricate events of translation, replication and packaging must be coordinated spatially and temporally for a productive infection, not to forget the continuous onslaught from host immune response. The information encoded in the viral genome is necessary and sufficient to carry out all these events (11).

The first round of RNA genome translation resulting in production of all the necessary proteins required for replication and other downstream steps is the rate limiting step in the viral life cycle. Eukaryotic initiation factor (eIF4F) and the poly A binding protein (PABP), respectively, bind to the 5′ cap and A-rich region adjacent to the dumbbell (DB) structure of 3′ UTR in the viral RNA thus establishing the translational initiation step on the surface of the ER membrane (12, 13). This results in the formation of an ER membrane associated polyprotein, which is cleaved co- and post translationally to give rise to individual viral proteins. The polyprotein on the ER membrane is processed by coordinated actions of the viral protease and host cell signalase. This will be discussed in more detail in following sections. The insertion of different membranotropic proteins brings about the changes in the ER membrane morphology resulting in membrane rearrangement and formation of replication factories (RF) where the genome replication takes place (9).
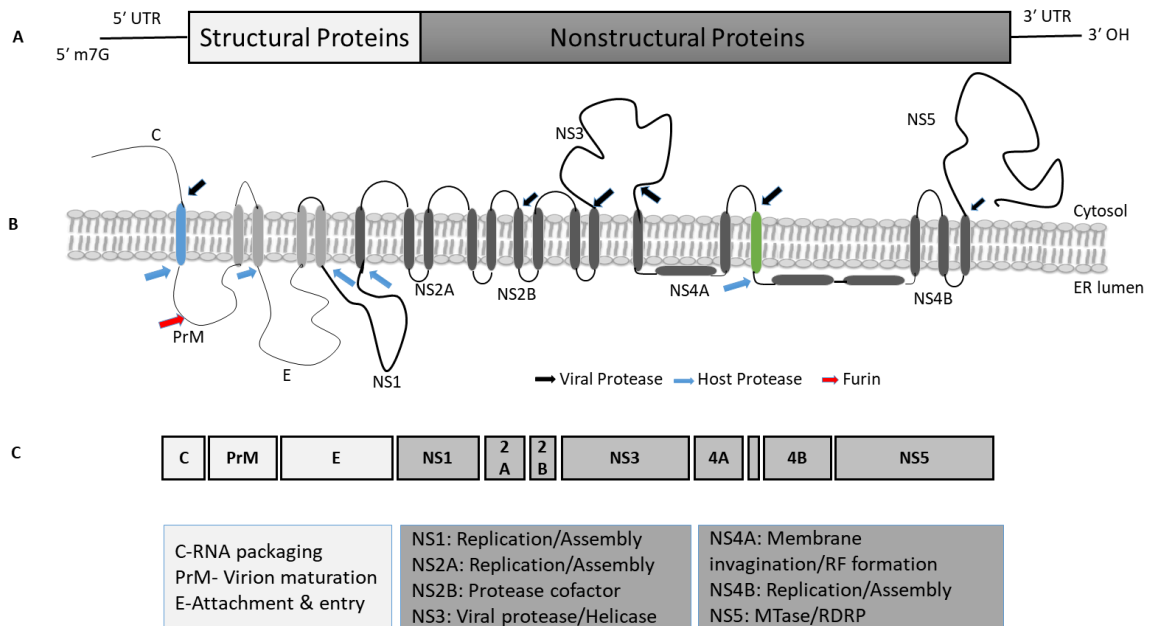
Fig. 1.1 Genome organization of flavivirus and polyprotein processing. A. Schematic of 5′ capped flavivirus positive sense RNA genome. B. Orientation and arrangement of polyprotein in the ER membrane. The positive sense RNA genome is translated to give rise to 3 structural proteins and 7 nonstructural proteins which are processed by host (blue and red arrow) and viral (black arrow) proteases to form mature proteins. Capsid (C) among structural and NS3 and NS5 among nonstructural proteins are cytoplasmic, while PrM, E and NS1 are found in ER lumen. The rest of the proteins NS2A, 2B, 4A and 4B are integral membrane protein of ER. C. Schematic of individual protein size (drawn to scale) and their general functions. RF-Replication factory, MTase-Methyltransferase, RDRP- RNA dependent RNA polymerase. True signal peptides encoded by the flaviviral genomes are colored; Blue- Capsid anchor, Green- 2K.

When enough replication proteins are synthesized, viral RNA replication is initiated. The RNA dependent RNA polymerase (RDRP) domain of NS5 and NS3 helicase domain play a major role in RNA synthesis. Flaviviral RDRP is capable of de novo RNA synthesis beginning at the 3′ end of UTR. Since the 5′ and 3′ end of the flavivirus genomes are strictly conserved, RDRP initiates the RNA synthesis with 5′ AG (14, 15). Viral RNA assumes a circular-panhandle like shape involving long range interactions between 5′ and 3′ UTRs. The RDRP bound to "stem loop A" (SLA) of 5′ UTR is then transferred to the 3′ Stem loop (SL) thus initiating negative strand RNA synthesis. The negative strand RNA copies are then used to synthesize many copies of positive strand viral RNA (16). Only the newly formed + strand RNA genomes are capped by the coordinated action of NS3 and the methyltransferase (MTase) domain of NS5. These + sense capped RNA genomes are then packaged in the budding particle lying opposite of the RFs (14, 17).

The packaging of a newly synthesized viral genome into a budding particle is an intricate process. This step of the virus life cycle must be finely tuned in such a way that – strand RNA genome and the cellular mRNA should be excluded and only the newly synthesized + strand RNA genome should be encapsidated. This process is further complicated by the fact that no recognizable packaging signals in the flaviviral genome have been reported. The negatively charged RNA genome is nonspecifically bound by numerous positively charged capsid molecules thus initiating the process of packaging (18). The flaviviral particles bud into the ER lumen and then transported via the ER-Golgi secretory pathway. In the trans-Golgi, host protease furin cleaves the prM on the viral surface to give rise to mature infectious particles (19). The basic life cycle of flaviviruses is depicted in Fig 1.2.

1.4   Flaviviral polyprotein processing and role of ER membrane proteins

Translation of the flaviviral + sense RNA genome results in the formation of a polyprotein consisting of three structural gene and seven nonstructural gene. Not only does the polyprotein helps condense the genetic material but also provides spatio-temporal control of protein in relation to polyprotein processing (20). Depending on its topology, polyprotein is either processed by
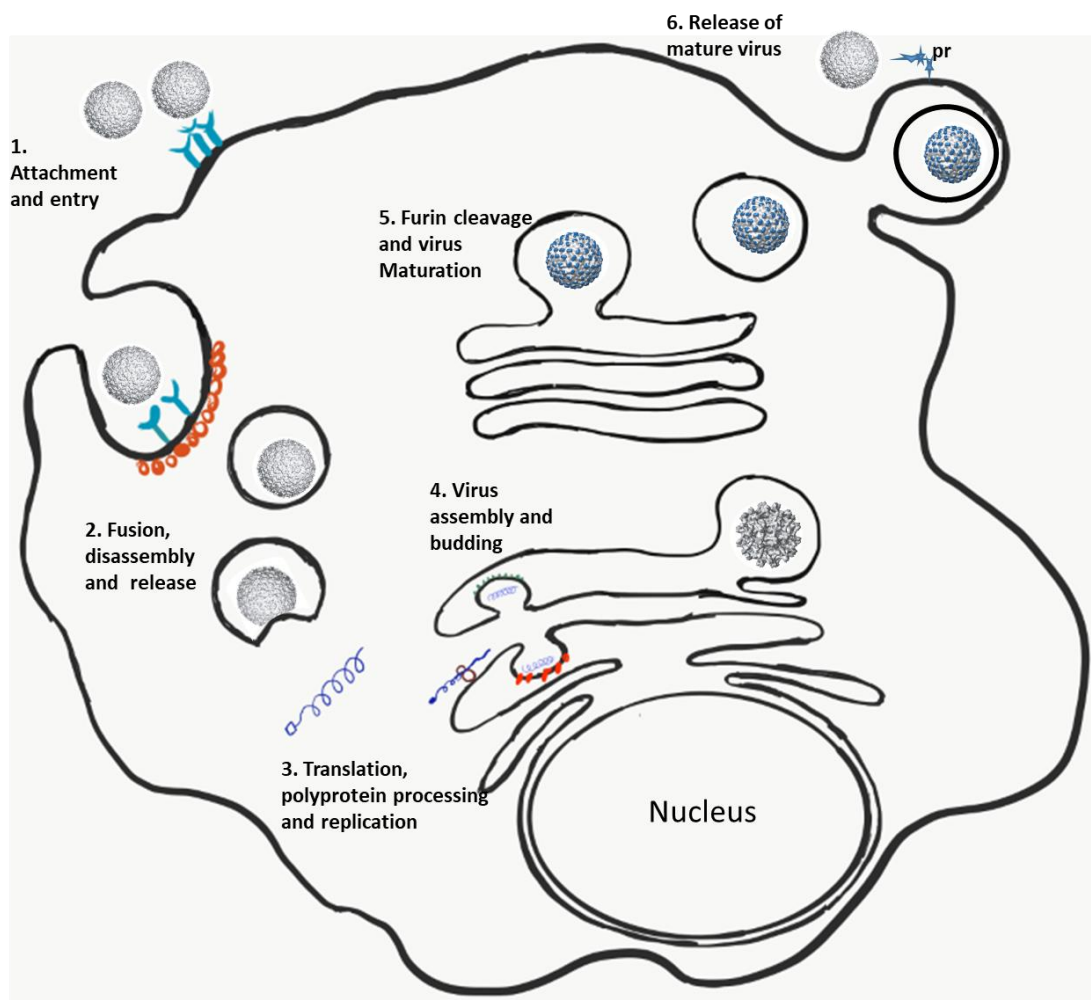
Fig. 1.2 Life cycle of flaviviruses: Viruses enter the cells via receptor mediated endocytosis aided by clathrin. Once inside the endosome, the low pH triggers the membrane fusion which leads to virus disassembly and release of single strand + sense RNA genome. The RNA genome is thus translated in the ER membrane to give rise to a single polyprotein which is processed by viral and host protease. These proteins aid in the genome replication which happens in the ER derived organelles called replication factories (RF). On the opposite side of the RF, the newly formed structural proteins initiate budding and bind to newly synthesized genome. The immature particles thus formed pass through the ER-Golgi network, where the furin in Golgi cleaves prM to give rise to mature virus which is released in a process known as exocytosis. Newly formed virion can infect new cells.

viral or host proteases to give rise to individual proteins (21). As the capsid (C) protein comes out of the ribosome, the signal anchor of C protein is bound by the signal recognition particle (SRP) thus targeting the protein translational complex to the ER membrane (12). An uninterrupted synthesis and simultaneous processing of the polyprotein happens in the ER membrane aided by the ER protein translocation complex, along with other enzymatic components to produce mature and fully functional individual proteins. This is summarized in Fig 1.1 B-C.

DNAJ homolog subfamily C member 14 (DNAJC14), a dopamine receptor transport protein of ER, interacts with nonstructural proteins of YFV helping form protein scaffolds that anchors the replication complex (20). Both overexpression and silencing of endogenous expression of DNAJC14 were deleterious for replication of YFV and BVDV suggesting a requirement for endogenous level of DNAJC14. (22). Hrd1 protein complex has also been indicated as one of the major host proteins that regulates the flaviviral replication. Derlin 2, a member of Hrd 1 complex, has been reported to interact with NS4B and NS5 of ZIKV (23). The oligosaccharyltransferase (OST) complex, consisting of STT3A and STT3B subunits, which catalyzes the N-glycosylation of the proteins is suggested to have a structural role rather than direct functional role in flaviviral replication (24). Similarly, Reticulon 3.1A, responsible for changing membrane curvature, is recruited to establish replication complex in flaviviruses. It interacts with NS4A of WNV, but not DENV and ZIKV (25). ER membrane protein complex (EMC) is recruited to the site of replication by NS4B of DENV and ZIKV where it also aids in the biogenesis of membrane proteins NS4A and NS4B (26). One of the major components of the ER membrane that has a direct role in the biogenesis of the flaviviral proteins is the protein translocation complex and the signal peptidase complex.

The continuous interaction at the membrane microenvironment involves a multitude of host proteins and several viral proteins. In the following sections, we will mainly focus on viral NS4A, 2K and NS4B proteins and host cell signalase for this part of the study. As host cell signalase has direct role in the morphogenesis of several viral proteins that are of unparalleled importance, the cleavage between NS4A-2K-NS4B and the role of signal peptide 2K hold a special place in the flaviviral lifecycle.

1.4.1 NS membrane proteins of flaviviruses

The NS membrane proteins of flaviviruses constitutes a major portion of nonstructural polyprotein that is synthesized in the ER membrane. NS2A, NS2B, NS4A and NS4B are integral membrane proteins of varied topologies and functions which are involved in different stages of replication and assembly of the viruses. NS2A, ~22 kDa integral membrane protein, plays an indispensable role in viral replication, assembly and immune evasion (27). NS2A orchestrates virion morphogenesis by modulating prM and E processing by interacting with them and recruiting viral RNA to site of assembly by interacting with the 3′UTR of RNA (28). NS2B, another integral membrane protein, acts as a cofactor of viral protease NS3. It interacts with the N-terminal serine protease domain of NS3 and anchors NS3 to the membrane for carrying out the proteolytic cleavage (29). NS4A and NS4B play an equally important role in flaviviral life cycle and would be detailed in the following sections.

The assembly of integral membrane proteins at the ER membrane is a multistep procedure involving cytosolic and ER membrane resident proteins. The targeting and insertion of membrane proteins to ER membranes is highly conserved and consists of either i) Classical co-translational pathway mediated by signal recognition particle (SRP) and Sec61 translocon or ii) The posttranslational pathway mediated by cytosolic ATpase (30). The polyprotein insertion of flaviviruses follow the co-translational insertion, and I will focus more on this topic henceforth.

The insertion of TMDs into the lipid bilayer is highly unfavorable, the machinery involved must overcome the biophysical barrier to achieve a functional membrane protein. The membrane insertion comprises 3 major steps, recognition of protein/TMDs as it emerges from the ribosome to prevent aggregation, targeting to the receptor in ER, and finally, migration of the TMDs from the polar surface of ER to the hydrophobic core of the membrane (31). As the signal sequence or the first TMD emerges from the ribosome, it is recognized by the SRP. The TMD of the nascent protein binds to the M-domain of the SRP which guides the ribosome bound complex to SRP receptor on the ER membrane involving GTPase domain in both the SRP and SRP receptor. In the next couple of steps, the energy obtained from the hydrolysis of GTP helps transfer the nascent chain from SRP to the Sec61 translocation channel and dissociation of SRP and SRP receptor (32). The Sec 61α subunit of the Sec61 serves as a major translocation channel for the lateral insertion of the signal peptide or the TMDs into the hydrophobic lipid core thus forming an interface

between two chemically different environments. The two subdomains consisting of helices TMD 1-5 and TMD 6-10 of the α-subunit form an hourglass-shaped pore opening laterally on the middle of bilayer and serves as a gate through which the signal peptides/ TMDs exit (30, 31). Thus, the Sec 61 translocon along with other accessory factors and cytosolic proteins, play an important role in the insertion of the integral membrane protein in the ER membrane in a series of closely coordinated events.

1.4.2   Signal peptide, Signal peptidases and role in flavivirus life cycle

During flaviviral genome translation, the signal peptide/signal anchor motif play an important role in homing the polyprotein to the ER membrane. The first signal peptide to appear is the capsid anchor (Ca) motif that must be recognized by the SRP-dependent protein translocation machinery (12). Also, there are several internal TMDs that would serve as an internal signal sequence for the insertion of the downstream protein into the ER membrane. The examples of which include the second TMD of M which serves as a signal for translocation of E protein and TMD2 of E for ER translocation of NS1. These kinds of phenomenon are common among +strand RNA viruses helping them condense the proteins to a specific location so as to manipulate the host immune response as well as efficiently carry out the replication (20). Another pronounced presence as a signal peptide is the 2K peptide that acts as a leader sequence for the translocation of the NS4B protein to the ER. These signal sequences are cleaved by ER resident host cell signalase/signal peptidase to give rise to a mature protein. However, in a flaviviral infected system, a series of uncleaved polyproteins has been detected (33–35), and only recently has a functional study on the relevance of these uncleaved polyprotein products has been conducted (36). The presence of uncleaved polyprotein suggests involvement of several factors in bringing out a complete cleavage as well as the role of the spatio-temporal coordination between host enzymes and the viral protease. For example, the cleavage between Ca and Pr is not carried out by the host cell signal peptidase unless the cytoplasmic portion of C is cleaved by the viral protease, which functions in cytoplasm vs. the signalase in the ER lumen. Any manipulation of these events results in severe inhibition in particle production (37).

Signal peptidase complex (SPC) comprising of five different subunits are involved in the removal of the signal peptide from the N-terminal of precursor protein. The five subunits; SPCS1,

SPCS2, SPCS3, Sec11A and Sec11C are integral membrane proteins of the ER and have very high specificity for cleaving a signal sequence. The bulk of the domains carrying out the peptidase function of SPC, Sec11A and Sec11C lie in the ER lumen anchored by a single TMDs of respective subunit (38, 39). Signal peptidases are one of the major host enzymatic components that is exploited by viruses. Even though, they specifically cleave at the signal peptide-protein junction, some of them are known to cleave in the internal sites without a proper TMD leading to the protein degradation (40) or formation of a protein with different topology (41). Signal peptidase cleavage happens predominantly co-translationally as the protein comes out of the translocon, and a short loop with conserved amino acids at P1 and P3 positions of signal peptides are encountered (42).

Components of SPCs have been shown to be essential for the flaviviral life cycle. A genome wide CRISPR screen study of the host gene indicated SPCS1 and SPCS3 as major contributors of flaviviral infectivity. SPCS1 knockout cells did not support the growth of many flaviviruses and showed a pronounced inhibition of NS4A-2K-NS4B cleavage (43). SPCS1 has also been found as an important component of HCV assembly as it interacts with NS2 and E2 and helps in particle formation (43).

Once the signal peptide is cleaved by the SPC, the peptide is further acted on by signal peptide peptidase (SPP). The SPPs are polytopic transmembrane proteins that consist of two conserved aspartate residues required for proteolytic activity lying in the adjacent TMDs (44). Because of their requirement for TMD aspartate for proteolytic activity, they are also known as aspartyl intramembrane cleaving proteases (I-CLiPs). SPPs preferably access the site in signal peptide/TMD fragment enriched with helix breaking amino acids and are subsequently cleaved within the lipid bilayer by the endoproteinase activity of SPP (45). Thus, cleaved products of the signal peptide are either degraded by proteases in the cytosol or are involved in signal transduction or presented in complex with MHC protein. The fragment derived from the N-terminal signal peptide of HIV gp160 interacts with calmodulin, however, the functional aspect of it needs to be established (46). Additionally, the fragments derived from the signal peptides are processed by the proteasome and can be complexed to MHC I in a transporter of antigen (TAP) dependent or independent way and presented to cytotoxic T cells. A small peptide fragment of GP1 of lymphocytic choriomeningitis virus is presented complexed with MHC I (47).

Not all signal peptide cleavages are straightforward and not all the cleaved products are acted on by the SPPs. The long signal peptide (SP) of Foamy virus envelope glycoprotein gp18 gets incorporated in viral particles (48) . Some of the SPs act as a regulator of viral gene expression. The envelope SP of Jaagsiekte–Sheep virus acts as a posttranscriptional regulator of viral gene expression. Similarly, SP of mouse mammary tumor virus is targeted to nucleoli post cleavage and modulates tumor formation (49, 50). In HCV, the conditional cleavage of P7 targets the protein either to mitochondria or ER (51). The signal anchor of the capsid protein Ca has been reported to play an important role in the assembly of the virus by maintaining the stability of E protein (52). Similarly, any changes in the order of SP cleavage from the polyprotein has been shown to be deleterious for particle production in flaviviruses (53).

1.5   Nonstructural protein 4A (NS4A)

NS4A is an integral membrane protein consisting of 127 amino acid residues and ~16 kDa in size. Together with other NS proteins (NS2A, NS2B and NS4B) it forms the structural framework of the replication complex of DENV. Both the N-terminal and C-terminal end of a mature NS4A is generated by the viral protease NS2B/3. Topological analysis along with biochemical characterizations have predicted NS4A to consist of an N-terminal cytoplasmic end and four transmembrane domains (TMDs) wherein the second TMD sits close to the inner leaflet of the ER membrane (Fig 1.3 A) and the fourth TMD, also known as 2K, acts as a signal peptide and will be discussed separately (54). A nuclear magnetic resonance (NMR) spectroscopy structure of full length NS4A of DENV serotype 4 showed the presence of six helices; three of the N-terminal helices interacted with the membrane on the cytoplasmic side and the remaining three inserted in the membrane, thus confirming the earlier notion of NS4A topology (55). The NS4A protein of DENV exists in different oligomeric forms. Oligomerization of NS4A is primarily the function of TMD1 with N-terminal cytoplasmic end playing a small role (56).

1.5.1   Role in formation of replication complex:

The seminal study by Miller *et al*. on determining the topology of NS4A also studied the role of NS4A in inducing ER membrane curvatures in virus-infected cells. They found that NS4A co-localizes with dsRNA in the ER derived membrane structures thus confirming its role in replication

36

complex formation. More importantly, NS4A induces membrane rearrangements that is dependent on cleavage of 2K peptide (54). The negative curvature of the resulting membrane structures has been contributed to the presence of the TMD2 helix which sits on the plane of the membrane. NS4A oligomerization and its interaction with NS4B also contributes to the membrane remodeling (57). The N-terminal cytoplasmic region of NS4A has been suggested to bind to the curved membrane thus further helping in membrane rearrangements (58).

1.5.2   Interaction with host and other viral proteins:

WNV NS4A recruits reticulon 3.1 to the site of replication and aiding further in membrane remodeling and stabilizing the replication complex (59). Also, NS4A with its N-terminal cytoplasmic end interacts with vimentin resulting in vimentin reorganization which helps anchor the replication complex (60). Dengue NS4A localized with a lipid droplet associated membrane protein (AUP1) during infection and triggered the re-localization of AUP1 to the autophagosome membrane. Interaction of NS4A with AUP1 induce lipophagy mediated by the acetyltransferase activity of AUP1 thus helping the virus thrive (61). It has been suggested that NS4A induces multiple mechanisms of autophagic control during the flaviviral life cycle of which PI3K is the most common one (62). NS4A being an ER membrane protein interacts with other viral protein to stabilize the replication complex. NS1, an ER lumen protein, interacts with NS4A thus helping NS1 communicate with the replicase complex (63). The C-terminal EELPD/E motif of NS4A in WNV acts as a cofactor of NS3 helicase domain and regulates its ATPase activity thus maintaining the balance between RNA unwinding and the availability of ATPs (64)

1.6   2K peptide

The fourth TMD of NS4A, also known as a signal peptide or 2K, is the least understood protein of DENV. For the better part of DENV research, the 2K peptide has simply been dismissed as a signal peptide that helps translocate NS4B into the ER lumen. However, recent studies elucidating its role in enhancing RNA synthesis (65), aiding in overcoming superinfection exclusion (66), and counteracting the activity of interferon-inducible 2′,5′-oligoadenylate synthetase 1b (Oas1b) in WNV and enhancing viral RNA synthesis (67) has shed slight into its functions.

When taken in the context of co- and post translational polyprotein cleavage, 2K can be considered either the last TMD of NS4A or the first TMD of NS4B or as an individual protein that mediates the function of both the proteins preceding and following it. NS2B/3, a viral protease is responsible for cleavage between C-terminal of NS4A and 2K, however, the 2K-NS4B junction, which is in the ER lumen, is cleaved by host cell signalase. The processing of 2K-NS4B is a prime example of how viral proteins exploit the host system. The 2K-NS4B cleavage site is held in cryptic confirmation (signalase inaccessible) unless the junction between NS4A and 2K is cleaved by NS2B/3 (35, 68). Cleavage by viral protease follows 2K-NS4B cleavage by signalase resulting in the formation of mature proteins. A comparable phenomenon exists during proteolytic processing between capsid and prM proteins in flaviviruses. By using series of mutants to uncouple the dependency of host signalase on viral protease, it has been shown that the sequential/inefficient cleavage between capsid anchor protein and prM helps in efficient nucleocapsid incorporation and enhancement of the cleavage leads to lethal phenotypes (37, 69).

1.6.1 2K as a signal peptide

A signal peptide consists of three distinct domains; a central core hydrophobic (H) domain, N-terminal domain and a C-terminal domain. The N-terminal domain which determines the length of signal peptide can range up to 15-50 amino acid residues in length and are characterized by the presence of positively charged residues. The core hydrophobic domain ranging from 10-15 residues in length is the major contributor of signal anchor properties and membrane insertion. The C-terminal domain is rich in amino acids with helix breaking properties and controls the signalase cleavage activity (47, 70). The 2K peptide of DENV and most other flaviviruses is 23 amino acid in length and mostly conforms to the established rules of a signal peptide. However, one notable exception includes the presence of a conserved 'DNQL' motif in the N-terminus of the 2K peptide that confers a negative charge to the N-terminus. The 2K peptide can be used as a signal peptide for the proper translocation of NS1 of dengue without affecting its functioning (unpublished data). Similarly, 2K can be functionally replaced by signal peptide from unrelated proteins in the context of an expression system resulting in proper translocation of the protein (71).

1.6.2   2K peptide: Role beyond signal sequence

NS4A plays a major role in the rearrangement of ER membrane to form the replication factories of flaviviruses. The cleavage of 2K from NS4A has been described as a major event for induction of membrane rearrangement in DENV (54). On the contrary, in Kunjin virus (KUNV), the retention of 2K i.e. uncleaved NS4A-2K is responsible for the membrane rearrangements. Further, in KUNV, cleavage resulted in localization of NS4A to Golgi apparatus (72). Thus, a complex interplay between viral protease, host signalase, cleaved and uncleaved products play an important role for productive viral replication. Furthermore, mutant selection in the presence of lycorine, a flaviviral inhibitor, selected a 2K V9M mutant. The V9M mutant had a direct effect on viral RNA synthesis possibly through differential binding of 2K with host protein thus overcoming the effect of lycorine (65). The same WNV mutant showed a propensity in overcoming superinfection exclusion, a result of a higher than normal viral dissemination rate without any replication enhancement (66). Interestingly, the 2K V9M mutant also interfered with the host interferon inducible Oas1b and promoted viral RNA replication (67).

Recently, Plaszczyca *et al* described the role of interaction between the connector region of Wing domain of NS1 and intermediate cleavage product NS4A-2K-NS4B in enhancing the RNA amplification in a more direct way rather than aiding in the formation of vesicle packets (36). Partially cleaved NS4A-2K-NS4B intermediates have been previously described in DENV and YFV infections (33, 34). 2K-NS4B and NS4A-2K-NS4B have been reported in DENV infected BHK cells, and not in mosquito cells, which were later processed post translationally (34). Even though, the cleavage intermediate products of NS4A-NS4B have been reported on several occasions, their functional roles haven't been yet investigated. A thorough understanding of how the cleavage between NS4A-2K-NS4B is regulated by viral protease and host cell signalase, and what role do these intermediate products and 2K play would further shed light into the viral life cycle.

1.7   Nonstructural protein 4B (NS4B)

An indispensable component of replication complex, NS4B of DENV is an integral membrane protein of ~27 kDa in size and largest of the NS membrane proteins. The N-terminus of NS4B is in the ER lumen as the protein is translocated to the ER lumen by 2K peptide and later

processed by host cell signalase to give rise to mature NS4B protein. To date, no crystal structure of NS4B is available and most of the functional studies are based on predicted and experimentally established topological models. A recent study using solution NMR spectroscopy of N-terminal 125 amino acid truncated NS4B protein suggested the presence of 5 α-helices with four of them (α2-α5) embedded in the micelles (73). More recently, solution NMR spectroscopy of full length DENV-3 NS4B showed a presence of eleven α-helices with five of them forming transmembrane domains (TMDs) (74). Seminal biochemical studies have shown that NS4B consists of three true TMDs and two membrane associated TMDs (75). These results were corroborated by another group who also reported cytosolic loop and C-terminal domain mediated dimerization of NS4B (76). Glycosylation of NS4B at amino acid residues N-58 and N-62 increases the efficiency viral RNA synthesis and possibly help in NS4B folding (77). The predicted topology is presented in Fig 1.3 B.

1.7.1 Interaction with other viral proteins

NS4B, in association with other viral proteins, is involved in different stages of viral replication. The ER luminal region of NS4B comprising the amino acid residue F86 interacts with NS1 and serves as a link between NS1 and the replication complex (78). NS4B complements the activity of NS3 helicase. This interaction which is dependent on NS4B conformation enhances the processivity of the helicase enzyme by increasing the RNA unwinding activity of the helicase (79). Using surface plasmon resonance, Zou *et al* showed that the cytosolic loop of NS4B interacts with subdomain 2 and 3 of NS3 helicase in bringing about its increase in processivity (80). Resistant mapping showed that NS4B with its cytosolic loop amino acid residue Q134 interacts with NS3 and increases the viral replication (81). Genetic and physical interactions of NS4B with NS4A have been reported. A lethal K79R mutation in JEV NS4A was rescued by Y3N mutation in the N-terminal luminal region of NS4B. Even though mechanistic studies were not performed, the revertant helped rescue the RNA replication (82). Further, NS4A-NS4B interaction mediated by the regions spanning the first TMDs of NS4A and NS4B helped enhance the viral replication (83).

1.7.2 Interaction with host proteins

Interactions of NS4B with several host proteins have been indicated, albeit lacking in functional studies. Even though phosphoglycerate kinase 1 (PGK1), type II cytoskeletal 8 keratin (KRT8) and Ube2i, a small ubiquitin-like modifier enzyme was identified as the major interacting partner of NS4B in a yeast two hybrid assay, their role alongside NS4B has not been established directly (84). NS4B of YFV, and not DENV, has been shown to bind to stimulator of IFN gene (STING) and block the RIG I mediated IFN activity (85). Recently, NS4B in coordination with NS4A have been found to suppress the AKT-mTOR pathway and perturb autophagy leading to cellular dysregulation in ZIKV infected neural stem cell lines. Interestingly, this phenomenon was not seen in DENV (86). Even though NS4B shares similar topology and significant homology within flaviviruses, the interference of cellular functioning might be completely different and virus specific. Flaviviruses replicate in the membrane organelles derived from the ER. The membranotropic proteins NS4A and NS4B interact with ER membrane protein complex (EMC) thus helping it localize to site of replication complex formation. The two N-terminal TMDs of NS4B located in the ER lumen are responsible for the interaction (26). Interaction of NS4B with EMC helps in its folding and post translational stability (87).

NS4B acts a hub to counteract the host immune system. In an intriguing phenomenon, the luminal region of NS4B of DENV encompassing amino acid residues 77-125 is involved in antagonizing the IFN α/β by inhibiting the nuclear localization of STAT 1 (88), even though, how the luminal NS4B inhibits cytoplasmic STAT 1 remains unexplained. Moreover, these events must be a complex process involving different viral and host proteins as these phenomena were not observed in different strains of multiple serotypes of DENV (89). TMD3 and TMD5 of NS4B bind with dicer and inhibit the generation of siRNA thus acting as a potent suppressor of viral RNAi silencing (90).

As an important component of the replication complex, NS4B interacts with different viral and host proteins driving the viral replication and particle production. Acting as a hub of host immune response antagonist, this protein aids in the successful establishment of viral infection. More importantly, the multi-pass membrane protein, NS4B, samples both the luminal and the cytosolic environments because of the loops connecting the TMDs. Its unique topology might

help bridge luminal and cytosolic proteins (both viral and host) to work in concert for a productive viral life cycle. A detailed study into the structural and functional aspects of NS4B is warranted.

1.8   Nonstructural protein 5 (NS5)

NS5, a protein of ~103 kDa in size and ~900 amino acids, is the largest and the most conserved protein of flaviviruses. It consists of two distinct N- and C-termini domains with enzymatic activities that are essential for the flaviviral genome replication and translation (91). The N-terminus domain of NS5 has been shown to add a 5'-cap to RNA genomes in a multistep reaction and is known as the methyltransferase (MTase) domain, whereas, the C-terminus domain has the RNA dependent RNA polymerase (RDRP) activity. The two domains are connected by a 5-6 amino acid linker (92). In addition to its role in genome amplification, NS5 plays a major role in viral pathogenesis. NS5 has been shown to perturb host immune system by downregulating interferon (IFN) and cytokine activities (93, 94). Further, NS5 has been reported to shuttle between cytoplasm and nucleus thus interacting with several host factors, and more recently, has been shown to modulate RNA splicing (95, 96).

1.8.1   The methyltransferase (MTase) domain:

MTase domains among flaviviruses share a 50-70% sequence identitiy, which explains the presence of the characteristic α/β fold present in the crystal structures of the MTase domains of most of the medically important flaviviruses (97). The MTase domain consists of three subdomains. The N-terminus subdomain that coordinates the GTP during 2'O adenosine methylation consists of helix turn helix motif, a β strand and a α-helix. The core subdomain between the N- and C-termini subdomains consists of seven β strands surrounded by four α helices forming a typical MTase fold and is responsible for binding of S-adenosyl methionine (SAM) and carrying out the major reaction. The C-terminal subdomain consists of seven β strands surrounded by four α helices thus forming a characteristic MTase fold (92). The MTase domain of NS5 is responsible for adding a type I cap (m^7GppAmG) to the 5'end of nascent RNA of flaviviruses as the first two nucleotides of the flaviviral genome are strictly conserved (98). The multistep reaction is carried out with the involvement of triphosphatase activity of the NS3. The RNA capping reaction is initiated after the removal of terminal phosphate from the positive sense RNA by triphosphatase activity of NS3

helicase. A GMP moiety is then transferred to the RNA by the guanylyltransferase activity of MTase domain. In the next sets of reaction, the methyltransferase activity of MTase domain adds a methyl group to the N-7 position of guanine followed by 2'-O position of the first nucleotide adenine (92, 99). S-adenosyl methionine (SAM) acts as methyl donor during the last two steps of the reaction and gets converted to S-adenosyl-L-homocysteine (AdoHcy).

Capping of viral RNA is one of the immune evasion mechanisms. As eukaryotic mRNAs are capped, capping helps mimic the host, disguising the viral RNA from the immune surveillance and degradation by 5'-3' exoribonucleases. Viral RNAs lacking a 2'-O adenine methylation were highly sensitive to IFN-induced proteins with tetratricopeptide repeats (IFIT). In addition to their immune evasion role, capping enhances stability and translational efficiency of the viral genome (100).
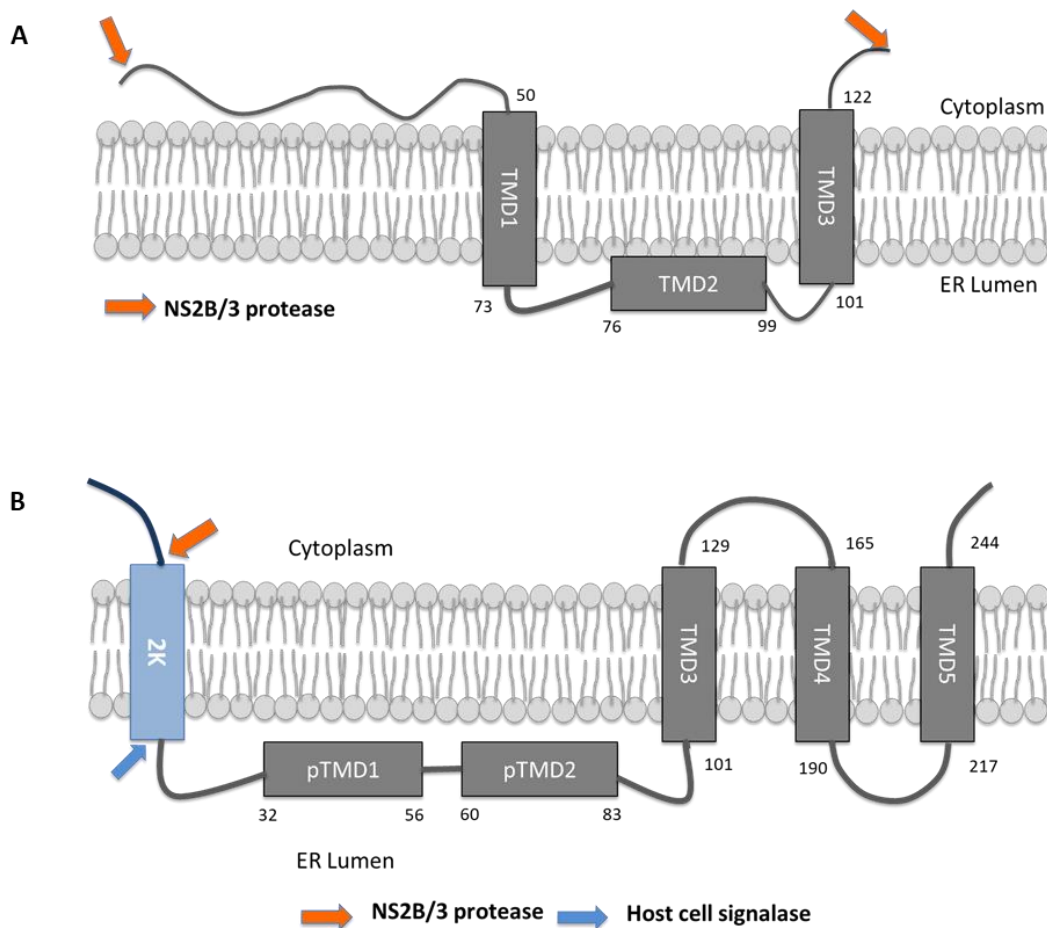
Fig. 1.3 Topological model of DENV-2 NS4A and NS4B. A) NS4A consists of 3 TMDs with TMD1 and TMD3 traversing the ER in opposite directions and TMD2 lying flush with the membrane. The 50-residue long N- terminal cytoplasmic tail is suggested to have 3 α-helices. Viral protease NS2B/3 (orange arrow) cleaves on both the N- and C-termini of the protein. B) NS4B consists of 5 TMDs with two of them (pTMD1-2) lying in the ER lumen. The remaining three traverse the ER membrane forming cytosolic loop between TMD3 and TMD4 and an ER loop between TMD4 and TMD5. The N-terminal of NS4B is generated after 2K is cleaved by host cell signalase (blue arrow) in the ER lumen whereas, the C-terminus is generated after NS2B/3 cleavage of NS5. In ~15% of the cases the TMD5 flips to the ER post NS5 cleavage from NS4B. (Model designed on topology predicted by Miller *et al*.)

1.8.2 The RNA dependent RNA polymerase (RDRP) domain

The RDRP domain of NS5 is ~74 kDa and accounts for two third of NS5 protein and has a nuclear localization signal. RNA synthesis in flaviviruses occurs in the specialized membrane structures formed by rearrangement/invaginations of ER membrane. The positive sense RNA genome acts as a template for the synthesis of negative strand RNA thus resulting in formation of the double stranded replication intermediates. Viral RDRP utilizes the negative strand in the replicative form to synthesize more positive sense RNA (101, 102). During late in infection, RNA synthesis is asymmetrical leading to almost ten time more positive sense RNA than negative strand (91). The flaviviral RDRP structure conforms to other established RDRP structures. The core region of RDRP assumes a cupped right-hand shape with fingers, palm and thumb subdomains. The palm domain consists of the active site of the enzyme and binds to RNA, nucleotides and metal ions to modulate the genome replication. The fingers subdomain which form a tunnel guides the single strand RNA to the active site. The thumb subdomain, which is the least conserved region of RDRP, is involved in de novo synthesis of RNA in addition to its role in guiding the RNA in and out of the active site (14, 103).

1.9 Flaviviral inhibitors

An effective small molecule inhibitor targeting a crucial step in the viral life cycle is a result of thorough understanding of structural, biochemical and mechanistic roles of target proteins involved in that step of life cycle. Even though the process seems straightforward, the design and development are not always a smooth road. Due to the lack of proofreading activity of the flaviviral RDRP, mutations accumulate in the viral genome over time which might affect the region targeted by the inhibitors, or the virus can quickly develop resistance against the lead compounds (104). The scenario is not helped by the presence of different serotypes of dengue, emergence and reemergence of other flaviviruses, as well as discoveries of newer modes of transmission (105).

Inhibitors of flaviviruses most commonly target the two nonstructural enzymatic proteins, NS3 and NS5 that are respectively involved in polyprotein processing and genome replication. Several inhibitors of viral entry targeting structural proteins and molecules targeting non-enzymatic nonstructural proteins involved in replication have been reported. The development of flaviviral inhibitors warrants a continued interest because of the lack of effective vaccine and

therapeutics. A combination of target based, and cell-based assays form the basis for development of potent antiflaviviral therapeutics. As viruses use plethora of host proteins to result in productive infection, inhibitors that target/perturb specific viral proteins function without affecting host proteins would be ideal candidates to proceed with in the drug development pipeline.

1.9.1 Flaviviral inhibitors against structural proteins

The major events of entry, assembly and exit during a viral life cycle involves structural proteins and involves many biochemical, structural and conformational changes. These critical events of the viral life cycle make them an attractive target for inhibitors. ST-148, a small molecule inhibitor, targeting capsid enhances its self-interaction affecting assembly and disassembly by introducing structural rigidity (106). Similarly, NITD-448 targets the hydrophobic pocket for β-N-octyl-glucoside in E protein and inhibits the membrane fusion. Similarly, compound 6, and highly basic compound like PO2 were developed targeting the same hydrophobic pocket but have not been successfully advanced for further trials (107).

1.9.2 Inhibitors against nonstructural proteins

Nonstructural proteins of flaviviruses are involved in the formation of replication complex machinery to amplify the viral genome. In addition to their constitutive role in replication, some NS proteins play an important role in virion assembly (NS1, NS2A, and NS3) and immune evasion (NS4A, NS4B and NS5). NS3 and NS5 of flaviviruses are multifunctional enzymatic proteins that are involved in different steps of viral replication. Owing to their indispensable roles, several flaviviral inhibitors are designed to inhibit their function and hence viral replication (104, 108).

Inhibitors of NS3

NS3 harbors protease and helicase activities, respectively, required for polyprotein processing and RNA genome replication. The protease activity of NS3 is very stringent with requirements for specific amino acids at polyprotein cleavage sites. Inhibitors targeting NS3 protease activity can inhibit polyprotein processing which has a debilitating effect in viral life cycle. Several compounds targeting the protease function of NS3 have been reported. Bowman-Birk inhibitor binds to the substrate binding S1 pocket of NS3 thus inhibiting its interaction with NS2B (109). Similarly,

compound 1, 166347 and ARDP0006 that block the protease activity of NS3 by competitive inhibition have been documented. Moreover, several compounds that inhibit the protease activity by mixed inhibitions are known. Though a wide variety of compounds have been reported to be active against the protease activity of NS3, not many have gone through lead to optimization pathway because of their poor solubility, off-target activity, and lack of virus inhibition *in vivo*. The NS3 helicase on the other hand does not have any specific pockets that can be exploited for potential inhibitor development. Despite the aforementioned reason, compounds like suramin, ivermectin, and several other compounds have been shown to effectively inhibit NS3 helicase activity.

Inhibitors of NS5

NS5 of flaviviruses is the key protein in amplifying the RNA genome and capping and readying it for translation. The N-terminal one third of the NS5 protein contributes to the methyltransferase and guanylyltransferase reactions, important steps of RNA capping. Whereas, the C-terminal two thirds of the protein has RDRP activity and can synthesize RNA de novo. Because of their vital role in the viral life cycle, these domains of NS5 are targets of many antiflaviviral inhibitors.

Inhibitors of NS5 MTase activity

The MTase domain of NS5 in conjunction with NS3 carries out the capping of newly synthesized positive sense RNA genomes. In a series of reactions, MTase catalyzes the transfer of a methyl group to N-7 of guanine cap as well as the 2′-OH group of the first nucleotide, adenine (110). The methyl donor in both the cases, SAM, gets converted to SAH as a byproduct. Inhibition of capping by mutagenesis studies has proven to be lethal for viruses. Similarly, inhibition of methylation of the internal adenosine increases its IFN susceptibility.

The crystal structure of most of the flaviviruses MTase show a characteristic core subdomain with MTase fold cradled between the N- and C-terminal subdomains. The core subdomain is highly conserved within MTase making it harder to design inhibitors that specifically target the viral MTase and not the host. Structure based inhibitors design targets several ligand binding pockets within the MTase domain. Specifically, the SAM-binding and GTP cap-binding

pockets have been attractive targets as they have been shown to bind to small molecule inhibitors (111, 112). Almost all of the viral MTase crystal structures have been solved with SAM tightly bound to the MTase. The higher affinity of binding of SAM within the binding pocket adds further complication in designing compounds that would compete with it (113). However, due to capping being a multistep reaction, SAM has to be displaced at some point. In addition, a highly conserved pocket that is present only on flaviviral MTase lying adjacent to SAM binding pocket has been reported in the crystal structure of MTase (114, 115). Since the extra pocket is absent in human MTase, competitive inhibitors of SAM like compound 10 with branching that would fit in the extra pocket have been designed (115). Similarly, sinefungin, a SAM analogue, has been shown to bind to the SAM binding site with higher affinity thus inhibiting the downstream reactions (113). The GTP-binding pocket of MTase is predominantly involved in the methylation of 2′-OH ribose of the adenosine. Inhibitors targeting the GTP-binding pocket thus inhibit the methylation at 2′-OH making the RNA more susceptible to identification by IFIT molecules. Inhibitors like BG-323 and Aurintricarboxylic acid are designed to bind to the GTP-cap binding pocket, however, have not been followed up further due to lack of cell permeability or other reasons (116, 117).

Inhibitors of NS5 RDRP activity

The flaviviral RNA polymerase has been the subject of many antiflaviviral inhibitors development as the protein is indispensable for the viral life cycle. The RNA polymerase is capable of initiating a de novo synthesis of RNA and is shaped like a semi-opened fist wherein the finger and thumb subdomains are connected by the loops encircling the palm subdomain (118). Inhibitors of NS5 RDRP have been broadly divided into nucleoside (NI) and nonnucleoside inhibitors (NNI). The nucleoside analogs compete with the nucleoside and get incorporated in the growing RNA chain thus terminating the elongation or introducing mutations. On the other hand, NNI act broadly by binding to different pockets of polymerase preventing its interaction with other proteins, locking the polymerase in inactive conformation or directly blocking the enzyme activity (119). Several NIs like NITD-008 and Balapiravir because of their potency to inhibit RDRP have been tested in preclinical and phase II trials, however, had to be pulled out because of toxicity or their inefficacy (108). Similarly, several NNIs like HPA 23, retinamide and Ivermectin have been identified as potential lead compound for inhibiting the polymerase activity (105).

1.9.3   Conclusions and perspectives

Flaviviruses have gained notoriety for causing a host of diseases ranging from congenital microcephaly, encephalitis, hemorrhagic fever to Guillain-Barre Syndrome. Vaccines are only available for few of the flaviviruses. The severity of the situation demands a continuous search for antiflaviviral compounds. NS proteins which are part of the replication complex and possess enzymatic functions make them logical and attractive targets. NS3 could be targeted to inhibit either its protease or the helicase activity. Inhibitors like compound 1 and ARDP0006 compete with the protease activity of NS3. Similarly, NS5 due to its critical role in RNA synthesis and capping has been exploited to develop antiflaviviral inhibitors. The availability of high-resolution crystal structures of both MTase and RDRP domains further aids in the process. Small molecule inhibitors competing with SAM binding site of MTase have been in the developmental pipeline for quite some time. NI and NNIs targeting the RDRP have had limited success as some candidate compounds made it to the phase II clinical trial. This clearly demands a more high-throughput structure-function based inhibitor design and screening approach.

A prime focus of the past has been to develop an effective antiviral therapy for flaviviruses. Due to increased urbanization and globalization, flavivirus infections are found in places where they would not be encountered normally. The Americas and the Asia have been home to many recent flaviviral outbreaks including the 2015/16 ZIKV outbreak. Despite several efforts from different groups, an effective drug against flaviviruses has not been approved. The problem not only lies in the emergence of resistant strains to inhibitors because of the error-prone nature of RDRP, but also due to the fact that not all the drugs have desired efficacy and pharmacokinetic properties. Thus, striking a balance to check the aforementioned problems in developing a desired inhibitor warrants a multidisciplinary approach. Structure based *in silico* studies, enzyme based high-throughput assays, and repurposing the FDA approved drugs form the basis of these approaches.

1.10   Thesis Synopsis

The family *Flaviviridae* consists of several medically important viruses of global public health concern. Despite the tremendous effort and resources poured to understand the biology of flaviviruses, we are still lacking a preventative vaccine that is effective against all four serotypes

of DENV. These problems are further complicated by the absence of chemotherapeutic agents and broadening mode of transmission for e.g. sexual/vertical transmission of ZIKV. With the difficult task faced to develop a broad-spectrum vaccine or chemotherapeutic agents, a thorough understanding of the viral life cycle and involvement of viral proteins in each step is justified.

Nonstructural proteins 4A (NS4A) and 4B (NS4B) of DENV and the regulated cleavage at the junction of NS4A-2K-NS4B presents us with an excellent substrate to probe in depth for the yet unidentified functions of these proteins. These two nonstructural integral membrane proteins are the least studied of the flavivirus proteins without any known crystal structures. Even though, several studies have been carried out based on the established topology, there are huge knowledge gaps regarding the role of 2K, presence of uncleaved polyprotein 2K-NS4B during viral infections. Similarly, less is known about the role of the TMDs of these nonstructural proteins. In this thesis, I have examined the role of 2K (a presumed signal peptide), NS4A and NS4B using a combination of reverse genetics and chimeric analysis and explained their role in viral replication and particle release. Moreover, I constructed and characterized a ZIKV replicon and investigated the efficacy of several small molecule inhibitors of flavivirus N-7-Methyltransferase against ZIKV, DENV and YFV.

In Chapter 2, I demonstrate that 2K peptide is not simply a signal peptide, as it carries more information than previously thought and plays a significant role in viral replication in a serotype specific manner. By generating different sets of 2K chimera, individual mutants and reciprocal mutants of 2K, we described how a 2 kDa peptide modulates viral replication. The major conclusions from this chapter can be summarized as: 2K peptides of DENV serotypes are functionally not replaceable even with signal peptides from other flaviviruses. Using mutagenesis, we demonstrated the importance of individual amino acid residues as well as conserved peptide "DNQL" within 2K, and the role they play in replication. Using completely new strategy of reciprocal mutation, we were able to demonstrate a partial rescue in replication and particle release in some mutants.

Chapter 3 dives into a more detailed study of the 2K peptide and how it might modulate the function of NS4B protein. Here we describe why the cleavage at 2K-NS4B junction is inefficient and why at any given time point in viral infection, there are two populations of NS4B; 2K-NS4B

and NS4B. We further explained why the chimeric Den 2K (2→3) and Den 2K (2→4) viruses were unable to cleave at the 2K-NS4B junction using a heterologous NS1 secretion system. Using the Den 2K (2→3) system, which is devoid in infectious particle production, we demonstrated the deficiency could be transcomplemented by providing NS4B (-2K) in trans. Furthermore, we detailed how the ER loop of NS4B is responsible for the rescue. Using alanine scanning mutagenesis of the conserved residues of ER loop, we showed that the T198A mutant within the ER loop most closely resembled the chimeric virus phenotype suggesting its involvement in the early stages of viral packaging. In summary, the data from this chapter point toward a differential role of 2K-NS4B and a mature NS4B with 2K-NS4B mostly involved in replication and NS4B in early packaging steps, however, the functions of these proteins are not mutually exclusive.

In chapter 4, I examined the role of different regions of NS4A and NS4B based on the established topological models. Precisely, we attempted to separate the role of TMDs in anchoring the viral proteins in the ER membrane vs. their role in viral replication and particle production using series of interserotypic NS4A and NS4B TMD chimeric viruses. TMD1 and TMD3 of DENV-2 NS4A were demonstrated to be conserved functionally across DENV serotypes albeit partially, whereas TMD2 functioned in a serotype specific manner. Similarly, different TMDs of NS4B were differentially conserved across DENV serotypes and showed varying levels of tolerance for interserotypic substitution. We further examined the effect of interserotypic substitution at TMD5 to test for its effect in post cleavage reorientation. Revertant analysis of TMD5 chimera pointed to the effect of substitution on TMD5 reorientation and suggested different mechanisms in different serotypes of DENV. Moreover, the study of interserotypic cytosolic and ER luminal loop chimeras of NS4B suggested that ER loop is functionally conserved across all serotypes of DENV, whereas, the cytosolic loop was more serotype dependent.

Chapter 5 details the construction and characterization of a ZIKV replicon system and screening of several small molecule inhibitors of flavivirus MTase designed to target the extra pocket present adjacent to the flavivirus SAM-binding site. We tested a total of eight compounds synthesized in Dr. Arun K Ghosh's lab for their ability to inhibit replication of ZKV, DENV and YFV. A ZIKV replicon capable of autonomous replication was constructed to facilitate the screening of large number of compounds. Even though, these compounds were targeted against the capping enzyme of flaviviruses, they showed a huge variation in their activity profile. GRL-

002- and GRL-004-16-MT specifically inhibited ZIKV replication with low micromolar IC_{50} value. On the other hand, compounds GRL-007-, GRL-0012- and GRL-0015-16-MT demonstrated a dual inhibitory effect against DENV and YFV, albeit the CC_{50} values of the GRL-012 and GRL-015 were concerning. Compounds GRL-007-16-MT showed a broad-spectrum activity against ZIKV, DENV and YFV even though it was slightly cytotoxic to Vero cells. Moreover, GRL-002-16 was inhibitory to YFV while ineffective against DENV, whereas, GRL-016-16 had the opposite effect. Our results reveal the differential efficacies of the small molecule inhibitors targeting N-7-MTase. The experimental data suggests these compounds have different cytotoxicities in different cell lines and the compounds act in a virus specific way. Nonetheless, we were able to shortlist some potent compounds for future modifications.

CHAPTER 2.   MUTAGENIC ANALYSES OF 2K PEPTIDE REVEALS PREVIOUSLY UNDEFINED ROLE IN VIRAL LIFE CYCLE

2.1   Chapter summary

The 2K peptide of dengue virus has long been considered a signal peptide for translocation of nonstructural protein 4B (NS4B) into the endoplasmic reticulum. The signal peptide, otherwise, a 4th TMD of NS4A protein, is cleaved from NS4A by viral NS2B/3 protease in the cytosol and subsequently processed by host cell signalase in the ER lumen. The fate of the 2K peptide and its functions have remained largely unknown. This chapter demonstrates how a small, 2 kDa protein carries more information than previously thought and how perturbation of this information negatively affects viral replication and subsequent steps of viral life cycle. To answer these questions, different sets of chimeras, individual mutants and reciprocal mutants of 2K were characterized using DENV-2 as a model system. The major findings from the study can be summarized as: i) The 2K peptide from DENV-2 can be replaced with 2K from closely related serotypes, albeit with compromised fitness, but not with 2K from other viruses or signal peptides from other proteins; ii) Mutations involving switching of corresponding amino acid that differed from DENV-2 to DENV-3 pointed to valine (V18) and threonine (T21) as being specific to DENV-2, the mutation of which led to reduced replication and significant decrease in infectious particle production; iii) Reciprocal/back mutation of some of the residues in chimeric background rescued replication and infectious particle production, however, not to wild type level; iii) The highly conserved DNQL region within the 2K peptide is essential for viral replication. Charge reversal and conservative mutations of this region suggested the importance of negatively charged aspartate (D4) at the N-terminal of 2K peptide. Thus, we concluded that 2K peptide carries information beyond signal sequence and necessary for viral life cycle.

2.2   Introduction

The signal sequence leading up to localization of NS4B into the ER lumen is about 2 kDa in size and referred to as the 2K peptide. The N-terminus of 2K is generated by viral protease NS2B/3 by cleaving it from rest of NS4A thus generating 2K-NS4B as an intermediate product. The intermediate product is then cleaved by host signalase in the ER lumen to generate a mature

NS4B protein. The sequential cleavage between NS4A-2K-NS4B presents us with a prime example of how a viral system hijacks the host machinery to its advantage. There have been a couple of examples when a similar succession of viral and host cell signalase cleavage was altered with debilitating effect on particle production (69). Flaviviruses undergo replication on the membranes of ER origin. The ER membrane originated replication factories are induced mainly by NS4A. As 2K is considered a 4th TMD of NS4A, the role of 2K in membrane rearrangement have been studied but with varied results. In KUNV, intact NS4A-2K resulted in the formation of replication organelles closely related to wild type virus, whereas, in DENV, the mature form of NS4A i.e. NS4A without 2K has been implicated in membrane biogenesis (54, 72). These differences in functions also point to the effect of cleavage between NS4A-2K and/or 2K-NS4B in forming the replication organelles and the subsequent steps of the viral life cycle. The nonstructural proteins 4A and 4B are the uncharted territories of dengue virus research. The 2K peptide is the least studied of all and needs to be put in the context of the viral life cycle in addition to its role as a signal sequence.

Signal peptides are 20–30 amino acid long consisting of a distinct three-domain structure. The N-terminus generally consists of basic amino acids, with a central hydrophobic region of about 7-13 residues, and a slightly polar C-terminus (70). The C-terminal signalase cleavage site normally conforms to the requirement of small and neutral residues in position -1 and -3 upstream of the cleavage site (Ala-X-Ala), however, eukaryotic signal peptidases have less stringent requirements (48). The 2K peptide normally conforms to the signal sequence requirement except for the lack of basic amino acid residues in its N-terminus and predominantly apolar residues in its C-terminus. The Ca and 2K are two genuine signal peptides of DENV that are formed during polyprotein processing. The Ca peptide that homes in the polyprotein coming out of the ribosome to the ER membrane has been implicated in efficient nucleocapsid packaging in Murray Virus Encephalitis Virus (MVEV) by modulating the proteolytic activity of the viral protease and the host cell signalase as well as stabilizing the E protein in ZIKV by manipulating the autophagic pathway (52, 53). A similar study wherein the sequence upstream of signalase cleavage site was mutated to perturb the sequential cleavage in YFV resulted in lethal phenotype (33).

Signal sequences in viruses have been reported to play major roles besides its conventional protein translocation functions. The signal peptide of the core protein of HCV helps in immune

modulation of the host by secreting the nonenveloped nucleocapsid (120). In Semliki Forest virus, signal peptide for p62, E3, has been shown to be essential for viral assembly by promoting the heterodimer formation between the viral surface proteins. The deletion of E3 resulted in the ER retention of E1 (121). The 2K peptide of flaviviruses have been shown to affect viral replication and aid in immune evasion. A V9M 2K escape mutant was able to overcome the inhibition offered by Lycorine by enhancing the viral RNA replication. The same mutant, V9M has been implicated in superinfection exclusion and immune evasion (65–67). Despite few studies pointing out the role of 2K in the viral life cycle, this remains a largely puzzling protein sequence whose role has not been properly identified.

2.3   Materials and methods

2.3.1   Cell culture and viruses

Baby Hamster Kidney BHK-15 (BHK-15) cells were obtained from the American Type Culture Collection (ATCC) and were maintained in minimal essential medium (MEM) supplemented with 10% fetal bovine serum (FBS). Dengue virus was propagated in the C6/36 cell line at 30°C in DMEM supplemented with 2% FBS, 25mM HEPES and 25mM L-Glutamine in the presence of 5% CO_2. The culture supernatant was clarified by centrifugation and filtered using 0.25μM filter. All chimeric viruses and mutants were generated in the DENV-2 (16681), PD2ICMO backbone.

2.3.2   Construction of chimeric viruses and replicons

All the chimeric viruses and replicons were generated in two steps. Unique restriction sites, BssHII and AgeI encompassing NS4A-2K-NS4B in the PD2ICMO were chosen. In a two-step overlap extension PCR; the 2K peptide was switched to 2K from DENV-3 (05k86), DENV-4 (06k2270), and ZKV (FSS13025) using unique sets of primers resulting in –NS4A-2K(3)-NS4B-, –NS4A-2K(4)-NS4B-, and –NS4A-2K(Zk)-NS4B- fragments. The final products were cloned into the PD2ICMO backbone using unique restriction sites BssHII and AgeI generating Den 2K (2→3), Den 2K (2→4), and Den 2K/Zika chimeric viruses. Using similar strategy, chimeric dengue replicon constructs were generated using in-house constructed DenvRLuc backbone. In a separate set of experiments, two more chimeric constructs with 2K switched to that of the signal sequence

of Receptor for Advanced Glycation Endproducts (RAGE) and leader peptide of Major Histocomapatibility Complex (MHC I) were constructed utilizing similar strategy generating PD2ICMO-RAGE and PD2ICMO-MHCLP chimeric viruses and replicons.

2.3.3 Site directed mutagenesis

A pair of complementary primers with two nucleotide substitutions corresponding to the target residues in the parental plasmid were designed using Primer X SDM software and synthesized by Integrated DNA Technology (IDT). An infectious cDNA clone of DENV and replicon were used for these experiments unless otherwise stated. Site directed mutagenesis was carried out using a modified PCR protocol using High Fidelity (HF) Phusion (NEB) enzyme. The products were transformed in DH5α competent cells, screened for mutants and confirmed by low throughput sequencing at the Purdue Genomics facility. For generation of reciprocal mutants, i.e., individual chimeric mutants, Denv 2K (2→3) chimeric virus or replicon were used as a backbone.

2.3.4 In vitro transcription and transfection

All the chimeric viruses and replicon constructs were linearized using XbaI and in vitro transcribed with T7 polymerase. Briefly, the linearized plasmid was mixed with T7 polymerase (NEB) and incubated at 37°C for 11/2 hours. Ten μgs of RNA thus obtained was electroporated into BHK-15 cells as described previously (122).

2.3.5 Immunofluorescence Assay

The electroporated BHK-15 cells that were plated in 24-well plates were fixed at 48 and 72 HPE using 3.7% paraformaldehyde and permeabilized using 0.1% TritonX-100. After blocking with 1% BSA, they were stained with mouse monoclonal antibody against NS4B (a kind gift of Dr. Pei Young Shi) or dsRNA or NS5 (Strauss). They were further stained with either FITC or TRITC secondary antibody and visualized using an Olympus 1X81 microscope and Metamorph basic software (Molecular Devices). The images were processed using ImageJ software.

2.3.6 Luciferase assay and Plaque assay

BHK-15 cells electroporated with different chimeric and mutant replicon constructs were plated in 24-well plates. At various time points post transfection, the cells were washed once with PBS and lysed using 100 µl cell lysis buffer (Promega). The lysed cells were stored at -80°C. Once samples for all time points had been collected, luciferase signals were measured using a Spectramax L Luminometer and Softmax Pro Software (LMAXII 384, Molecular Devices) according to the manufacturer's protocol. Briefly, 20 µl of cell lysates in triplicates were added to an opaque 96-well plates, the injector of the Spectramax L was primed with Luciferase assay reagent and 100 µl was added to each well with 2-second measurement delay and 5-second measurement read for luciferase activity. As a negative control, a replication deficient RNA (ΔDD) construct, with a mutated GDD motif within RDRP was used to account for any background signal. For plaque assays, supernatants from transfected cells were collected at different time points, centrifuged to clarify and processed. BHK-15 cells plated in 6 well plates were infected with 6 ten-fold dilutions of the supernatant and rocked for an hour. It was overlayed with MEM supplemented with 5% FBS and 1X agarose, incubated for 5 days at 37°C, stained with neutral red and plaques were counted.

2.3.7 SDS-PAGE and Western Blot

Transfected and infected cells were collected at different time points (24, 48 or 72 Hrs) post electroporation/infection depending on the samples. They were lysed using Pierce Co-IP buffer containing protease inhibitor cocktail (Roche) and frozen at -80°C until all the time points were collected. 10%, 12% and 13% acrylamide gels were used according to samples being processed. The nitrocellulose membrane was probed with mouse monoclonal anti-NS4B (44-4-7), rabbit polyclonal anti-NS1 and mouse anti-NS3 and -NS5 (Strauss). Infrared-labeled GαM 680 or GαR 800 secondary antibodies were added, and the proteins were visualized using an Odyssey infrared imager (LI-COR) and the Odyssey version 3 software.

2.3.8 Intracellular vs. extracellular infectious particle assay

At 24, 48 and 72 hours post electroporation (HPE) supernatants and cells were collected. Supernatants were clarified by centrifugation and frozen at -80°C until used. Cells were washed

with 1X PBS, scraped off, resuspended in 2.5% FBS containing MEM and pelleted down. Cells were then subjected to two more washes with 1XPBS. Cells were then resuspended in 2.5% FBS MEM and subjected to three rounds of freeze-thaw using liquid nitrogen and incubation at 37°C. Samples were centrifuged to remove the debris, and the supernatants were subjected to plaque assay as explained in section 2.3.8.

2.3.9 Intracellular vs extracellular RNA extraction

Transfected cells were washed thrice with 1X PBS at 6 HPE to remove s residual RNA from electroporation. At 24, 48, 72 HPE, supernatants were collected and processed for viral RNA extraction using RNeasy mini kit (Qiagen) or Pure Link RNA mini kit (Thermo Fisher) according to the manufacturer's instructions. In parallel, the cells were washed three times with 1X PBS and total RNA was extracted using the same kit. The extracted viral RNAs were frozen in aliquots at --80°C until used for further experiments. A ΔDD control was used a negative control for the background level of signal arising from RNA in downstream analyses.

2.3.10 Quantitative Real Time (qRT) PCR

SYBR Green One-step qRT kit (Invitrogen) along with dengue specific primers was used to carry out the qRT-PCR for various samples. A standard curve was generated according to the manufacturer's instructions using purified in vitro RNA samples and was used as a reference point to calculate the RNA molecules.

2.4 Results

2.4.1 In silico analysis of 2K peptide and structure prediction

The aims of these in silico analyses were to reiterate the role of 2K as signal sequence and predict the tentative N-, hydrophobic core (h) and the C-termini of the 2K peptide. Five different models were predicted when the 2K peptide was subjected to I-TASSER analysis (Fig 2.1 A, left panel) (123). The quality of the predicted models was based on the confidence (C-) score with model 1 being scored the highest (Fig 2.1 A, right panel). The 2K peptide was further analyzed using SignalP 3.0 Server (124), which correctly predicted it as a signal anchor sequence. Moreover, the analysis predicted the residues within the N-, h- and C-termini of the 2K peptide along with

the signalase cleavage site between 2K and NS4B (Fig 2.1 B). Since the amino acid composition of the signal peptide play a major role in coordinated cleavages by viral and host protease, these form the important basis in the current study. Another important feature of 2K is their high variability within the flaviviruses, although they are mostly conserved among DENV serotypes (Fig 2.1 C).
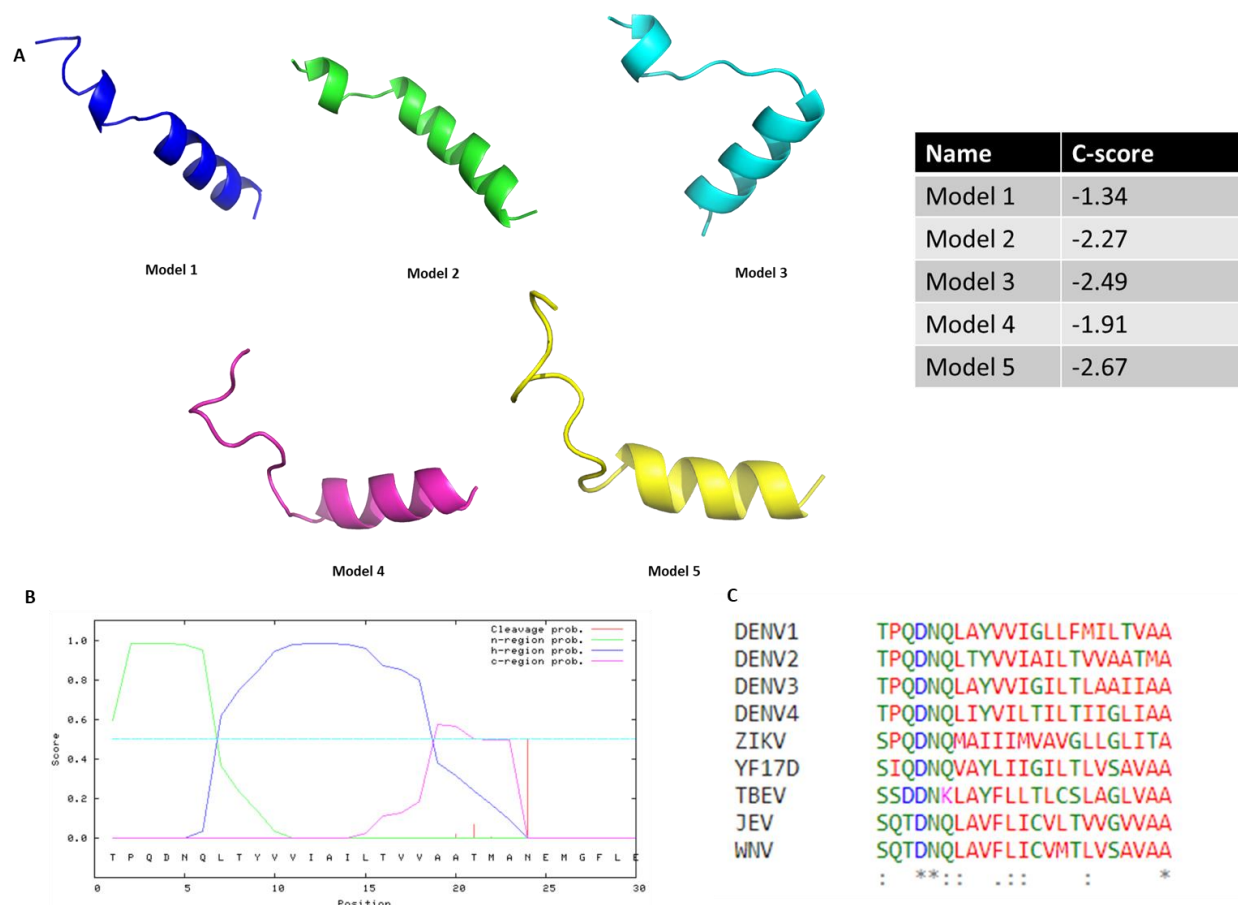
Fig. 2.1 In silico analysis of DENV-2 2K peptide and sequence alignment. A) Different structural models of DENV-2 2K as predicted by I-TASSER. The quality of the predicted models is estimated using the C-scores (confidence score) which are shown in the left panel. B) The SignalP-HMM model predicting the N-, h- and C- region and cleavage probability of the 2K peptide using neural network and hidden Markov model in eukaryotic organisms. C) Sequence alignments of 2K from different flaviviruses using Clustal omega software (125). Color coding scheme- Red: Small (small+ hydrophobic); Blue: Acidic; Magenta: Basic; Green: Hydroxyl+ sulfhydryl+ amine+ G. Asterisk (*)- Fully conserved; colon (:)- Conservation between groups of strongly similar properties; period (.)- Conservation between groups of weakly similar properties (Similar coloring/coding scheme would be used throughout this study).

2.4.2   Establishing the role of 2K peptide beyond its signal sequence activity

If 2K peptide is just a signal sequence with relatively low or no information, it should be replaceable with heterologous or closely related signal sequences with minimal to no effect on the viral life cycle. To test the hypothesis, we generated several chimeric DENV-2 constructs in the context of a full-length virus and replicon system. The 2K peptide in these constructs was switched from DENV-2 to either the leader peptide of human RAGE (receptor for advanced glycation end-products) or the more closely related ZIKV 2K (Fig 2.2 A). The schematic of the constructs is shown in Fig 2.2 B.
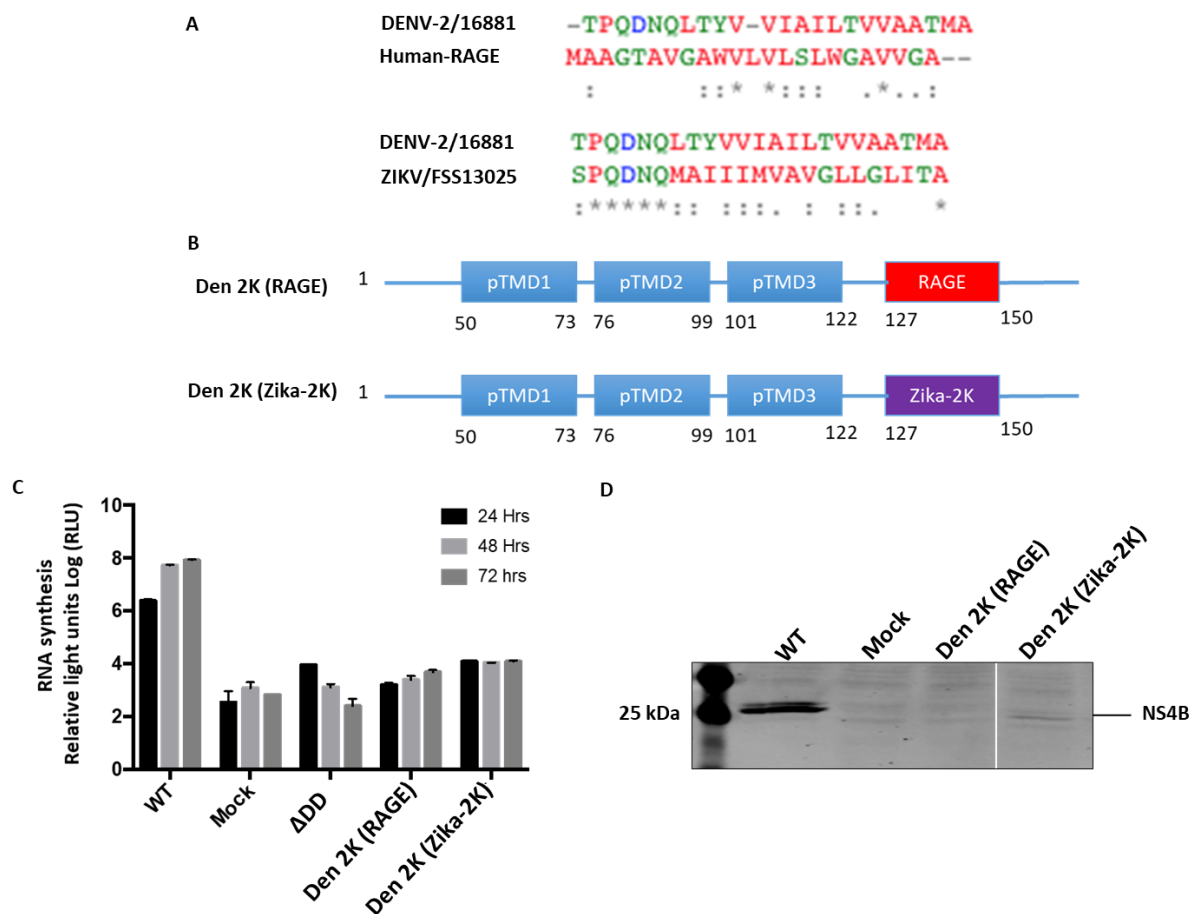
Fig. 2.2 Generation and characterization of chimeric DENV. A) Sequence alignments of the 2K peptide with leader peptide of human RAGE protein (top panel) and 2K of ZIKV (bottom panel) showing little to no sequence conservation (RAGE) to some similarity (ZIKV-2K). B) Schematic of the chimeric constructs as drawn to scale. C) The cells transfected with the corresponding chimeric constructs were analyzed for their luciferase activity at 24, 48 and 72 HPE. A replication deficient ΔDD control was used as a negative control for background level of translation obtained from the input RNA. D) Western blot of the lysates collected from the BHK cells electroporated with the chimeric full-length virus constructs and probed with anti-NS4B antibody.

These chimeric constructs were tested for their ability to replicate using a *Renilla* luciferase-based replicon system. The *in vitro* transcribed RNAs from these constructs were electroporated into BHK cells and the cell lysates were assessed for luciferase activity at 24, 48 and 72 HPE. Both the chimeric constructs were unable to replicate as demonstrated by the luciferase assay and western blot (Fig 2.2 C-D). As the substitution of 2K was lethal for replication, the full-length chimeras did not yield any infectious particles (data not shown). These results clearly demonstrate that the 2K peptide of flaviviruses is not just a signal peptide and cannot be replaced by a heterologous signal peptide like the leader sequence of RAGE or even from the closely related flavivirus ZIKV. This indirectly suggests that 2K peptide carries more information than required to translocate NS4B protein to ER lumen and is essential for the viral life cycle. Moreover, the inability to substitute 2K even within flaviviruses suggest their inherently different role in different viral context.

2.4.3   Assessing the effect of 2K substitution from other DENV serotypes

Now that we have established 2K is essential for the viral life cycle and cannot even be replaced with a signal peptide form other flavivirus species, we wanted to test whether these peptides can be replaced using 2K from other DENV serotypes. For this purpose, we chose 2K from DENV-3 and DENV-4 as the sequence identities of 2K were 69% and 56%, respectively. To test the hypothesis, we created two different chimeric constructs with 2K substituted in similar way as previously described (Fig 2.3 A-B). The chimeric replicon constructs were transfected into BHK cells with the luciferase assays being carried out at 4, 12, 24, 48 and 72 HPE. The 4 HPE time period serves as control of input RNA, at this time point, all the samples should show similar, if not identical, luciferase activity.

The 12 HPE time point represents the measure of early replication in DENV. As evident by the reduced luciferase activity of the chimeric constructs in 12 HPE (Fig 2.3 C), it clearly shows the delay in early stages of RNA synthesis in these constructs. The rate of RNA synthesis gradually increases, however, at 72 HPE, the luciferase activity is reduced by a ~1-1.5 log compared to the wild type. The establishment of this system wherein the chimeric 2K viruses were able to replicate albeit with some defect, provided the opportunity to assess the effect on infectious particle production. Surprisingly though, the chimeric constructs which replicated comparable to wild type

levels, did not produce infectious viral particles when the samples were processed at 48 HPE. Samples were collected every 24 HPE for 5 DPE for assessing the particle production. Chimeric Den 2K (2→3) virus did not show any infectious particle production until 4 DPE, whereas Den 2K (2→4) until 3 DPE. In both the cases, infectious particle production was severely affected with smaller plaque phenotypes (Fig 2.3 D-E). The absence of infectious particle production at 72 HPE in Den 2K (2→3) is interesting as a reduction in ~1-1.5 log reduction in RNA synthesis cannot simply explain the phenomenon of complete lack of infectious particle production. The differences in the amount of different proteins (NS3, NS4B and NS5) observed in the 48 HPE samples processed for western blot (Fig 2.3 F) is representative of ~1.5 log reduction in level of replication in different chimeras at that time point. Additionally, the western blot represents samples transfected with full length chimeras, a system slightly different than replicon system, which might add up for some of the differences seen in this case. Moreover, the amount of 2K-NS4B, NS3 and NS5 were quantitated using densitometry. For this purpose, the amount of proteins produced by wild type virus was normalized to 100%. It is evident from the densitometry that the amount of 2K-NS4B produced in both the chimeras were reduced by ≥50% (Fig 2.3 G). Interestingly, the amount of NS5 produced by the chimeric viruses were reduced by ~80% in case of Den 2K (2→3) and by ~74% in case of Den 2K (2→4). These results suggest that a lack of processing at the 2K-NS4B junction could affect the production of NS5 which might have influenced viral replication and downstream effects seen in the chimeric viruses.

However, an interesting trend with the processing of NS4B protein in both the Den 2K (2→3) and Den 2K (2→4) chimera was observed in the western blot. In both the samples, the lower band of NS4B (-2K) was missing and the product thus formed was not cleaved at the 2K-NS4B junction forming a product of ~29 kDa (Lane 1 and 2 from left, Fig 2.3 F). This suggested how specific the 2K peptides are even for the DENV serotypes such that in the context of NS4A and NS4B of DENV-2 virus, a 2K peptide from either DENV-3 or -4 cannot be processed by host cell signalase.
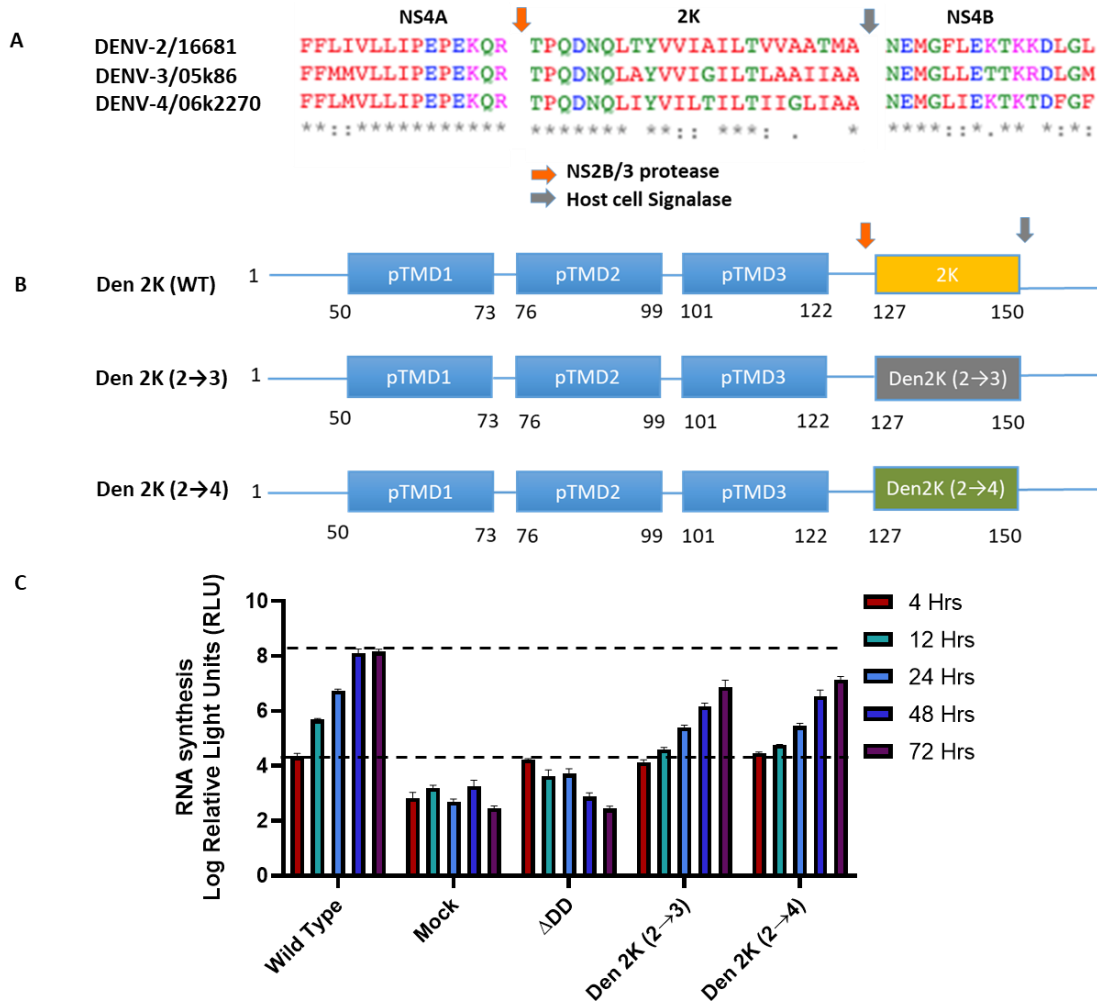
Fig. 2.3 Generation and characterization of interserotypic 2K chimeric viruses. A) Sequence alignment of 2K from different serotypes of DENV depicting the viral NS2B/3 and host signalase cleavage sites. B) Schematic of the interserotypic DENV-2K chimeric constructs. C) Indirect quantification of RNA synthesis using *Renilla* luciferase as a reporter from BHK cells transfected with chimeric viruses from 4 to 72 HPE. D) and E) Quantification of infectious particle production over 5 DPE. Supernatants were collected from BHK cells transfected with the chimeric constructs over the 5-day period and were processed for amount of infectious particle released using plaque assay. E) depicts the smaller plaque morphology of the chimeric viruses. F) Western blot analysis of NS3, NS4B and NS5 proteins from the WT and chimeric viruses transfected cells. The lysates were run on a 14% polyacrylamide gel, transferred to nitrocellulose membrane and probed with anti-NS4B (44-4-7), -NS3 and -NS5 (Strauss) antibodies. G) Amount of protein produced by the chimeric viruses were quantitated using densitometry.

Figure 2.3 continued
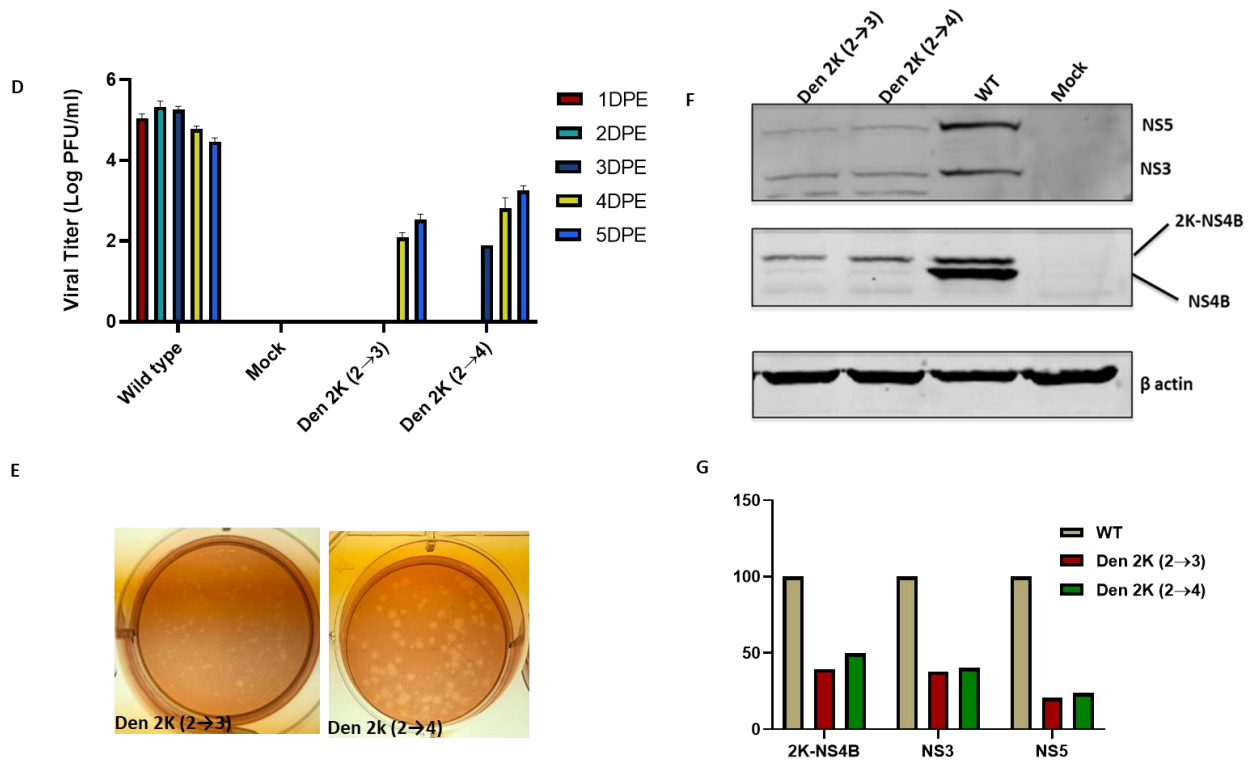
Moreover, the amino acid sequences of the 2K peptide from DENV-2, -3 and -4 were submitted to Heliquest server (126) to analyze their helix properties. Interestingly, in DENV-3 and -4, the 2K peptide formed a more prominent hydrophobic face compared to the DENV-2 (Fig 2.4). The resultant hydrophobic faces in the chimeric viruses due to the switching of 2K from DENV-2 to either DENV-3 or -4 might have pulled the 2K closer to the membrane thus impacting the cleavage by host cell signalase. The lack of cleavage at 2K-NS4B junction in the chimera results in reduced and delayed viral particle production. As evident from the western blot (Fig 2.3 F), the lack of cleavage at this junction might also affect the production of NS5 protein, a major replication protein. These data taken together points, in part, to differential function a mature (NS4B) vs uncleaved version (2K-NS4B) of NS4B play during viral life cycle. This will be probed in more detail in the following chapter.

Den 2K (WT)

Hydrophobic Face: ILVVML

Den 2K (2→3)

Hydrophobic Face: LVIILAVALAAIA

Den 2K (2→4)

Hydrophobic Face: IVIILIIALIGLA
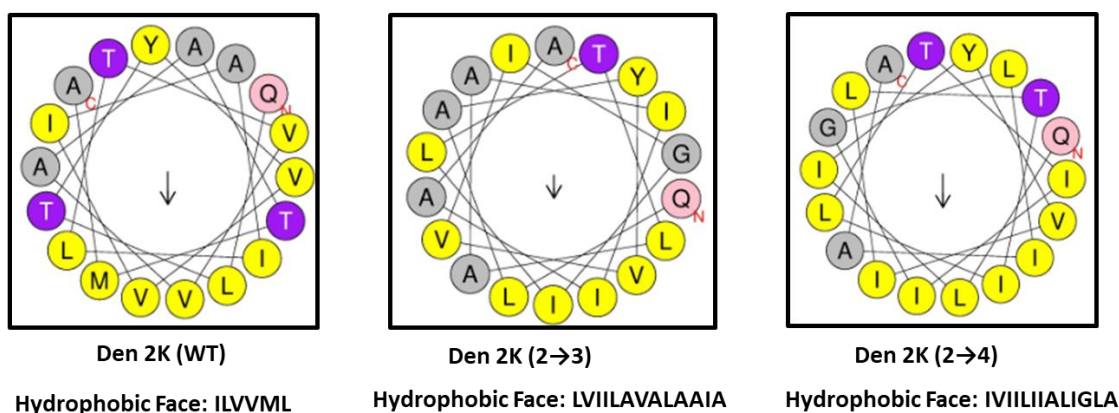
Fig. 2.4 Helical wheel analysis of amino acid residues of the 2K peptide in wild type DENV-2 vs Den 2K (2→3) and Den 2K (2→4) chimera. A switch of seven and ten amino acid residues in Den 2K (2→3) and Den 2K (2→4) chimera, respectively, resulted in a prominent shift in the hydrophobic face of the α-helices formed by the chimeric constructs.

2.4.4 Role of non-conserved amino acid residues of 2K

The revelation that the 2K can be replaced within dengue serotypes with compromised replication and a significant effect in infectious particle production prompted us to ask if any of the individual amino acid residues were responsible for the observed phenotype. For this purpose, we chose to use Den 2K (2→3) chimeric virus as this construct demonstrated prominent effect in our previous assays. Experiments were performed to generate 7 sets of mutants (full-length and replicon) in which the non-conserved amino acid residues in DENV-2 2K were substituted to amino acid at the corresponding position of DEN-3 2K (Fig 2.5 A). All these mutant constructs were analyzed for their RNA synthesis ability, infectivity and the effect of these substitution on the cleavage of 2K-NS4B.

The mutants were divided into two subgroups from the results of *Renilla* luciferase assay. The first group included T8A, A13G, V17L and M22A mutants that were not affected by the substitutions. The members of this group showed comparable level of replication (Fig 2.5B), infectious particle production (Fig 2.5 C) as well as similar pattern of 2K-NS4B cleavage (Fig 2.5 D). The second group consisting of V18A, A20I and T21I mutants each showed characteristic features. The V18A mutant was severely affected in replication, the effect of which could be translated in the infectious particle production (Fig 2.5 B, C). However, the 2K-NS4B cleavage pattern in V18A mutant remain unchanged with both NS4B and 2K-NS4B species being produced.

The second member of this group included A20I which was comparable to wild type in replication and infectious particle production. Interestingly, the A20I mutant displayed a differential 2K-NS4B cleavage pattern in which the amount of 2K-NS4B and NS4B were reversed compared to the wild type (Fig 2.5 D). The third member of this group, T21I mutant, was very similar to the Den 2K (2→3) chimera wherein the replication was reduced by ~2 log and the infectious particle production was significantly reduced. Moreover, the 2K-NS4B cleavage pattern of T21I mutant showed the production of higher molecular weight uncleaved version of NS4B (Fig 2.5 D).

The change in the property of the α-helix after introduction of the individual amino acid residues from the second group was analyzed using the helical wheel analysis (Fig 2.6). In case of V18A and A20I, there were no significant changes in the hydrophobic faces of the α-helix. These amino acid residues might play a role in DENV replication independent of the helix property. However, the in T21I mutant, the introduction of isoleucine made a prominent effect in the hydrophobic face. The resultant change might have affected the helix such that the signalase cleavage is inhibited resulting in the complete lack of mature NS4B protein (Fig 2.5 D). The requirement for small amino acid residues at position P1 (-1) and P3 (-3), as has been suggested for host signalase, is further iterated by the demonstration that substitution of threonine to isoleucine abrogated the cleavage of NS4B from the precursor protein.

In summary, the residues in the hydrophobic core of 2K peptide closer to the N-terminus are replaceable with corresponding residues from a different serotype, however, the residues closer to the signalase cleavage site (V18 and A20) and the residue that fits in the pocket of signalase cleavage enzyme has a pronounced effect in viral replication. This also suggests how the same host cell signalase is manipulated in a different way when the 2K peptide from DENV-3 is presented in a different context i.e. the proteins preceding and following it.
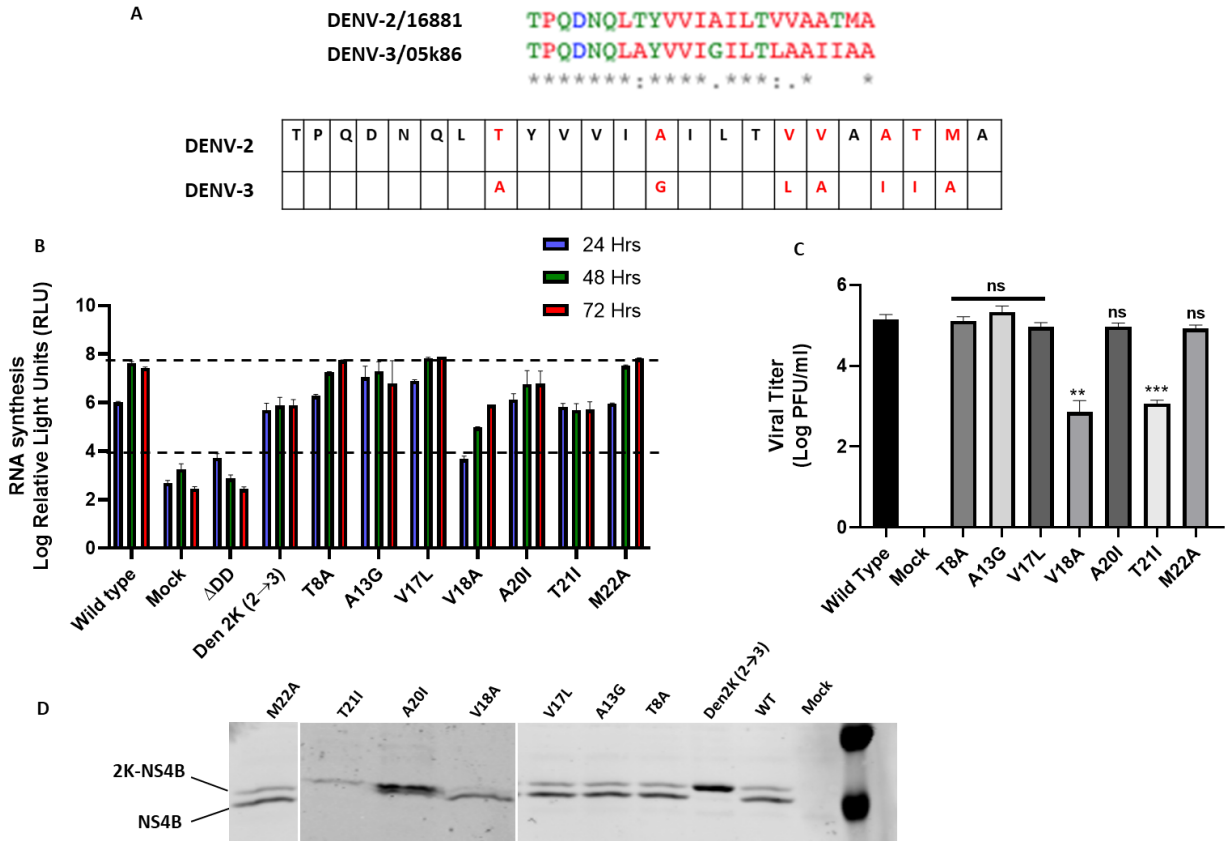
Fig. 2.5 Effect of individual mutations of 2K. A) Sequence alignment of DENV-2 and -3 2K peptide showing the amino acid residues that were mutated to corresponding residues of DENV-3. B) RNA synthesis in 7 different 2K mutants as measured by the luciferase signal at the indicated time points. Den 2K (2→3) was also used as a chimeric control against which the other mutants were compared. C) Viral titer as calculated by plaque assay from the samples collected at 3 DPE. D) Western blot analysis of lysates transfected with the mutant RNA were run on 13% or 14% gel and transferred to nitrocellulose membrane and probed with anti-NS4B antibody.
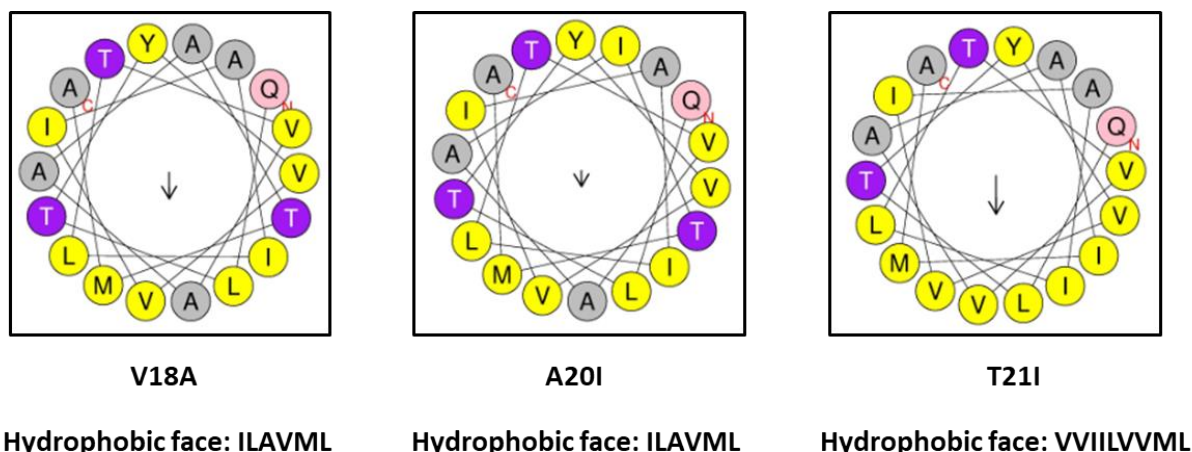
Fig. 2.6 Helical wheel analysis of amino acid residues of mutants V18A, A20I and T2. The hydrophobic faces in V18A and A20I changes from ILVVML (WT) to ILAVML. However, a bigger change in the hydrophobic face is observed after introduction of isoleucine in place of T21.

2.4.5 Assessing the role of amino acid residues in chimeric backgrounds:

The next step involved asking the question as to which individual amino acids, if any, can be substituted back to the corresponding amino acid residues in DENV-2 2K in a chimeric virus background (Den 2K (2→3)) such that the observed defects can be compensated. This method is traditionally equivalent to revertant generation, the only difference being the amino acid residues are being forced at the specific position. Briefly, the seven non-conserved amino acids in the Den 2K (2→3) chimeric constructs were individually mutated back to the corresponding amino acids of DENV-2 2K peptide (Fig 2.7 A). These mutants were then analyzed for RNA synthesis, infectious particle production and tested for their effect in 2K-NS4B cleavage.

Broadly, the reciprocal mutants were categorized into two groups. The first group comprising of A8T, G13A, L14V and A22M showed comparable or even lower rate of RNA synthesis than the chimeric construct as evident from the *Renilla* luciferase assay. These reciprocal mutants did not show any significant increase in infectious particle production compared to the Den 2K (2→3) chimeric virus. Additionally, there were no changes in the cleavage pattern of NS4B compared to the chimeric viruses; uncleaved 2K-NS4B being the only product. The lower intensity of the band corresponds to the lowered replication at 48 HPE at which the lysates were collected (Fig 2.7 B-D).

The second group included the remaining A18V, I20A and I21T mutants. Each of these mutants showed unique characteristics. The A18V mutant (Fig 2.7 B) was comparable to the chimeric virus in terms of RNA synthesis, however, showed significant increase in infectious particle production compared to Den 2K (2→3) chimeric virus (Fig 2.7 C), even though the cleavage pattern of NS4B remained the same as the chimeric virus (Fig 2.7 D). This result was interesting compared to the V18A mutant discussed in previous section (Fig 2.5 A) which was severely affected in replication and infectious particle production. This emphasizes the requirement of a hydrophobic residue at this position. Similarly, the substitution I20A was not able to rescue the replication to the wild type level, even though there was a significant increase in particle production compared to the chimeric viruses (Fig 2.7 C). More importantly, the I20A mutant restored the cleavage at 2K-NS4B junction, although the amount of cleaved (NS4B) vs uncleaved (2K-NS4B) product was reversed (Fig 2.7 D) and comparable to the A20I mutant discussed in previous section. The third mutant in this subgroup, I21T showed a modest increase in replication, however, a significant increase in infectious particle production was observed (Fig 2.7 B and C). This result was also surprising in a sense that the cleavage at 2K-NS4B junction was complete resulting formation of only mature NS4B protein (Fig 2.7 D). This suggested an increase in specific infectivity of this mutant as a greater number of infectious particles were being formed even if less amount of RNA molecules were synthesized.

In summary, none of the reciprocal (back) mutations with Den 2K (2→3) chimera as a background were able to completely rescue the replication and infectious particle production. Of note was the restoration of the partial cleavage at 2K-NS4B junction in A20I mutant albeit the ratio of cleaved vs uncleaved NS4B was reversed. On the other hand, the I21T mutant which restored the small amino acid requirement at the P3 (-3) position for signalase cleavage showed a complete cleavage at 2K-NS4B junction. The I21T mutation even though did not rescue the RNA replication, showed significant increase in infectious particle production compared to the chimeric virus.
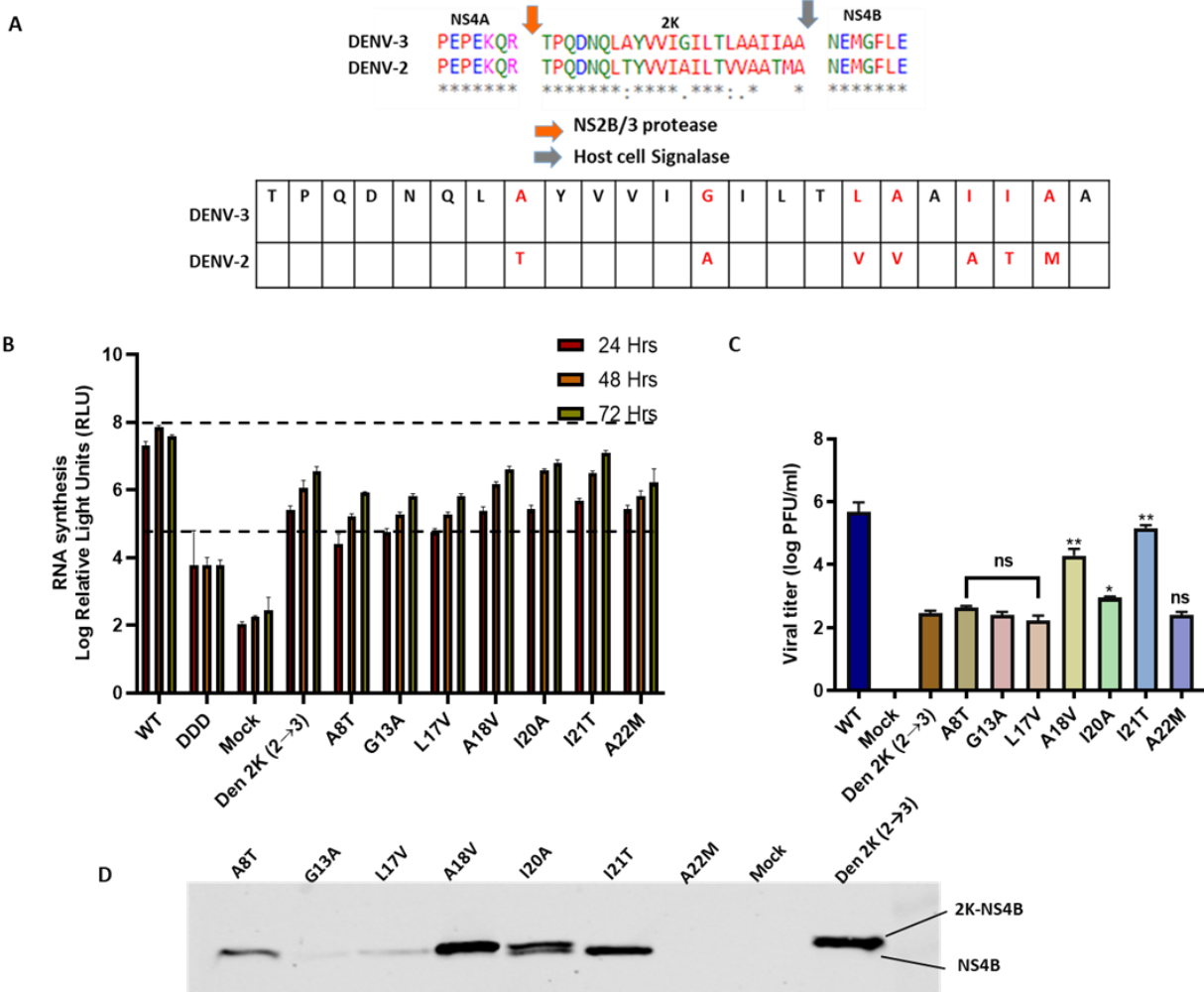
Fig. 2.7 Effect of reciprocal mutations in chimeric background. A) Sequence alignment of the 2K peptide from DENV-3 and DENV-2 along with the NS2B/3 and signalase cleavage site (Top panel). Bottom panel showing the amino acids residues in the Den 2K (2→3) chimera that were mutated back to the corresponding residue. B) RNA synthesis in the reciprocal mutants as measured by the *Renilla* luciferase reporter assay. Samples collected at 24, 48 and 72 HPE from BHK cells transfected with the mutant viruses were used in the assay. C) Viral titer as calculated by plaque assay from the supernatants collected 3 DPE. D) Western blot analysis of lysates collected from cells transfected with the mutant viruses collected at 48 HPE run on 12% gel and transferred to nitrocellulose membrane and probed with anti-NS4B antibody. Student's t-test was performed to test the significance at P<0.05.

2.4.6   Role of conserved residue "DNQL" of 2K

The N-terminus of the 2K peptide harbors a small stretch of amino acids that are almost identical in the flaviviruses (Fig 2.8 A). The presence of a highly conserved residue prompted us to ask whether these residues are important for viral replication and/or the polyprotein processing. By convention, the N-terminus of the signal sequence should be basic in nature, however, the presence of aspartate (D4) as well as two other uncharged polar amino acids (N5 and Q6) provide an exception for the 2K peptide. We analyzed the importance of these residues in two sets of experiments. The first step included alanine scanning mutagenesis of the conserved residues and assessing their effect in viral replication and infectious particle production. Assessing the effect of conservative and charge reversal mutations, as well as deletion of "DNQL" residues was part of the second step to figure out the role of these residues in viral replication.

The alanine scanning mutagenesis yielded some interesting results. The D4A, N5A and L7A mutants all were lethal for replication hence in infectious particle production (Fig 2.8 B&C). However, Q6A mutant was able to tolerate alanine at this position with a prominent compensation seen in replication and infectious particle production. The RNA synthesis ability, as measured by luciferase assay, was reduced by >2 logs for this mutant with a significant reduction in the infectious particle production (Fig 2.8 B&C). The inability to substitute these residues with alanine suggest their critical role in viral replication, even though these residues are part of the signal sequence. The Q6A mutant was able to replicate and make virus, although the titer was reduced significantly and along with the plaque size (data not shown). The substitution of glutamine (Q6) with some success is not entirely unexpected as this residue is not as strictly conserved as D4 and N5 residues suggesting the less critical role this residue play in viral replication and infectious particle production. Western blot analysis (Fig 2.9) also showed the complete inhibition of replication (absence of NS5 and NS4B) in all other alanine mutants except for Q6A.

We then asked whether conservative mutations at these positions will restore the replication of the virus. For this purpose, we generated D4E, N5D and Q6E mutants and tested them for their ability to restore replication and infectious particle production. Even though the D4E and N5D mutations rescued replication to some extent, they did not restore the infectious particle production measured at 48 HPE (Fig 2.10 A-B). In both mutants, the replication was reduced by ~1.5-2 logs compared to wild type at 72 HPE (Fig 2.10 A) and is evident in the western blot assay (Fig 2.10

C). The inability of same charge substitution mutant D4E to produce infectious particle was quite surprising and stresses the absolute requirement of these residues at this position for replication and hence infectious particle release. On the other hand, Q6E mutant showed comparable property to that of Q6A, with a ~1.5-2 log reduction in replication and a significant reduction in infectious particle production (Fig 2.10B). Moreover, we assessed the effect of charge reversal mutant D4K and a ΔDNQL mutant on viral replication. As evident from the data shown in Fig 2.10, they were lethal for replication and hence no infectious particle production was observed. Western blot analysis of the mutants shows how even the conservative mutation is unable to completely restore replication (Fig 2.10 C).
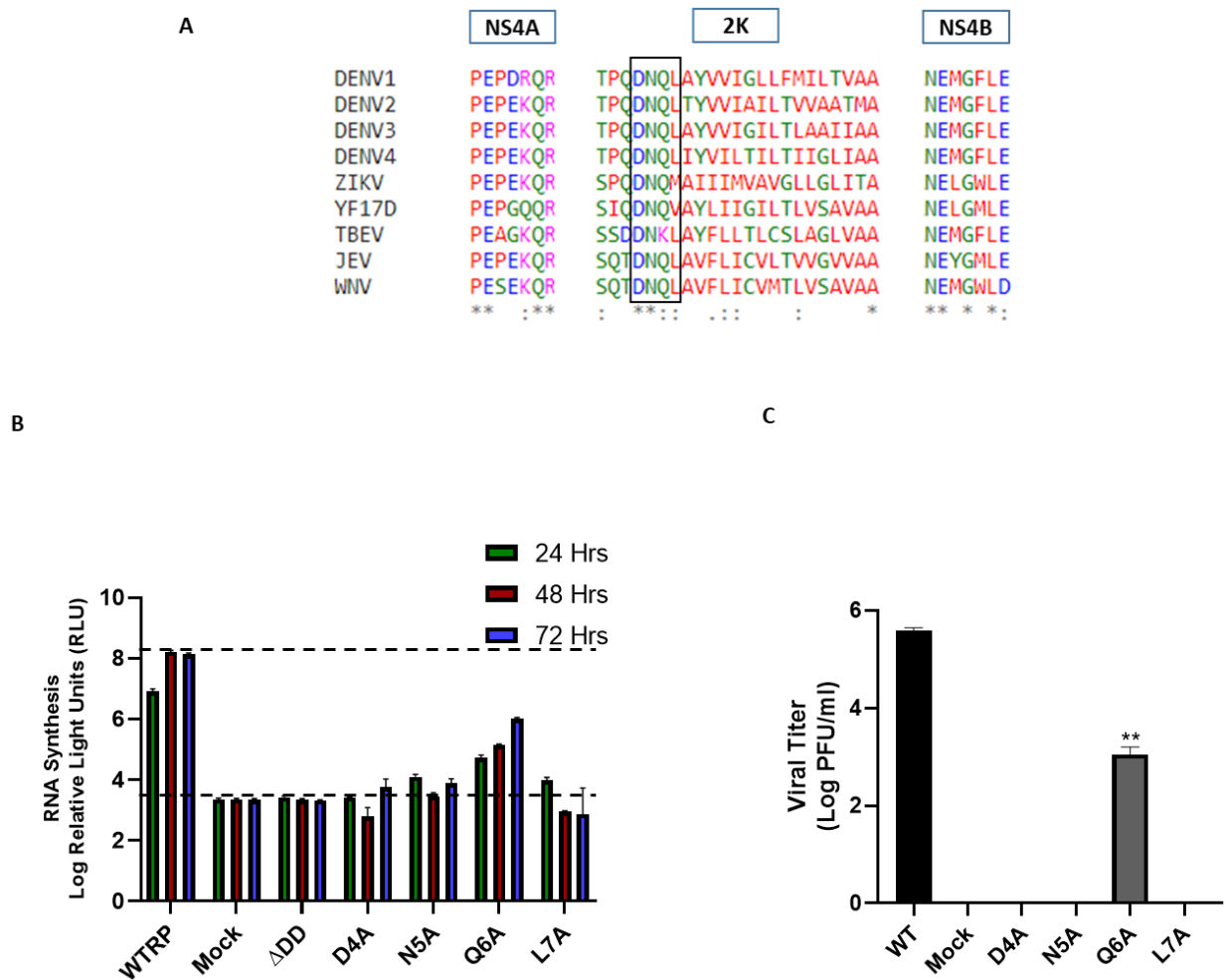
Fig. 2.8 Alanine mutations of DNQL residues within 2K abolish replication of DENV. A) Sequence alignment of the 2K peptide from different flaviviruses showing the conservation in DNQL region. Also shown are the C-and N-termini of NS4A and NS4B, respectively. B) *Renilla* luciferase assay for the alanine mutants of the DNQL residues. Samples were collected at 24, 48 and 72 HPE and measured for their RNA synthesis activity using luciferase assay. C) Viral titer determined by plaque assay using supernatants collected 48 HPE. Significance was calculated using student's t-test at $p < 0.05$.
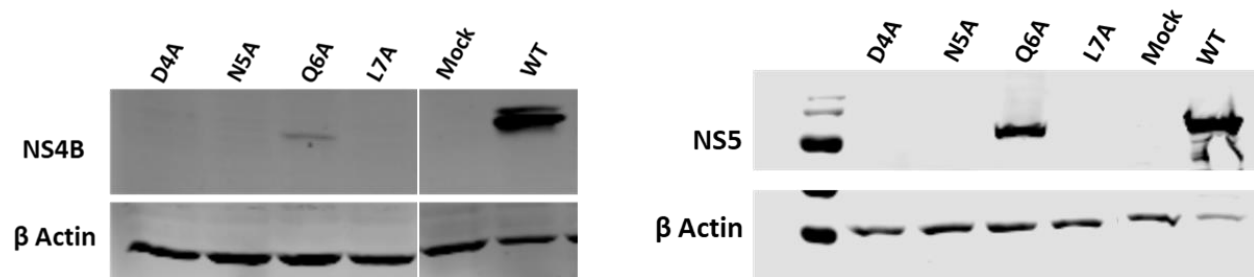
Fig. 2.9 Western blot analysis of the DNQL alanine mutants. Sample lysates collected from BHK cells transfected with the mutants were collected at 48 HPE and ran on 12% or 13% SDS-PAGE and transferred to nitrocellulose membrane and blotted with anti NS4B or NS5 Abs.
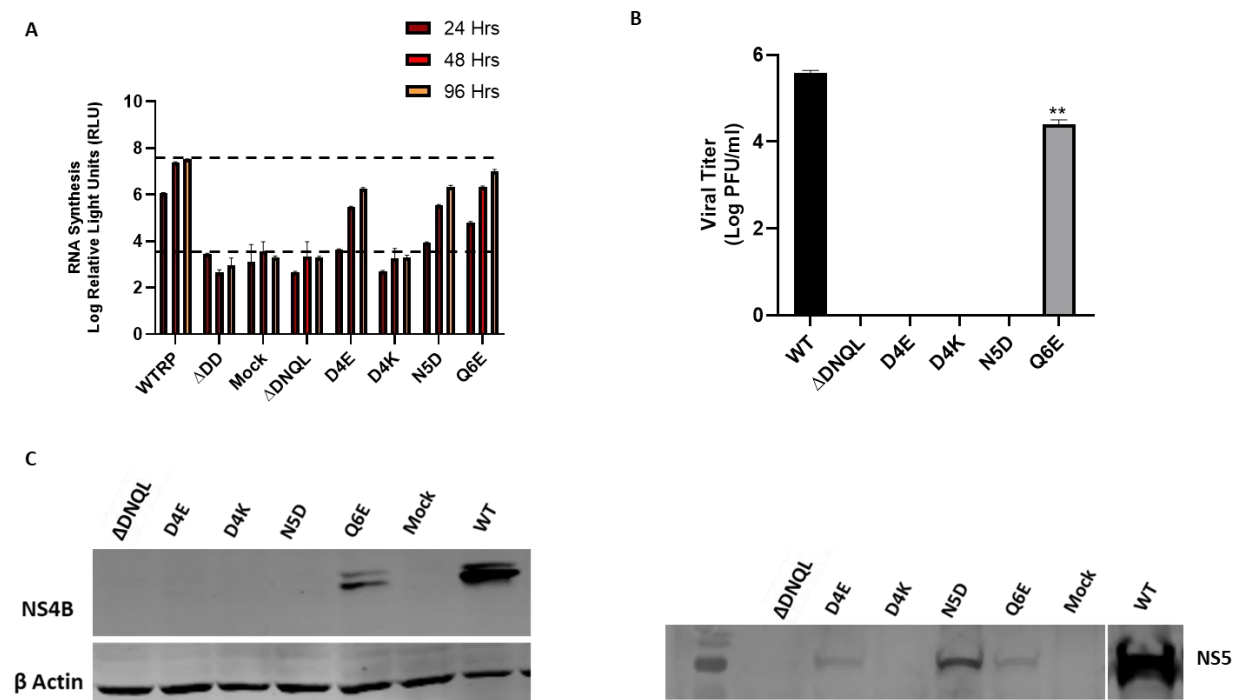
Fig. 2.10 Conservative mutation of DNQL partially restores the replication of DENV. A) *Renilla* luciferase assay for DNQL mutants. Samples were collected at 24, 48 and 72 HPE from the BHK cells transfected with the mutant constructs followed by measurement of RNA synthesis using luciferase assay B) Viral titer determined by plaque assay using supernatants collected 48 HPE. C) Western blot analysis of sample lysates against NS4B and NS5 protein. Significance was calculated using student's t-test at $p < 0.05$.

2.5   Discussion

Signal peptides are considered low information containing short peptide sequences that help target a protein to specific membranes/organelles in the cell. The flaviviral genome codes for two such peptides Ca and 2K, that aid in the translocation of the downstream protein to the ER lumen. In ZIKV, Ca peptide plays a role in virus assembly and morphogenesis by stabilizing the downstream E protein and making it available for particle formation (52). However, there is not much information available for 2K functions. In this chapter, we began to address that issue by generating and analyzing several 2K chimeric viruses and mutants.

2.5.1   The 2K peptide plays role beyond its conventional signal activity

2K peptide as shown by the *in-silico* analysis consists characteristic N-, h- and C-termini ends with a well-defined signalase cleavage site (Fig 2.1). We hypothesized that if 2K simply serves as a signal sequence for translocation of NS4B, it should not have any other role in viral life cycle and should be replaceable without consequences. However, the switch from the DENV-2 2K to leader peptide from human RAGE protein or more closely related 2K from ZIKV resulted in a lethal phenotype as shown from the *Renilla* luciferase assay and Western blot analysis (Fig 2.2). The inability to successfully replace the 2K in DENV-2 with 2K from another flavivirus or evolutionary distant leader peptide of RAGE suggests role of 2K beyond its established function as signal peptide. There are very few studies where functional role of 2K has been studied by itself. In testing the efficacy of Lycorine against flaviviruses, resistant mutant V9M was mapped to 2K. The same mutation in 2K was responsible for enhancing viral replication by interfering with host immune component (65–67). In both the chimera described in this section, the V9 position is occupied by different amino acids. The change in the signal peptide might have adversely affected the interaction between the 2K peptide and host protein. The use of unnatural signal peptide sometimes has deleterious effect on the function of protein, its folding and where it is targeted. Either of these resulting in slight modification of protein function or stability can have a serious effect in viral replication. *E. coli* thioredoxin protein was targeted to inclusion bodies rather than to the periplasmic space when an unnatural signal peptide was used, suggesting not all signal peptides function in the same way and can act in a sequence dependent manner (127). Moreover, the way signal peptide interact with the translocation machinery also determines the protein fate

76

and hence the functional outcome. The results from these sections helped us conclude that even though 2K is a signal peptide, it cannot be replaced with an unrelated signal peptide and might play an organism specific role in stabilizing/folding the protein it helps translocate.

In the next step, we chose to replace these 2K peptides with closely related signal peptides from other DENV serotypes. Both chimeras thus generated were capable of replicating but were severely affected in their ability to produce infectious particles (Fig 2.3). The ability of 2K to be replaced by very closely related signal peptide with a fitness cost in infectious particle production suggests several possibilities. First, the individual amino acids of 2K might play different role in different DENV serotypes, or the 2K peptide as a functional unit may behave differently. A ~1.5 log reduction in RNA replication cannot simply explain the absence of infectious particle production. The 2K must be investigated in context of NS4A and NS4B to get a clear picture of the ongoing phenomenon. Since the N-terminus of 2K is generated by the viral NS2B/3 protease, when switched to a different 2K in DENV-2 background it might not function in the same way. Similarly, serotype specific interactions between proteins have been reported. In a chimera of NS5 protein of DENV-2, wherein the RDRP and MTase domain were replaced by corresponding domains of DENV-4, virus replication and particle production were severely affected (128). In both Den 2K (2→3) and Den 2K (2→4) chimeric viruses, the prominent difference from the wild type was the absence of 2K-NS4B cleavage. Upon analysis of the protein lysates from 48 HPE, both chimeric viruses showed a prominent ~30 kDa protein band corresponding to uncleaved 2K-NS4B (Fig 2.3 F). The ability of these chimeric viruses to replicate but not produce infectious particle at a time point where wild type would peak, combined with their inability to be cleaved at 2K-NS4B junction suggests a differential role 2K-NS4B plays vs a mature NS4B. This is an interesting finding as the cleavage is catalyzed by host cell signalase, which suggests the way polyproteins from other DENV serotypes are processed is slightly differently than DENV-2 serotype or the viral sequences are optimized for a particular context. Based on the data, we propose that the switching of the 2K among DENV serotypes results in an increased hydrophobic face in the helix pulling it further up in the membrane and making the 2K-NS4B cleavage site inaccessible for host cell signalase (Fig 2.11).
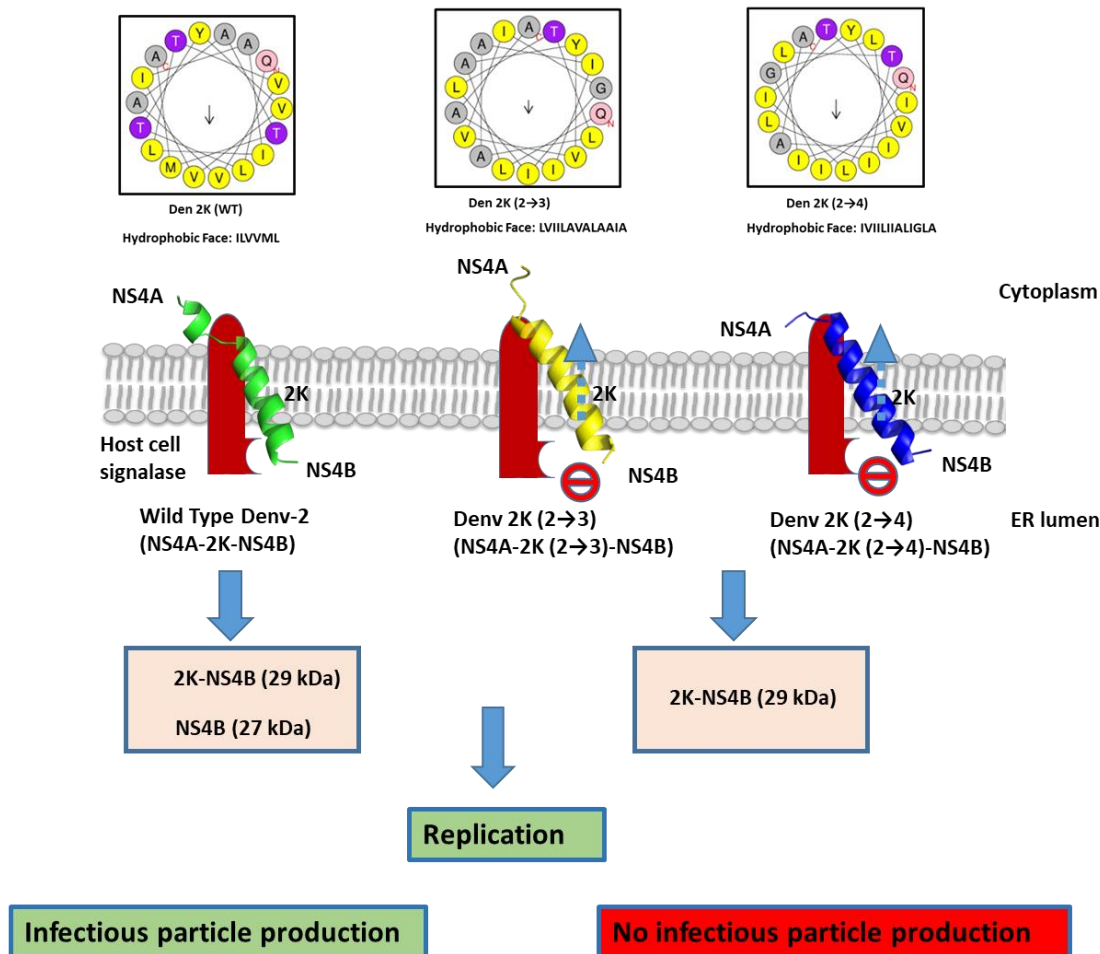
Fig. 2.11 Proposed model of processing of NS4A-2K-NS4B cleavage in interserotypic 2K chimeric viruses. In a wild type virus, after the cleavage of NS4A-2K junction by viral NS2B/3 protease, the cryptic 2K-NS4B becomes accessible to host signalase resulting in normal processing of the precursor protein producing a mature NS4B and 2K-NS4B precursor (left panel). However, upon substitution of the 2K in DENV-2 to that of 2K from DENV-3 (yellow α-helix) or DENV-4 (blue α-helix), due to an extensive change in the hydrophobic face, the α-helix is pulled up (dotted blue arrow) resulting in 2K-NS4B junction being inaccessible to host cell signalase. This results into production of 2K-NS4B precursor protein only which severely affects infectious particle production.

Thus, the 2K peptide, a 23 amino acid residue single-pass membrane protein, carries information necessary for viral replication and possibly beyond that which will be discussed in more detail in the next chapter.

2.5.2 Individual amino acid residues impart a significant role in viral replication and 2K-NS4B cleavage:

In order to define the importance of the amino acid residues within 2K, we devised a strategy wherein the non-conserved amino acids of DENV-2 2K were mutated to corresponding residues of DENV-3 2K (Fig 2.4 A). Amino acid residues in these 2K peptides mostly differed in their hydrophobic core or C-terminal region. A total of seven mutants were generated with different effects on their replication, infectious particle production and cleavage properties. As 2K serves as a signal peptide, it must fulfill the criteria of having a slightly basic N-terminal end, hydrophobic core and slightly polar C-terminal end. Among the seven different mutants generated, three of them are of special interest. The A20I mutant which was affected slightly in the replication and infectious particle production produced unique 2K-NS4B cleavage pattern where the normal cleavage pattern was reversed. The proximity of this residue to the signalase binding site (P3) might have disturbed the cleavage by signalase. The more hydrophobic residue isoleucine with branch chain instead of alanine might have created the steric hinderance or pulled the peptide closer to the hydrophobic membrane thus inhibiting the signalase activity. The V18A residue that showed a prominent effect in the replication and hence particle production underscores the requirement of bulky amino acids at the core of the 2K peptide. The helix breaking alanine residue might have affected the proper translocation of the protein or its interaction with the translocation machinery. Mutations in the core domain of signal sequences have long been reported to have negative consequences. One such example is C18R mutation in the core region of the signal sequence of preproparathyroid hormone which resulted in the loss of secretion of this hormone leading to hypoparathyroidism (129). In HIV-1 gp160 signal sequence, its conserved residues along with the residues downstream of cleavage site form an extended helix preventing the co-translational signalase cleavage (130). It would be interesting if similar phenomenon existed in DENV where the hydrophobic core residue of the 2K in coordination with residues from NS4B aid in the prevention of premature cleavage of 2K-NS4B.

The third mutant T21I was phenotypically closest to the chimeric Den 2K (2→3) virus. This mutant corresponds to the mutant in the cleavage site. For a cleavage to occur, the amino acids at position -1 and -3 must be small and nonpolar. The substitution of isoleucine instead of threonine at this position completely abrogated the 2K-NS4B cleavage which is surprising given that the same residue is present in the DENV-3 serotype, which gets cleaved and produces infectious particles. The mutagenesis around the cleavage site of C-prM that enhanced the C-prM cleavage was lethal for particle production (69), suggesting that signalase cleavage is highly regulated, and any perturbation is translated in replication and particle production.

In the next step, we tried to answer which amino acid residues within 2K are important from a different approach in what we call a reciprocal mutation. In these experiments, we used the chimeric Den 2K (2→3) chimeric virus as our starting point then replaced each of the non-conserved amino acid residues back to DENV-2 2K residues (Fig 2.5 A). Reciprocal mutations as mentioned earlier are equivalent to revertant generation except for they are not naturally selected. Reciprocal mutations within Den 2K (2→3) chimera gave some interesting results. The substitution of valine in place of alanine (A18V) rescued infectious particle production although ~2 logs less than the wild type and in the absence of the cleavage of 2K-NS4B as evident in the western blot (Fig 2.5 D). As discussed earlier, this points to the importance of a hydrophobic residue at this position. This result should be interpreted in a different vein with A18V mutant as A18V is in the DENV-2 background.

The other noteworthy result from this set of experiment was demonstrated by the reciprocal mutant I21T. The substitution resulted in a significant increase in infectious particle production to within a log of wild type. The I21T mutant produced characteristic 2K-NS4B cleavage pattern, predominantly forming NS4B as evident by the band shift in the Western blot (Fig 2.7 D). It is interesting to assume that the restoration of cleavage might have helped rescue the infectious particle production. The absence of the uncleaved 2K-NS4B in this reciprocal mutant should be taken with caution. Western blot analysis might not have picked up the very low amount of 2K-NS4B that was produced in the reciprocal mutant. If there is a complete processing of 2K-NS4B junction, a more detailed characterization of this phenotype is warranted.

The mutagenic analyses points to the importance of amino acid sequence/residue in or near the signalase cleavage site in the 2K peptide. The V18A mutation had a major effect in replication leading to a significant reduction in virion production. The importance of this site was further reinforced by the reciprocal mutation A18V, which resulted in rescuing of infectious particle production without any significant cleavage of 2K-NS4B residue. Even more pronounced was the effect of mutation on the signalase cleavage site. The T21I mutant was phenotypically similar to Den 2K (2→3) chimera, with fitness cost in replication and a significant effect in infectious particle production. Reciprocal mutation at this position resulted in increase in replication and infectious particle production with a unique 2K-NS4B cleavage pattern. These results clearly demonstrate the importance of amino acid residues of the 2K peptide and the role these residues at cleavage site play in particle release by affecting the 2K-NS4B cleavage.

2.5.3   Conserved residue in the N-terminal of 2K play role in replication

Signal peptides are surprisingly complex with modest conservation across the board (131). By convention, the N-terminus of a signal peptide is basic in nature, however, the presence of negatively charged aspartate (D4) as well as polar uncharged residues asparagine (N5) and glutamine (Q6) confers 2K of flaviviruses unique features. A sequence alignment of 2K from different flaviviruses showed a region of high conservation in the N-terminus of 2K termed "DNQL" for the conservation seen among these amino acid residues. The location of the "DNQL" along with its amino acid composition are unique as this region is closer to NS2B/3 cleavage site between NS4A and the 2K (Fig 2.10A); also, the presence of aspartate and other polar residues pointed towards the importance of this region. This underscored the need to study the detailed role of these residues in the flaviviral life cycle. Hence, we performed site-directed mutagenesis and deletion of these residues to determine their role in viral life cycle.

The first set of experiments involving alanine substitution at these positions provided some insights into the role these residues play in the viral life cycle. All the alanine mutants completely inhibited DENV viral replication and hence infectious particle production, except mutant, Q6A. The Q6A mutant was severely affected in replication (~2 log reduction) and showed a significant reduction in virion production as well as reduced protein production. When we compared the sequence-alignment results (Fig 2.10 A), Q6 is replaced by lysine (K) residue in TBEV, suggesting

the tolerance of other amino acid at this position. This clearly suggested the less strict requirement of Q6 for DENV life cycle. However, the rest of the mutants were lethal for replication and hence the infectious particle production demonstrating the need for a negatively charged D4 at this position in addition to polar uncharged N5 and a hydrophobic L7. The overall effects seen in the lethal mutants might have been caused by the overall low RNA synthesis resulting in diminished viral protein production or the mutations in 2K might have affected the replication complex formation thus interfering with RNA synthesis and the downstream process. A study carrying out the mutagenic analysis of the conserved residue "QQWS" in signal peptide of parathyroid hormone showed a loss of signal peptide cleavage, resulting in diminished nuclear localization (132). In this study, the signalase cleavage at 2K-NS4B was not affected, however, we could not check the NS2B/3 cleavage between NS4A and the 2K peptide.

Since alanine substitutions of the residues resulted in severe defect in viral replication and infectious particle production, we generated some conservative mutants in a hope that they would rescue defects seen in the alanine mutants. Surprisingly, none of the mutations completely restored the replication and infectious particle production. Although the same charge substitution mutant, D4E, rescued replication to some extent, there was no production of infectious particles. This might be due to the side chain specific interaction of aspartate vs glutamate. Mutation of D to E in the RGD motif of the Rhodostomin, a snake venom, affected its activity, structure and dynamics thus reduced its potency. Further, in the D to E mutant of the RGD motif, interaction of aspartate side chain with integrin molecule was disrupted (133). It would be interesting to probe for loss of protein-protein interactions between wild type 2K and the D4E mutant, if any. The N5D mutant was phenotypically similar to D4E, with a prominent effect in replication and infectious particle production, suggesting these two residues might play a role in particle assembly, which this needs to be probed in more detail. Additionally, the charge reversal mutant, D4K, and the deletion mutant, ΔDNQL, were lethal for replication, suggesting an absolute requirement for these residues at the N-terminal of the flaviviral 2K peptide.

Since the "DNQL" residues are closer to the NS2B/3 cleavage site, any changes in the amino acid composition might affect the way it is cleaved, interfere with protein-protein interaction mediated by the 2K or may affect the folding of downstream protein adversely affecting viral

replication. All these possibilities need to be probed in more detail before a definitive role is teased out.

Overall Chapter 2 shed light on how information rich 2K peptides are. From their inability to be replaced by unrelated signal peptides to their sequence specific role in 2K-NS4B cleavage 2K peptide with their complexity play an important role in viral life cycle.

CHAPTER 3.   THE CLEAVAGE OF 2K PEPTIDE BY HOST CELL SIGNALASE MODULATES NS4B FUNCTIONS

3.1   Chapter summary

DENV polyprotein processing taking place at the interface of ER membrane is a fundamental step in the viral life cycle. A productive viral replication and virion formation involve coordinated activities of host cell signalase and viral protease (NS2B/3) working in tandem to generate mature viral proteins from a polyprotein generated by the single ORF of DENV genome. The signal peptides that DENV genome code for, target the ensuing proteins into the ER membrane or the lumen where they are acted upon by signalase during polyprotein processing. The modulation of host signalase cleavage and effect thereof on viral life cycle is largely unknown. how modulation of the host signalase activity affects viral replication/assembly has remained largely unknown. Following up on establishing 2K as more than just a signal peptide, in this chapter we describe how the differential cleavage at 2K-NS4B modulates the function of NS4B. The major findings can be summarized as: i) Cleavage at 2K-NS4B junction is incomplete at any given time post infection; ii) NS4B can be supplemented in trans to rescue infectious particle production only when there is an active replication complex as evident in the 2K-NS4B cleavage deficient chimera; iii) The ER loop of NS4B is required to rescue the defect seen in 2K-NS4B cleavage deficient chimera with T198A within the ER loop playing a major role in particle assembly. Together these data pointed towards the dual role of NS4B with an uncleaved 2K-NS4B participating in the replication and a mature NS4B modulating the viral assembly. However, it must be noted that the functions of these proteins are not mutually exclusive.

3.2   Introduction

NS4B, an integral transmembrane protein of ~27 kDa, has a multivariate role in the DENV life cycle. From its ability to antagonize the IFN pathway to its role in replication complex formation by interacting with other viral proteins, NS4B plays a critical role in the viral life cycle. The established topological models of NS4B point to the basis of its multifaceted role during virus infection. NS4B consists of five potential TMDs, the two N-terminal amphipathic helices (pTMD1 and pTMD2) are found in the ER lumen while the three remaining TMDs; TMD3, TMD4 and

TMD5 traverse the ER membrane resulting in formation of cytoplasmic and ER loops in between TMD3/TMD4 and TMD4/TMD5 respectively (75). A solution NMR study of N-terminal 125 amino acid residues of NS4B revealed the presence of five α-helices, the C-terminal four helices of which were membrane embedded (74). The presence of the cytosolic loop (35 amino acid) and ER loop (26 amino acid) gives it an advantage to encounter viral as well as host proteins in both cytosolic and luminal environment, which might explain its varied role. Moreover, the N-terminal luminal pTMDs have recently been presented as the candidate that bind to EMC and aid in anchoring the replication complex in the ER membrane (26).

Host cell signalase cleavage of 2K from the N-terminal end of NS4B in the ER lumen results in the formation of a mature NS4B protein. The highly coordinated event of polyprotein processing occurring at the interface of cytosol and ER lumen forms the checkpoint for protein biogenesis and stability. Flaviviruses co-opt host cell proteases in tandem with the viral protease to process several of its proteins. These events happening at two completely different environments inside the cells are temporally coordinated. For instance, the capsid anchor, Ca, cannot be cleaved by host cell signalase unless NS2B/3 cleaves it from the C-terminus of the capsid. Any changes in the order of the cleavage results in defects in particle production (134). NS4A-2K-NS4B junction offers another example of spatially and temporally controlled polyprotein cleavage in flaviviruses. The signalase site between 2K-NS4B in the ER lumen is in cryptic conformation unless NS2B/3 cleaves NS4A from the N-terminal end of 2K. However, data on consequences of altered cleavage at this site have not been reported so far.

Earlier studies on polyprotein processing from flavivirus infected cells have revealed the presence of uncleaved or partially cleaved polyproteins. Uncleaved NS4A-2K-NS4B polyprotein intermediates were reported in YFV infected cells (33, 34). These studies also reported the complex but rapid cleavage pattern in the NS3-NS4-NS5 junction resulting in several uncleaved precursor proteins. The importance of these precursor proteins has remained largely unknown until recently when Plaszczyca et al. discovered that NS1 interacts with the uncleaved precursor protein NS4A-2K-NS4B directly enhancing the amplification of RNA without playing any significant role in the formation of the vesicle packets/replication factories (36). In contrary, a heterologous expression of NS4A-2K has been reported to form replication factories that closely resembled the one formed by wild type KUNV. In a flavivirus infected cells, due to the sequential cleavage of

85

NS4A-2K-NS4B, NS4A-2K should be technically equivalent to NS4A-2K-NS4B as the 2K-NS4B stays in cryptic confirmation until NS4A is cleaved from N-terminus of 2K peptide. This also indirectly suggested the role of precursor proteins in viral life cycle (72). The role of these intermediates in flaviviral life cycle has remained largely rudimentary and remains to be studied in detail.

Flaviviruses adopt a strategy in which the RNA replication and packaging of the newly synthesized genome are closely linked. The budding particles only package the newly synthesized RNA genome (135). In the absence of any recognized packaging signal, the encapsidation of the RNA is believed to be driven by electrostatic force and non-specific interactions (136). There have been several notions that NS proteins of flaviviruses act as a bridge to transport the actively synthesized genome from the replication site to the assembly site which lies opposite of each other. In this regard, several NS proteins of flaviviruses have been implicated in viral assembly. Nonstructural protein 2A (NS2A) has been described as the orchestrator of DENV assembly. NS2A interacts with 3' UTR of RNA genome which serves as a tentative packaging signal, thus initiating the recruitment of the structural proteins, RNA and viral protease to site of assembly (28). Similar findings/mechanisms of role of NS2A in assembly were reported for ZIKV (137). Similarly, two different sets of NS2A molecules have been reported with each subset playing distinct role in replication and viral assembly (27). DENV NS1 interacts with prM and E proteins and enhances virion production (138). Similarly, Patkar *et al.* showed a single mutation within the helicase domain of NS3 completely abrogated particle production in YFV without having any effect on genome replication (139).

The role of NS4B in viral assembly is still debatable. It is mostly considered a replication protein and has just once been reported to be involved in ER membrane rearrangements (140), otherwise a major function of NS4A. A large scale mutagenesis study of different regions of NS4B protein mostly pointed to amino acid residues that are involved in replication, the mutation of which would disrupt its interaction with NS3 (81). In a study of dimerization of DENV NS4B, Zou *et al.* selected several lethal mutants of NS4B, the defects in which were not transcomplemented when NS4B was heterologously expressed (141). The notion of a successful transcomplementation only when an active replication complex is present supports the idea of co-translational NS4A-2K-NS4B processing and assembling closer to other replication proteins. This

when analyzed from a different perspective stirs the idea, what if a partially cleaved/uncleaved polyprotein at the replication complex aid in the RNA synthesis and the mature protein is involved in additional functions. In chapter 2, we were able to characterize chimeric viruses which were deficient in 2K-NS4B cleavage. These viruses, though severely affected in infectious particle production, showed comparable levels of replication. This prompted us to ask questions about the role of the uncleaved vs cleaved protein. In this chapter, we explain how precursor polyprotein 2K-NS4B plays an important role in viral replication and how it differs from its mature NS4B version.

3.3   Materials and Methods

3.3.1   Cell culture and viruses

Baby Hamster Kidney BHK-15 cells obtained from the American Type Culture Collection (ATCC) and were maintained as previously described in section 2.3.1. Human Embryonic Kidney (HEK) 293T cells were maintained in a high-glucose Dulbecoo's Modified Eagles Medium (DMEM). Chimeric viruses and mutants were generated in the DENV-2 (16681), PD2ICMO backbone.

3.3.2   Construction of heterologous NS1 secretion system

A heterologous NS1 secretion system was generated to indirectly measure the cleavage of 2K-NS4B by host cell signalase. The pcDNA based heterologous NS1 secretion system was generated in a two-step overlap PCRs. Using specific sets of primers; NS4A was amplified from PD2ICMO in the first step. In a second step, using primers containing FMDV2A and portion of 2K, 2K-NS1 was amplified. In a two-step overlap extension PCR, a final product –NS4A-FMDV2A-2K-NS1- was generated which was cloned into pcDNA using unique restriction sites BamHI and XbaI. Using a similar strategy, -NS4A-FMDV2A-2K(3)-NS1- and –NS4A-FMDV2A-2K(4)-NS1- were generated in a two-step overlap extension PCR and cloned into pcDNA 3.1 using the unique restriction sites.

3.3.3 Construction of NS4B truncation constructs

A series of seven different MHCLP-NS4B-Flag truncation constructs in pcDNA3.1(+) were generated based on the established topology of NS4B (75). MHCLP-NS4B (Δ218-248), MHCLP-NS4B (Δ191-248), MHCLP-NS4B (Δ165-248), MHCLP-NS4B (Δ130-248), MHCLP-NS4B (Δ101-248), MHCLP-NS4B (Δ84-248), and MHCLP-NS4B (Δ61-248) were generated in a series of PCR reactions that would either delete the transmembrane domains (TMDs) and/or the loops in between TMDs. The reverse primers were designed in such a way that they would introduce a Flag tag at the C-terminus. The truncated PCR products were cloned into pcDNA3.1 using unique restriction sites BamHI and XbaI.

3.3.4 Site directed mutagenesis

Sets of direct complementarity primers with two nucleotide substitutions corresponding to the target residues in the parental plasmid were synthesized using Primer X SDM software. An infectious cDNA clone of DENV and replicon were used for these experiments unless otherwise stated. Site directed mutagenesis was thus carried out using a modified PCR protocol using High Fidelity (HF) Phusion (NEB) enzyme. The products were transformed in DH5α competent cells, screened for mutants and confirmed by low throughput sequencing at the Purdue Genomics facility. For generation of reciprocal mutants, i.e., individual chimeric mutants, PD2ICMO-2K (2$\rightarrow$3) chimeric virus or replicon were used.

3.3.5 In vitro transcription and transfection

All the chimeric viruses and replicon constructs were linearized using XbaI and in vitro transcribed with T7 polymerase as described in section 2.3.4. For transfection of pcDNA constructs, Lipofectamine 2000 was used. Briefly, 293T cells at 80-90% confluency were treated with 1:1 ratio of Lipofectamine: DNA made in Optimem. Six hours post transfection; the media with lipofectamine and plasmid DNA was replaced with fresh media.

3.3.6 Luciferase assay and plaque assay

BHK-15 cells electroporated with different chimeric and mutant replicon constructs were plated in 24-well plates. At various time points post transfection, the cells were washed once with

PBS and lysed using 100 µl cell lysis buffer (Promega). The lysed cells were stored at -80^{0}C. Once samples for all time points had been collected, luciferase signals were measured using a Spectramax L Luminometer and Softmax Pro Software (LMAXII 384, Molecular Devices) according to manufacturer's protocol. Briefly, 20 µl of cell lysates in triplicates were added to an opaque 96-well plates, the injector of the Spectramax L was primed with Luciferase assay reagent and 100 µl was added to each well with 2-second measurement delay and 5-second measurement read for luciferase activity. As a negative control, a replication deficient RNA (ΔDD) construct, with a mutated GDD motif within the RDRP was used to account for any background signal. For plaque assays, supernatants from transfected cells were collected at different time points, centrifuged to clarify and processed. BHK-15 cells plated in 6 well plates were infected with 6 ten-fold dilutions of the supernatant and rocked for an hour. They were overlayed with MEM supplemented with 5% FBS and 1X agarose, incubated for 5 days at 37ºC, stained with neutral red and plaques were counted.

3.3.7 SDS-PAGE and western blots

Transfected and infected cells were collected at different time points (24, 48 or 72 Hrs) post electroporation/infection (HPE) depending on the samples. They were lysed using Pierce Co-IP buffer containing protease inhibitor cocktail (Roche) and frozen at -80ºC until all the time points were collected. A 10%, 12% and 13% acrylamide gels were used according to samples being processed. The nitrocellulose membrane was probed with mouse monoclonal anti NS4B (44-4-7), rabbit polyclonal anti NS1 and mouse anti NS3 and NS5 (Strauss). Infrared-labeled GαM 680 or GαR 800 secondary antibodies were added, and the proteins were visualized using an Odyssey infrared imager (LI-COR) and the Odyssey version 3 software.

3.3.8 Intracellular vs. extracellular infectious particle assay

At 24, 48 and 72 HPE supernatants and cells were collected. Supernatants were clarified by centrifugation and frozen at -80ºC until used. Cells were washed with 1X PBS, scraped off, resuspended in 2.5% FBS containing MEM and pelleted down. Cells were then subjected to two more washes with 1XPBS. Cells were then resuspended in 2.5% FBS MEM and subjected to three rounds of freeze-thaw using liquid nitrogen and incubation at 37ºC. Samples were centrifuged to

remove the cell debris, and the supernatants were subjected to plaque assay as explained in section 2.3.8.

3.3.9 Intracellular vs extracellular RNA extraction

Transfected cells were washed thrice with 1X PBS at 6 HPE to get rid of residual RNA from electroporation. At 24, 48, 72 HPE, supernatants were collected and processed for viral RNA extraction using RNeasy mini kit (Qiagen) or Pure Link RNA mini kit (Thermo Fisher) according to the manufacturer's instructions. In parallel, the cells were washed three times with 1X PBS and total RNA was extracted using the same kit. The extracted viral RNAs were frozen in aliquots at -80^0C until used for further experiments. A ΔDD control was used as a negative control for the background level of signal arising from RNA in downstream analyses.

3.3.10 Quantitative Real Time (qRT) and Reverse Transcriptase (RT) PCR

SYBR Green One-step qRT kit (Invitrogen) along with dengue specific primers was used to carry out the qRT-PCR for various samples. A standard curve was generated according to the manufacturer's instructions using purified in vitro RNA samples and was used as a reference point to calculate the RNA molecules. RT PCR was carried out using the One TAQ RT-PCR kit (NEB). Region specific primers were used to amplify the DNA fragments which were later run on a gel, purified using GFX columns (Invitrogen) and send for sequencing.

3.3.11 Selection of revertants and identification of mutations

BHK-15 cells were electroporated with 10 μg of in vitro transcribed mutant RNA. Culture supernatants were collected 5 DPE and plaqued as described previously. Individual plaques were picked and passaged for 5-6 passages or until big plaques were visible with culture supernatant at each passage being collected, clarified and frozen at -80ºC until further analysis.   At this point, the corresponding supernatant samples were subjected to RNA extraction and RT PCR analysis as described previously. The targeted DNA fragments thus obtained were purified and analyzed by nucleotide sequencing.

3.3.12 Trans-complementation assay

BHK-15 cells were electroporated with 10 µg of in vitro transcribed chimeric RNA and plated in T-25 flasks. Twelve to 16 HPE, pcDNA NS4B truncation plasmids were transfected using Lipofectamine 2000 (Thermo Fisher) according to the manufacturer's instruction. Culture supernatants were collected 48 hours post transfection (HPT) and analyzed by plaque assay as described previously. Cells were washed thrice with 1X PBS and resuspended in 2.5% FBS MEM and pelleted down, washed twice with 1XPBS and processed for calculation of intracellular particle assay.

3.3.13 Trans-packaging assay

BHK-15 cells were electroporated with 10µg of in vitro transcribed chimeric and full-length replicon RNA and plated in a T-75 flask. Sixteen HPE, the electroporated cells were subjected to second round of electroporation with SIN-CprME. The culture supernatants were collected at 24 HPE and used to infect naïve BHK cells. BHK cells thus infected were incubated for 48 hours and subjected to luciferase assay as described in section 3.3.6.

3.3.14 Statistical analysis

GraphPad Prism Software 7 was used to analyze the data. Student's t-tests were used to determine significance wherever applicable.

3.4 Results

3.4.1 The chimeric viruses are delayed in packaging

Interserotypic 2K chimeras that are competent in replication yet defective in host cell signalase cleavage at 2K-NS4B junction can be used as a tool to understand how signalase cleavage at this junction influences viral life cycle. As described in Chapter 2, the interserotypic chimeras, Den 2K (2→3) and Den 2K (2→4), did not produce any infectious particles when measured at 48 HPE. To further analyze the defect in infectious particle production, we performed series of experiments to determine if the block was in packaging or release of the virus. BHK cells were transfected with the wild type and chimeric viruses and subjected to quantitation of

intracellular RNA synthesis using qRT-PCR or plaque assay for viral titer determination. As shown in Fig 3.1 A, at 48 HPE, in case of chimeric Den 2K (2→3) virus, intracellular infectious particles were not detected. Similarly, the Den 2K (2→4) shows ~ 3 log reduction in intracellular infectious particle production compared to wild type virus. As discussed in section 2.4.3 of chapter 2, there were no infectious particles being secreted at 48 HPE in either of the chimeric viruses as shown in Fig 3.1 B.
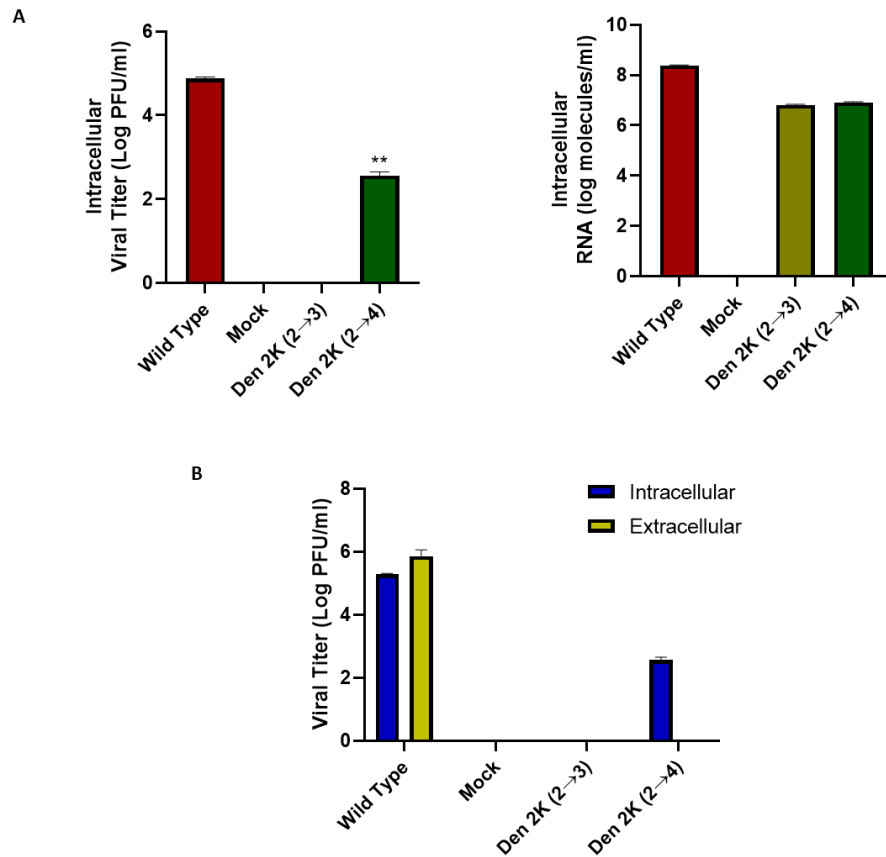
Fig. 3.1 Analysis of infectious particles and intracellular RNA genome release in the 2K chimeric viruses. A) Quantification of intracellular infectious particles (Left panel) and RNA genome (Right panel). BHK cells transfected with the WT and chimeric viruses were lysed and processed accordingly for viral titer determination using plaque assay and qRT pCR for quantification of RNA genome. B) Intracellular vs extracellular viral titer. BHK cells transfected with the WT and chimeric viruses were lysed at 48 HPE after thorough washing. The clarified lysate was processed for viral titer determination using plaque assay. Data were collected from experiments performed in duplicates (for RNA quantitation) and triplicates. Student's t-test was performed to determine the significance at $p<0.05$.

The absence or severely reduced intracellular infectious particle production at 48 HPE in both the chimeric viruses points toward delayed packaging or other defects in assembly. As evident from the release of reduced number of infectious particles later in the infection (4 DPE), we can conclude that some early steps in the viral packaging have been affected. At 48 HPE, the amount of RNA genome synthesized in both chimeric viruses were ~1.5 log lesser than the wild type. However, a lack of intracellular infectious particle production in the context of chimeric viruses at the same time point was surprising. The ~1.5 log reduction in RNA synthesis is unlikely to account for the more severe defect seen in infectious particle production (Fig 3.1A). A transpackaging assay where structural proteins were supplied in trans was used to assess the packaging of the WT vs the chimeric replicons. Both the chimeric replicons were prominently reduced compared to the wild type (data not shown). Similarly, There are evidences demonstrating efficient packaging of RNA molecules when there is maximal RNA synthesis (135). Using a DNA-based KUNV construct and a control virus with GDD mutation, *Khromykh et al*., showed an active replication will lead to packaging of the viruses (135).
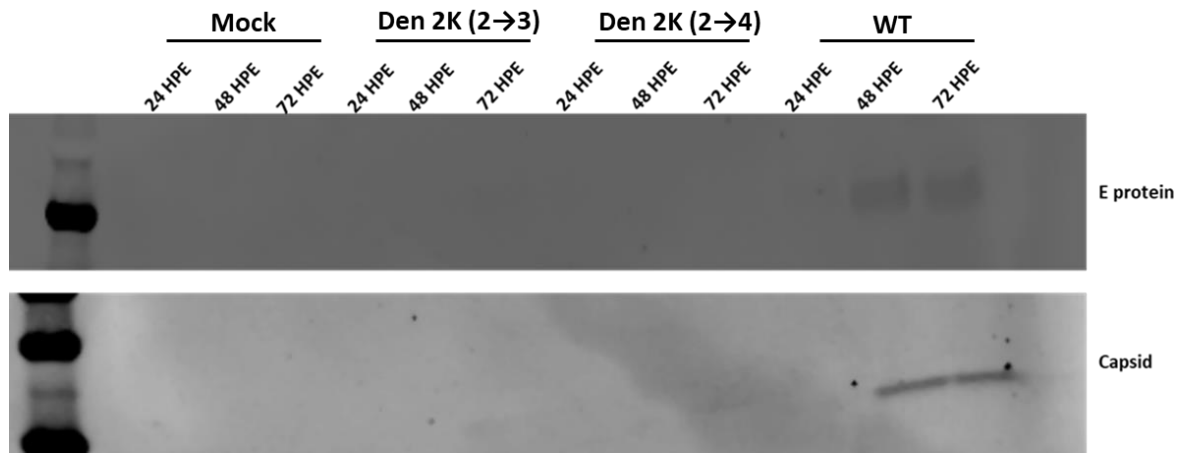
Fig. 3.2 Western blot analysis for C and E proteins over 72 HPE. Supernatants from BHK cells transfected with the chimeric and wild type virus were collected at 24, 48, and 72 HPE. After clarifying the supernatant by centrifugation, the samples were run on a 12% SDS-PAGE and transferred to nitrocellulose membrane and probed with anti-E (4G2) and anti-C antibody.

To further probe for the defect in packaging vs release, we then analyzed the supernatants collected from the transfected cells over the period of 72 HPE. Samples collected at 24, 48, 72 HPE were subjected to western blot analysis. Not surprisingly, both the chimeric viruses did not release any capsid in the supernatant compared to wild type virus where capsid was clearly visible at 48 and 72 HPE (Fig 3.2). Similarly, there was absence of any detectable E protein until 72 HPE in both the chimeric viruses.

In the next step, we analyzed the lysate of BHK cells transfected with the chimeric and the wild type viruses at 48 HPE (Fig 3.3). Lysates from the cells transfected with both chimeric viruses showed the presence of C and E protein at levels similar or greater than the WT. This further supports the idea that the interserotypic chimeras were delayed in packaging.
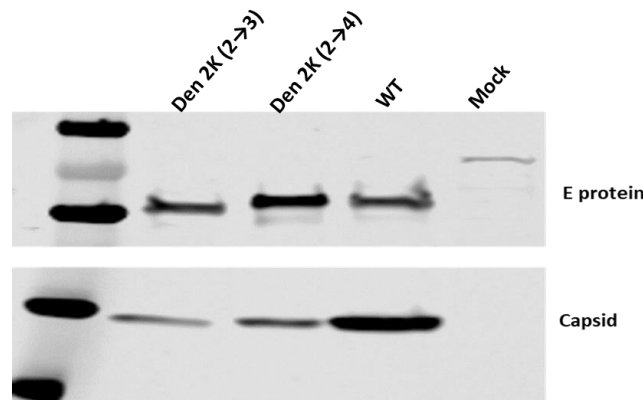
Fig. 3.3 Western blot analysis of C and E protein from the lysate. Lysates from BHK cells transfected with the chimeric and wild type viruses were collected 48 HPE. Samples were run on a 12% SDS-PAGE and transferred to nitrocellulose membrane and probed with anti-E (4G2) and anti-C antibody.

3.4.2 Processing of NS4A-2K-NS4B junction in DENV-2 infected cells

As we have noticed in the previous chapter, the cleavage at 2K-NS4B junction is not complete. Western blot analysis of DENV-2 transfected cells at 48 HPE showed the presence of a doublet band representing 2K-NS4B and NS4B. This raised a question whether the partial/incomplete cleavage at the 2K-NS4B was temporally regulated. Does this happen only when more protein accumulates during the latter stages of viral life cycle? To address these questions, we went ahead to establish the pattern of polyprotein processing at the NS4A-2K-NS4B

94

junction in virus infected cells. To this end, BHK cells were infected at an MOI of 1 with DENV-2 and the infected cell lysates were collected every six hour intervals from 6 HPI to 72 HPI and subjected to Western blot analysis.

A ~15 kDa band of NS4A protein was visible at 24 HPI post infection with a peak band intensity observed around 66 HPI (Fig 3.4, top panel). This experiment mainly focused on the 2K-NS4B junction so other uncleaved polyprotein bands won't be discussed. Interestingly, a ~27 kDa band corresponding to NS4B was visible at 30 HPI and peaked around 72 HPI. Of note was the presence of the doublet band (2K-NS4B and NS4B) from early in infection (30 HPI) and maintained throughout the time of experiment (72 HPI) (Fig 3.4, bottom panel). In another set of experiments, BHK cells were infected with DENV-3 virus at an MOI of 1, the lysate was collected at 48 HPI and probed for the evidence of partial cleavage at 2K-NS4B junction in DENV-3 serotype. Interestingly, the partial cleavage at 2K-NS4B junction is not serotype specific and is present in DENV-3 serotype as well.
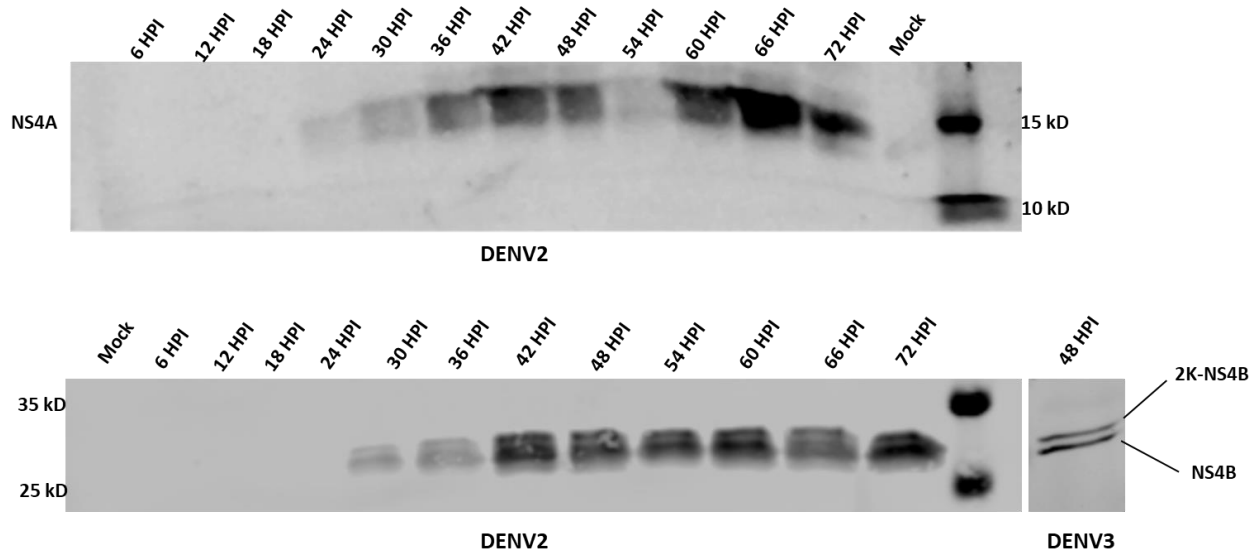
Fig. 3.4 Western bot analysis of NS4A and NS4B proteins of DENV-2 infected BHK cells. BHK cells in a 6 well plate was infected by DENV-2 at an MOI of 1. Cell lysates were collected at every 6 HPI interval and then ran on a 12% or 13% gel, transferred to nitrocellulose paper and probed with anti-NS4A antibody (Top panel) or anti-NS4B antibody (Bottom panel). Lysate collected at 48 HPI from BHK cells infected with DENV-3 were collected and processed the same way and probed with anti-NS4B antibody (Bottom right panel).

This proved to be a proof of concept that in a DENV infected system, there are always two distinct sets of NS4B present, a mature NS4B (~27 kDa) and an uncleaved 2K-NS4B (~29 kDa). The differences brought about in the viral life cycle, if only one or other species is present in the system form the basis of Chapter 3. Herein, we study how these two species of NS4B are involved in different steps of viral life cycle and try to tease out their role.

3.4.3   Indirect assessment of cleavage at 2K-NS4B junction:

The signal peptide property of the 2K peptide can be exploited by using it as a signal sequence for translocation of an ER luminal protein other than NS4B. We created a system wherein the 2K was cloned at the 5' terminus of NS1 replacing its natural signal peptide in a pcDNA 3.1 backbone. NS1 of DENV is an ER luminal protein that gets secreted. In a viral system, the last 24 amino acid residues of E protein serve as the signal for translocation of NS1 to the ER lumen. Inside the lumen, the E-NS1 junction must be cleaved by the host protease for it to be secreted. If the 2K from DENV-2, -3 and -4 serotypes are cleaved equivalently, the amount of NS1 released in the supernatant should be equal or similar.

In order to test if all three 2K peptides from DENV-2, -3 and -4 could translocate NS1 to ER lumen and get cleaved in a similar manner by host cell protease, we transfected 293T cells with four different constructs pcDNA-NS1, pcDNA-2K-NS1, pcDNA-2K (3)-NS1, and pcDNA-2K (4)-NS1. At 72 HPT, the supernatants and cells were collected and further processed. The amount of NS1 secreted was calculated by measuring the band intensity. pcDNA-2K-NS1 was used as a control as this construct has the E24 amino acid residues as a signal peptide. The amount of NS1 secreted and translocated using a pcDNA-2K-NS1 was comparable to the pcDNA-NS1 construct with natural signal peptide (Fig 3.5 A). This suggested that 2K from DENV-2 can be used as a heterologous signal peptide in an expression system as it was processed in the same way as the natural signal sequence. On the other hand, the amount of NS1 translocated and secreted were significantly reduced in the system wherein the natural signal peptide was replaced with 2K from either DENV-3 or -4 (Fig 3.5 A).

The amount of NS1 thus secreted using different 2K peptide from different DENV serotypes were quantified using densitometry. For this purpose, the amount of NS1 secreted using the DENV-2 2K peptide was normalized to 100%. This normalization was relevant as both Den 2K

(2→3) and Den 2K (2→4) chimeric viruses used in the current study were generated in the DENV-2 background, replacing the 2K with 2K from the respective serotypes. It was evident from the densitometry that the amount of NS1 secreted in both the 2K (3)-NS1 and 2K (4)-NS1 system were significantly lesser than the one using DENV-2 2K system ($P<0.0001$) (Fig 3.5 B).

This is an indirect measurement of the cleavage happening at 2K-NS4B junction. As is seen from the above results, 2K from DENV-3 and -4 are not a good signalase substrate thus are not cleaved properly from the protein thus creating a pool of partially cleaved proteins. These results further consolidate the idea of involvement of two different species of NS4B in the viral life cycle.
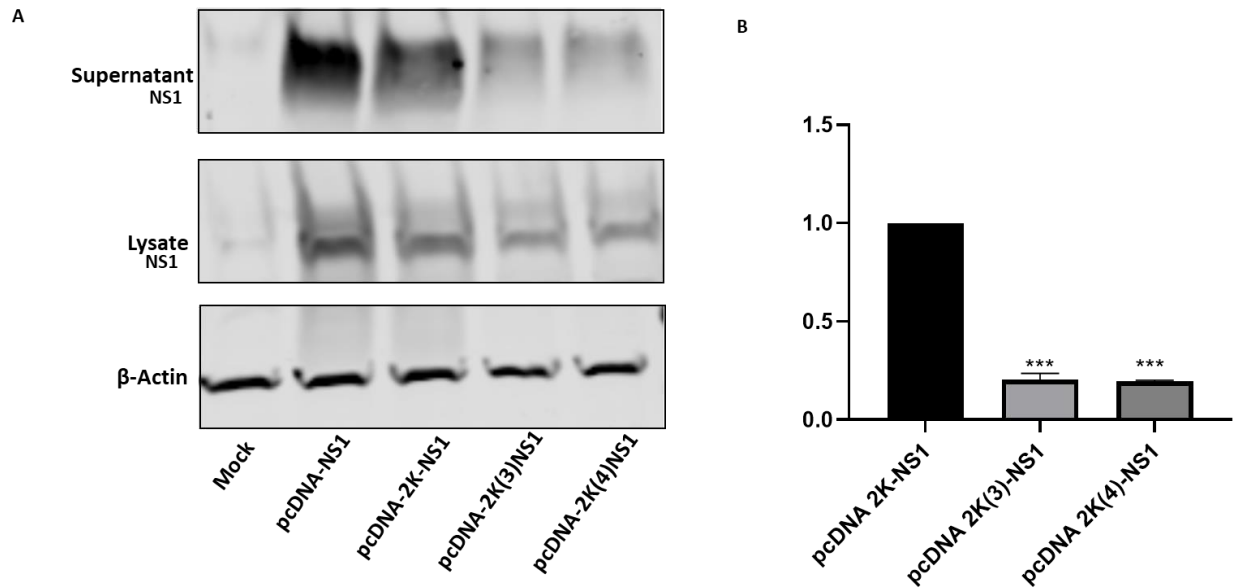
Fig. 3.5 Measurement of cleavage using a heterologous expression system. A) Four different pcDNA-NS1 constructs with different signal peptides were transfected in 293T cells. The cells and supernatant were harvested at 72 HPT and subjected to western blot analysis. B) The amount of NS1 protein secreted in the supernatant were quantified using densitometry. Amount of protein secreted from the pcDNA 2K-NS1 was normalized as 100%. Results are shown as means (± SEM) of two independent experiments. Student's t-test was performed to measure the significance at $P<0.0001$.

3.4.4 Defect in particle production can be transcomplemented

Now that we have established that an uncleaved 2K-NS4B is capable of functioning as a replication protein, we asked whether a mature NS4B has additional functions. If a mature NS4B has a role in particle production or any related role in accelerating the assembly process, we should be able to supply a mature NS4B in trans and it should rescue the particle production. However, translocation of NS4B to the ER requires a signal peptide and it cannot be 2K in this case. To overcome this issue, we relied on published data wherein a murine leader peptide of murine major histocompatibility complex I (MHC I) molecule has been successfully used to translocate NS4B to the ER without affecting its function (71) as depicted in Fig 3.6 A (bottom panel).

After 12 hours post electroporation with the Den 2K (2→3) chimera, NS4B with the leader peptide from MHC I was transfected using Lipofectamine. Supernatants from the transcomplementation reaction were collected 48 HPT and subjected to plaque assay. The results clearly showed that the defect in particle production seen in the chimeric Den 2K (2→3) can be transcomplemented if NS4B is supplied in trans with its 2K peptide substituted to unrelated signal peptide. Though the rescue was not to the wild type level, it was significantly different ($p<0.005$) from the chimeric virus (Fig 3.6 C).

In a separate experiment, we tried to transcomplement a replication dead full-length DENV-2 with Zika 2K peptide (Zika-2K) (described in chapter 2) using a pcDNA construct expressing full length 2K-NS4B and were not successful (Data not shown). Taken together, these experiments suggest the requirement of an active replication complex for a defect in NS4B to be transcomplemented. Similar observations were made in a study wherein individual NS4B mutants dead in replication could not be transcomplemented by a full length NS4B (76).

3.4.5 The ER loop between TMD4 and TMD5 is required to rescue infectious particle production

To further narrow down the regions within NS4B responsible for infectious particle production, we generated series of NS4B-truncation constructs with C-terminal FLAG tag (Fig 3.7 A and B). We then analyzed the role of these truncated proteins in rescuing the deficiency in particle production in the chimeric Den 2K (2→3) virus. The deletion constructs were individually transfected into the BHK cells already harboring the chimeric virus. The transcomplementation

experiment involving TMD5 deletion construct (Δ218-248), significantly increased the particle production compared to the chimeric virus alone. However, as soon as the ER loop was deleted (Δ191-248), the ability of NS4B to transcomplement the defect in infectious particle production decreased significantly, suggesting the importance of the ER loop in rescuing the defect seen in the chimeric virus lacking in 2K-NS4B cleavage (Fig 3.7 C). All other truncation constructs upstream of the ER loop did not bring about any significant difference in rescuing the defect in virion production. Thus, we concluded that the region consisting of 26 amino acid residues (191-216) corresponding to ER loop region of NS4B is responsible for rescuing the infectious particle production. ER loop can interact with other viral proteins or host proteins in the ER lumen to bring about the effect seen in the chimeric viruses. NS1 interacts with NS4B in the loop region between TMD2 and TMD3 which lies in ER lumen with its wing domain (142). Similarly, first 125 amino acid residues of NS4B that are located in the ER also interfere with the IFN α/β signaling (71), suggesting the importance of residues in the ER lumen.
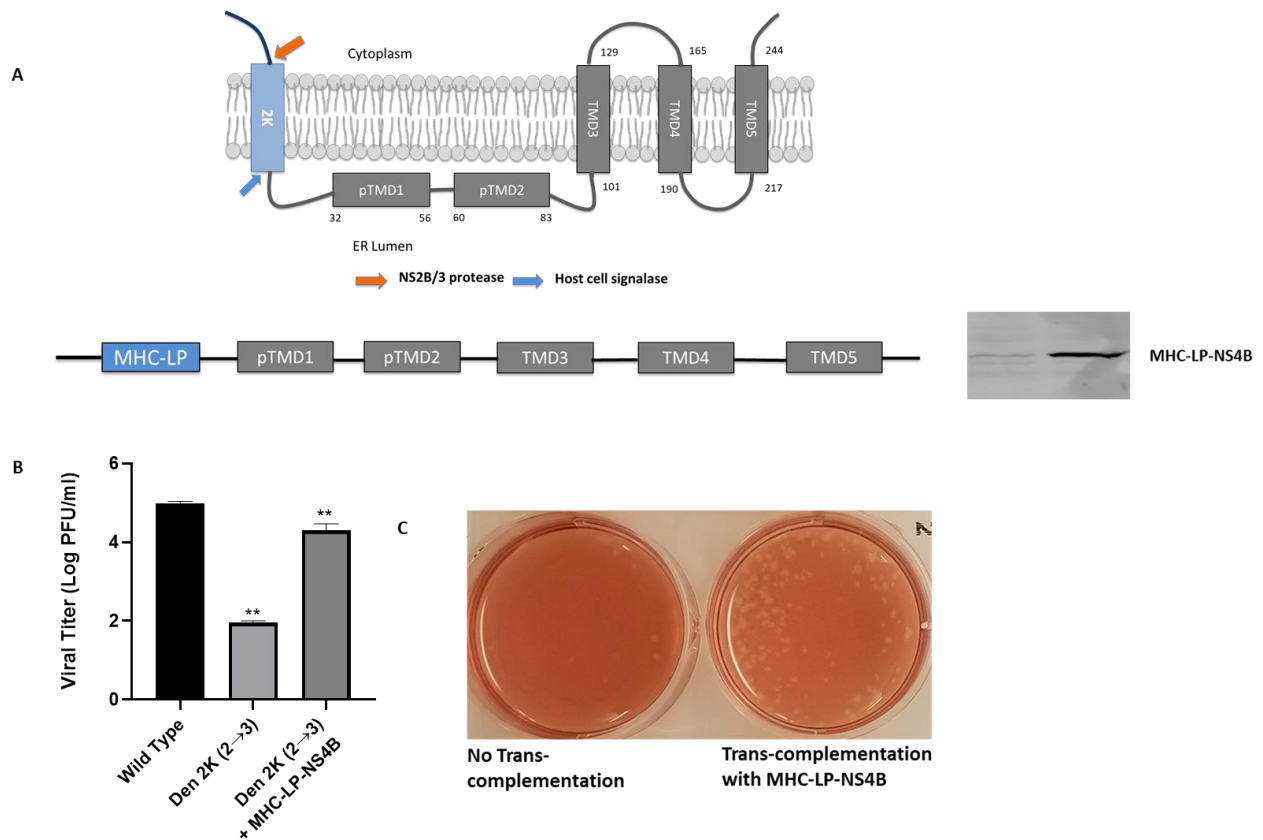
Fig. 3.6 Rescue assay using transcomplementation with MHC LP-NS4B. A) Predicted topology of NS4B adapted from Miller *et al* (top panel). The schematic of MHCLP-NS4B and the western blot showing the expression of the protein (bottom panel). B) Rescue assay using MHC LP-NS4B. At 12 HPE of BHK cells with the chimeric virus, pcDNA3.1 expressing NS4B with leader peptide from murine MHC (MHC LP) was transfected using Lipofectamine 2000. 48 HPT, the supernatants were collected and subjected to viral titer determination using plaque assay. Data were collected from experiments done in triplicates. Student's t-test was used to determine the significance ($p<0.05$) C) Representative of plaque assay result is shown.
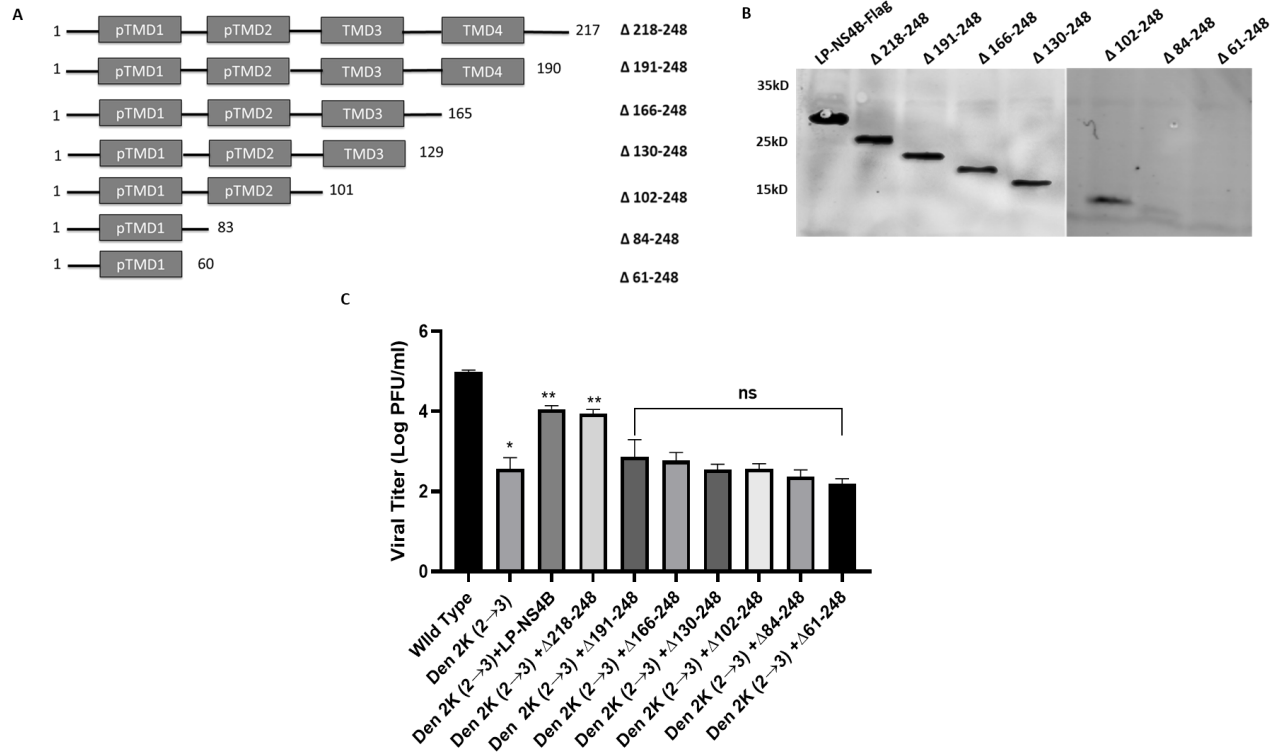
Fig. 3.7 Rescue assay using transcomplementation with MHC LP-NS4B with NS4B truncations. A) Schematic of MHC LP-NS4B truncates with amino acid positions specified. A total of seven truncations were made and cloned into pcDNA 3.1 with C-terminal FLAG tag. B) Western blot analysis showing the expression of the truncated protein. The truncation constructs were transfected in 293-T cells using lipofectamine 2000, lysed at 48 HPT and run on a 13% gel. It was then transferred to nitrocellulose membrane and was blotted using anti-FLAG Ab.   C) Rescue assay using MHC LP-NS4B deletion constructs. At 12 HPE of BHK cells with the chimeric virus, pcDNA3.1 expressing different NS4B truncations with leader peptide from murine MHC (MHC LP) was transfected using Lipofectamine 2000. At 48 HPT, the supernatants were collected and subjected to viral titer determination using plaque assay. Student's t-test was used to determine the significance ($p<0.05$).

3.4.6 Mutations of the conserved residues within ER loop points to Threonine (T198) as a potential modulator of the rescue function

Now that we have established the role of ER loop in rescue the defect in infectious particle production, we wanted to narrow down residue/s within the ER loop that are responsible for the observed functions. A sequence alignment of the ER loop residues of different DENV serotypes were carried out (Fig 3.8 A). To this end, we mutated most of the conserved residues (excluding alanine, glycine and prolines) totaling to 14 mutants of the ER loop. We analyzed the RNA synthesis pattern of these mutants using the *Renilla* luciferase assay (Fig 3.8 B), followed by viral titer determination using plaque assay (Fig 3.8 C). These mutants could be divided into four groups.

1) Mutants with none to some defect in replication and particle release. C191A, T195A, T203A, W205A, E206A, T215A, and T216A were comparable to wild type or within a log of wild type in replication as measured by the luciferase assay. There were no significant differences in the infectious particles formed by these mutants. T195A and T215A, although were affected higher in replication compared to others in this group, they did not show any significant differences in the viral titer, suggesting these mutants have higher infectivity. 2) Second group includes mutations that are lethal for replication and particle production. F212A, W213A and N214A all showed luciferase activity lower/equal to the background control. These mutants did not produce any infectious particles. 3) Mutants severely affected in replication and particle production. E192A, L196A and L204A showed luciferase activity slightly higher than the background level. These mutants did not produce any infectious particles at 48 HPE. These mutants were subjected to intracellular particle production assay, the intracellular viral titer corroborated their lower replication efficiency. 4) Mutant slightly affected in replication but severely reduced in infectious particle production. The T198A mutant was reduced by ~1.5 log in RNA synthesis activity as measured by luciferase assay, however, did not produce any infectious particles at 48 HPE. To this end, the mutant was subjected to intracellular infectious particle production assay showing a ~3 log reduction compared to the wild type virus (Fig 3.7 D).

A

```
DENV1   CESITLATGPLTTLWEGSPGKFWNTT
DENV2   CEALTLATGPISTLWEGNPGRFWNTT
DENV3   CEALTLATGPITTLWEGSPGKFWNTT
DENV4   CEVLTLATGPILTLWEGNPGRFWNTT
        ** .*******. ***** **.*****
```
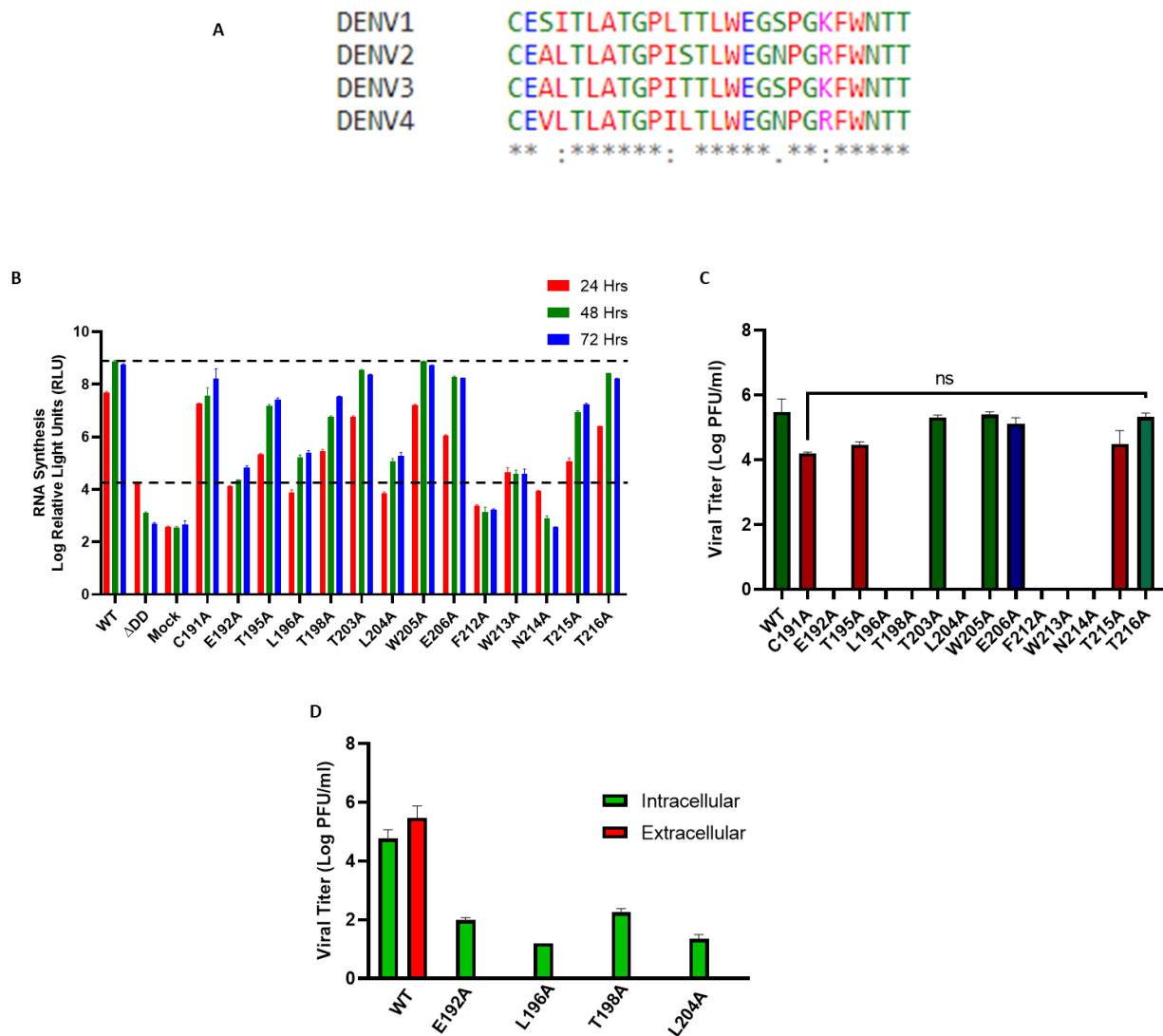
Fig. 3.8 Mutational analysis of conserved residues of ER loop. A) Sequence alignment of ER loop residues among different DENV serotypes. B) RNA synthesis of mutant viruses measured by luciferase assay. Sample lysates collected at 24, 48 and 72 HPE were compared for their luciferase activity against the ΔDD background. C) Viral titer measured by plaque assay. At 48 HPE of BHK cells with the respective mutants, supernatants were collected and subjected to plaque assay. D) Intracellular vs extracellular plaque assays. Cells at 48 HPE were washed thrice with PBS and subjected to three freeze-thaw cycles. The clarified supernatants were subjected to plaque assay and compared to the supernatants from the same sample. Student's t-test was performed to determine the significance at $p<0.05$.

From this data, threonine (T198) within the ER loop of NS4B seems as a plausible candidate in orhestrating the rescuing of infectious particle production. The properties of T198A mutant to replicate to comparable level of wild type and not produce any infectious particles at 48 HPE was similar to Den 2K (2→3) chimeric viruses, the only difference being the lack of intracellular particle production at 48 HPE in the chimeric virus. As the ER loop lies proximal to other viral proteins in the ER lumen, we speculate that the T198 residue interacts with other viral proteins, most probably NS1 to bring the packaging machinery together. A more in-depth analysis of this mutant is warranted.

3.4.7 A reversion at I21 position of chimeric virus rescues particle production with some fitness cost

The chimeric Den 2K (2→3) virus was passaged for seven passages every 4-5 days in order to select for a reversion that would rescue infectious particle production, supporting the results described in this chapter. Supernatants from each passage were subjected to plaque assay. The supernatant from the 7th passage yielded higher titer even though the plaque size remained the same. The corresponding supernatant was used to generate cDNA using RT-PCR, which was then sequenced to look for reversions. As shown in Fig 3.8 A, in both our replicates the isoleucine (I21) within the 2K region of the chimeric virus had reverted to leucine (L), called I21L here onwards. The chromatogram (Fig 3.8 B) shows the respective nucleotide change.

 The leucine residue was thus cloned back into the chimeric background in order to generate a I21L chimeric revertant virus. The I21L virus was thus subjected to measurement of RNA synthesis using *Renilla* luciferase assay and viral titer measurement using plaque assay. The RNA synthesis level in the I21L revertant virus as indirectly measured by luciferase assay was comparable to wild type level (Fig 3.9 A) with no significant differences between the viral titer of wild type and I21L revertant (Fig 3.9 B). The interesting characteristic about the revertant was the tiny size of the plaques (~1 mm) (Fig 3.9 B right panel). Surprisingly, the 2K-NS4B cleavage pattern in the revertant remained the same as chimeric virus (Fig 3.10 B).

Because of the characteristic property of the revertant in the chimeric background, we asked what happens if the threonine (T21) residue is mutated to leucine (L) in the wild type virus background. To this end, we introduced T21L mutation in the 2K of wild type virus and

characterized the mutant. Interestingly, the mutant was phenotypically similar to the revertant virus with a tiny plaque morphology (Fig 3.10 A) with a significantly reduced infectivity (~1.5 log) compared to the wild type virus. A higher molecular weight protein corresponding to 2K-NS4B was observed in the mutant suggesting the absence of cleavage in the mutant (Fig 3.10 B).

In the following set of experiments, we analyzed the particle to PFU ratio of the chimeric Den 2K (2→3), I21L revertant and T21L mutant and compared them with the wild type virus at 48 HPE. Compared to the wild type, the specific infectivity of the I21L revertant chimeric virus was reduced by ~5-fold and ~ 2-fold reduced in the T21L mutant (Fig 3.10 C). These results also consolidate the notion of 2K-NS4B cleavage requirement as a part of productive particle assembly.

A

Virus	Expt.	Revertant	Amino acid at 2K-NS4B junction
Den 2K(2→3)			PEKQR TPQDNQLAYVVIGILTLAAIIAA NEMGF
Den 2K(2→3) I21L	2	I$_{21}$⟶L (ATA→TTA)	....L.. .....

B
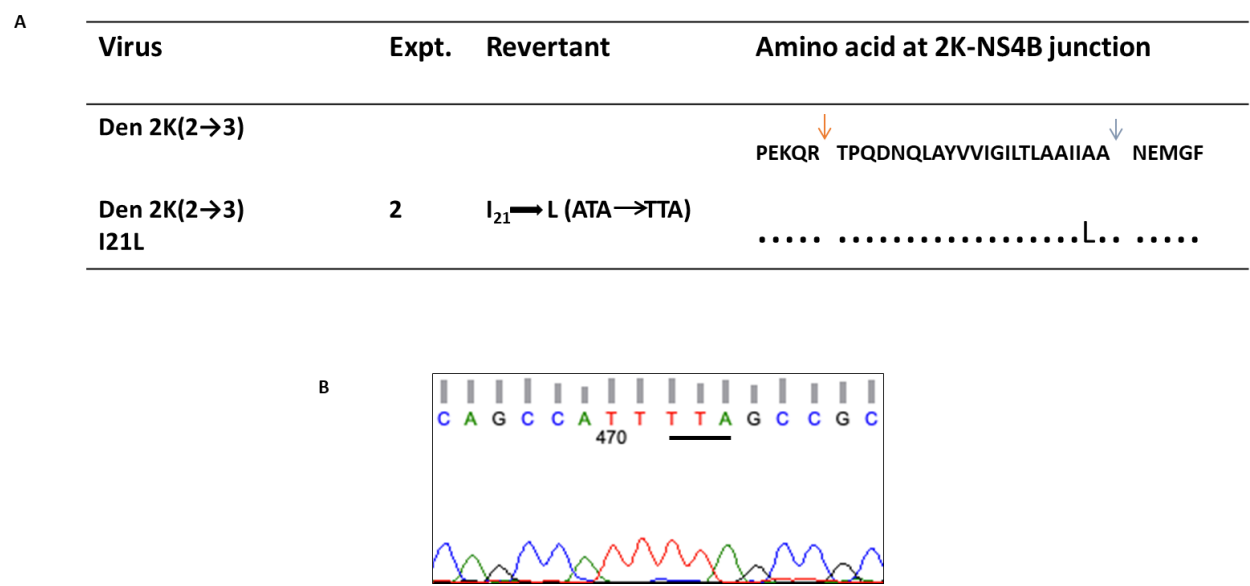
Fig. 3.9 Reversion in the Den 2K (2→3) chimeric virus. A) I21L reversion in the 2K peptide of the chimeric virus. Chimeric viruses were passaged seven times before an increase in titer was observed. The RT PCR followed by sequencing of the cDNA confirmed the amino acid change. Experiments were performed in duplicate. The orange and blue arrow show the respective viral protease and host signalase cleavage site. B) Chromatogram showing the nucleotide change corresponding to I21L reversion.
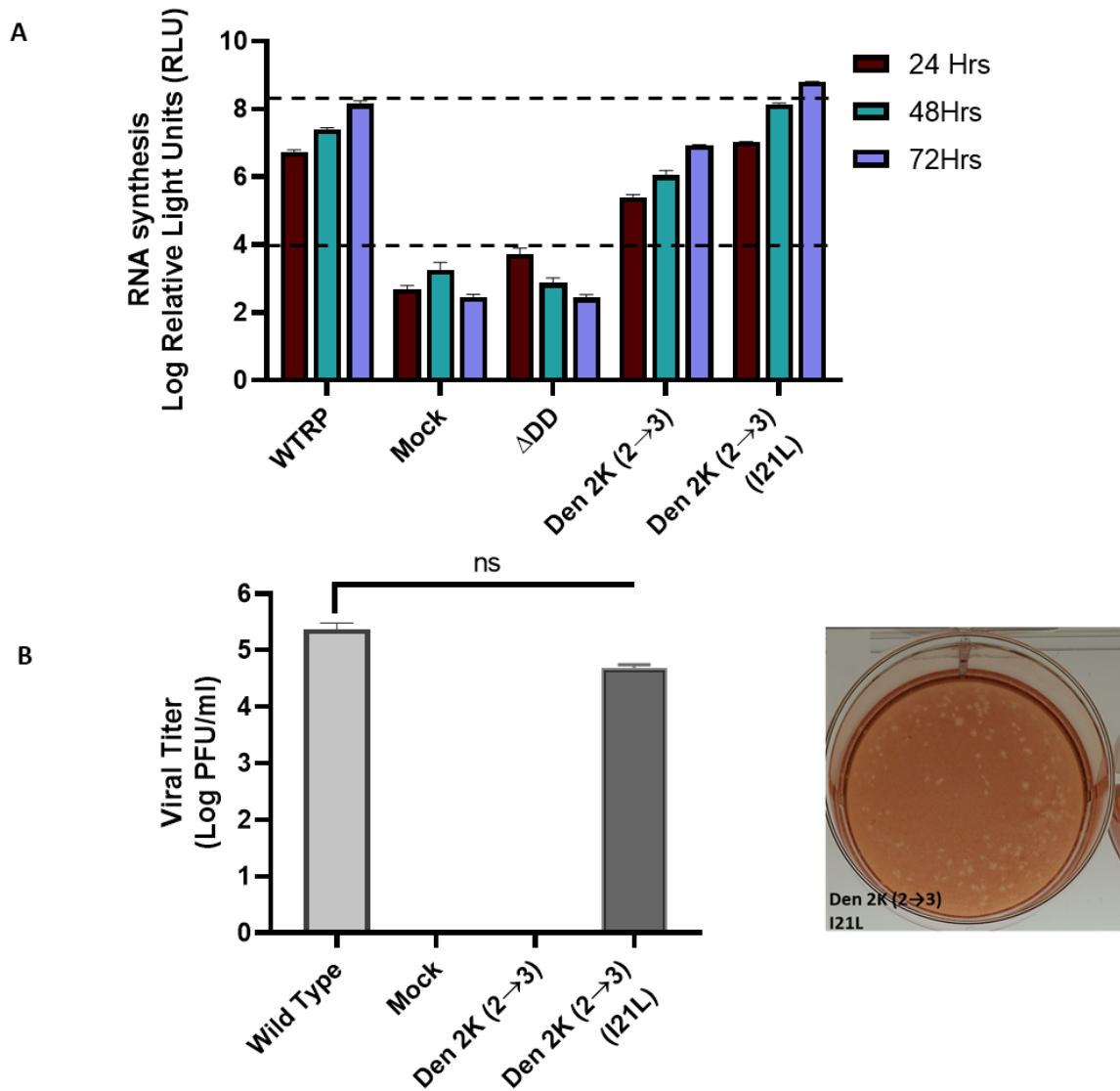
Fig. 3.10 Characterization of I21L chimeric revertant. A) *Renilla* luciferase assay depicting the amount of RNA synthesis in the wild type replicon, chimeric replicon and I21L chimeric replicon. ΔDD was used as a translational control of the luciferase activity. B) Viral titer calculated by plaque assay. The supernatant collected at 48 HPE were used to infect fresh BHK cells and subjected to plaque assay as described in previous sections. Data were collected from experiments performed in triplicates. Bottom right panel shows the tiny plaque morphology of the revertant chimeric virus. Student's t-test was performed to determine the significance at $p<0.05$.
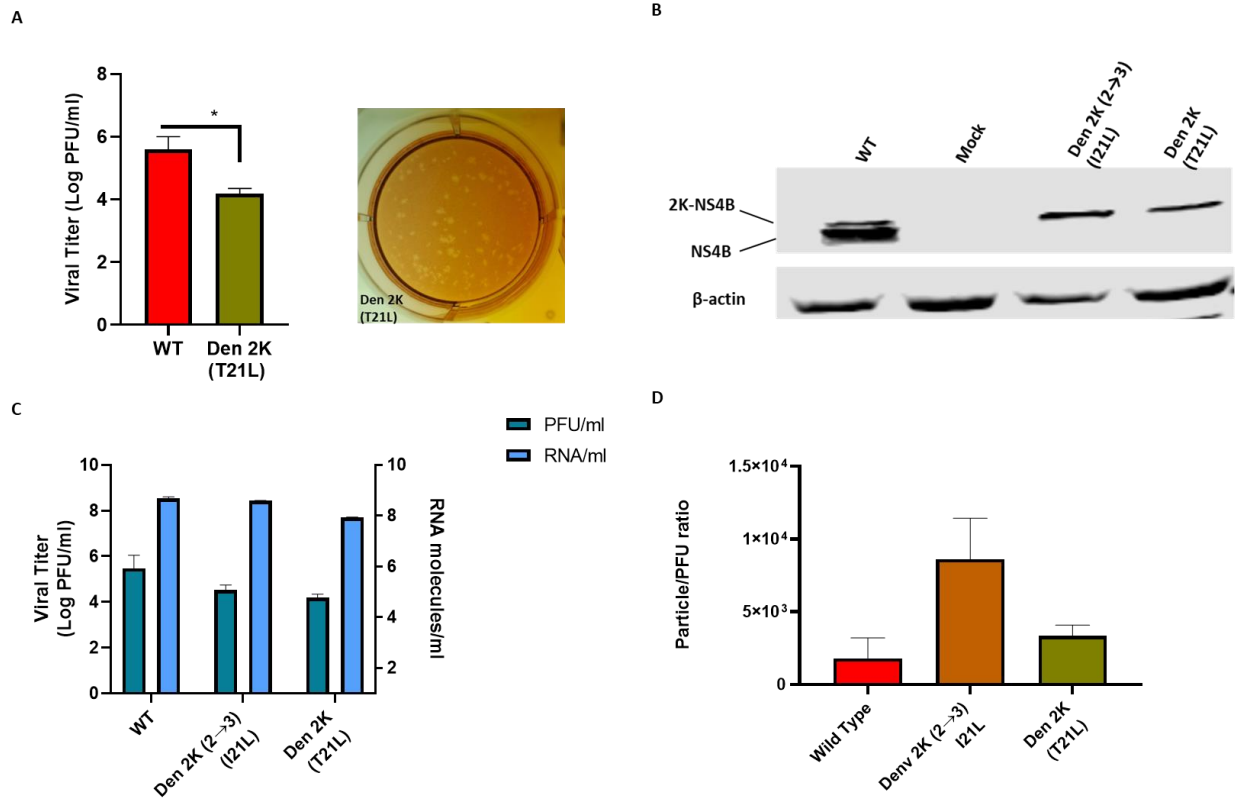
Fig. 3.11 Characterization of T21L mutant and I21L chimeric revertant. A) Viral titer of T21L mutant as determined by plaque assay. The right panel shows the plaque morphology of the mutant. B) Western blot analysis of sample lysates collected at 48 HPE from the BHK cells transfected with the respective mutants. The samples were run on a 13% SDS-PAGE gel and transferred to nitrocellulose membrane and probed with anti-NS4B Ab C) A comparison of viral titer (left Y-axis) vs RNA molecules (right Y-axis) among the wild type, Den 2K (2→3) chimera, I21L revertant and T21L mutant. Supernatants from the BHK cells transfected with respective construct were collected at 48 HPE. The supernatant was used to calculate the viral titer by plaque assay. The same supernatant was used to quantitate the number of RNA molecules using qRT PCR. D) Comparison of particle to PFU ratio of the I21L revertant and T21L mutant to wild type virus. The data obtained from (C) was used to determine the particle/PFU ratio. Student's t-test was performed to determine the significance at $p < 0.05$.

3.5 Discussion

3.5.1 The uncleaved 2K-NS4B results in delayed packaging

The cleavage at NS4A-2K-NS4B junction mediated by the viral NS2B/3 protease and host cell signalase is a coordinated event. Host cell signalase cannot act on the 2K-NS4B junction, which is normally in cryptic conformation, unless NS4A is removed from the N-terminus of 2K by the viral NS2B/3 protease. In this study, we generated chimeric viruses which were deficient in cleavage at 2K-NS4B junction resulting in the accumulation of uncleaved 2K-NS4B protein. The ensuing chimeric viruses where the 2K-NS4B cleavage was disrupted were defective in replication with a more pronounced effect in infectious particle production. The system thus generated gave us a tool to study functions of NS4B in other stages of viral life cycle than replication.

The chimeric viruses were unable to form any intracellular as well as extracellular infectious particles at 48 HPE. The absence of extracellular particle corroborated with the Western blot data probing for the C and E proteins over the period of 72 hours (Fig 3.2). The presence of active replication complexes as evident by intracellular RNA synthesis data (Fig 3.1 B) and the production of comparable levels of C and E proteins in the chimeric viruses but lack of any intracellular particles clearly hinted at either a defect in packaging or any other steps of particle assembly in these chimeric constructs. But it must be kept in mind that these chimeric constructs do release infectious particles later in the life cycle (3/4 DPE) (Fig 2.4D) thus suggesting there is a delayed packaging but not a complete abrogation. The failure to cleave 2K-NS4B might have affected the early stage of packaging. NS4B is known for its multivariate function. NS4B interacts with NS1 within the ER lumen and helps connect NS1 to the cytosolic replication complex (142). NS4B is known to enhance the helicase activity of NS3 by dissociating it from single stranded RNA (79). Also, in HCV, the helicase domain of NS3 has been implicated in intracellular particle assembly (143). Moreover, the cleavage at NS4A-2K-NS4B junction holds an importance in the way the viral replication factories-membrane rearrangements are formed. In KUNV, NS4A-2K is required for the formation of membrane rearrangements unlike DENV, where a complete cleavage of 2K from NS4A is required to form the replication organelles (54, 72). It is interesting to suggest that the uncleaved version of 2K-NS4B plays a role in replication and a mature NS4B (-2K) acts as a checkpoint to initiate packaging by bringing together necessary viral proteins.

Indeed, in a viral infected system there is always an abundance of NS4B over 2K-NS4B, but both are present from early on in infection. We ran a western blot analysis of a BHK cell infected with DENV-2 and analyzed the lysate over a period of 72 hours at 6-hour intervals. It is clear from the results (Fig 3.4) that the processing at 2K-NS4B junction is not 100% suggesting the functional role of these uncleaved products. Recently, it has been shown that the uncleaved protein precursor NS4A-2K-NS4B interacts with NS1 thus helping in the RNA replication in a more direct way. Interestingly, this sort of interaction was not seen with mature NS4A or NS4B protein. Also, these interactions did not have any role in membrane rearrangements (36). This clearly suggests the role of mature vs uncleaved polyprotein in the DENV life cycle. Taken together these evidences plus the ability of NS1 to interact with mature NS4B (142), it could be suggested that there is a temporal and spatial protein-protein interaction between these proteins occurring at different stages of viral life cycle.

The cleavage at the 2K-NS4B junction is not complete, however, we showed it had better cleavage efficiency when used as a heterologous signal peptide for assessing the secretion of NS1 compared to 2K from either DENV-3 or DENV-4. This information could thus be inferred to suggest that the 2K-NS4B junctions of DENV-3 and DENV-4 serotypes are cleaved less efficiently. We generated a heterologous NS1 expression system wherein the NS1 was translocated to ER lumen using either its original signal peptide or using either 2K from DENV-2, 3 or 4. The amount of NS1 thus secreted from the system were measured and used to infer the cleavage occurring at 2K-NS4B junction. It came as no surprise why in both the chimeric viruses, accumulation of uncleaved 2K-NS4B occurred. These suggested that 2K from different serotypes of DENV have different substrate affinity or they are context dependent. In a context of NS4A and NS4B from DENV-2, a 2K from DENV-3 might not be recognized as efficiently as in its natural context. Moreover, the use of 2K to translocate the NS1 to ER lumen and thus getting it secreted consolidates its function as signal peptide.

3.5.2   NS4B without 2K (-2K) has an additional role during early stage of packaging

The defect in particle assembly can be rescued by transcomplementing NS4B(-2K). Since NS4B is an ER membrane protein, it needs to be preceded by a signal peptide for it to be translocated and folded properly in the ER. As we are teasing the role of 2K-NS4B and NS4B

separately, 2K-NS4B could not be used in this context. To avoid these scenarios, we used a leader peptide from murine MHC I molecule to construct MHC LP-NS4B (71). The results from plaque assay data at 48 HPT, which is equivalent to 60 HPE, clearly showed that the block in packaging early in the life cycle can be rescued with a NS4B (-2K). It has been reported that defects in NS4B functioning cannot be transcomplemented in the absence of active replication complex (141). The chimeric virus has a functional replication complex mediated by 2K-NS4B, and when a functional NS4B is supplied in trans, acceleration of particle packaging happens.

To further narrow down the region within NS4B responsible for the described role, a series of NS4B truncations were tested for their ability to rescue the particle production. The region corresponding to the ER luminal loop (AA 191-216) was enough to bring about the same change as NS4B (-2K) suggesting the critical role of this loop during an early stage of the viral lifecycle. We speculate the floppy ER loop interacts with other viral proteins or ER membrane resident proteins to bring about the changes necessary to initiate packaging. Flaviviral nonstructural proteins play varied roles in viral assembly. An assembly defect mutant of the NS2Aα cleavage site of DENV has been rescued by second site reversion in the NS3 helicase domain suggesting the role of an integral ER membrane protein in viral assembly (144). More recently, NS2A has been described as a hub of viral assembly which coordinates the complex event of genome shuttling, assembling structural proteins and protease at the site of assembly (28). NS4B may act in the same vein, as the topological structure of NS4B is similar to NS2A. As seen in the western blot for the capsid protein 60 HPT (data not shown), the level of capsid protein was comparable to wild type. It is interesting to suggest that NS4B (-2K) can facilitate the capsid-RNA binding thus initiating the packaging of the viral particle. With the ability to sample both the ER lumen and cytosol with the ER loop and cytosolic loop, NS4B can interact with plethora of host and viral proteins. NS4B with its cytosolic loop interacts with NS3 helicase domain and aids in viral replication (80). No such functions have been assigned to ER loop of NS4B. This is the first time where the role of NS4B and its ER loop in particle production have been addressed.

We further analyzed the residues within the ER loop of NS4B, hypothesizing one or more of these residues when mutated should show similar characteristics with the chimeric viruses i.e. should be comparable to wild type in terms of RNA synthesis and defective in infectious particle production. After sequence alignment, we proceeded with 14 alanine scanning mutations of the

candidate residues. Some of these mutations were lethal, while some did not affect viral replication and infectious particle production. However, a T198A mutant, was surprisingly close to the chimeric viruses phenotypically. The T198A mutant was severely affected in extracellular as well as intracellular particle production even though RNA synthesis was within a ~1.5 log of the wild type. This suggested that the T198 residue within the ER loop has a major role in orchestrating the early stage of packaging. A single amino acid residue Q134 within the cytosolic loop of NS4B modulates its interaction with NS3 and enhance the RNA replication (145). Similarly, a separate study identified Q134, G140 and N144 of cytosolic loop as residues that are important for viral replication and interaction with NS3 (80).

3.5.3 The 2K-NS4B cleavage can be bypassed for infectious particle release but there is a huge fitness cost

We passaged the Den 2K (2→3) chimeric virus for several passages to select for a revertant in order to figure out an interacting partner or a mutant that will restore the 2K-NS4B cleavage. Rather interestingly, we recovered a revertant within the 2K peptide that rescued infectious particle production that was not significantly different from the wild type level. The revertant thus recovered displayed some characteristic properties with regard to the location of reversion and the effect it had on 2K-NS4B cleavage. The isoleucine (I) to leucine (L), I21L revertant, did not lead to cleavage of the 2K-NS4B junction, even though the reversion was in the P3 position of signalase cleavage site. Amino acids at P1 and P3 position guide the enzymatic activity of the signalase. This surprising finding can be discussed under several topics.

Amino acid residues at the P1 and P3 position not only function as a signalase substrate, but also play a direct role in replication. As seen in the chimeric revertant virus, upon I21L substitution, RNA synthesis as measured by the luciferase assay was like wild type virus level. The increased replication resulted in increased infectious particle production that was not significantly different from wild type. This result was quite surprising as the rescue in infectious particle release happened in the absence of 2K-NS4B cleavage (discussed below). This suggests that the viruses can adapt to lack of 2K-NS4B cleavage by adjusting the amino acid composition within the 2K. This further supports the idea that 2K is an important entity of the viral genome rather than just a signal sequence.

In the chimeric revertant virus, even in the absence of 2K-NS4B cleavage, there was an increase in RNA synthesis and infectious particle production. However, the resultant viruses displayed a tiny plaque morphology (~1mm) as well as decreased specific infectivity. The DEN 2K (2→3) I21L revertant virus had aa five-fold lower specific infectivity compared to that of the wild type virus. Similarly, the T21L mutant (in a wild type background) which was also deficient in 2K-NS4B cleavage, was significantly affected in infectious particle production, showed a tiny plaque morphology and a two-fold decrease in specific infectivity. Taking together these data, it would be interesting to reason that amino acid composition at the P3 position, in the absence of 2K-NS4B cleavage, plays an important role in infectious particle production. As the revertant amino acid i.e. Leucine (L) is not present in any of the flaviviruses 2K at that position (Fig 2.1 A), it would be very interesting to characterize this virus further.

This further supports the idea of requirement of 2K-NS4B cleavage in mediating a proper packaging of the RNA genome. We speculate that in the absence of NS4B (-2K), which acts as a scaffolding for the RNA genome to be picked up by capsid protein doesn't happen efficiently. In the revertant virus, the RNA genome is synthesized in similar number to wild type but due to the absence of a scaffolding to help it get packaged. The same mutation when introduced on a wild type virus, resulted in an inhibition of 2K-NS4B cleavage and reduced infectious particle production by ~1.5 logs and with smaller plaque morphology similar to the revertant virus (Fig 3.10 A). These results combined with the decrease in specific infectivity of the revertant I21L and mutant T21L resulting in loss of 2K-NS4B cleavage suggest the need for cleavage at this junction. The proposed role of NS4B in the viral life cycle has been detailed in Fig 3.12.

Fig. 3.12 Proposed role of 2K-NS4B cleavage in viral life cycle. A) The NS4A-2K-NS4B junction is cleaved by viral NS2B/3 protease and host cell signalase in a sequential manner, however, the cleavage at 2K-NS4B is not complete resulting in two populations of NS4B; 2K-NS4B and NS4B. In a normal viral infection, this will result in normal replication and packaging of the genome B) However, if the population of NS4B is skewed to 2K-NS4B, this will not have a significant effect in replication but results in packaging delay, and none to very less particle being produced. Our data suggest that in the absence of NS4B (-2K), packaging is severely affected and can be rescued by supplying NS4B in trans. Further, the ER loop of NS4B was required to rescue the packaging defect seen in the 2K-NS4B producing virus. We speculate the ER loop of NS4B interacts with some NS1 or other proteins and help bring the capsid and RNA together to initiate the packaging. C) The outcomes of the viral lifecycle where 2K-NS4B is exclusively present also depends on the amino acids at the signalase cleavage site. In the presence of permissive amino acids, though, uncleavable by host signalase, RNA synthesis increases, however, we predict in the absence of ER loop interacting with the putative partner results in deficient packaging.

A

B

C

Signalase   2K   RNA   Thr198   Capsid

114
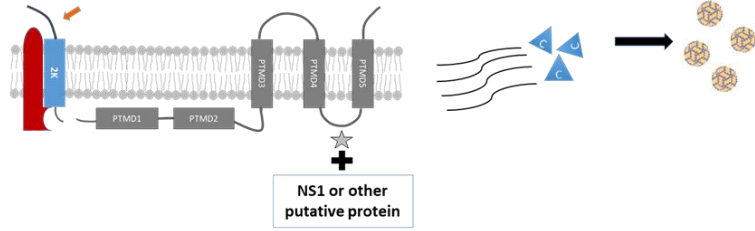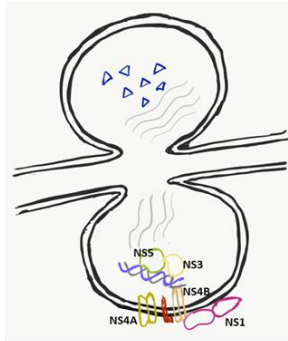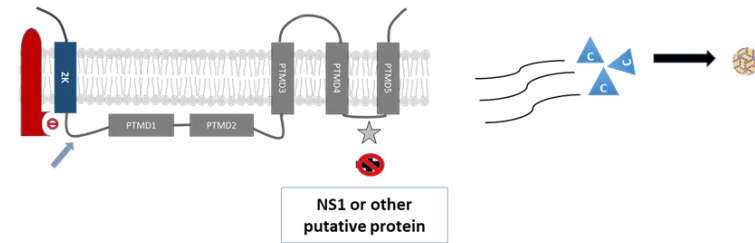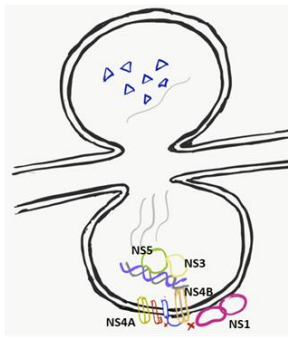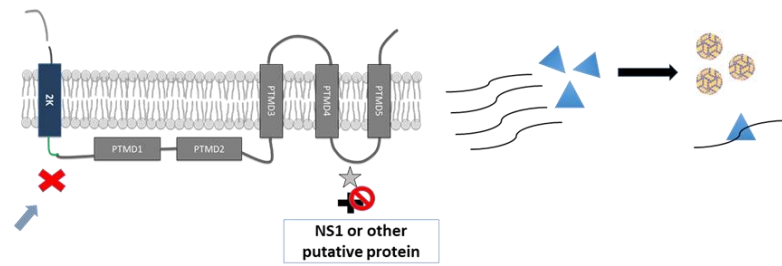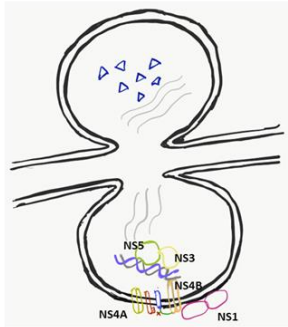
CHAPTER 4. TRANSMEMBRANE DOMAINS OF NS4A AND NS4B PLAY A MAJOR ROLE IN VIRAL REPLICATION

4.1 Chapter summary

NS4A and NS4B of DENV are multi-pass integral membrane proteins. They help anchor the replication complex to the ER membrane by virtue of their transmembrane domains (TMDs). In this chapter, we attempted to probe for the role of TMDs of NS4A and NS4B using interserotypic chimera as a tool. Using the chimeric viruses, we tried to separate the role of TMDs in anchoring the viral proteins in the ER membrane vs. their role in viral replication and infectious particle production. We found that the TMD1 and TMD3 of DENV-2 NS4A could be replaced with partial success across the DENV serotypes, whereas TMD2 is highly specific to DENV-2. Moreover, the substitution of these TMDs had a pronounced effect in viral replication and infectious particle release, suggesting the residues within TMDs function additionally in viral replication other than anchoring the protein to the ER membrane. Similarly, analysis of interserotypic NS4B viruses suggested different TMDs of NS4B function in different ways. The TMD1 was functionally conserved among DENV-2 and -3 whereas other TMDs showed varied effect upon interserotypic substitutions. The NS4B TMD4(2→3) chimera was severely affected in replication and infectious virion production, whereas NS4B TMD3(2→3) and NS4B TMD5(2→3) chimeras were partially affected by the substitution. Revertant analysis of the NS4B TMD5(2→3) chimera pointed to how reorientation of TMD5 post NS2B/3 cleavage may vary in different serotypes. The M240T revertant in the NS4B TMD5(2→3) chimera perturbed its hydrophobic face possibly allowing the reorientation of TMD5. Moreover, by generating interserotypic cytosolic and ER luminal loop chimera, we studied their functional conservation among DENV serotypes. The results pointed toward a tolerance of the ER loop as a functional domain across all serotypes of DENV, whereas, the cytosolic loop was more serotype dependent.

4.2 Introduction

The association of flaviviral nonstructural proteins with the ER membrane and interactions with several host factors results in the formation of replication factories that harbor the viral replication complex. The nonstructural integral membrane proteins of flaviviruses are best known

for their role in anchoring the replication complex in the ER membrane by virtue of their TMDs. These hydrophobic/amphipathic TMDs of nonstructural proteins function possibly by interacting with ER resident proteins to bring about the membrane rearrangements permissive for flaviviral replication (146). NS4A and NS4B of DENV are two integral membrane proteins that are central to viral replication, immune evasion and protein-protein interactions. NS4A, in particular, has been implicated in the formation of the membrane rearrangements that are requisites for the flaviviral replication (54). However, several studies have suggested involvement of more than one nonstructural proteins in the formation of the replication factories arising from membrane invaginations (147, 148).

NS4A of DENV is an integral membrane protein predicted to consists of a long N-terminal cytoplasmic tail, and three TMDs. The TMD1 and TMD3 traverse the ER membrane in opposite directions, whereas, the TMD2 remains flush with the inner leaflet of the ER membrane (54). NS4A interacts with vimentin (DENV) with its N-terminal cytoplasmic tail and reticulon 3.1 (WNV) with possibly TMD1 to stabilize the replication complex (59, 60). The TMD1 of NS4A is also involved in the oligomerization of NS4A and interaction with NS4B (56). There is less information available on what roles these TMDs play during the viral life cycle other than anchoring the protein and replication complex. A systematic mutagenesis of the conserved residues of the TMDs of JEV NS2B pointed towards its role in viral assembly through its interaction with NS2A protein (149). Similarly, TMD amino acid residues of influenza virus neuraminidase domain were found to be responsible for lipid raft association and budding. By using systematic mutagenesis and chimeric viruses in the neuraminidase region, influenza viruses with reduced titer and elongated morphology were generated (150). Similar studies regarding the role of TMDs of NS4A is warranted.

NS4B is a multifunctional protein with its role extending from viral replication to immune evasion. The diverse functions of the protein can be attributed to its unique topological nature. Different studies have established topology of NS4B as having five potential TMDs with three of them traversing the ER membrane, while the remaining two lies in the ER lumen (75, 76). The TMD3 and TMD4 that traverse the ER in opposite direction form a 35 amino acid long cytosolic loop that has been implicated in the dimerization of NS4B (76). Similarly, an ER luminal loop of 26 amino acid residues is formed between TMD4 and TMD5. In 5-10 % of the cases, when the

NS2B/3 protease acts on the NS4B-NS5 junction in the cytosolic side, the TMD5 flips to the ER lumen (Fig 4.9 A). The unique topology of the NS4B provides it with the chance to interact with different cellular environments and act as one of the crucial proteins in viral life cycle. The TMDs of NS4B have varieties of role to play in viral life cycle. The N-terminal luminal TMDs bind to EMC and help anchor the replication complex in the ER membrane (26). Similarly, these luminal TMDs are involved in the IFN α/β antagonism (71). NS4B has also been identified as hotspot of mutation to develop resistance from antivirals. Some of these mutations were concentrated in the TMD3 (151). The cytoplasmic loop and the C-terminal domain of NS4B including the TMD5, to lesser extent, have been implicated in the dimerization of NS4B. Despite studies probing and providing information about different regions of NS4B, roles of TMDs have not been studied directly. The basic questions like the role of TMDs in viral replication and particle production other than anchoring the protein to the ER membrane remains unanswered. Similarly, if these TMDs are there to anchor the replication complex, are they functionally conserved across the DENV serotypes? These questions need to be answered to better understand the biology of DENV and specific role NS4B plays.

One way to answer these questions would be to generate interserotypic chimera wherein different regions of the protein are exchanged for corresponding regions of same protein from a different serotype. This will shed light if these regions are functionally conserved and if there are any interserotypic interactions that are important for viral replication and particle release. In this chapter, we exlored the role of different regions of NS4A and NS4B using a similar strategy. Several interserotypic TMD (NS4A and NS4B) chimeric viruses were generated and they were probed for their ability to replicate and produce infectious virions.

4.3   Materials and methods

4.3.1   Cell culture and viruses

Baby Hamster Kidney BHK-15 cells obtained from the American Type Culture Collection (ATCC) and were maintained as previously described in section 2.3.1. Chimeric viruses and mutants were generated in the DENV-2 (16681), PD2ICMO backbone.

4.3.2 Site directed mutagenesis

Sets of direct complementarity primers with two nucleotides substitution corresponding to the target residues in the parental plasmid were synthesized using Primer X SDM software. Infectious cDNA clone of DENV and replicon were used for these experiments unless otherwise stated. Site directed mutagenesis was thus carried out using a modified PCR protocol using High Fidelity (HF) Phusion (NEB) enzyme. The products were transformed in DH5α competent cells, screened for mutants and confirmed by low throughput sequencing at the Purdue Genomics facility. For generation of reciprocal mutants, i.e., individual chimeric mutants, PD2ICMO-(2→3) chimeric virus or replicon were used.

4.3.3 In vitro transcription and transfection

All the chimeric viruses and replicon constructs were linearized using XbaI and in vitro transcribed with T7 polymerase as described in section 2.3.4.

4.3.4 Luciferase assay and Plaque assay

BHK-15 cells electroporated with different chimeric and mutant replicon constructs were plated in 24-well plates. At various time points post transfection, the cells were washed once with PBS and lysed using 100µl cell lysis buffer (Promega). The lysed cells were stored at -80^0C. Once samples for all time points had been collected, luciferase signals were measured using a Spectramax L Luminometer and Softmax Pro Software (LMAXII 384, Molecular Devices) according to manufacturer's protocol. Briefly, 20 µl of cell lysates in triplicates were added to an opaque 96-well plates, the injector of the Spectramax L was primed with Luciferase assay reagent and 100 µl was added to each well with 2-second measurement delay and 5-second measurement read for luciferase activity. As a negative control, a replication deficient RNA (ΔDD) construct, with a mutated GDD motif within RDRP was used to assess background signal. For plaque assays, supernatants from transfected cells were collected at different time points, centrifuged to clarify and processed. BHK-15 cells plated in 6 well plates were infected with 6 ten-fold dilutions of the supernatant and rocked for an hour. It was overlayed with MEM supplemented with 5% FBS and 1X agarose, incubated for 5 days at 37ºC, stained with neutral red and plaques were counted.

4.3.5 SDS-PAGE and Western Blot

Transfected and infected cells were collected at different time points (24, 48 and 72 Hrs) post electroporation/infection depending on the samples. They were lysed using Pierce Co-IP buffer containing protease inhibitor cocktail (Roche) and frozen at -80^0C until all the time points were collected. A 10%, 12% and 13% acrylamide gels were used according to samples being processed. The nitrocellulose membrane was probed with either mouse monoclonal anti-NS4A and -NS4B (44-4-7), mouse anti-NS3 and NS5 (Strauss). Infrared-labeled GαM 680 or GαR 800 secondary antibodies were added, and the proteins were visualized using an Odyssey infrared imager (LI-COR) and the Odyssey version 3 software.

4.3.6 Intracellular vs. extracellular infectious particle assay

At 24, 48 and 72 HPE, supernatants and cells were collected. Supernatants were clarified by centrifugation and frozen at -80ºC until used. Cells were washed with 1X PBS, scraped off, resuspended in 2.5% FBS containing MEM and pelleted down. Cells were then subjected to two more washes with 1XPBS. Cells were then resuspended in 2.5% FBS MEM and subjected to three rounds of freeze-thaw using liquid nitrogen and incubation at 37ºC. Samples were centrifuged to remove the debris, and the supernatants were processed for plaque assay as explained in section 2.3.8.

4.3.7 Intracellular vs extracellular RNA extraction

Transfected cells were washed thrice with 1X PBS at 6 HPE to remove residual RNA from electroporation. At 24, 48, 72 HPE, supernatants were collected and processed for viral RNA extraction using RNeasy mini kit (Qiagen) or Pure Link RNA mini kit (Thermo Fisher) according to the manufacturer's instructions. In parallel, the cells were washed three times with 1X PBS and total RNA was extracted using the same kit. The extracted viral RNAs were frozen in aliquots at -80ºC until used for further experiments. A ΔDD control was used as a negative control for the background level of signal arising from RNA in downstream analyses.

4.3.8 Quantitative Real Time (qRT) and Reverse Transcriptase (RT) PCR

SYBR Green One-step qRT kit (Invitrogen) along with dengue specific primers was used to carry out the qRT-PCR for various samples. A standard curve was generated according to the manufacturer's instructions using purified in vitro RNA samples and was used as a reference point to calculate the RNA molecules. RT PCR was carried out using the One TAQ RT-PCR kit (NEB). Region specific primers were used to amplify the DNA fragments which were later run on a gel, purified using GFX columns (Invitrogen) and sent for sequencing.

4.3.9 Selection of revertants and identification of mutations

BHK-15 cells were electroporated with 10 μg of in vitro transcribed mutant RNA. Culture supernatants were collected 5 DPE and plaqued as described previously. Individual plaques were picked and passaged for 5-6 passages or until plaques were visible with culture supernatant at each passage being collected, clarified and frozen at -80ºC until further analysis. At this point, the corresponding supernatant samples were subjected to RNA extraction and RT PCR analysis as described previously. The targeted DNA fragments thus obtained were purified and analyzed by nucleotide sequencing.

4.3.10 Statistical analysis

GraphPad Prism Software 7 was used to analyze the data. Student's t-tests were used to determine significance wherever applicable.

4.4 Results

4.4.1 Construction and characterization of NS4A interserotypic chimeras

NS4A is an integral membrane protein, a property that contributes to the formation of membrane rearrangements resulting in replication factories. Topologically, NS4A has been described to possess three TMDs, with TMD1 and TMD3 traversing the ER membrane while TMD2 sits parallelly with the inner leaflet of the ER membrane (Fig 4.1 A). The role TMDs of NS4A play during viral life cycle is little known except for the fact that they anchor the viral replication complex in the ER membrane. We hypothesized that if TMDs just play a role in

anchoring the protein in the ER, we should successfully be able to replace it without significant effect on viral replication and particle production. To test this hypothesis, we generated three different chimeras wherein the TMDs of NS4A of DENV-2 were substituted with that of DENV-3 TMDs (Fig 4.1 B-C). The interserotypic chimeras thus obtained were analyzed for replication and infectious particle production.

Interestingly, of the three chimeras thus generated and analyzed, NS4A TMD1(2→3) and TMD3(2→3) chimera were affected severely in replication resulting in significant reduction in infectious particle production, whereas, TMD2(2→3) chimera was lethal for replication and infectious particle production (Fig 4.2 A-B). Both NS4A TMD1(2→3) and TMD3(2→3) were delayed in replication that peaked gradually up to 72 hours, however, was comparable to the 24 hour luciferase activity shown by the wild type replicon suggesting the nine and eight amino acid residue changes made in the NS4A TMD1(2→3) and TMD3(2→3) chimeras, respectively, affected the replication (Fig 4.2 A). In both the cases, the reduced replication translated in significant reduction in infectious particle production determined at 48HPE (Fig 4.2 B). On the other hand, the NS4A TMD2(2→3) chimera was the most affected of all. With a total of twelve amino acid residue changes in the TMD2(2→3) chimera, it was lethal for replication, with the luciferase signal similar to background level (ΔDD construct). No infectious particle release was observed for TMD2(2→3) when measured at 48 HPE (Fig 4.2 B) and beyond (Data not shown).

The western blot analysis of the chimeric constructs depicts the amount of NS4A and NS4B proteins (Fig 4.3 A) as well as NS3 and NS5 proteins (Fig 4.3 B) being produced in the chimeric viruses vs the wild type. Surprisingly, monomeric NS4A bands were hardly visible in the wild type as well as in the chimeric constructs. However, a prominent oligomeric band around ~100 kDa was observed in the TMD1 chimeric virus and the wild type. The absence of the NS4A and NS4B was quite concerning for TMD3 chimeric construct. However, it might be due to several reasons. The replacement of TMD3 might have negatively affected the antibody binding or these membrane proteins were produced in reduced amount as seen in the case of NS3 and NS5 protein (Fig 4.3 B) in TMD3(2→3) chimera or the proteins might have degraded more rapidly in this case.
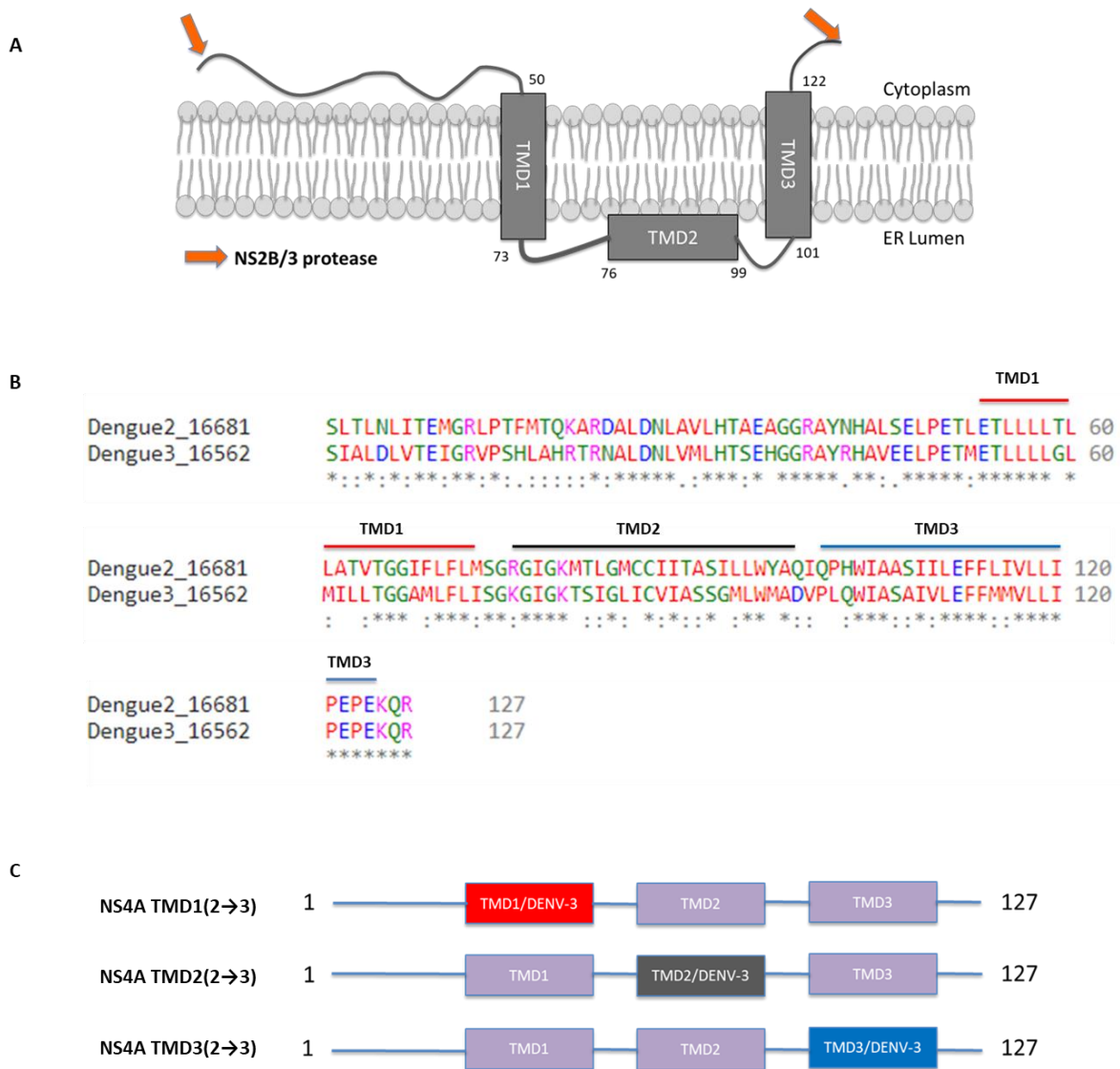
Fig. 4.1 Construction of interserotypic NS4A chimera A) Topology of NS4A. The established topology of NS4A based on Miller *et al* showing the TMDs. B) Sequence alignment of DENV-2 and DENV-3 NS4A with TMD1, TMD2 and TMD3 labeled. C) Schematic of the interserotypic NS4A TMD chimeric constructs.
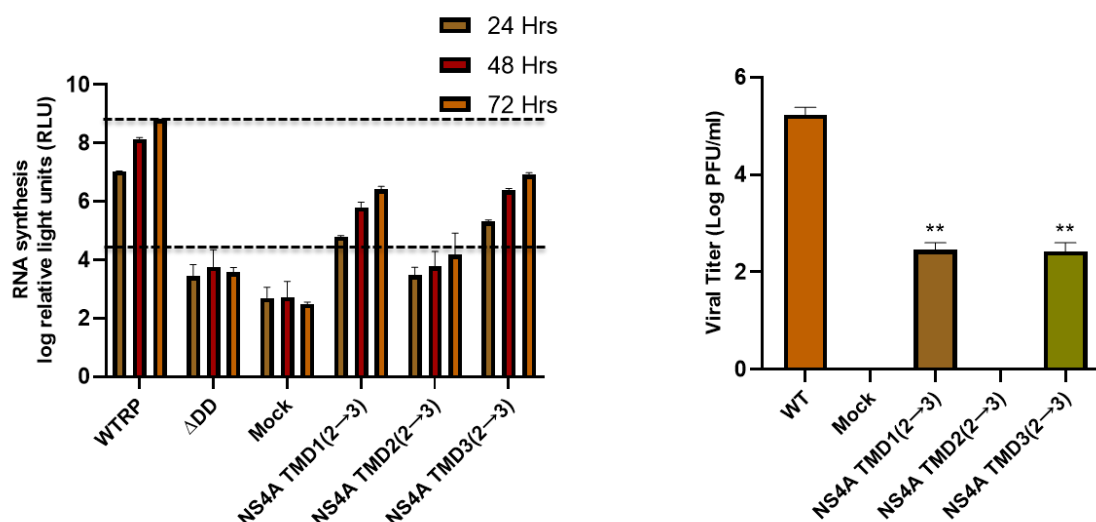
Fig. 4.2 Characterization of interserotypic NS4A TMD chimera. A) *Renilla* luciferase assay for an indirect measurement of RNA synthesis. The chimeric constructs were transfected in BHK cells and cell lysates were collected at 24, 48 and 72 HPE and subjected to *Renilla* luciferase assay. B) Viral titer determination using plaque assay. Supernatants from BHK cells transfected with full-length chimeric constructs were collected at 48 HPE and processed for plaque assay, plaque being counted on 6th day. Student's t-test was carried out to determine the significance ($p<0.05$).

To further analyze the effect of amino acid changes due to the TMD substitutions, sequences of the TMDs of DENV-2 and DENV-3 were submitted to Heliquest server (126). Interestingly, NS4A TMD1(2→3) and TMD3(2→3) chimera had a bigger change in the hydrophobic faces of the respective TMDs compared to TMD2 (2→3) (Fig 4.4). Both chimeras were significantly reduced in infectious particle production (Fig 4.2 B). On the other hand, the TMD2 switch did not result in much change at the hydrophobic face (Fig 4.4), but the lethality of the switch could be attributed to the number and drastic amino acid changes at the ER surface and luminal interface as the TMD2 of NS4A lies flush with the inner leaflet of ER membrane.
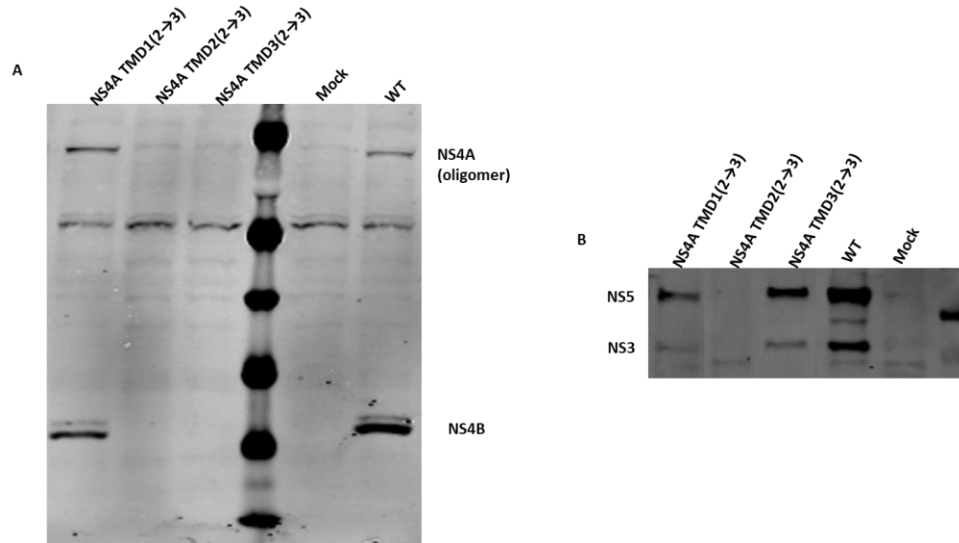
Fig. 4.3 Western blot analysis of interserotypic NS4A TMD chimera. BHK cell lysates transfected with chimeric constructs were collected at 48 HPE and ran on a 4-16% SDS gel. Proteins were transferred to nitrocellulose membrane and blotted with anti-NS4A and NS4B abs (A) and with anti-NS3 and NS5 Abs (B).
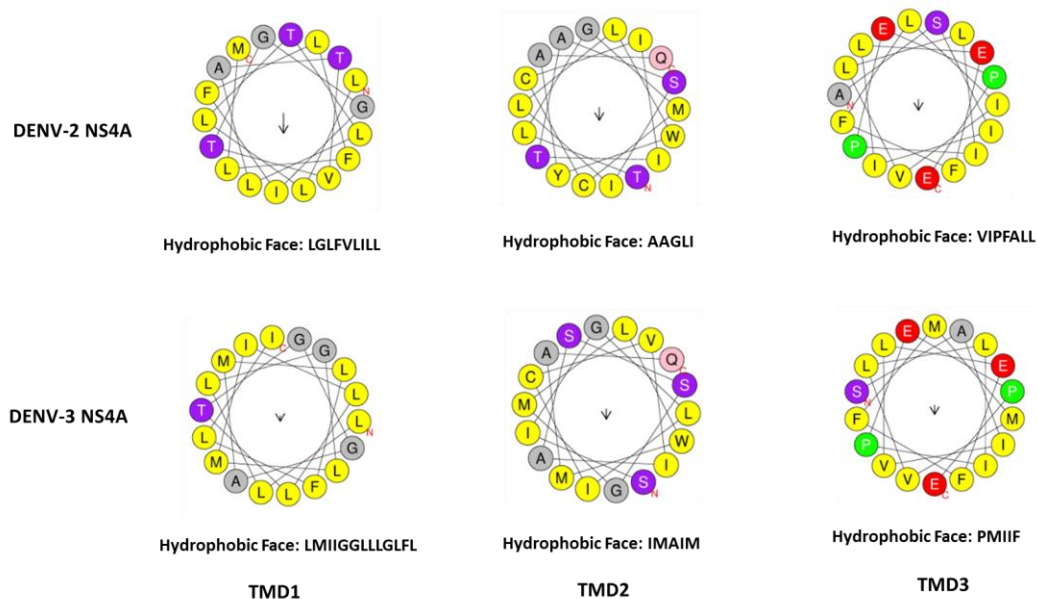
Fig. 4.4 Helical wheel analysis of amino acid residues of TMDs of NS4A of DENV-2 and DENV-3. The top panel shows the hydrophobic faces formed by the TMDs of DENV-2 NS4A. Upon substitution of TMDs from DENV-2 to DENV-3 which accounted for nine, twelve and eight amino acid residues, respectively, the changes in the hydrophobic faces of the TMDs of the chimeric viruses are depicted in the bottom panel.

4.4.2 Analysis of reciprocal mutation in the chimeric background

In the next sets of experiment, we analyzed whether individual amino acids within the TMDs of NS4A are responsible for the phenotypic effect seen in the interserotypic chimeric viruses. To test the hypothesis, we chose chimeric viruses as the starting point and mutated select amino acids to the original ones to assess the effect. Amino acid residues switched from the chimeric background to the original ones are highlighted in the schematic shown in Fig 4.5. A total of three amino acid changes were brought about in TMD1 chimera, five amino acid residues in case of TMD2 and four amino acid changes in case of TMD3.

Fig. 4.5 Schematic of reciprocal mutation in NS4A TMDs. Reciprocal mutations introduced in A) TMD1 B) TMD2 and C) TMD3 chimeric viruses highlighted in blue.

In the first set of reciprocal mutations to probe for the important amino acids in TMD1 of NS4A, we made three changes; G59T, L63T and M69F on the chimeric background. The G59T mutation which introduces a polar uncharged residue instead of a helix breaker glycine, had a very small effect on the overall phenotypic property of the TMD1 chimera. There was ~1 log increase in replication as evident by the luciferase assay, which was translated in particle production,

although insignificant. The other two mutations, L63T and M69F did not have any significant effect on the way TMD1 chimera behaved (Fig 4.7 A-B).

TMD2 of NS4A sits on the inner layer of the ER membrane and possibly plays a role in introducing membrane curvature during the viral replication complex formation. Switching from TMD2 of DENV-2 to DENV-3 introduces a total of 12 amino acid changes in the chimeric virus. The introduction of the DENV-3 TMD2 in NS4A was lethal with no replication and infectious particle production. Furthermore, the reciprocal mutations chosen to probe if individual amino acid replacement can rescue this loss in replication was unsuccessful, as shown in Fig 4.7.
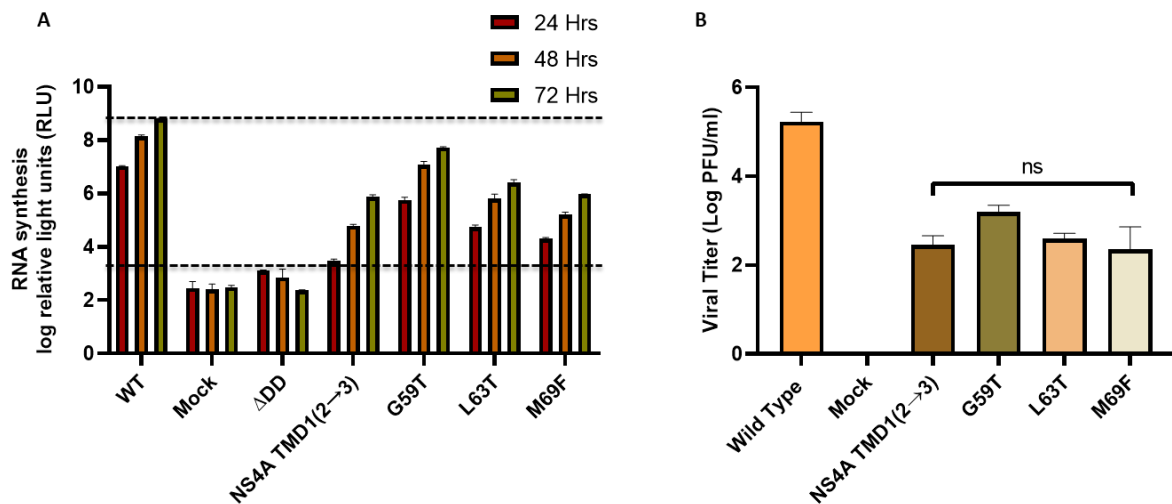
Fig. 4.6 Effect of reciprocal mutation in TMD1 chimera of NS4A. A) *Renilla* luciferase assay for the reciprocal mutant of NS4A TMD1 chimera. *Renilla* luciferase assay depicting the amount of RNA synthesis in the wild type replicon, chimeric replicon and reciprocal mutant replicons. ΔDD was used as a translational control of the luciferase activity. B) viral titer calculated by plaque assay. The supernatants collected at 48 HPE were used to infect fresh BHK cells and plaqued as described in previous sections. Student's t-test was carried out to determine the significance at $P<0.05$.
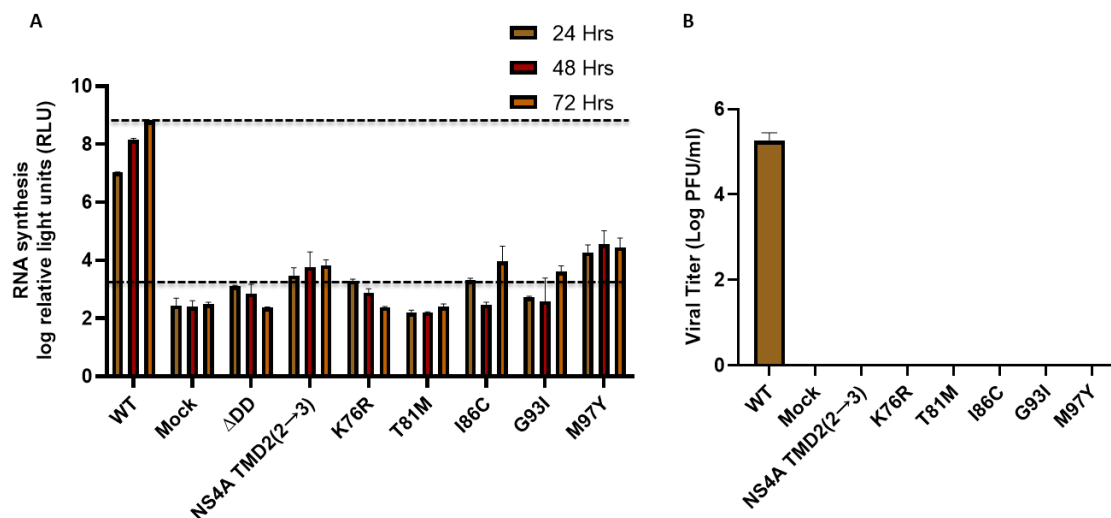
Fig. 4.7 Effect of reciprocal mutation in TMD2 chimera of NS4A. A) *Renilla* luciferase assay for the reciprocal mutant of NS4A TMD1(2→3) chimera. *Renilla* luciferase assay depicting the amount of RNA synthesis in the wild type replicon, chimeric replicon and reciprocal mutant replicons. ΔDD was used as a translational control of the luciferase activity. B) Viral titer calculated by plaque assay. The supernatant collected at 48 HPE were used to infect fresh BHK cells and determine the viral titer. Student's t-test was carried out to determine the significance at P<0.05.

Similar experiments were carried out to determine if the re-introduction of individual amino acid residue could rescue the replication and infectious particle production in the TMD3 chimera. L102P and Q103H did not have any significant effect on the replication as well as particle production. Surprisingly, S107A gained some replication competence and a significant increase in infectious particle production, suggesting the requirement of small amino acid at this position. However, this reciprocal mutant never reached the level of the wild type virus (Fig 4.8).
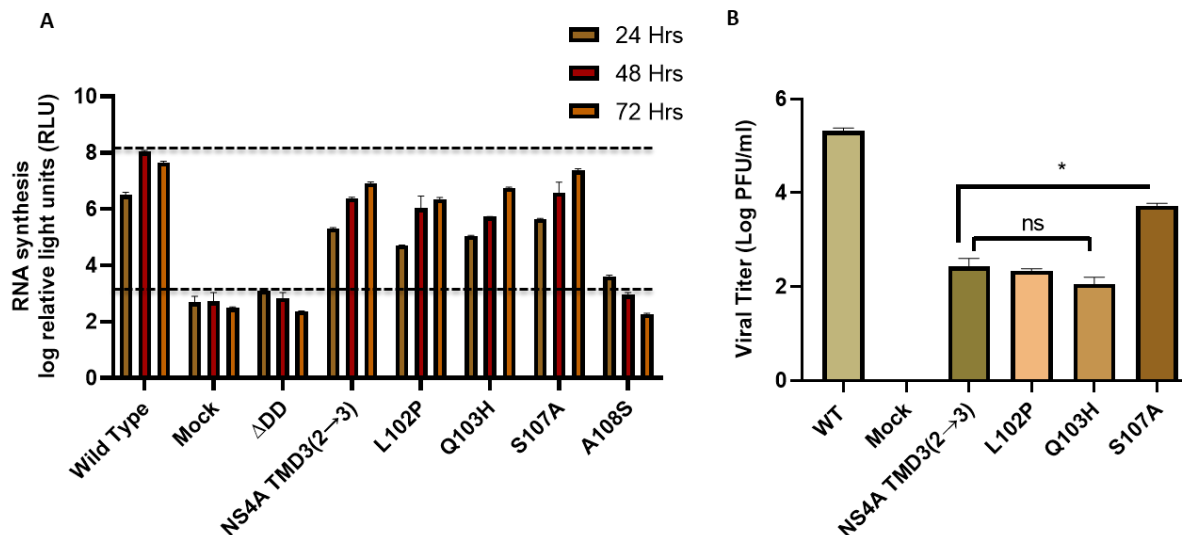
Fig. 4.8 Effect of reciprocal mutations in TMD3 chimera of NS4A. A) *Renilla* luciferase assay for the reciprocal mutants of NS4A TMD1 chimera. *Renilla* luciferase assay depicting the amount of RNA synthesis in the wild type replicon, chimeric replicon and reciprocal mutant replicons. ΔDD was used as a translational control of the luciferase activity. B) Viral titer calculated by plaque assay. The supernatant collected at 48 HPE were used to infect fresh BHK cells and plaqued as described in previous sections.

4.4.3   Construction and characterization of NS4B interserotypic chimera

NS4B, the largest nonstructural membrane protein of DENV, consists of five potential TMDs. The first two TMDs do not traverse the ER membrane and lie in the lumen. TMD3, TMD4 and TMD5 traverse the ER lumen resulting in formation of cytoplasmic and ER luminal loop in between TMD3/TMD4 and TMD4/TMD5, respectively (75). Different regions within NS4B have been attributed with different functions. The loop region between pTMD2 and TMD3 interacts with NS1 and helps in viral replication (142), the cytosolic loop interacts with NS3 enhancing its helicase activity (81) among others. These properties made NS4B a good candidate to probe for roles of different regions within NS4B. We hypothesized that if the TMDs and loops are functionally conserved across different serotypes of DENV, we should be able to successfully replace them with corresponding regions from other DENV serotype without any effect on viral life cycle. To test the hypothesis, we constructed five different interserotypic TMD NS4B chimera (Fig 4.9 B-C) and three each of the cytosolic and ER loop chimera (discussed later in the chapter).

The chimeric viruses in the context of replicon and full-length genome were transfected in BHK cells and analyzed for their ability to synthesize RNA and make infectious particles. The NS4B TMD chimeras showed varied and interesting results (Fig 4.10). Based on the data obtained from the luciferase assay and plaque assay, they can be divided into three subgroups. The first group consists of NS4B TMD1(2→3) chimera which showed a comparable RNA synthesis level to wild type. There were no significant differences in infectious particles produced by this chimera compared to wild type virus suggesting the four amino acid residues which differ between DENV-2 and DENV-3 are interchangeable. The second group of chimeras consisted of NS4B TMD2(2→3), NS4B TMD4(2→3) and NS4B TMD5(2→3). In all these chimeras, the switching of the TMDs from DENV-2 to DENV-3 resulted in varying degree of effect on replication and infectious particle production. The TMD2 switch resulted in lethal phenotype which completely abrogated the replication and infectious particle production. The NS4B TMD4(2→3) chimera was severely affected in replication and showed a highly significant reduction in infectious particle production. The TMD4 switch which account for six amino acid changes might explain the effects seen in the chimeric virus. Similarly, the NS4B TMD5(2→3) showed reduced level of RNA synthesis and infectious particle production and will be discussed in more detail in the following sections. The third group consisted of NS4B TMD3(2→3) chimera which was reduced in replication but did not show a significant difference in infectious particle production. Even though the RNA synthesis as measured by the luciferase assay was reduced by ~1.5-2 log at 48 HPE, there was no significant difference in the release of infectious particle produced compared to the wild type. This suggests that the chimeric viruses are more infectious than the wild type viruses or the RNA genome is packaged more efficiently in this chimera.

The Western blot analysis (Fig 4.10 C) shows a very faint band of TMD3(2→3) compared to that of TMD1(2→3). This is concerning but the antibodies against NS4B are targeted against the cytosolic loop which is formed by TMD3 and TMD4 and the substitution in the TMD3 (a change of four amino acids) might have affected the binding. Also, compared to TMD1(2→3), less amount of RNA is synthesized at 48 HPE when the samples were collected for Western blot.
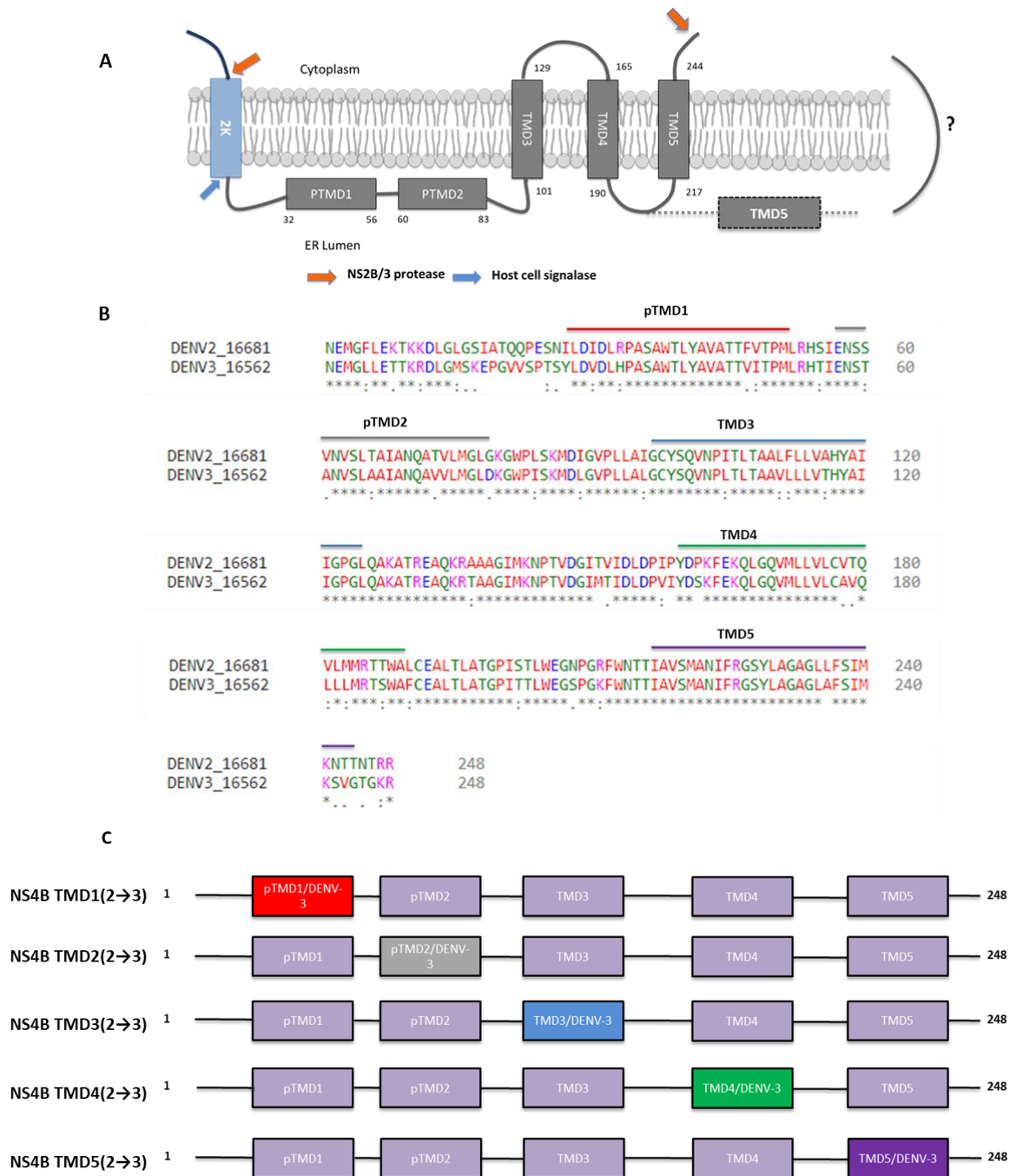
Fig. 4.9 Construction of interserotypic NS4B TMD chimeras. A) Topology of NS4B based on Miller *et al*. NS4B consists of five predicted TMDs and loops connecting these TMDs. The TMD5 in many cases flips inside to ER lumen after NS2B/3 cleavage. B) Sequence alignment of DENV-2 and DENV-3 NS4B with the corresponding TMDs indicated. C) Schematic of interserotypic NS4B TMD chimeric constructs.
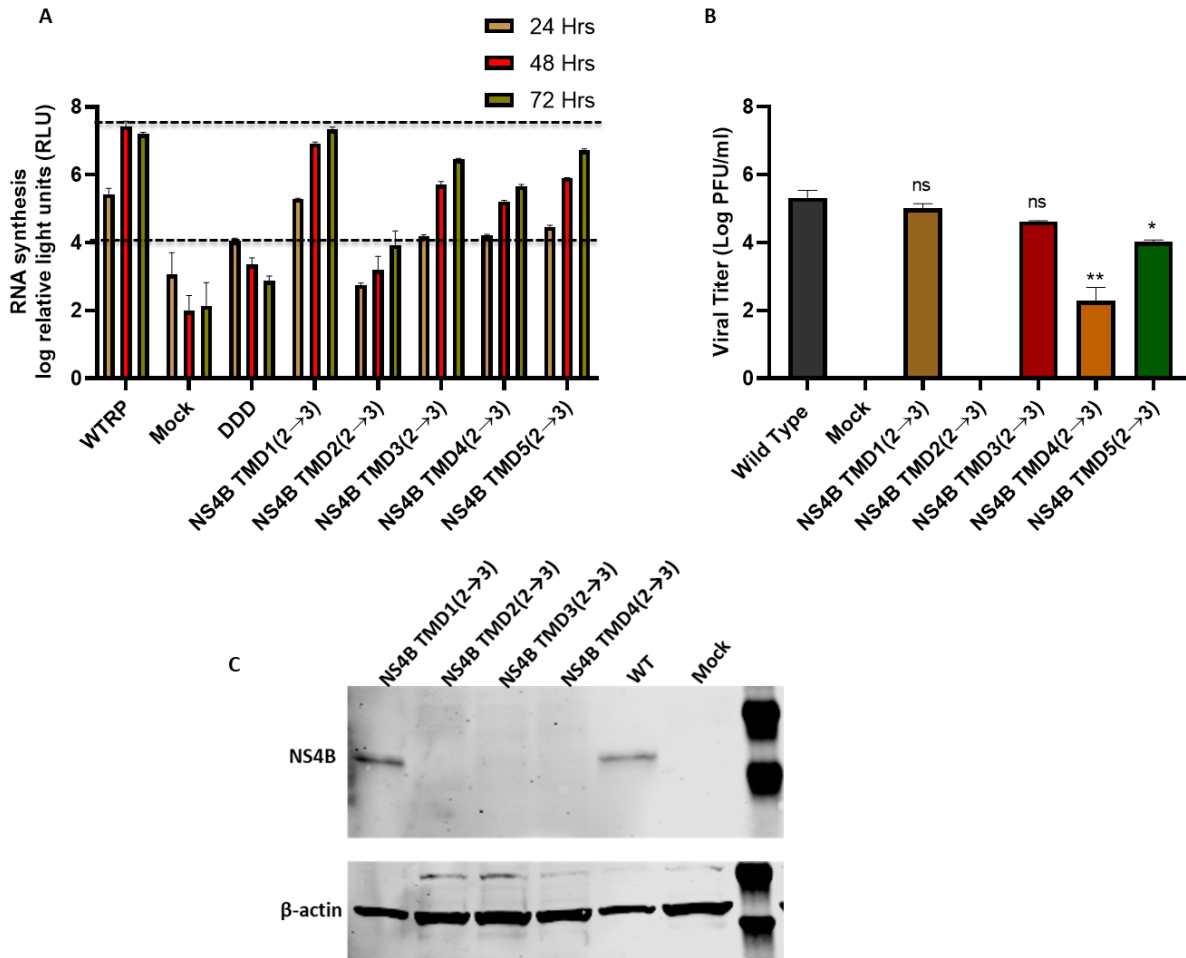
Fig. 4.10 Characterization of interserotypic NS4B TMD chimeras. A) *Renilla* luciferase assay for an indirect measurement of RNA synthesis. The chimeric constructs were transfected in BHK cells and cell lysates were collected at 24, 48 and 72 HPE, and *Renilla* luciferase activity was measured. B) Viral titer determination using plaque assay. Supernatants from BHK cells transfected with full-length chimeric constructs were collected at 48 HPE and processed for plaque assays. Plaques were counted on day 6. Data were collected from experiments performed in triplicates. C) Western blot analysis of interserotypic NS4B TMD chimeras. BHK cell lysates transfected with chimeric constructs were collected at 48 HPE and ran on a 12% SDS gel. Proteins were transferred to nitrocellulose membrane and blotted with anti-NS4B antibody. β-actin was used as a loading control. Student's t-test was carried out to test the significance at p<0.05.

131
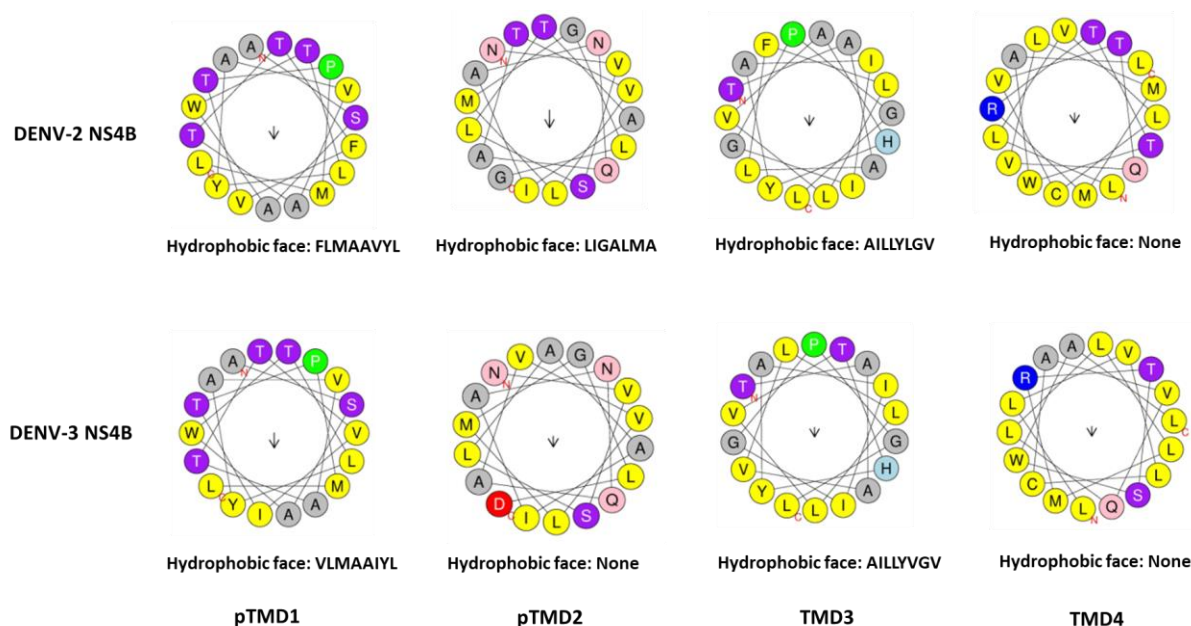
Fig. 4.11 Helical wheel analysis of amino acid residues of TMDs of NS4B of DENV-2 and DENV-3. The top panel shows the hydrophobic faces formed by the TMDs of DENV-2 NS4B. Upon substitution of TMDs from DENV-2 to DENV-3 which accounted for four, five, four, and six amino acid residues, respectively, the changes in the hydrophobic faces of the TMDs of the chimeric viruses are depicted in the bottom panel.

We analyzed the TMDs of NS4B of both DENV-2 vs. DENV-3 were analyzed by Heliquest server (126) for any major changes that might have played role in the interserotypic chimeric phenotypes (Fig 4.11). There were no major changes in the hydrophobic faces in the interserotypic TMD1(2→3), TMD3(2→3) and TMD4(2→3) chimeras. However, the TMD2(2→3) chimera showed a loss of hydrophobic face compared to the wild type virus. Interestingly, the TMD2(2→3) substitution was lethal.

4.4.4   Analysis of reciprocal mutations of NS4B in the chimeric background

In the following experiments, we analyzed whether individual amino acids within the TMDs of NS4B are responsible for the phenotypic effect seen in the interserotypic chimeric viruses. For this purpose, we chose the TMD2(2→3) chimera, which was replication incompetent and TMD5(2→3), which was affected in replication and infectious particle production. Also, TMD5 is proximal to NS2B/3 cleavage site and is assumed to flip inside the lumen post cleavage in 5-10% of the cases (75).   Using TMD2(2→3) and TMD5(2→3) chimeric replicons and viruses as the

starting point, we mutated select amino acids to the original ones to assess the effect of individual amino acids. Amino acid residues switched from the chimeric background to the original ones are highlighted in the schematic shown in Fig 4.12.

Fig. 4.12 Schematic of reciprocal mutation of select NS4B TMD chimeric constructs. TMD2 chimera (top panel) and TMD5 chimera (bottom panel).

Effect of reciprocal mutation in TMD2 chimeric viruses

A total of 3 reciprocal mutations were made in the TMD2 chimeric virus background, A66T, V73T and D79G in context of both full-length and replicon construct. The mutations of the selected individual amino acids in TMD2 chimeric background did not have any effect on the replication and particle production (Data not shown).

Effect of reciprocal mutation in TMD5 chimeric viruses

Three amino acids at the end of TMD5, which are close to NS2B/3 cleavage site, were chosen for the reciprocal mutation. Each amino acid was mutated back to the original residue and analyzed.
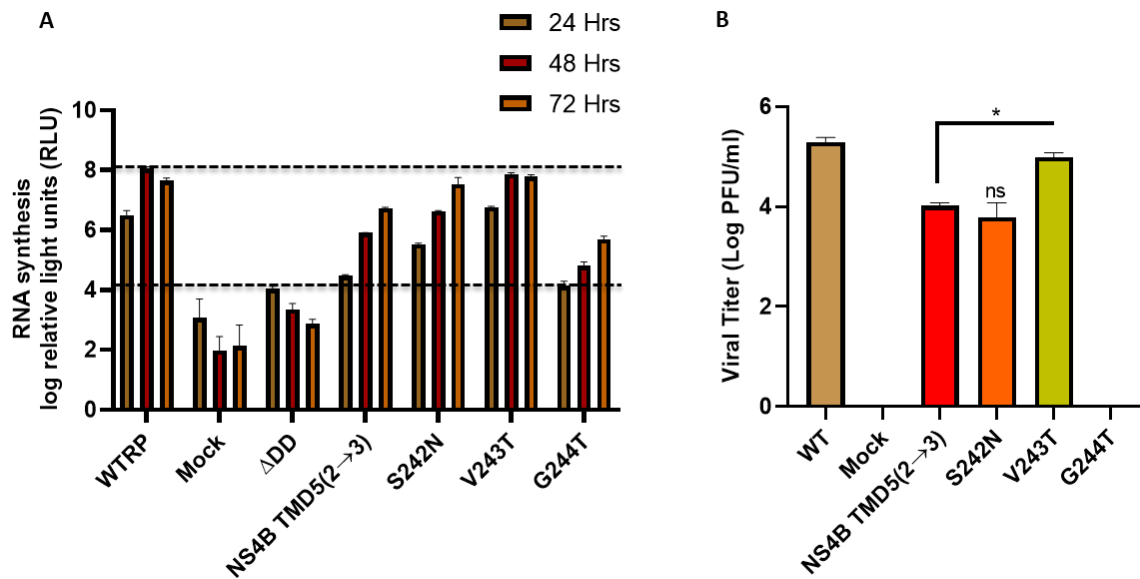
Fig. 4.13 Effect of reciprocal mutation in TMD5 chimera. A) *Renilla* luciferase assay of reciprocal mutants. The reciprocal chimeric constructs were transfected in BHK cells and cell lysates were collected at 24, 48 and 72 HPE and subjected to the *Renilla* luciferase assay. B) Viral titer determination using plaque assay. Supernatants from BHK cells transfected with full-length chimeric constructs were collected at 48 HPE and processed for plaque assays. Data were collected from experiments performed in triplicates. Significance was calculated using student's t-test at $p<0.05$.

Of the three reciprocal mutants, S242N showed a log increase in replication at 72 HPE, however, there was no significant change in infectious particle production suggesting the interchangeability of this residue. On the other hand, V243T rescued the replication to wild type level and a significant change in particle production compared to the chimeric virus suggesting a requirement of polar/uncharged residue at this position. Interestingly, G244T resulted in a prominent reduction of RNA synthesis and a loss of infectious particle production (Fig 4.13). The G244T mutation in the chimeric virus resulted in -SVT- in the chimeric virus which points to the context dependency of this amino acid residue. The substitution might have affected the folding of downstream protein or affected the cleavage at NS4B-NS5 junction. In order to assess the polyprotein processing at NS4B-NS5 junction in these reciprocal chimeric mutants, western blot analysis was carried out. There were no differences in the molecular size of the NS5 bands compared to wild type virus suggesting absence any aberrant proteolytic processing. Of note was

lower band intensity in the chimeric and reciprocal constructs in which reduced replication was observed (Fig 4.14).
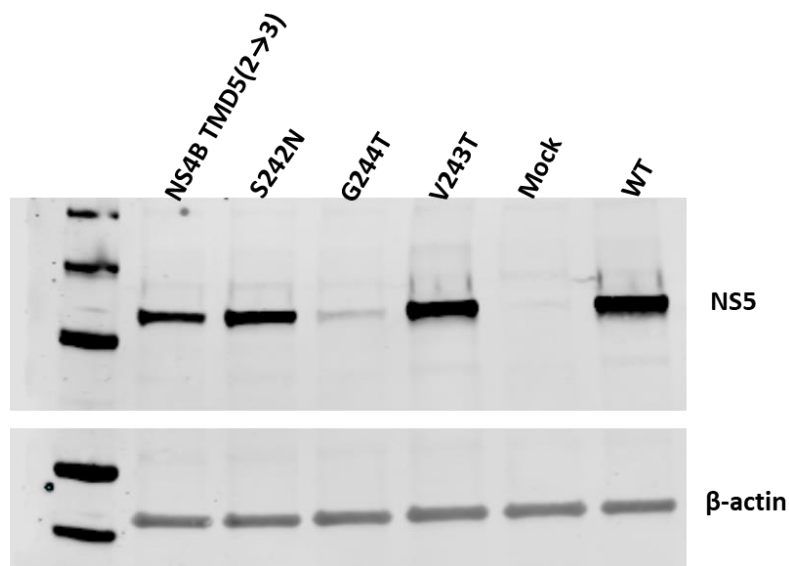
Fig. 4.14 Western blot analysis of the NS4B TMD5(2→3) chimeric viruses. BHK cells at 48 HPE were lysed and run on a 12% SDS-PAGE gel. They were transferred to a nitrocellulose membrane and blotted with anti-NS5 antibody. WT and NS4B TMD5(2→3) chimera were, respectively, used as a control for the chimeric and reciprocal chimeric virus.

4.4.5 Same site reversion rescues the replication and particle production in TMD5 chimera

Due to the unique nature of TMD5 to flip inside the lumen as it is cleaved from the NS5 protein, we were interested in knowing if the reduction in replication and particle production in the TMD5 chimeric construct was due to loss of interaction with any other viral proteins. The introduction of -SVG- in place of -NTT- might affect the stability/amphipathicity of the TMD5 in the ER membrane. Hence, to select for a reversion, we passaged the TMD5 chimeric viruses for several passages. After seven passages, we observed a slight increase in plaque size compared to the chimeric TMD5 virus. The revertant virus was plaque purified, subjected to RT-PCR for cDNA generation and subjected to sequencing. Interestingly, the reversion was with in the TMD5 itself. The methionine (M240) mutated to threonine (T) as shown in Fig 4.15.

Virus	Expt.	Revertant	Amino acid residues in NS4B TMD5(2→3)
NS4B TMD5(2→3)			IAVSMANIFRGSYLAGAGLAFSI**M**KSVG
NS4B TMD5(2→3) M240T	2	M$_{240}$T (ATG →ACG)	......................T....
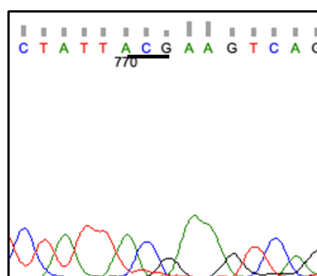
Fig. 4.15 Reversion in the NS4B TMD5(2→3) chimeric virus. A) M240T reversion in the TMD5 of the chimeric virus. Chimeric viruses were passaged seven times before an increase in plaque size was observed. The RT PCR followed by sequencing of the cDNA confirmed the amino acid change. Experiments were performed in duplicate. B) Chromatogram showing the nucleotide change corresponding to M240T reversion.

The corresponding mutation was thus introduced into the chimeric virus background and subjected to further analysis for their effect in replication and particle production. The introduction of M240T helped increase replication to wild type level and significantly increased infectious particle production (Fig 4.16).
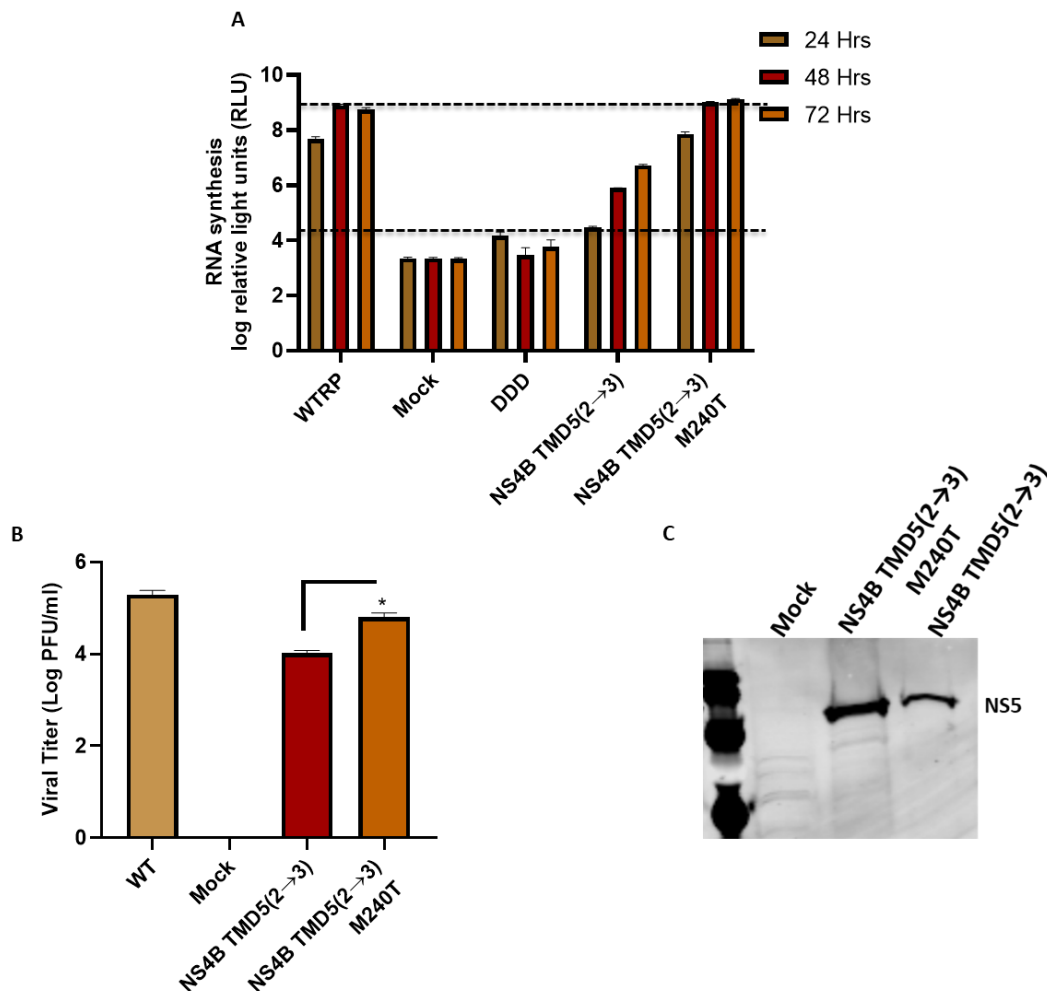
Fig. 4.16 Characterization of M240T chimeric revertant. A) *Renilla* luciferase assay depicting the amount of RNA synthesis in the wild type replicon, chimeric replicon and M240T chimeric replicon. ΔDD was used as a translational control of the luciferase activity. B) Viral titer calculated by plaque assay. The supernatant collected at 48 HPE were used to infect fresh BHK cells and perform plaque assay as described in the previous sections. C) Western blot analysis of the M240T revertant. The lysates from BHK cells transfected with the chimeric revertant constructs were collected at 48 HPE, run on a 12% gel, transferred to nitrocellulose membrane and probed with anti-NS5 Ab. Student's t-test was carried out to determine the significance at $p < 0.05$.

The sequence of the TMD5, TMD5 chimera and TMD5 chimeric revertant were submitted to the Heliquest server (126) to analyze the effect brought about by the introduction of threonine instead of methionine. With T in the backbone, the helix has a smaller hydrophobic face, which is (Fig 4.17 C) closer to the wild type helix (Fig 4.17 A) than the chimeric TMD5 helix.

A	B	C
NS4B-TMD5	NS4B TMD5(2→3)	NS4B TMD5(2→3) revertant
Hydrophobic face: None	**Hydrophobic face: IGVAYMAGFL**	**Hydrophobic face: IGVAY**
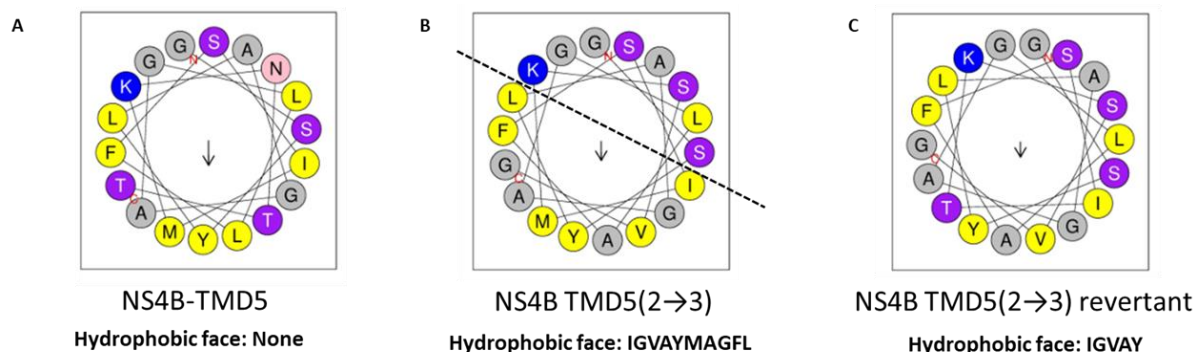
Fig. 4.17 Helical wheel analysis of amino acid residues of TMD5, TMD5 NS4B (2→3) chimera, and TMD5 NS4B (2→3) chimeric revertant. A) In the wild type TMD5, there is absence of hydrophobic face, however, upon introduction of SVG in place of NTT, a ten amino acid residue hydrophobic face is formed (B). C) In the M240T revertant, there is a smaller hydrophobic face compared to the chimeric virus.

4.4.6 Construction and characterization of interserotypic cytosolic and ER luminal loop chimera

The TMDs of multi-pass integral membrane proteins of flaviviruses are connected by amino acid residues that are either exposed to the cytosolic or the luminal environment in the cell. These amino acid residues (loops) play varied role during viral life cycle. In the case of NS4B, the TMD3 and TMD4 traversing the ER membrane in opposite direction form a 35 amino acid residues long cytosolic loop. The cytosolic loop is an interacting partner for NS3 helicase as well as a domain required for NS4B dimerization (152). Similarly, the TMD4 and TMD5 traversing the ER membrane form an ER luminal loop of 26 amino acid length. The ER luminal loop has not been attributed any specific role so far but in some cases mutations of ER loop residues is demonstrated to abrogate viral replication (145). Since the cytosolic and the ER loop are in different chemical environments and are the soluble regions of the membrane protein NS4B, they can be target of many protein-protein interactions.

We asked whether the functions of these soluble loops are conserved among different serotypes of DENV, and if so, can these loops in DENV-2 background be replaced by corresponding loops from other DENV serotypes. To test this hypothesis, we generated a total of 12 interserotypic chimeras (6 each in full-length virus and replicon system) and tested their ability to replicate and to produce infectious particles.

The cytosolic loop in the DENV-2 background was switched to that of the cytosolic loop of DEN-1, -3 and -4. The ER loop was switched in a similar fashion to generate 3 other interserotypic chimeras. The sequence alignment of the cytosolic loops (Fig 4.18 A) and ER loops (Fig 4.18 B) were carried out using Clustal Omega (125) and the chimeric viruses and replicons were generated accordingly.
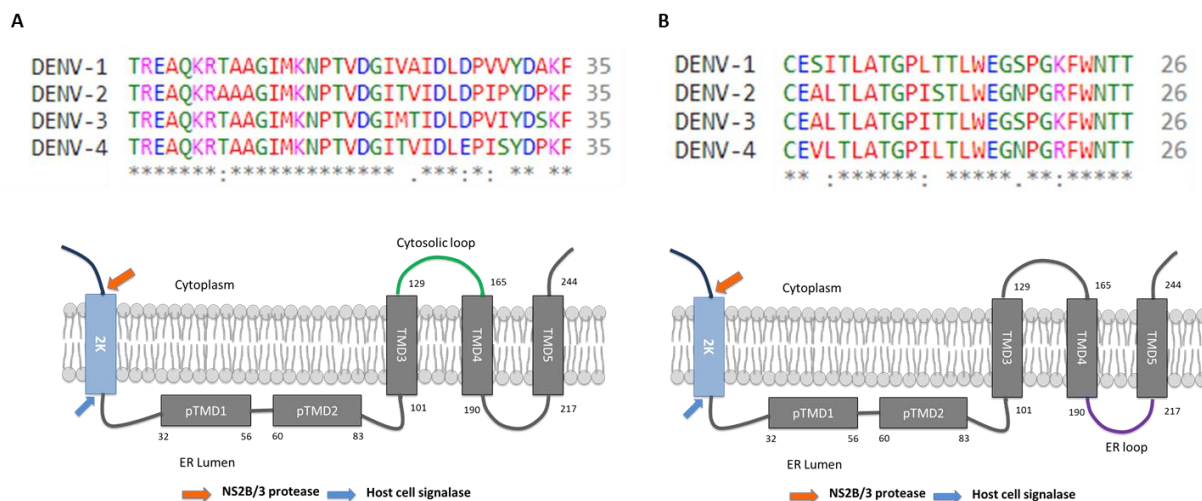
Fig. 4.18 Sequence alignment and topology of the cytosolic and ER loop of NS4B A) The amino acid residues of NS4B encompassing 129-165 were subjected to sequence alignment using Clustal Omega software (125). Bottom panel highlights the cytosolic loop (green) that was switched. (B) The amino acid residues of NS4B encompassing 190-217 were subjected to sequence alignment using Clustal omega software. Bottom panel highlights the ER loop (violet) that was switched.

The substitution of the cytosolic loop had a variable effect on viral replication, as shown in Fig 4.19 A. The NS4B Cyt(2→1) and NS4B Cyt(2→3) interserotypic chimeras were severely affected in terms of RNA synthesis. Both chimeras showed a maximum luciferase activity at 72 hrs that was smaller than luciferase activity of wild type at 24 hrs (Fig 4.19 A). With the reduced RNA synthesis as measured by luciferase activity, both chimeric viruses, NS4B Cyt(2→1) and NS4B

Cyt(2→3), showed a highly significant reduction in infectious particle production (Fig 4.19 B). This suggests the incompatibility of the cytosolic loop from either DENV-1 or -3 in replacing the loop from DENV-2. Whereas in case of NS4B Cyt(2→4) chimera, it showed an RNA synthesis level comparable to wild type at later time points (48 and 72 HPE). There was no significant difference in the release of infectious particle compared to wild type suggesting the interchangeability of this loop (Fig 4.19). The switching of the loop from DENV-2 to DENV-4 results in switching of only three amino acid residues suggesting their dispensable nature.
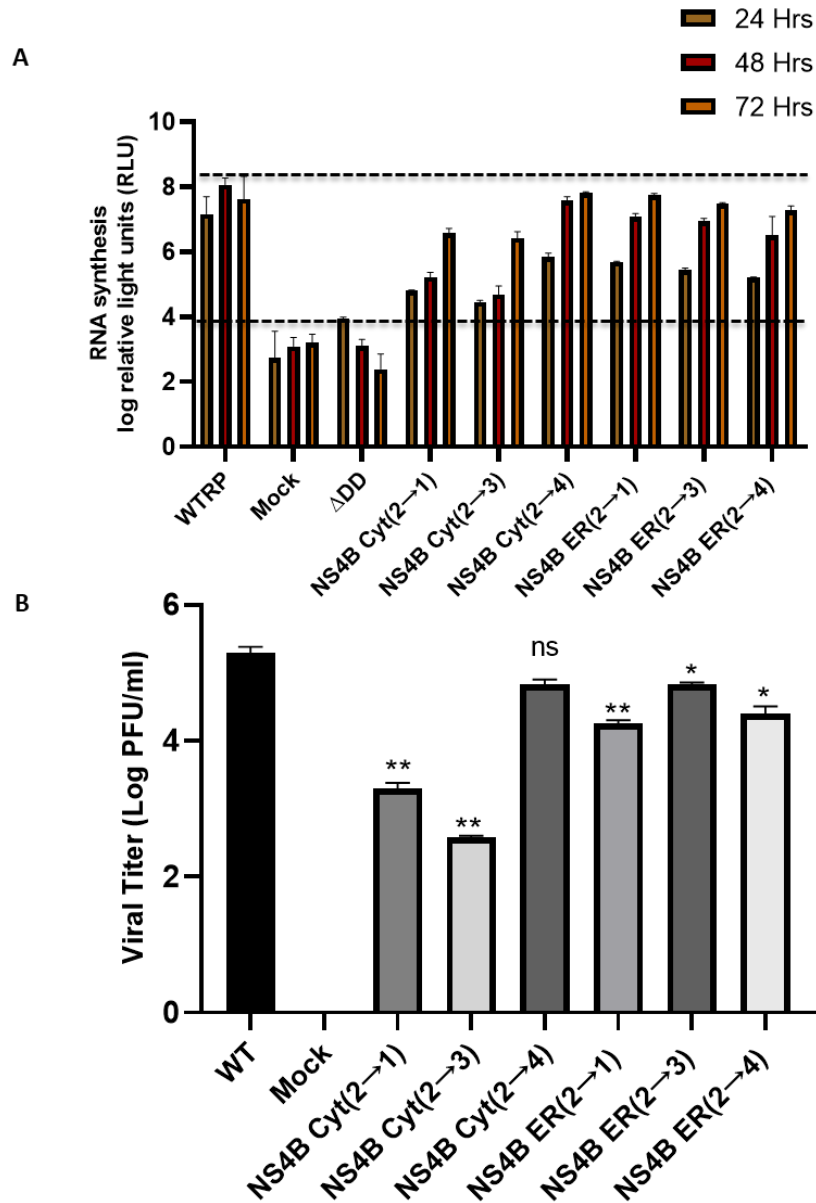
Fig. 4.19 Characterization of interserotypic cytosolic and ER luminal loop chimeras A) *Renilla* luciferase assay of interserotypic loop chimeras. The interserotypic chimeric constructs were transfected into BHK cells and cell lysates were collected at 24, 48 and 72 HPE and subjected to *Renilla* luciferase assays. B) Viral titer was determined using plaque assay. Supernatants from BHK cells transfected with full-length interserotypic chimeric constructs were collected at 48 HPE and processed for plaque assay. Student's t-test was carried out to determine the significance at p<0.05.

Interestingly, the substitution of the ER luminal loops from DENV-2 to either DENV-1, -3 or -4 had less drastic effects on viral replication compared to the cytosolic loop chimeras (Fig 4.19 A). The RNA synthesis level as measured by luciferase activity at 72 HPE were comparable to wild type. In all three chimeras, RNA synthesis at 24 HPE was mostly affected which gradually rose. The viral titer of the ER loop chimera calculated at 48 HPE shows a significant reduction in viral titer for NS4B ER(2→3) and NS4B ER(2→4) chimeras and a highly significant reduction in case of NS4B ER(2→1) chimera (Fig 4.19 B). In the NS4B ER(2→3) and ER(2→4) chimeras, the switching of the loop results in switching of two and three amino acid residues, respectively, which might have accounted for the less severe effect compared to ER(2→1) switch where a total of six amino acid residues are switched. The western blot analysis is reflective of the effects seen in these interserotypic chimera where a a comparable level of NS4B protein synthesis is seen in NS4B Cyt(2→4), NS4B ER(2→3) and WT virus (Fig 4.20).
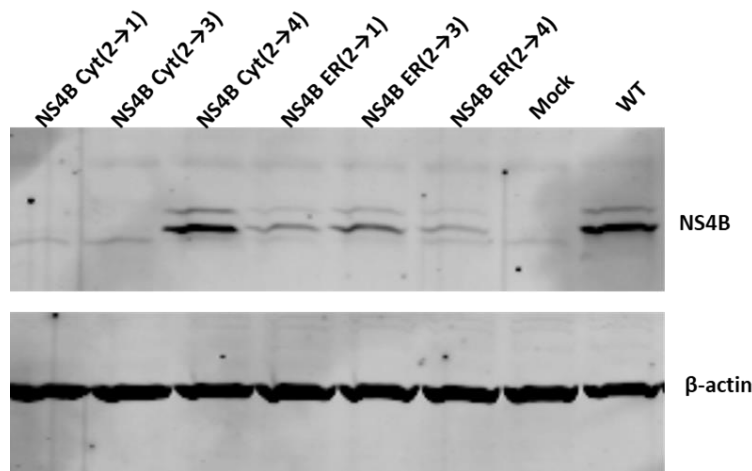
Fig. 4.20 Western blot analysis of interserotypic cytosolic and luminal loop chimera. BHK cell lysates from cells transfected with the interserotypic chimeric constructs were run on a 13% SDS gel, blotted onto nitrocellulose membrane and probed with anti NS4B antibody. β-actin was used as loading control.

4.5 Discussion

This chapter describes the role of different TMDs in viral replication and assembly. By creating interserotypic chimeras, we tried to define the functional role of TMDs of the integral membrane proteins other than anchoring the protein in the ER membrane. Generation of chimeric

viruses involved a bulk change in specific regions, subunits or an entire protein. The bulk changes allow assessing the functional conservation among wide varieties of substrate. This also allows us to assess, if these regions/domains are functional in their original niche. Generation of chimeric viruses as a tool to figure out the role of different regions of viral protein or role of the entire protein in general has been used quite frequently. Chimeric DENV-2 virus, wherein the MTase domain of NS5 in DENV-2 was switched to MTase of DENV-4, was severely affected in replication. The chimeric virus developed an adaptive mutation within the RDRP domain which partially rescued the replication, suggesting the interserotypic interaction between RDRP and the MTase domain (153). These interserotypic chimeras were probed further demonstrating a requirement for an interserotypic genetic interaction between NS5 and NS3 helicase domain as well as interdomain NS5 interactions for successful DENV replication (128).

4.5.1 TMDs of NS4A are serotype specific and play important role in viral replication

In this chapter we utilized the interserotypic chimeras as a tool to define roles of different TMDs of NS4A of DENV. The interserotypic NS4A TMD chimeras could be divided into two groups. The first group includes NS4A TMD1(2→3) and TMD3(2→3) chimeras which were severely affected in replication and showed significantly reduced infectious particle production (Fig 4.2). These chimeras accounted for a bulk change of nine and eight amino acids, respectively. Since NS4A is one of the major players in membrane rearrangement for the formation of replication factories, any changes in the TMDs negatively affect that property. As can be seen from the helical wheel analysis of the TMD1, the switch to TMD1 from DENV-3 introduces a bigger hydrophobic face. Whereas in TMD3, the composition of the amino acids forming the hydrophobic face differs completely. Since these changes might affect the replication factory formation, the resultant chimeras, NS4A TMD1(2→3) and TMD3(2→3) were prominently affected in replication as a result showed a significant reduction in virion production. Also, the interserotypic changes involve switching from hydrophobic to polar uncharged residues, from aliphatic to bulky aromatic groups and from stable to helix breaker residues (Fig 4.5). These changes when imposed at the same time might have affected the replication efficacy of these chimeric constructs. Moreover, TMD1 of NS4A is responsible for its oligomerization. The amino acids L52, E53, G66, and G67 of TMD1 have been shown by NMR to be involved in the oligomerization (56). E53, G66 and G67 are conserved across DENV-2 and DENV-3. However, there is a methionine in place

of L52 in DENV-3. This might be one of the reasons for the reduced rate of replication seen. However, western blot data (Fig 4.3) does not completely support this notion as oligomers of NS4A are produced by this chimera. Similarly, a unique PEPE motif in the TMD3 of WNV-Kunjin plays a role in the cleavage of the 2K from NS4A by NS2B/3. In mutant viruses where these residues were mutated, there was deficient cleavage at NS4A-2K junction resulting in defective replication complex formation (154). With the substitution of eight amino acids in TMD3(2→3) chimera, the function of conserved peptide PEPE might have been affected. Also, we did not observe any NS4A and NS4B in the western blot for this interserotypic chimera. However, no higher molecular weight bands of NS4A-2K-NS4B were also seen. This must be due to poor binding of antibody or due to rapid degradation of the membrane protein as both NS3 and NS5 production could be seen for the same chimeras (Fig 4.3 B).

The second group consisted of the NS4A TMD2(2→3) chimera. The TMD2 switch was lethal for replication and infectious particle production. The TMD2 of NS4A sits parallel with the inner leaflet of the ER membrane. The TMD2 of NS4A also plays a major role in membrane bending, rearrangement and formation of replication factories. An interserotypic chimeric switch from DENV-2 to DENV-3 results in a bulk change of twelve amino acid residues. The introduction of helix breaker G93, and to some extent S82 and S91, might have destabilized the helix in DENV-2 context and might have resulted in improper folding and degradation of the protein. Moreover, as TMD2sits on the inner leaflet of the ER membrane, the large substitution might have affected the protein-protein interaction mediated by the residues of TMD2 of DENV-2 and not DENV-3.

All these observations led us to ask why these TMDs work in the context of DENV-3 and not in DENV-2. One way to answer that question is to generate a revertant which would probably point to its specific interaction partner. However, several attempts to select for a revertant virus in NS4A TMD1(2→3) and TMD3(2→3) chimeras were unsuccessful. Alternatively, to pinpoint individual amino acid residues responsible for the phenotypic effect seen, we chose a different strategy in which select amino acid residues were mutated back to their original residues in the chimeric background. None of the reciprocal mutations of the NS4A TMD1(2→3) chimera significantly helped restore the replication and infectious particle production, although G59T reciprocal mutation showed some restoration of replication and infectious particle production (Fig 4.6). Our attempts to pinpoint residues of TMD2 that could rescue the replication in TMD2(2→3)

chimera were unsuccessful, as none of the reciprocal mutations rescued replication in this chimera. This supports the idea that rather than a single amino acid, a group of amino acid residues interact with the membrane, thus keeping it bound to the inner leaflet of ER membrane. Any disturbances in the membrane homeostasis maintained by these domains are detrimental for viral life cycle. It is also possible that TMD2 might interact with other viral proteins or TMDs of same serotype; thus, any changes to this TMD results in non-replicative chimeras. One prominent example of the rescue of replication and significant increase in infectious particle production using reciprocal mutation is exemplified by the S107A mutant of NS4A TMD3(2→3) chimera. The introduction of alanine on the chimeric background resulted in a gradual increase in RNA synthesis as measured by luciferase assay and a significant increase in infectious particle production compared to the chimeric viruses (Fig 4.8).

4.5.2 TMDs of NS4B vary in their ability to tolerate interserotypic substitutions

NS4B with its unique topology is one of the major replication proteins of DENV. Presence of soluble domains (Cytosolic loop and ER loop) and TMDs make it a protein with multivariate functions. In order to understand the role of TMDs in viral life cycle, several interserotypic TMD chimera of NS4B in DENV-2 were generated. The TMDs of NS4B could be substituted with corresponding TMDs of DENV-3 NS4B with varying degree of success. TMD1 of NS4B was the most permissive one. The TMD1 chimera did not have any major defect in terms of replication and virion production as they were comparable to that of wild type (Fig 4.10). pTMD1 and pTMD2 of NS4B are believed to be membrane associated, however, do not traverse the membrane (75). A chimeric switch from TMD1 of DENV-2 to DENV-3 introduces a total of four amino acid changes and most of them are conservative substitutions which explains the result obtained from this chimeric virus. The substitution of pTMD2, however, resulted in the loss of viability of the virus which could not be rescued even by reciprocal mutation (Data not shown). As shown from the helical wheel analysis of pTMD2, the TMD switch from DENV-2 to DENV-3 results in loss of hydrophobic face (Fig 4.11). Also, pTMD1 and pTMD2 of NS4B have been reported to interact with EMC and help in the biogenesis of NS4B protein (26). The loss of hydrophobic face might have affected the way pTMD2 interacts with the membrane and hence the EMC resulting in instability of the protein. The NS4B TMD3(2→3) chimera showed a reduced replication, however, there was no significant difference in infectious particle production suggesting the production of

145

virions with higher infectivity. With only four amino acid substitutions in the interserotypic TMD3 (2→3) chimera, the result was quite interesting. However, role of TMD3 of DENV in viral pathogenesis and adaptability has been reported. DENV-4 adapted to Vero cell lines develops L112F mutation. Interestingly, the switching also resulted in L112F substitution in our experiment. Similarly, V109, and G119 residues within TMD3 of NS4B were responsible for enhanced replication of DENV-4 when mutated to alanine in Vero cells (155). With a bulk change of six amino acid residues, mostly conservative, TMD4(2→3) chimera was severely reduced in replication and infectious particle production. Although there were no changes in the hydrophobic face when switched from DENV-2 to DENV-3 (Fig 4.11), other interactions mediated by individual amino acids within TMD4 might have been disrupted.

The NS4B TMD5(2→3) chimera in which the last TMD of NS4B (close to NS4B-NS5 junction), was reduced in RNA synthesis and was significantly affected in infectious particle production (Fig 4.13). Since most of the amino acid changes in the chimera were closer to the NS4B-NS5 cleavage site, we took a special interest in the NS4B TMD5(2→3) chimera. As mentioned earlier, the substitution of TMD5 in DENV-2 to DENV-3 resulted in reduced replication efficiency that was translated in terms of infectious particle release (Fig 4.10). The predicted topology of NS4B supports that TMD5 of NS4B can be reoriented after NS2B/3 cleavage. The TMD5 can flip to the inside of the lumen (75). We suspected the introduction of SVG instead of NTT might have introduced more hydrophobic residues to the TMD which might have affected TMD5 flipping to the ER lumen. In order to select for a revertant, the TMD5 chimeric virus was passaged several times. A M240T reversion in TMD5 rescued the replication and infectious particle production of the TMD5 chimeric virus. We analyzed the sequences of wild type TMD5, TMD5 chimeric virus, and the revertant virus using helical wheel projection. Interestingly, in TMD5 chimeric virus, with the introduction of residues from DEN-3 TMD5 a huge hydrophobic face was introduced (Fig 4.15 B) compared to DENV-2 TMD5. With the M240T reversion, the hydrophobic face is reduced to few amino acids, suggesting the critical role of the NTT residues towards the end of TMD5 in possibly helping reorient the TMD5 to the lumen post cleavage. This phenomenon points to how the reorientation of TMD5 post NS2B/3 cleavage might vary in different serotypes. Similar post cleavage reorientation of TMDs have been described in N-terminal of NS4B of HCV, where posttranslational processing of the N-terminal of NS4B results in it being translocated to the lumen of the ER (156). Similarly, the M protein of

gastroenteritis coronavirus adopts two topologies with the –COOH group inside or outside the virion surface (157). These revertant data is also supported by the reciprocal mutations we did in the TMD5 chimeric background. The introduction of V243T also rescued replication and infectious particle production, albeit not to wild type levels (Fig 4.13).

In summary, the different TMDs of NS4B function in different ways as they interact with different environments. The TMD1 and 2 are in the lumen while TMD3 and TMD4 meet different fate in the bilipid layer of the ER. TMD5 could sample both the membranous environment and the lumen as it flips into ER lumen post cleavage. The contribution of unique properties from different regions within NS4B makes it one of the major replication proteins in the viral life cycle.

4.5.3   ER loop of NS4B is functionally more conserved than the cytosolic loop

The cytosolic and ER loop consist of soluble domains of an otherwise integral membrane protein NS4B. The cytosolic loop of NS4B has a diverse role ranging from its involvement in NS4B dimerization to interacting with helicase domain of NS3 to help replication. We were interested in testing if these functions are conserved across the DENV serotypes. The interserotypic cytosolic chimera were used as a tool to answer these questions. As seen in Fig 4.19 A, the substitution of cytosolic loop from DENV-2 to DENV-1 or -3 resulted in a drastic defect in viral replication and infectious particle production. However, the substitution to DENV-4 did not have any significant effect. When a switch of a cytosolic loop is made from DENV-2 to either DENV-1 or DENV-3, a total of five and six amino acids, respectively are replaced with new ones. In other words, the conservation or amino acid identities among DENV-2 and DENV-1 and -3 cytosolic loops are ~83%. However, a switch from DENV-2 to DENV-4 results in three amino acid residue changes in the resulting chimera and the sequence identity among these two is ~91%. The phenotypic changes brought about by the cytosolic loop switch could result from several of the reasons discussed here. The amino acids within cytosolic loop participate in protein-protein interaction, which might have been disrupted by the substitution. The conserved amino acids Q134, G140 and N144 of cytosolic loop are involved in interaction with NS3 (80). The substitution of the cytosolic loop introduces different amino acid environment compared to native one, and even though these residues are conserved, the way they behave in changed environment needs to be studied. Moreover, the same study using NMR spectroscopy showed that the cytosolic loop of

DENV-2 formed three turn α-helices and two β-strands. The introduction of new amino acids might have affected the structure and thus interfered with the functions of the loop. The other possibility includes the perturbation of the interserotypic interaction mediated by these loops. For instance, the cytosolic loop of DENV-2 might just interact with NS3 from DENV-2 or DENV-4 and not with other serotypes. These disruption in interactions mediated by the cytosolic loop might have affected the chimeric viruses. Attempts to get a revertant for NS4B Cyt(2→1) and NS4B Cyt(2→3) chimeric viruses were unsuccessful.

On the other hand, the ER luminal loop could be replaced with less pronounced effect on viral replication within DENV serotypes (Fig 4.19). However, the substitution significantly affected the infectious particle production. The switching of the ER loop from DENV-2 to DENV-1 resulted in the most prominent effect. The resultant chimera NS4B ER(2→1) had six different amino acids compared to the wild type virus. These amino acids change might have negatively affected the function of the ER loop. The NS4B ER(2→3) and NS4B ER(2→4) were affected to a lesser extent as the switching of the ER loop in these chimeras account for two and three amino acid residues, respectively. Also, the amino acid identities of the ER loop vary from ~77% (DENV-2 vs -1) to 92% (DENV-2 vs -4). Although the switching of the ER loop among DENV serotypes resulted in less pronounced effect in viral replication, there was significant effect in the infectious particle production corroborating our data from Chapter 3 suggesting the role of ER loop in viral assembly. However, a detailed study is warranted before drawing a conclusion.

The results are summarized in Fig 4.21.

Fig 4.21 Summary of effects of interserotypic NS4A and NS4B TMD chimeras on DENV-2 replication and virion release. A) Effect of interserotypic NS4A TMD switch between DENV-2 and DENV-3. The TMD1(2→3) and TMD3(2→3) chimera tolerated the bulk amino acid changes, although they were severely affected in replication and infectious virion release (green dotted line). Reciprocal mutation in these chimeras could not rescue the defects except for S107A mutant of NS4A TMD3(2→3) chimera (green solid line). The TMD2 switch, however, was lethal, the defect of which could not be rescued upon reciprocal mutation of select residues of TMD2 in TMD2(2→3) background (red solid line). B) Effect of interserotypic NS4B TMD switch between DENV-2 and DENV-3. The interserotypic switch of TMD1 and TMD3 did not have any significant effect on the release of infectious particle. However, the NS4B TMD3(2→3) chimera, even though affected in replication, was not significantly affected in infectious particle release (blue dotted and solid line). The TMD2 switch in NS4B resulted in lethal phenotypes. Even the reciprocal mutations of the select residues could not rescue the defect (Red lines). On the other hand, the TMD4(2→3) and TMD5(2→3) chimeras were severely affected in replication and infectious virion release (green dotted line). Interestingly, the reciprocal mutation of G244T in TMD5(2→3) background was lethal (red solid line) for the chimera, whereas V243T rescued the defects of this chimera (green solid line). Also, M240T revertant of the TMD5(2→3) chimera rescued replication and virion production in the chimera.

A

Interserotypic NS4A TMD chimera	Residue-changes	Hydrophobic face
TMD1(2→3)	9	++
TMD2(2→3)	12	+
TMD3(2→3)	8	+

Replication → Infectious particle release

G59T, L63T, M69F — TMD1(2→3)

K76R, T81M, I86C, G93I, M97Y — TMD2(2→3)

L102P,Q103H — TMD3(2→3)

S107A

Reciprocal mutation

B

Interserotypic NS4B TMD chimera	Residue-changes	Hydrophobic face
TMD1(2→3)	4	-
TMD2(2→3)	5	+++
TMD3(2→3)	4	-
TMD4(2→3)	6	-
TMD5(2→3)	4	++

Replication → Infectious particle release

A66T, V73T, D79G — TMD2(2→3)

S242N

V243T

G244T

TMD5(2→3)

M240T — TMD5(2→3)

Reciprocal mutation

Revertant Generation

150

CHAPTER 5.   SMALL MOLECULE INHIBITORS OF N-7-METHYLTRANSFERASE OF FLAVIVIRUSES

5.1   Chapter summary

Nonstructural protein 5 (NS5) of flaviviruses has an indispensable role in viral life cycle because of its dual function in carrying out methyltransferase (MTase) and RNA-dependent RNA polymerase (RdRp) activities. The MTase domain of NS5 carries out the transfer of a methyl group to N^7 of guanine using S-adenosyl methionine (AdoMet) as a donor forming a type 1 cap. Several AdoMet analogs were synthesized that would compete with AdoMet for the binding pocket, in addition, would also fill the conserved adjacent pocket of the flaviviral MTase. We carried out molecular docking of these compounds into MTase domain of NS5 of ZIKV, DENV-2 and YFV, and further tested these compounds for their ability to inhibit replication of ZIKV, DENV and YFV. In parallel, a ZIKV replicon capable of autonomous replication was constructed to facilitate the screening of a large number of compounds. Two compounds identified in this study, GRL-002- and GRL-004-16-MT specifically inhibited ZIKV replication with low micromolar IC_{50} value. Using a *Renilla* luciferase assay system, three other compounds; GRL-007-, GRL-0012- and GRL-0015-16-MT were shown to have a dual inhibitory effect against DENV and YFV. At least one of these compounds, GRL-007-16-MT showed a broad spectrum activity against different members of flaviviruses. Our results reveal the efficacy of compound design targeting the extra pocket conserved in flaviviruses and help identify the lead compounds against different flaviviruses.

5.2   Introduction

Flaviviruses are a group of enveloped positive strand RNA viruses responsible for diseases ranging from febrile illness to more severe microcephaly, encephalitis and hemorrhagic fever. Most flaviviruses are arthropod borne and commonly transmitted by mosquitoes or ticks. Some prominent flaviviruses include ZIKV, DENV, YFV, WNV, and JEV. These viruses cause significant human disease and are considered a global health problem (158, 159). This is exemplified by the recent outbreak of ZIKV in the Americas and its long-term effect on the children in the affected areas, underlying their importance among the potent human pathogens (160). DENV has been estimated to infect approximately 390 million people each year of which

more than 500,000 cases result in the more severe form of disease, dengue hemorrhagic fever. Similarly, WNV was found to be the major cause of reported arbovirus related encephalitic mortality in the US (161).

The single strand positive sense RNA genome of flaviviruses codes for a single polyprotein that is co- and post-translationally modified by cellular and viral proteases into 3 structural proteins and 7 nonstructural proteins. In a mature virion (~50 nm in diameter), Capsid (C) surrounded by Membrane (M) and Envelope (E) proteins form a protective coating that encase the single strand RNA genome (5). The nonstructural proteins are responsible for genome replication, immune evasion, and interaction with host proteins as well as their potential role in viral assembly (6).

The incidence of flavivirus infections are ever growing as evidenced by the recent outbreaks of ZIKV and YFV in Brazil. Despite advances in understanding these viruses, there are currently no licensed human vaccines against ZIKV and WNV in the US. This is further complicated by the fact that no preventive and prophylactic antiflaviviral therapies are currently approved by the FDA. This underscores the need for rational drug design in order to develop therapeutic agents that selectively target the flaviviral replication machinery (164). Nonstructural protein 5 (NS5) of flaviviruses consists of an N-terminal methyltransferase (MTase) and C-terminal RNA-dependent RNA polymerase (RdRp) domains that have been exploited as antiviral targets because of their indispensable role in viral RNA replication. Moreover, the role of NS5 in inhibiting type I interferon has also been described, which is an additional benefit as an antiviral target (165).

The MTase domain of NS5 is responsible for adding a type 1 cap onto the 5' end of the RNA genome. To do so, it utilizes S-adenosyl methionine (AdoMet) as a methyl group donor for adding the N-7 methyl group on the guanine (8, 9). Experiments have shown that mutations within the AdoMet binding sites disrupt viral replication (10, 11). Thus, compounds that target this pocket and displace AdoMet have been identified as good candidates for screening against flaviviruses. However, the AdoMet binding motif is conserved among diverse organisms, and developing compounds that selectively inhibit the flaviviral MTase but not cellular MTases is considered challenging. Moreover, the S-Adenosine-L-Homocysteine (AdoHyc) produced during the capping reaction is tightly associated with the AdoMet binding pocket as seen in most of the NS5 crystal structures that have been solved so far (168). AdoMet analogs that can displace the AdoMet from

the binding pocket would be a good starting point towards development of effective MTase inhibitors.

Several AdoMet and AdoHyc analogs have been tested for their potency to inhibit the 5' capping of MTase and interfere with the viral life cycle (12, 14). To search for a novel and potent inhibitor of flaviviral N-7 MTase, we screened several AdoMet analogs that not only bind to the AdoMet binding pocket but also to the adjacent conserved pocket of the flavivirus MTase. We used replicon and live virus assays to identify two compounds, GRL-002-16-MT and GRL-004-16-MT, which were potent inhibitors against ZIKV with low IC_{50} values. Moreover, compounds specific against either DENV or YFV, as well as compounds inhibiting both viruses were found in the current study.

5.3   Materials and Methods

5.3.1   Cell culture and viruses

BHK-15 cells were obtained from the American Type Culture Collection (ATCC) and were maintained in minimal essential medium (MEM) supplemented with 10% fetal bovine serum (FBS). Vero cells (ATCC) were maintained in a high-glucose Dulbecoo's Modified Eagles Medium (DMEM). ZIKV was propagated in a Vero-furin cell line at 37°C in DMEM supplemented with 2% FBS in the presence of 5% CO_2. The culture supernatant was clarified by centrifugation and filtered using 0.25μM filter (Nalgene, Thermo Scientific).

5.3.2   Plasmid construction

Using a clone of pFLZIKV (a kind gift of Dr. Pei-Yong Shi) (171), a ZIKV replicon (*Renilla* luciferase) was constructed. A unique restriction site (AgeI) was chosen upstream of the T7 promoter site in the pFLZIKV cDNA construct. Using a specific set of primers, T7 promoter-5'UTR-Nter21 capsid was amplified from pFLZIKV. In a second step, the sequence encompassing RLuc-FMDV2A was amplified from a dengue replicon that was constructed in our lab. A third fragment with a unique restriction site (SphI) within NS1, along with the signal sequence for NS1 was amplified. In a two-step overlap extension PCR, a final product consisting of T7 promoter-5'UTR-Nter21-RLuc-FMDV2A-E23-NS1 was generated that was cloned in the pFLZIKV cDNA backbone using unique restriction sites AgeI and SphI resulting in plasmid pZIKVRLuc.

As a control, a replication defective replicon was constructed wherein the conserved GDD motif (corresponding to residues Gly664, Asp665, and Asp666) within the RDRP domain of NS5 was deleted using site directed mutagenesis resulting in plasmid pZKVRluc ΔGDD.

5.3.3   RNA transcription and transfection

The pZKVRLuc was linearized using ClaI and purified using a GFX column (Invitrogen) followed by incubation with T7 polymerase (NEB) at 37°C for 11/2 hours for in vitro transcription of RNA. For DENVRepLuc and WNVRepLuc, XbaI was used to linearize the plasmid followed by in vitro transcription using T7 polymerase, whereas, for YFVRepLuc, XhoI was used for linearization followed by in vitro transcription using SP6 polymerase (NEB). pZKVRLuc, DENVRepLuc, WNVRepLuc and YFVRepLuc transcripts (10 μg) were electroporated into confluent BHK-21 cells using 2mm cuvettes with the GenePulser apparatus (Bio-Rad) at settings of 1.5kV, 25μF and 200Ω, pulsing two times, with 2s intervals. After a 5 min recovery at room temperature, the transfected cells were mixed with 2% FBS containing media, mixed properly and divided into several 1 ml aliquots. This was followed by addition of different concentration of compounds or 0.5% DMSO to the cell suspension, which were plated in 96-well plates and incubated until samples were collected at different time points.

5.3.4   Luciferase assay

At various time points post transfection, the cells were washed once with PBS and lysed using 50 μl cell lysis buffer (Promega). The lysed cells were clarified by centrifugation and stored at -80°C. Once samples for all time points had been collected, luciferase signals were measured using a luminescence microplate reader (LMAXII 384, Molecular Devices) according to manufacturer's protocol. IC_{50} values were determined using GraphPad Prism 7 Software.

5.3.5   Compound synthesis

Eight different compounds that would compete with SAM for SAM-binding site were synthesized in the laboratory of Dr. Arun K Ghosh, Department of Chemistry, Purdue university. These AdoMet analogs were designed rationally in a way that the branching of these compounds fills in the conserved hydrophobic pocket of the flaviviral MTase.

5.3.6 Protein structure and ligand preparation

The crystal structure of MTAse domains of ZIKV (PDB ID: 5M5B) DENV-2 (PDB ID: 3EVG), and YFV 17D (PDB ID: 3EVA) were retrieved from Protein Data Bank (PDB). All these structures were solved with SAM-bound to the active site of the MTAse domain which served as reference for initiating the docking of the compounds discussed in this study. For generating PDB ID of the compounds, Online SMILES Translator and Structure File Generator (National Cancer Institute) was used. Additionally, Chimera software (172) was used for sequence alignments and generation of models.

5.3.7 Molecular docking

All the eight compounds were docked into the MTase domains of ZIKV, DENV and YFV using AutoDock Vina (173). For this study, the receptors (MTase) were kept rigid while the flexible compounds were docked against them. AutoDock Vina utilzes steric and hydrophobic interactions as well as hydrogen bonding wherever applicable to calculate docking scores and ranking the different orientation of the compounds.

5.3.8 Antiviral assay

Vero cells were seeded 5×10^5 cells per well in a 24 well plates. After overnight incubation, the cells were infected with ZIKV at a MOI of 5, the inoculum was removed after 2 hours of attachment, cells were washed 3X with PBS then treated with different concentrations of compound or 0.5% DMSO as a vehicle control. At 72 HPI, culture supernatants were collected, clarified by centrifugation and stored at -80°C until plaque assay was performed.

5.3.9 Cytotoxicity assay

Cytotoxicity (CC_{50}) was measured using a standard WST (Tetrazolium salt) assay measuring cellular proliferation in the presence of compound as a function of cellular mitochondrial dehydrogenase activity using the Quickcell Proliferation assay Kit (Biovision). Briefly, ~50,000 Vero or BHK cells were seeded in 96-well plates and allowed to attach for 6-8 hours. Different dilutions of compounds and vehicle at an amount of 100μl were added to each well. Following 48 hours of incubation at 37°C, the supernatant was removed and 100μl of diluted proliferation

substrate was added to each well and further incubated for 2-4 hours at 37°C. The supernatant was then transferred to a new 96 well plate, absorbance measured at 450 nm with a 96 well plate reader (Spectramax M5, Molecular devices).

5.3.10 Statistical analysis

GraphPad Prism Software 7 was used to analyze the data and calculate the CC_{50} and IC_{50} values using non-linear regression analysis.

5.4   Results

5.4.1   Construction and characterization of Zika virus replicon

Replicons are frequently used as a tool to measure RNA synthesis, which in turn indirectly measures virus proliferation. Replicons for different flaviviruses have been described and are used on a regular basis for replication analyses and antiviral compound screening (174, 175). Replicons are viral genomic RNAs with an in-frame deletion of the structural proteins. They are non-infectious; however, they can still undergo autonomous replication provided the necessary RNA signals remain intact. Replicons are commonly used as a measure of RNA turnover via the use of quantitative tags such as *Renilla* luciferase (RLuc), which are cloned in place of the structural genes. For this reason, different flavivirus replicons have been used for low and high throughput antiviral compound screening. The ZIKV replicon (pZIKVRLuc) was constructed from the full-length infectious cDNA clone of ZIKV (171). As a control, the pZIKVRLucGDD construct was made wherein the NS5 (RdRp) active site GDD was deleted (Fig 5.1).

Luciferase activity measured at 6-hour intervals from 12 hours post transfection (HPT) to 60 HPT showed ZIKV-Rluc exhibited a lag phase in proliferation between 0-18 HPT, and then proliferated approximately linearly to peak luciferase intensity at 60 HPT (Fig 5.2 A). In contrast, the replication deficient ZIKVRLuc GDD showed a gradual decrease in the luciferase activity over the same 60 hour time period (Fig 5.1 B).

The replication kinetics of ZIKVRLuc was compared with several other flavivirus members including WNV, YFV and DENV. Unique to the ZIKV replicon was a short lag phase followed by a steady increase in RNA synthesis that peaks at 60 hours, and the kinetics of replication was

156

comparable to dengue replicon which peaked at later time points (Fig 5.2 B). WNV, YFV and DENV replicons showed a sharp increase in replication from 6-24 HPT. Following this period, the DENV replicon plateaued while YFV and WNV decreased gradually for the duration of the experiment. As in Fig 5.2 A, the ZIKV replicon showed an initial lag phase of proliferation followed by a replication rate comparable to DENV. Like DENV, proliferation also appeared to plateau from approximately 42 HPT. Compared to the other flaviviral replicons, the luciferase signal from Zika replicon is relatively low. This can be attributed to the use of BHK cell lines used in the experiments, which are less favorable for Zika replication.
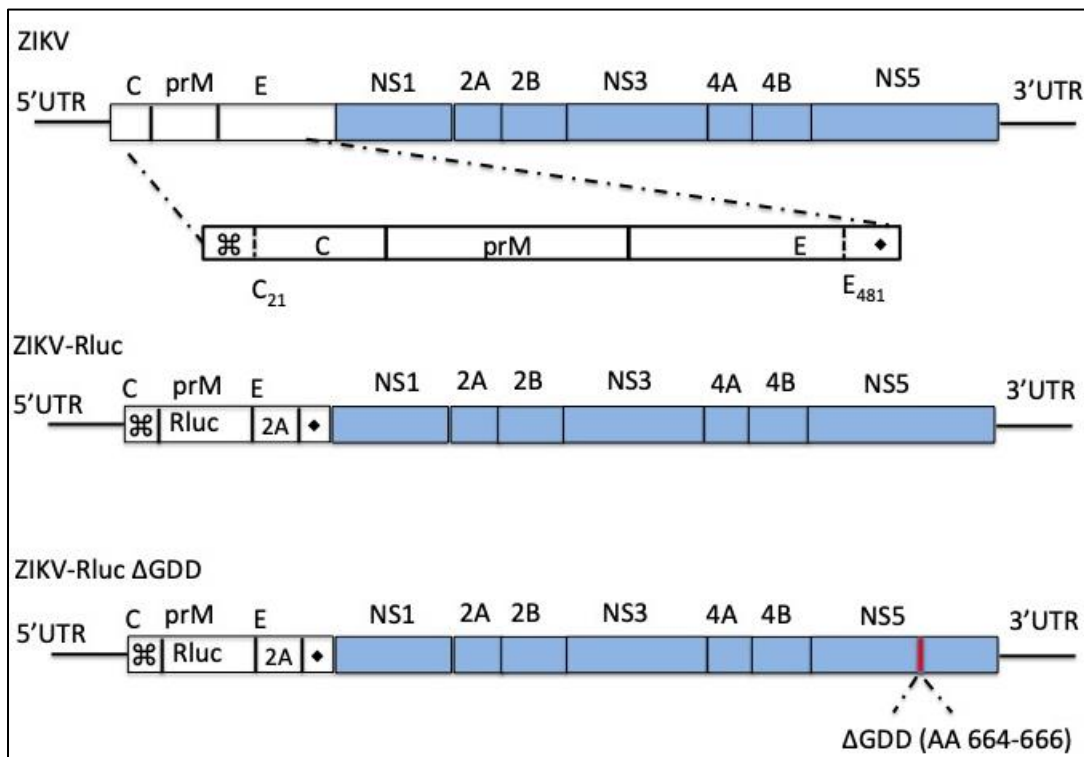
Fig. 5.1 Construction of ZIKV replicon. Genome organization of ZIKV and ZIKV replicon. The structural genes are depicted in open boxes and nonstructural genes in light blue boxes. The zoomed in portion shows the presence of cyclization sequence in capsid (⌘) and signal sequence (□) for NS1 in E protein. A Dengue replicon was used to amplify the *Renilla* luciferase-FMDV2A gene. The resulting RLuc-FMDV2A was cloned in frame between C_{21} and E_{482} in place of the deleted C_{22}-E_{481} region by overlap extension PCR. The bottom panel shows a replication defective ZIKV-Rluc ΔGDD construct in which the amino acids at position 664-666 in active site of RDRP have been deleted.
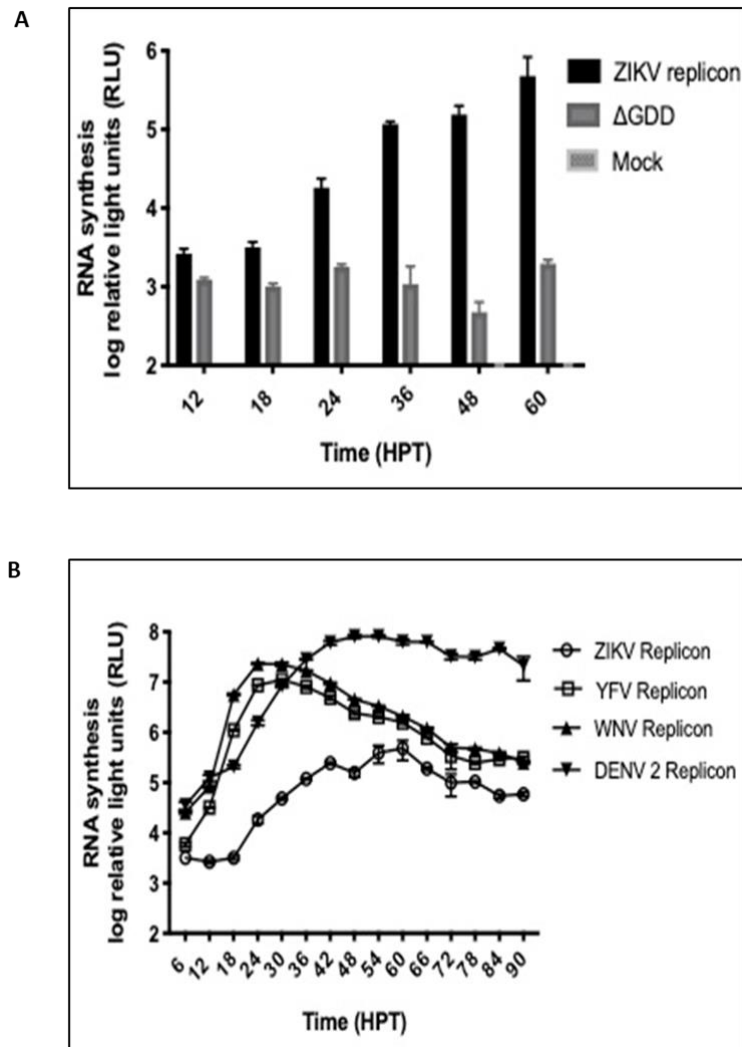
Fig. 5.2 Characterization of Zika replicon. A) Transient luciferase assay over a 60 hour time period. Equal amounts of wild type ZIKVRLuc and ZIKVRLuc ΔGDD were electroporated in BHK-15 cells. Lysates from the transfected cells were collected, clarified by centrifuge and *Renilla* luciferase activity measured at indicated time points. The means and standard error of means (SEM) are shown. B) Comparison of replication kinetics of different flaviviral replicons. *Renilla* luciferase activity of DENV, WNV, YFV and ZIKV replicons were measured every 6 hours post electroporation up to 60 hours. Luciferase activity is expressed in relative light units (RLU) and each time point represents triplicate samples with mean and SEM shown.

5.4.2 Small molecule inhibitors of MTase

The MTase domain of the NS5 protein of flaviviruses adds a type I cap to the 5' UTR of the RNA genome. This reaction involves the use of SAM as a methyl donor and is catalyzed by the multifunctional MTase domain. The capping mechanism and the enzyme used for the capping, MTase are mostly conserved evolutionarily (166). The challenge is to selectively inhibit the MTase activity of the targeted pathogen and not the host, which needs a rational design of compounds. The presence of a conserved pocket lying adjacent to the SAM binding pocket in flaviviruses (167) can be exploited to design compounds against them rationally.

For the purpose of this study, eight different small molecule competitive inhibitors of SAM were synthesized in the laboratory of Dr. AK Ghosh, Purdue University that would be analyzed for their ability to inhibit a battery of flaviviruses. The structure of the compounds synthesized are shown in Fig 5.3.
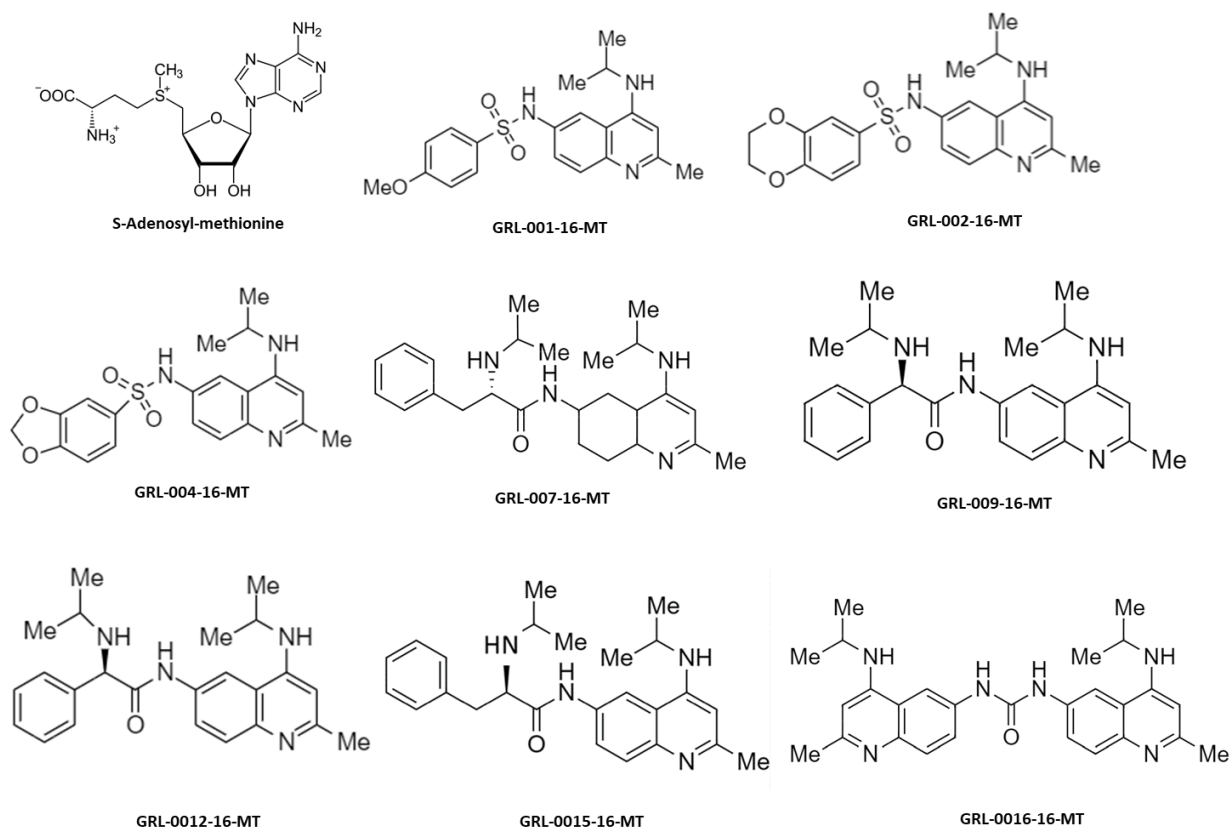
Fig. 5.3 Structure of SAM and different compounds used in this study.

5.4.3 Amino acid composition of the SAM binding pocket:

The SAM binding pocket of the MTase in chain A of ZIKV (PDB ID: 5M5B) is formed by the β-strands, β1, β2 and β4 and the α-helices αX and αA (Fig 5.4 A). The hydrophobic pocket formed by the amino acid side chains of Val138, Phe139, and Ile153 adjust the adenine base of the SAM molecule (Fig 5.4 B). Additionally, hydrogen bonds formed by Asp 137 and Lys111 stabilizes it in the pocket. The carboxylic group of Glu117 forms the hydrogen bond with the sugar molecule of SAM which is further stabilized by interactions with amino acid side chains of Ser62, Trp93, and Asp152 and main chain of Gly92 (176).
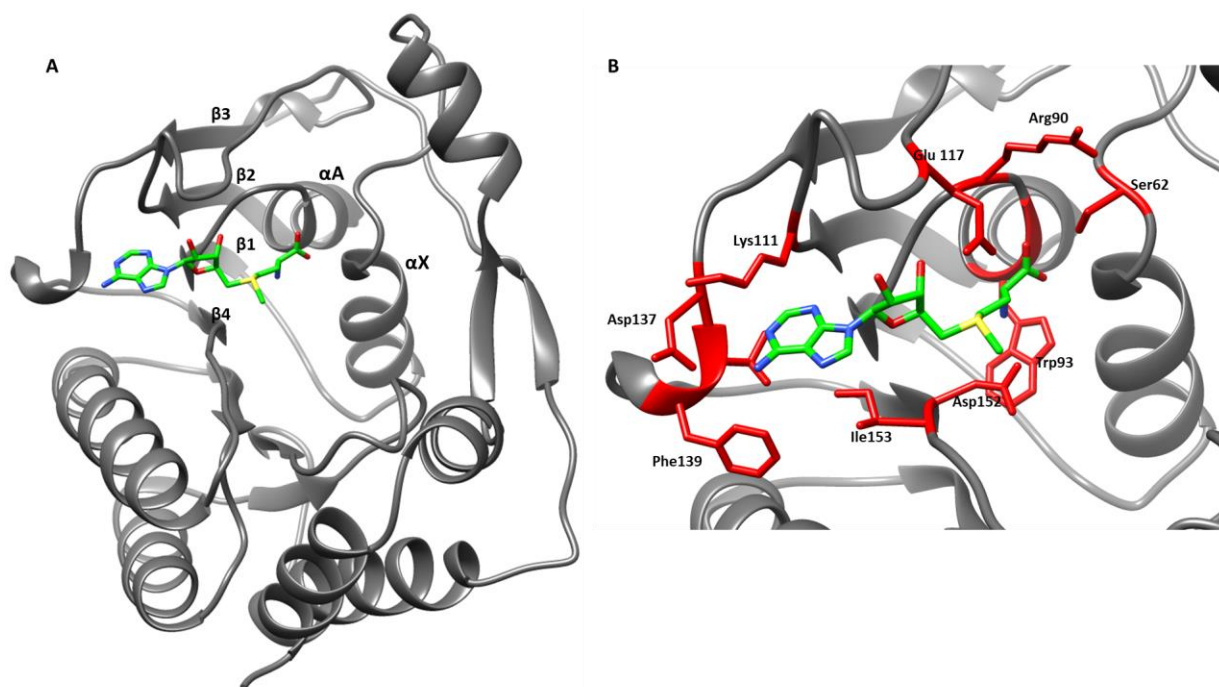
Fig 5.4 Crystal structure of ZIKV MTase (PDB ID: 5M5B). A) Ribbon diagram of ZIKV MTase chain A showing the β-strands and α-helices that form the SAM-binding pocket. B) Zoomed in view of the SAM-binding pocket with amino acid side chains (red) that stabilize the SAM molecule colored in green.

Since the small molecule inhibitors in this study were tested against DENV-2 and YFV in addition to ZIKV, the structural composition of the SAM-binding pockets of these MTases were compared (Fig 5.5). Most of the amino acid residues involved in the stabilization of SAM in the pocket were same in all three MTases except for Lys111, Val137 and Phe138 which were replaced by Leu111, Ile137 and His138 in YFV MTase (Fig 5.5 A).

A

		1	11	21	31	41	51	61
Consensus		.TLGEkWKar	LNalskseFq	iYKksgIqEV	dReeArralk	rGkad.ghAV	SRGsAKLRWf	vERgyvqpeG
Conservation		**** ** .	** :. :*	**::.* **	* *:. :	* . **	***:*****:	**. : *
DENV-2_3EVG	8	.TLGEKWKSR	LNALGKSEFQ	IYKKSGIQEV	DRTLAKEGIK	RGETD.HHAV	SRGSAKLRWF	VERNMVTPEG
ZIKV_5m5b	12 E	TLGEKWKAR	LNQMSALEFY	SYKKSGITEV	CREEARRALK	DGVATGGHAV	SRGSAKLRWL	VERGYLQPYG
YFV 17D_3EVA	6 K	TLGEVWKRE	LNLLDKRQFE	LYKRTDIVEV	DRDTARRHLA	EGKVDTGVAV	SRGTAKLRWF	HERGYVKLEG

		71	81	91	101	111	121	131
Consensus		kViDLGCGRG	GWsYYaaaik	kVqeVKGyTk	GgpGHEePmp	vqsyGWNivr	lksgvDvfhi	apekCDTLLC
Conservation		:*:*******	**.**.. :	:* *** **	* ***:*:	:.: *** ::	::. .*:. : .	******
DENV-2_3EVG	76	KVVDLGCGRG	GWSYYCGGLK	NVREVKGLTK	GGPGHEEPIP	MSTYGWNLVR	LQSGVDVFFI	PPEKCDTLLC
ZIKV_5m5b	82	KVIDLGCGRG	GWSYYAATIR	KVQEVKGYTK	GGPGHEEPML	VQSYGWNIVR	LKSGVDVFHM	AAEPCDTLLC
YFV 17D_3EVA	76	RVIDLGCGRG	GWCYYAAAQK	EVSGVKGFTL	GRDGHEKPMN	VQSLGWNIIT	FKDKTDIHRL	EPVKCDTLLC

		141	151	161	171	181	191	201
Consensus		DIGESSsspe	vEaaRTlRVL	smVekWL..r	.ptqFCikVL	aPYmpsviEk	lEaALQRryGG	alvRnPLSRN
Conservation		******...	.* **:***	.* .**	**:***	** . ::*.	:* ***::**	::* *****
DENV-2_3EVG	146	DIGESSPNPT	VEAGRTLRVL	NLVENWL..N	NNTQFCIKVL	NPYMPSVIEK	MEALQRKYGG	ALVRNPLSRN
ZIKV_5m5b	152	DIGESSSSPE	VEEARTLRVL	SMVGDWLEKR	.PGAFCIKVL	CPYTSTMMET	LERLQRRYGG	GLVRVPLSRN
YFV 17D_3EVA	146	DIGESSSSSV	TEGERTVRVL	DTVEKWLACG	.VDNFCVKVL	APYMPDVLEK	LELLQRRFGG	TVIRNPLSRN

		211	221	231	241	251	261
Consensus		STHEMYwVSg	AssNiissVn	qtSrlLirRm	rrpykkvtyE	aDViLgsGTR	a..
Conservation		******:**.	* .* :*.	*::*: *:	.. *	** ** ***	
DENV-2_3EVG	214	STHEMYWVSN	ASGNIVSSVN	MISRMLINRF	TMRYKKATYE	PDVDLGSGTR	N..
ZIKV_5m5b	221	STHEMYWVSG	AKSNTIKSVS	TTSQLLLGRM	DGPRRPVKYE	EDVNLGSGTR	AV.
YFV 17D_3EVA	215	STHEMYYVSG	ARSNVTFTVN	QTSRLLMRRM	RRPTGKVTLE	ADVILPIGTR	S.V

B

Fig 5.5 Sequence alignment and structural comparison of MTase domains of ZIKV (PDB ID: 5M5B), DENV-2 (PDB ID: 3EVG) and YFV 17D (PDB ID: 3EVA). A) Amino acid sequence alignment of NS5 MTase domains using Chimera software. The amino acid residues different in YFV compared to ZIKV and DENV-2 involved in SAM-binding are highlighted in red. B) Superposition of chain A of ZIKV MTase (blue), DENV-2 MTase (pink) and YFV MTase (golden) bound to SAM (green). Amino acid residues, Leu111, Ile137 and His138 unique to YFV MTase SAM-binding pocket are highlighted in red.

161

5.4.4   Virtual Screening using AutoDock Vina

Based on the SAM-binding pocket in the MTase domain, all eight small molecule compounds were docked into the NS5 MTase domains of ZIKV, DENV-2 and YFV using AutoDock Vina, the docking scoring of which is based on the PDBbind data. Default settings from Vina were used to dock the compounds against the rigid receptors, MTases. The hits of each compounds were ranked on the docking score/energy. To this end, all the eight small molecule inhibitors were docked against the flaviviral MTases (Fig 5.6) and the best energy score for each compound shown in Table 5.1
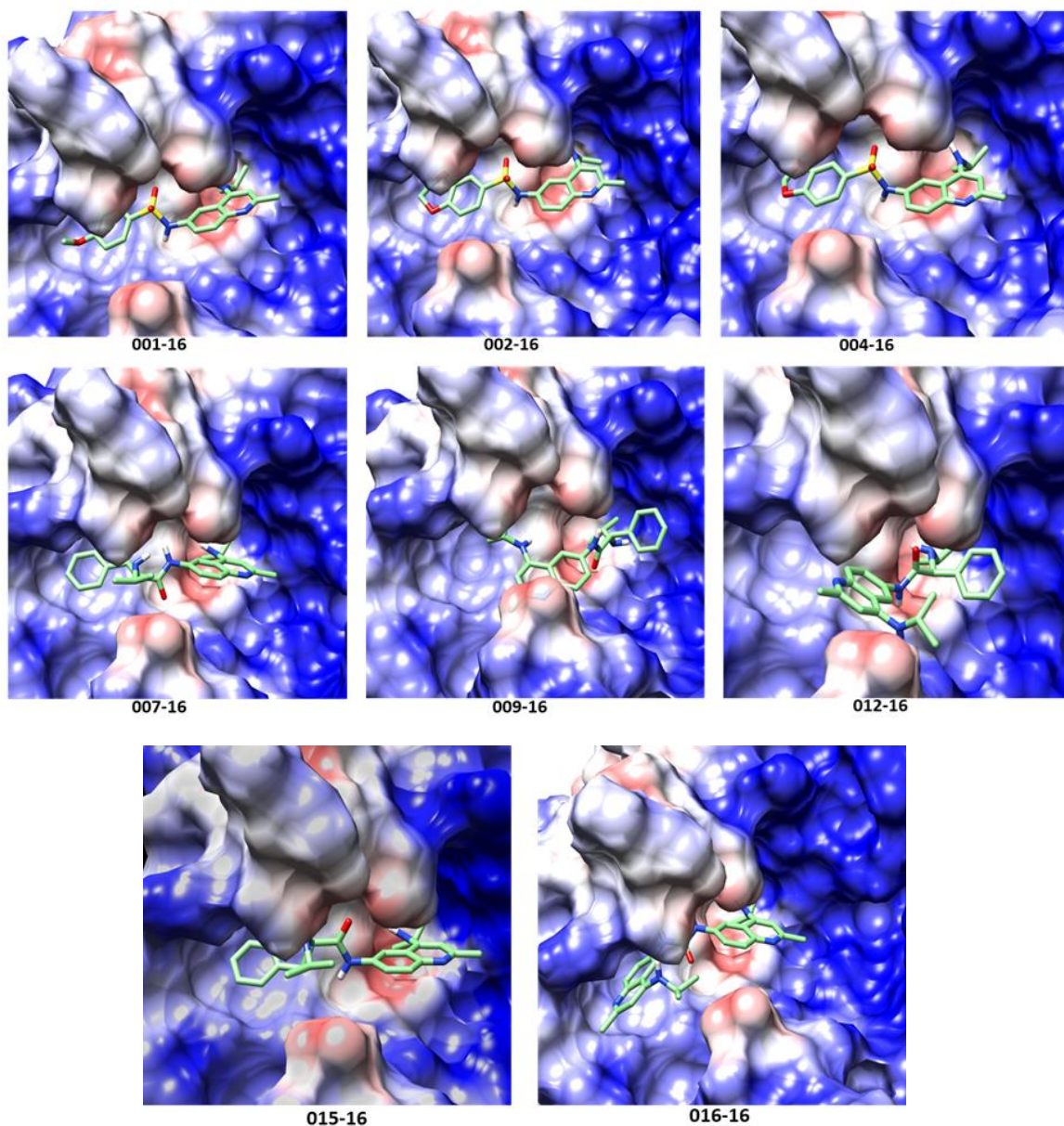
Fig, 5.6 Proposed docking of the small molecule inhibitors against MTases of ZIKV (PDB code 5M5B), DENV-2 (PDB code 3EVG) and YFV 17D (PDB code 3EVA). A) Docking of small molecule inhibitors against MTase of ZIKV within the SAM-binding pocket. An adjacent pocket is present next to SAM-binding pocket. B and C) Docking of small molecule inhibitors against DENV-2 and YFV, respectively.

Figure 5.6 continued

Figure 5.6 continued

001-16

002-16

004-16

007-16

009-16

012-16

015-16

016-16
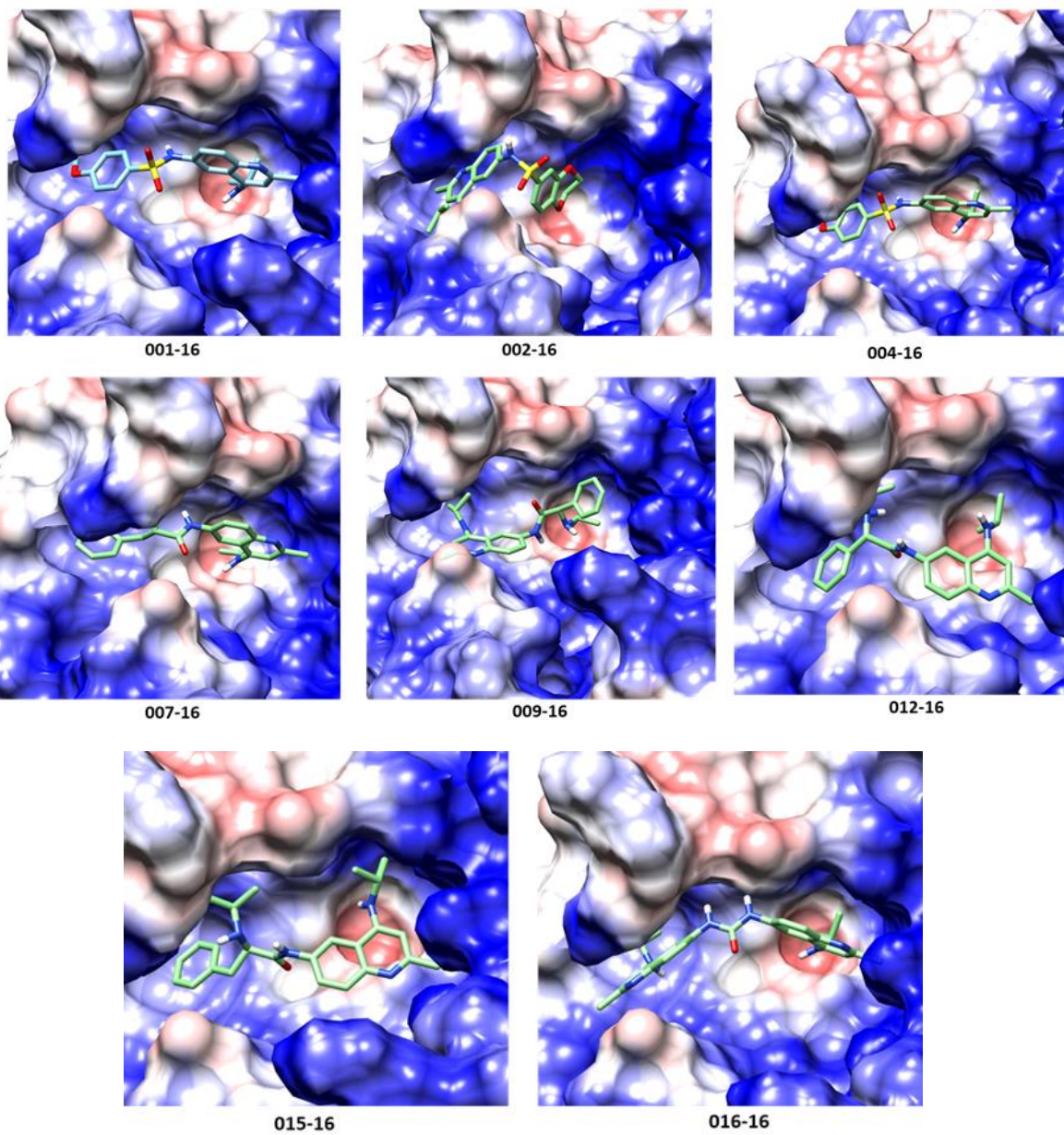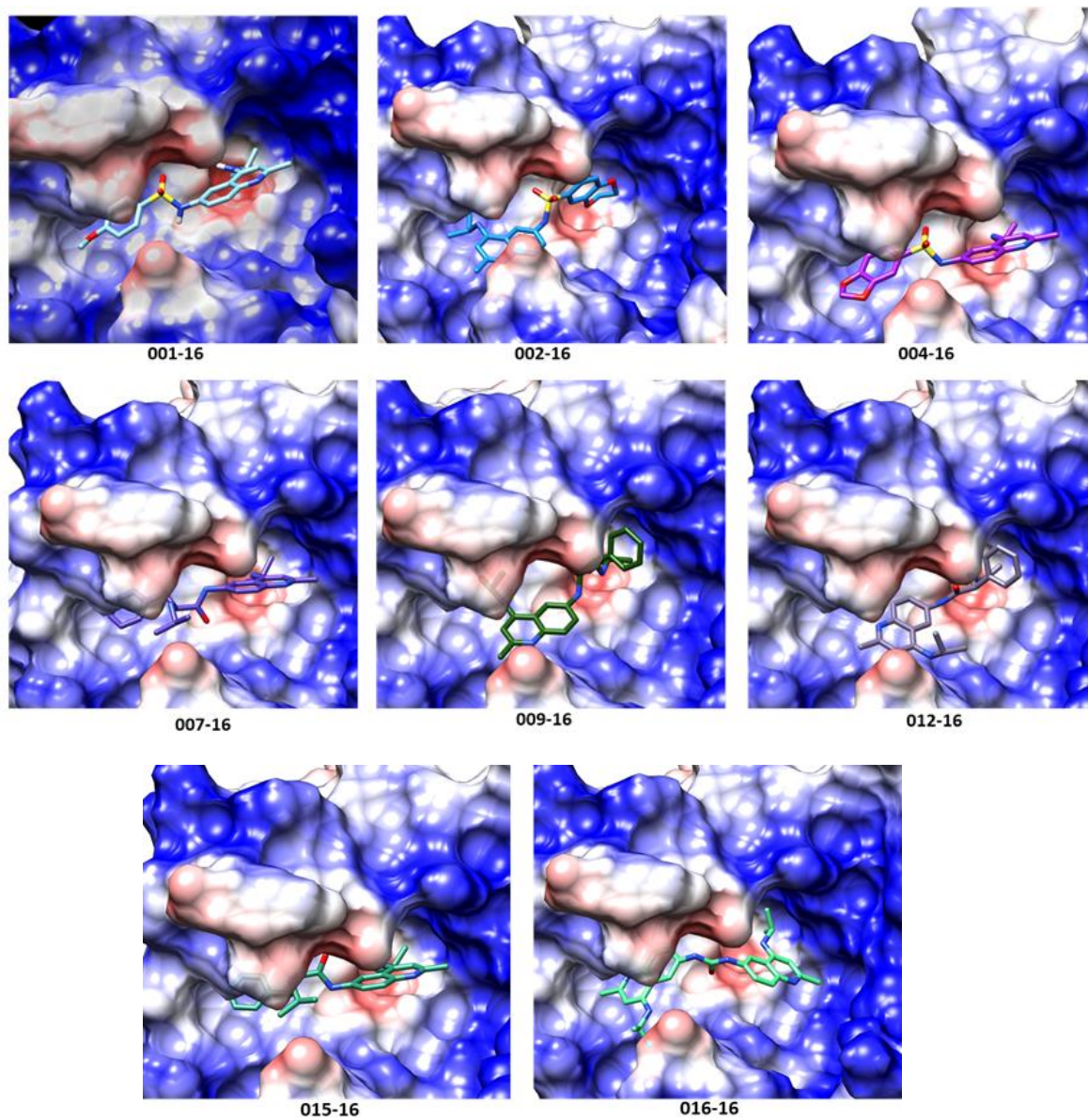
Table 5.1 Docking score generated by AutoDock Vina for small molecule inhibitors against MTases of ZIKV, DENV and YFV

Docking Score			
Compound	ZIKV	DENV-2	YFV
GRL-001-16-MT	-8.6	-8.6	-8.8
GRL-002-16-MT	-9.5	-8.4	-8.9
GRL-004-16-MT	-8.9	-9.1	-9.1
GRL-007-16-MT	-8.5	-9.4	-9.1
GRL-009-16-MT	-7.6	-8.2	-7.9
GRL-012-16-MT	-8.7	-8.1	-8.1
GRL-015-16-MT	-7.6	-8.8	-9.3
GRL-016-16-MT	-9.5	-9.5	-9.2

The docking scores obtained in the AutoDock Vina are derived from PDBind data set and represent the binding affinity (free energy of binding) of the compound in kcal/mol. The scoring function takes into consideration the number of favorable intermolecular hydrogen bonding as well as hydrophobic contacts that a certain pose make with the target molecule. The higher the energy scoring, the compound in question is more likely to fit in the binding pocket and bring about the desired effect.

5.4.5   Determination of cell cytotoxicity of the compounds

Before moving on to test the antiviral activity of the compounds, we tested these compounds for their suitability to be used in a living system. For this purpose, we tested the Cell Cytotoxicity (CC_{50}) value of all the eight compounds using a standard WST (Tetrazolium salt) assay measuring cellular proliferation in the presence of compound as a function of cellular mitochondrial dehydrogenase activity. Since two different types of cells were used in the study, CC_{50} of the compounds against both the Vero cells as well as the BHK cells were determined. The results are summarized in Table 5.2.

Table 5.2 CC_{50} values of different compounds on Vero and BHK cells

CC_{50} (µM)		
Compound	**Vero cells**	**BHK cells**
GRL-001-16-MT	>100	>100
GRL-002-16-MT	>100	>100
GRL-004-16-MT	>100	>100
GRL-007-16-MT	78.3	>100
GRL-009-16-MT	22.1	19.5
GRL-012-16-MT	49.4	42.0
GRL-015-16-MT	56.0	57.7
GRL-016-16-MT	43.5	>100

5.4.6 Determination of antiviral activity of the compounds against ZIKV

Eight different compounds (GRL-001, 2, 4, 7, 9, 12, 15, 16- 16MT) were screened for their ability to inhibit ZIKV replication using a viral system followed by screening of select compounds against the newly constructed ZIKV replicon. Of the 8 different compounds tested against ZIKV, 004-16-MT appeared to be the most effective against ZIKV with an IC_{50} value of 3.6 µM followed by 002-16-MT (Fig 5.7 A). However, selective index (SI) couldn't be calculated for these compounds as the cytotoxicity was tested only up to 100 µM. Both of these compounds scored highly when these compounds were docked against ZIKV MTAse. Compound 007-16-MT, on the other hand, was able to inhibit ZIKV at an IC_{50} value of 18.9 µM; however, the lower CC_{50} was a drawback for this compound. For the compounds: GRL 009-16 and 0012-16, the cell cytotoxicity was of major concern. Because of the low CC_{50} values of these compounds, IC_{50} values for compound inhibition could not be calculated accurately. GRL-0015-16 and 0016-16 both had low IC_{50} values, but they were also compromised in their activities because of relatively poor CC_{50} values. The calculation of IC_{50} values become increasingly difficult and inconsistent with lowered CC_{50} values. The results from these experiments are summarized in Table 5.3.

Table 5.3 Summary of cytotoxicity and inhibitory concentration values of the compounds used in the study against ZIKV

Replication of ZIKV in Vero cells			
Compound	[a]CC_{50} (μM)	[b]IC_{50} (μM)	[c]SI (CC_{50}/IC_{50})
GRL-001-16-MT	>100	66.8	>1.5
GRL-002-16-MT	>100	12.3	>8.1
GRL-004-16-MT	>100	3.6	>27.8
GRL-007-16-MT	78.3	17.7	4.4
GRL-009-16-MT	22.1	-	-
GRL-012-16-MT	49.4	-	-
GRL-015-16-MT	56.0	17.4	3.2
GRL-016-16-MT	43.5	13.3	3.3

[a]CC_{50}: CC_{50} values in μM were calculated after normalizing data to 100% cell viability based on 0.5% DMSO treated cells. Each experiment was carried out in triplicate

[b]IC_{50} values were calculated from viral titer reduction assay experiments that were done in triplicate.

[c]SI= CC_{50}/IC_{50}

CC_{50} and IC_{50} (wherever applicable) values were calculated using GraphPad prism 7 using a non-linear regression fit analysis.

To further quantify the inhibitory effects of these compounds, GRL-002-16, GRL-004-16 and GRL-0016-16-MT were tested using a ZIKV replicon Fig 5.7 B. Of the three compounds tested using the replicon system, GRL-016 was the most inhibitory followed by GRL-002 and GRL-004-16-MT. All 3 compounds were near equally effective with replicon experiments, but GRL-002-16-MT and GRL-004-16-MT stood out as being the most inhibitory without being cytotoxic. There was an apparent difference in the IC_{50} values obtained using two different systems, which also utilized two different cell lines. The differences can be in part attributed to use of Vero cells for virus infection versus BHK cell lines for the replicon system.

A

B
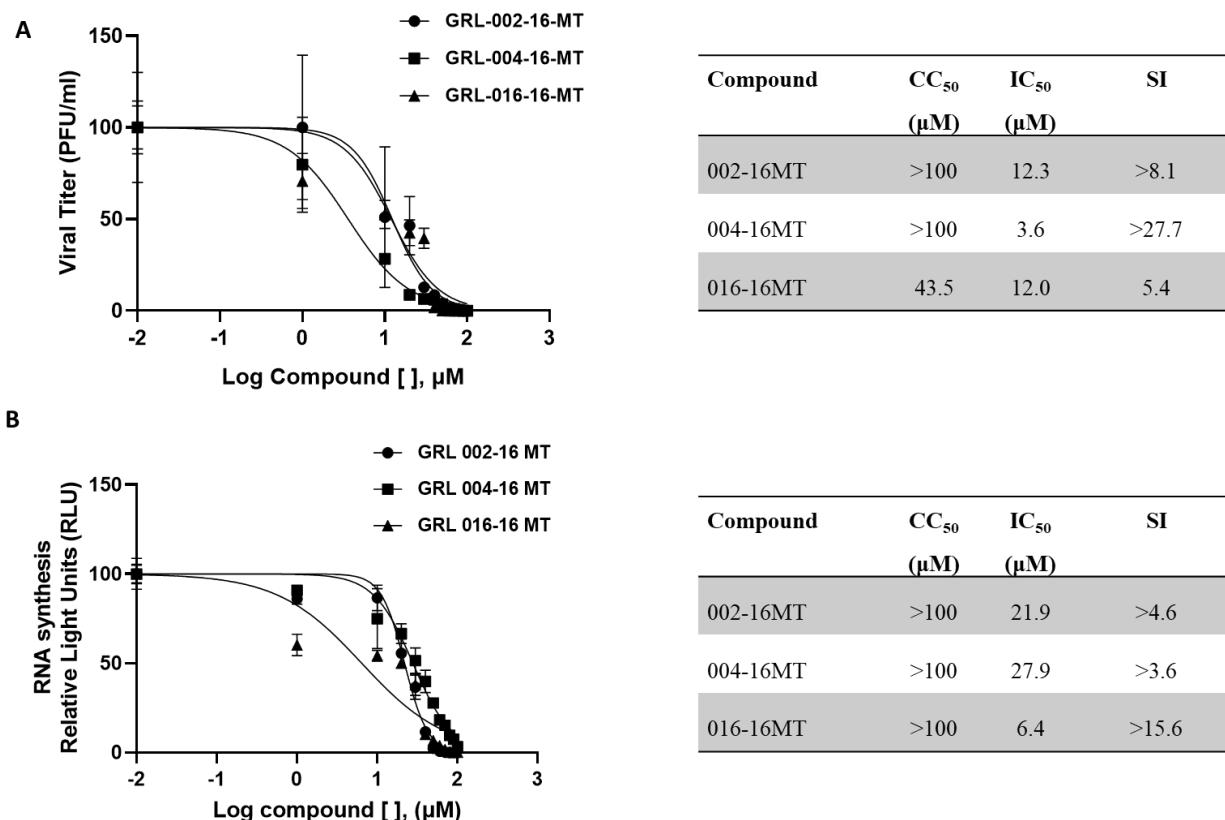
Fig. 5.7 Antiviral activity of select N-7-MTase inhibitors against ZIKV A) Antiviral activity of compounds GRL-002-, GRL-004- and GRL-016-16-MT using ZIKV plaque reduction assay. Vero cells at a confluency of ~90% were infected with ZIKV at an MOI of 5. The cells were washed after viral attachment, and overlayed with media containing different dilutions of each compound. Supernatants collected after 72 HPI were subjected to plaque assays to determine the virus titer and subsequently the IC_{50} B) Antiviral activity of compounds GRL-002-, GRL-004- and GRL-016-16-MT using ZIKV replicon. BHK cells were electroporated with 10 μg of WT replicon RNA and the transfected cells were immediately treated with different dilutions of compounds or 0.5% DMSO as a control. The luciferase activities were measured at 48 HPE. The *Renilla* luciferase activity from 0.5% DMSO control was used as 100%

Table for panel A (ZIKV plaque reduction assay):

Compound	CC_{50} (μM)	IC_{50} (μM)	SI
002-16MT	>100	12.3	>8.1
004-16MT	>100	3.6	>27.7
016-16MT	43.5	12.0	5.4

Table for panel B (ZIKV replicon):

Compound	CC_{50} (μM)	IC_{50} (μM)	SI
002-16MT	>100	21.9	>4.6
004-16MT	>100	27.9	>3.6
016-16MT	>100	6.4	>15.6

5.4.7 Determination of antiviral activity of the compounds against DENV and YFV

The small molecule inhibitors were further tested for their ability to inhibit replication of other members of the flaviviruses i.e. DENV-2 and YFV. Screening of these compounds against DENV was done using the replicon developed in our laboratory. Of the 8 different inhibitors tested against DENV, GRL-016- and -007-16 were the most promising compound with an IC_{50} values of

14.6 μM and 31.7 μM with CC_{50} value above 100 μM. The docking scores of these compounds were among the highest among the compounds docked against DENV MTase (Table 5.1). As the CC_{50} for these compounds were not tested above 100 μM, we were unable to determine the exact SI value for these compounds. GRL-009, -012, and -015 compounds were cytotoxic to BHK cells to varying degree with GRL-009-016 being the most cytotoxic with 19.5 μM CC_{50} value. However, these compounds showed promising IC_{50} values. Side chain modifications to these compounds could be promising in developing more potent inhibitors of DENV. The effect of these compounds on DENV replication is depicted in Fig 5.8.
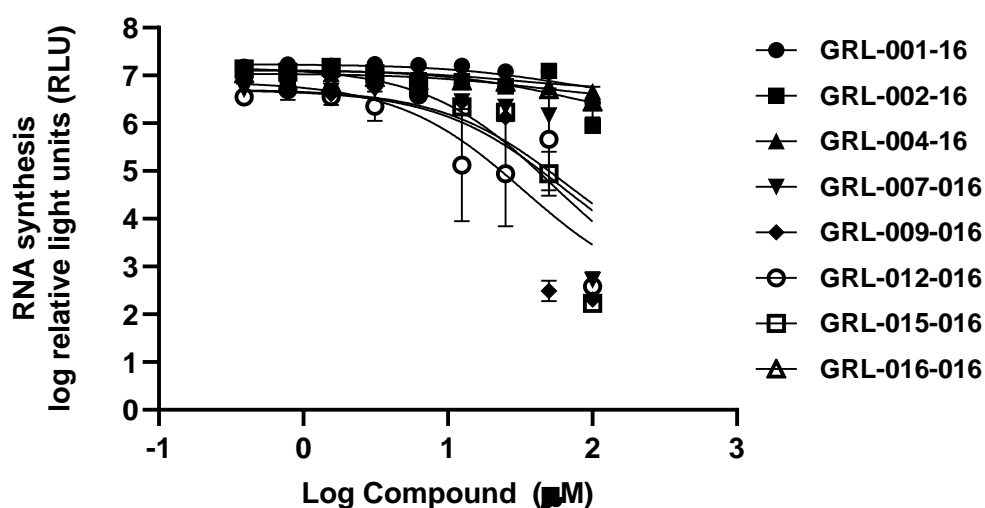
Fig. 5.8 Antiviral activity of N-7-MTase inhibitors against DENV. Antiviral activity of all the eight compounds were tested against DENV using a DENV replicon system. BHK cells were electroporated with 10μg of DENV replicon RNA, the transfected cells were immediately treated with different dilutions of compounds or 0.5% DMSO as a control. The BHK cell lysates were collected at 48 HPE and the luciferase activities were measured after clarifying the lysate. *Renilla* luciferase activity from 0.5% DMSO control was used as 100%
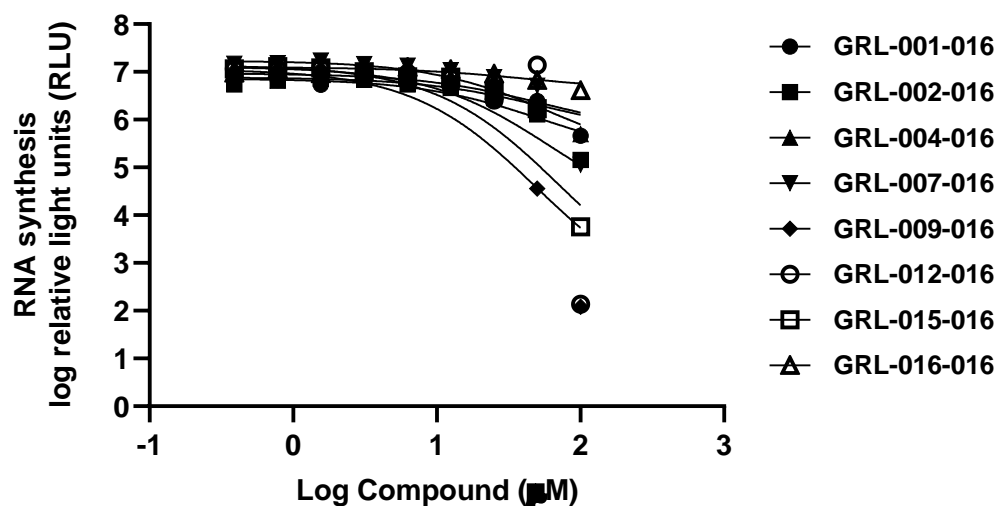
Fig. 5.9 Antiviral activity of N-7-MTase inhibitors against YFV. Antiviral activity of all the eight compounds were tested against YFV using a YFV replicon system. BHK cells were electroporated with 10µg of YFV replicon RNA, the transfected cells were immediately treated with different dilutions of compounds or 0.5% DMSO as a control. The BHK cell lysates were collected at 24 HPE and the luciferase activities were measured after clarifying the lysate. *Renilla* luciferase activity from 0.5% DMSO control was used as 100%

Similarly, all these compounds were tested against YFV using a YFV replicon constructed in our lab. The luciferase activities were measured from the BHK cells transfected with YFV replicon and treated with different concentrations of the compounds. Interestingly, the activities of these compounds against YFV and DENV varied significantly. The most effective compound GRL-0016-16 against DENV was not effective against YFV even though the docking scores of these compounds against respective MTases were comparable demonstrating the compounds unique inhibitory specificity. Whereas, compound GRL-002-016 which was not inhibitory to DENV showed the most promising effect with an IC_{50} value of 38.8 µM. Relatively, YFV showed a broad range of resistance to these compounds compared to DENV. The activity of these compounds in inhibiting YFV replication is shown in Fig 5.9.

Compound GRL-007-016 showed broad range inhibition of both DENV and YFV with an IC_{50} value of 31.7 and 53.5 µM, respectively. Moreover, both compounds were not cytotoxic at a concentration of 100 µM which provides a platform to work on modification of these compounds

to make it more potent. Compounds GRL-0012-16 and GRL-0015-16, despite being cytotoxic at a concentration less than 100 μM were also potent inhibitors of DENV and YFV replication. Importantly, compound GRL-009-16, which was cytotoxic to Vero cells was also cytotoxic to BHK cells, thus the efficacy of this compound could not be determined accurately. The results of these experiments are summarized in Table 5.4.

Table 5.4 Summary of CC_{50}, IC_{50} and SI of different small molecule inhibitors against DENV and YFV.

Replication of DENV and YFV in BHK cells					
Compound	[a]CC_{50} (μM)	DENV		YFV	
		[b]IC_{50} (μM)	[c]SI (CC_{50}/IC_{50})	[b]IC_{50} (μM)	[c]SI (CC_{50}/IC_{50})
GRL-001-16-MT	>100	66.3	1.6	81.4	1.3
GRL-002-16-MT	>100	>100	-	38.8	>2.6
GRL-004-16-MT	>100	53.9	>1.9	>100	-
GRL-007-16-MT	>100	31.7	>3.2	53.5	>1.9
GRL-009-16-MT	19.5	10.5	1.9	-	-
GRL-012-16-MT	42.0	7.6	5.5	6.3	6.7
GRL-015-16-MT	57.7	6.6	8.7	20.1	2.9
GRL-016-16-MT	>100	14.6	>6.8	No Inhibition	-

[a]CC_{50}: CC_{50} values in μM were calculated after normalizing data to 100% cell viability based on 0.5% DMSO treated cells. Each experiment was carried out in triplicate

[b]IC_{50} values were calculated from Luciferase assay experiments using DENV and YFV replicons that were done in triplicate.

[c]SI= CC50/IC50

CC_{50} and IC_{50} (wherever applicable) values were calculated using GraphPad prism 7 using a nonlinear regression fit analysis

5.5   Discussion

There are no approved chemotherapeutic agents against ZIKV or any other flaviviruses. The recent outbreak of ZIKV, once a neglected pathogen, underscores the need for identification and development of anti-flaviviral therapeutics. We screened eight different compounds that could compete with binding of SAM against ZIKV using a plaque reduction assay as well as a cell-based

replicon assay. This was further extended to two other members of the flaviviruses having global public health importance, DENV and YFV. Here we tested compounds that were synthesized to compete with AdoMet during the 5' capping of flaviviral RNA by the MTase domain of NS5. Using a newly constructed Zika replicon system as well as ZIKV, we were able to identify three compounds, GRL 002-16-, 004-16- and 007-16-MT that were able to inhibit ZIKV replication with low IC_{50} values and which could be promising candidates for further modifications to develop them into more potent compounds. Moreover, compounds that were effective against either one or both DENV and YFV were discovered in the current study.

Luciferase-based ZIKV replicons have been previously described (175, 177). Replicons can be used to easily screen efficacy of different compounds avoiding the risk of handling infectious virus. Even though replicons can't be used to study compounds targeted against viral entry, release and maturation, they can readily be used to screen compounds that target the nonstructural proteins (178). Even though in vitro enzyme inhibition assays are more quantitative, replicon-based assays, where permeability of the compounds has to be taken into account, would be closer to animal models, and can be the first significant step in developing potent antivirals (179). The pZIKVRLuc described in this study was used to screen anti ZIKV compounds targeting the capping enzyme.

The pZIKVRLuc showed a gradual but significant increase in luciferase activity compared to the replication deficient construct pZIKVRLuc ΔGDD over 12 to 60 hours post transfection with a replication peaking at 48 hours to 60 hours. The replication kinetics of the ZIKV replicon was compared to other flaviviral replicons. Unlike YFV and WNV, ZIKV replicon had a short lag phase before a gradual increase in luciferase signal was observed. Xie *et al.*, reported a comparable pattern of luciferase activities for their replicon construct (175). This delay can be attributed to the use of less permissible BHK-15 cells for these experiments. Due to poor efficiency of Vero cells to electroporation, BHK cell lines were used throughout this study for ZIKV replicon assays. Moreover, the replication kinetics seemed more comparable to DENV than WNV or YFV with the replication peaking up from 48 hours to 60 hours.

Of the 8 compounds tested against ZIKV, three of them were promising while the remaining compounds exhibited either high IC_{50} values or were highly cytotoxic to the cells. The three compounds that were examined further using the ZIKV replicon assay showed relatively different

IC_{50} values, compared to the IC_{50} value obtained from the plaque reduction assay. This might be due to the use of different cell lines in the viral system (Vero) versus the replicon system (BHK) for each experiment. The replication kinetics of virus differs in different cell lines owing to different innate immunological factors. Vero cells are known for the acquired absence of type 1 IFN locus and relatively inefficient interferon regulator factor 3 (IRF3), a trait different than BHK cells (180). Moreover, when using a viral system several factors like entry, assembly and exit have to be taken into consideration unlike a replicon system, which directly introduces an infectious genome into the cells (181).

YFV and DENV replicons were also used to test the potency of the compounds against these viruses. These compounds, based on their abilities to inhibit viral replication, could be classified into two groups: compounds showing dual inhibition or specific against either DENV or YFV (Table 5.4). Three of the compounds; GRL-007-, GRL-0012- and GRL-0015-MT were active against both DENV and YFV with low micromolar IC_{50} values, however, GRL-0012- and GRL-0015 were comparatively more cytotoxic. Inhibition shown by these compounds across different flaviviruses can be explained by the amino acid conservation of the MTase domain as well as conservation of the AdoMet binding pocket among the flaviviruses (167). Amino acid residues that stabilizes the SAM molecule in the conserved MTase pocket were analyzed. Interestingly, only YFV MTase had Leu111, Ile137 and His138 instead of conserved Lys111, Val137 and His138. This might have affected some of the differential activities seen in YFV compared to ZIKV and DENV. The structure of the compounds, their permeability across different cell lines, and their off-target activities among others play a major role in their ability to inhibit viral replication without being cytotoxic. Interestingly, compound GRL-002-MT was specifically active against YFV whereas compounds GRL-004-16- and GRL-0016-MT were effective against DENV only. The specificity of some of these compounds can be defined in part by the way they dock against the respective MTase. For example, the docking score of GRL-002-MT is higher in YFV compared to DENV. Although, some of these compounds have higher docking score compared to other, their lower CC_{50} resulted in them being less effective. Moreover, the MTase of ZIKV has 61% and 55% sequence identity respectively with DENV and YFV (182). Even though they form similar structures, the way these compounds interact with the AdoMet binding pocket may be different which can contribute to their specificity against one virus and not others. Also, flaviviral MTase have an extra pocket lying adjacent to AdoMet binding site forming an

extended pocket, which is highly hydrophobic in nature (11, 12). All three flaviviruses used in this study have same amino acid composition in the extended pocket region suggesting properties of these compounds and the nature of their interactions with the extended pocket may determine their efficacy in inhibiting the flaviviral replication. Similar kind of study testing the efficacy of compounds which were already proven to be effective against DENV, $GpppAC_4$ and A_{27}, against MTase of ZIKV showed these compounds inhibit ZIKV with low IC_{50} compared to DENV and were more potent (176).

In summary, the current study investigated the potency of several flaviviral N-7 MTase inhibitors using an established replicon system for dengue and yellow fever as well as a newly constructed ZIKV replicon system. The ZIKV replicon can be used to study several aspects of viral replication as well as can be used to develop a virus like particle (VLP) system for high throughput compound screening. Moreover, we were able to narrow down few compounds that inhibited ZIKV, DENV and YFV with low IC_{50} values and can be used as starting molecules for development of more potent inhibitors.

CHAPTER 6.   CONCLUSIONS AND FUTURE DIRECTIONS

6.1   The 2K signal peptides of flaviviruses are not functionally conserved

The concept of signal peptides carrying less information and being readily interchangeable was put to test in the current study and was disproved using a chimeric (2K) DENV-2 as a model system. The 2K peptides of DENVs are unique to each serotype and play roles beyond signal sequence was supported by several sets of evidence.

First, the chimeric viruses with signal peptides from ZIKV or human RAGE protein, switched in place of 2K, were not viable. The chimeric viruses were replication incompetent, suggesting a lack of proper translocation of protein or rapid degradation/misfolding resulting in the lack of formation of active replication complex. This observation pointed to the evolutionary conservation of the signal peptides and the protein they help translocate or secrete. A successful biogenesis of an ER membrane protein like NS4B depends on several factors. A significant portion of the success depends on a balanced interaction between signal peptides, the Sec61 translocation machinery, chaperones and various proteases. Any changes in the translocation efficiency (increased or decreased) of the substrate protein because of a heterologous signal peptide, results in improper folding of the target protein and activation of stress related protease resulting in their degradation (48).

Second, the interserotypic DENV-2 chimeric viruses with 2K peptide from either DENV-3 or DENV-4 were severely affected in replication and their ability to release infectious particles. These observations not only point to the different information each signal peptides carry, even if they are very closely related, but also their substrate specificities. The 2K peptide from DENV-3 won't be able to properly translocate the NS4B from DENV-2 suggesting an optimal match between a signal peptide and a target protein as an essential first step in the biogenesis of that protein. Even if the heterologous signal peptide can translocate the protein to the ER lumen, the resultant precursor protein might not be processed properly by the host cell signalase. As shown in Chapter 2, both the interserotypic chimeras (Den 2K (2→3) and Den 2K (2→4)) were deficient in signalase cleavage at the 2K-NS4B junction. The observed result when taken in the context of target protein (NS4B) only, suggests a requirement for specificity at the structural level for

different signal peptides. Also, 2K peptides from different serotypes interact differentially with the translocation machinery owing to the differences in their sequences. The interserotypic chimeric viruses with deficient 2K-NS4B cleavage were capable of replicating, albeit to reduced level, raising the question of role of signalase cleavage of the 2K peptide as well as the role of precursor protein vs the mature protein. In the cells expressing KUNV NS4A-2K, the resultant membrane rearrangements were comparable to KUNV infected cells, suggesting the requirement of 2K in bringing about the membrane rearrangements in the infected system (72). Whereas in the case of cells expressing DENV precursor proteins, NS4A without 2K expression closely resembled the membrane rearrangements seen in the DENV infected cells (75). Taken together these observations, and the temporal and spatial coordination of cleavage at NS4A-2K-NS4B junction, it is easy to deduct that there are partially cleaved, uncleaved and mature NS4A and NS4B in a viral infected system and 2K as a signal peptide regulates this event. A more detailed study of how these precursor proteins affect viral life cycle would be very helpful. A recent study revealed region within NS1 that interacts only with the NS4A-2K-NS4B precursor protein and not with the mature NS4A or NS4B in bringing about the enhancement in RNA replication independent of membrane rearrangements (36). It would be interesting to see how different the replication factories are in the interserotypic chimeric viruses and how the interaction between NS1 and the precursor protein is affected in a system where no mature NS4B protein is produced.

Third, mutations of select amino acid residues of 2K demonstrated effect on viral replication without affecting the 2K-NS4B cleavage, suggesting a direct role of 2K in DENV replication. Signal peptides have been established to play role independent of their signal activity. Signal peptide of Foamy virus envelope glycoprotein gp18 gets incorporated in viral particles and interacts with Gag proteins and controlling the amount of viral and sub-viral particles coming out of infected cells by ubiquitination (131). Similarly, mutations within capsid anchor peptide have been shown to interfere with ability of virus to effectively incorporate nucleocapsid and produce infectious particles (69). Any residue changes in the signal sequence might affect the total charge, potential energy and the dipole moment (183). Hence, in silico measurement of the changes arising from mutations of individual amino acid residue would be a welcome event to further characterize the function of these peptides. As described in Chapter 2, residues like Val18 and Ala20 affected viral replication without interfering signalase cleavage. Similarly, mutations of the conserved patch "DNQL" directly affected the viral replication. To this end, all these mutational analyses

177

were done in either a replicon or a viral system which has several limitations. If because of a mutation, there is no replication, one won't be able to tell whether enough protein is being formed or not, if the protein is being targeted properly to the ER or not. Hence, if these mutations were introduced in a pcDNA-like system, where the expression and localization of the protein could be studied, it would shed more light in the role of individual amino acids of 2K signal peptide.

6.2   2K-NS4B and NS4B coordinate a productive infectious particle release

Flavivirus assembly is a complex and highly regulated process where newly synthesized RNA genomes in the replication sites are transported to assembly site for encapsidation and envelopement. A successful packaging and release of the virus involves interplay between various viral and host proteins. Several replication proteins have been shown to play a major role in virion assembly and infectious particle release. NS1 interacts with structural proteins and aids in infectious particle production (138). NS2A of flaviviruses has recently been shown to orchestrate virion assembly. NS2A by interacting with the 3'UTR of the newly synthesized RNA initiates packaging by recruiting C-prM-E polyprotein to the assembly site (28). Similarly, our lab showed that a W349A mutation in the helicase domain of NS3 abrogates YFV assembly without affecting viral replication (139). Moreover, two different species of NS2A have been reported in DENV infected cells, each set playing a distinct role in replication and viral assembly (27). Our data in Chapter 3 demonstrated that NS4B also has two distinct sets of molecules, 2K-NS4B and NS4B at any given time in a DENV infected cells and these molecules can dictate replication and packaging without being mutually exclusive. The idea of a differential role of precursor protein 2K-NS4B vs. mature NS4B is supported by the finding that in the interserotypic chimeric viruses, where the signalase cleavage at 2K-NS4B junction was blocked, there was minor effect in replication, however, significant reduction in infectious particle release was observed. The notion of having distinct sets of NS4B for replication and assembly sounds tempting, however, our data from revertant virus lacking the 2K-NS4B cleavage partially disproved it. The revertant produced significantly higher infectious particles even in the absence of mature NS4B, although, these particles had reduced specific infectivity and tiny plaque morphology. This points to a synergistic role 2K-NS4B and NS4B play in the production of infectious particle. A mature NS4B might play a more effective role in helping the newly synthesized RNA genome get packaged more efficiently in co-ordination with other viral proteins that interact with NS4B.

The generation of replication competent interserotypic chimera that are significantly reduced in infectious particle production could be exploited for therapeutic purposes. One way to test for this would be using a virus infected system where a chimeric 2K-NS4B peptide is added in increasing concentration to assess if it can competitively inhibit the host signalase cleavage of viral 2K-NS4B. Studies using non-cleavable mutant protein to competitively inhibit ER signal peptidases have been reported. A preproinsulin with a mutation adjacent to the signalase cleavage site inhibited ER signalase in a dose dependent manner (184). The same protein cargo inhibited processing of HCV polyproteins. In the absence of any known and potent eukaryotic signalase inhibitor, it would be interesting to use both the chimeric 2K-NS4B peptide (from DENV-3 and DENV-4) to assess their antiviral activity.

Our data from Chapter 3 illustrated that the defect in infectious particle production in the replication competent chimeric viruses could be rescued by providing NS4B in trans, in the absence of its natural signal peptide 2K. The notion of requirement of active replication complex for a successful transcomplementation of NS4B is supported by this piece of data. The chimeric viruses with 2K replaced with signal peptide from ZIKV and RAGE protein were unable to be rescued as they were replication incompetent. Moreover, the data from Chapter 3 suggested that the ER luminal loop formed by the TMD4 and TMD5 of the NS4B is required in the packaging of the RNA genome in the chimeric viruses lacking in 2K-NS4B cleavage. This was further demonstrated by a systematic mutagenesis of the conserved residues of the ER loop. The Thr198 residue showed minor effect in replication, however, was severely depleted in infectious particle production.

It would be difficult, however, interesting to determine if the ER luminal loop is sufficient to rescue the infectious particle production. Since this is a short twenty-six amino acid peptide that is present in the ER lumen, it would be difficult to express it in a normal way without affecting its folding and other functions. An alternative way to test this would be to use another chimeric NS4B system wherein just the ER loop is from DENV-2. The next step would be determining how the luminally located ER loop is helping rescue the infectious particle production. A plausible hypothesis would be via its interaction with NS1 protein which is also located in the ER lumen and has been shown to be involved in particle production. The simplest way to figure this out would be to select for a second site revertant in NS1 using either the chimeric virus or the T198A

mutant. It would be interesting to define the interacting partners of 2K-NS4B vs mature NS4B. With the interactome thus generated, we can figure out if the cleavage of 2K by host cell signalase results into differential binding of mature NS4B, and any of these differences could be mapped to the ER loop of NS4B. It would be interesting if the signalase cleavage of 2K-NS4B leads to change in orientation of the ER loop that will modulate a differential function than when it was in the precursor form. However, we have very limited understanding of the structure of individual as well as precursor proteins of NS4A-2K-NS4B junction. There are evidence showing the regions of NS4B situated in the ER lumen participate in protein-protein interactions with host and other viral proteins. Intriguingly though, the first 125 amino acid residues of NS4B situated in the ER lumen interacted with the cytosolic IFN- α/β and inhibited their activity (71). Amino acid residues 40-76 were involved in interaction with NS4A (185). The small loop between pTMD2 and TMD3 interacts with NS1 of WNV and enhances RNA replication (78).

6.3   TMDs of NS4A and NS4B contribute to viral replication

NS4A and NS4B of DENV are multi-pass integral membrane proteins, the TMDs of which are believed to anchor the replication complex to the ER membrane. The interaction of TMDs with ER resident proteins induces membrane rearrangements resulting in formation of replication factories (146). However, their direct role in the viral life cycle remains unanswered. Chapter 4 illustrated that, the TMDs of these integral membrane proteins are unique to different serotypes. By generating interserotypic TMD chimera between DENV-2 and DENV-3, we demonstrated that, the TMDs of NS4A are not interchangeable to other DENV serotype. Any such changes resulted in a major effect in replication which significantly affected the infectious particle production. Chimeric proteins derived from closely related proteins could have several fates; new functional protein with properties encompassing its parental substrates, protein with complete loss of function or gain of function (186). The later scenarios are less informative and harder to analyze; however, a functional chimeric protein could be used as tool to study intra- and inter-protein interactions. Two of the interserotypic NS4B TMD chimeras, TMD1 and TMD3, with corresponding TMDs of NS4B from DENV-3 were demonstrated to function normally. A detailed study of differential protein-protein interactions, protein-viral RNA interaction in the chimeric viruses vs the wild type could give us a more detailed role of these TMDs and could explain the different strategies adopted by different serotypes of DENV in bringing about a successful infection.

Chimeric viruses either formed in natural habitats or generated in the laboratory have been used for studying pathogenesis, determining interaction partners of target proteins, or as a vaccine candidate for a long time. When two different strains of enteroviruses replicated within a single cell, a chimeric strain of coxsackievirus B4(CV-B4) was formed with a recombination in VP3 capsid gene (187). Generation of interserotypic chimera between DENV-2 and DENV-4 in the MTase domain resulted in drastic decrease in replication, however, an adaptive mutation in RDRP rescued the replication suggesting an interaction between MTase and RDRP domain (153). TMD5 of NS4B in 5-10% of the cases have been shown to flip back to the ER luminal side post NS2B/3 cleavage at NS4B-NS5 junction (75). The physiological significance of this mechanism is still unknown. Also, there are questions whether this phenomenon is common in all DENV serotypes. In Chapter 4, we demonstrated that a substitution of an amphipathic helix, TMD5 in DENV-2, with that of corresponding TMD5 of DENV-3 resulted in compromised replication and significant reduction in infectious particle production. Helical wheel analysis of the resultant chimera suggested a formation of a longer hydrophobic face, which possibly could have altered the flipping of TMD5. A reversion within the TMD5 of the chimeric virus, which restored the original hydrophobic face, rescued the replication and infectious particle formation. A tagged version of the chimeric protein could be used to probe the intriguing phenomenon of TMD flipping and determine its function in viral life cycle.

The integral membrane proteins, NS4A and NS4B, remain as a black box of flaviviruses. Despite several attempts from various groups, no structure has been solved for these proteins. Based on the established topology of these proteins, the study conducted here attempted to answer: a) The role of 2K peptide and their functional conservation among DENV serotypes; b) What happens if a coordinated event of polyprotein processing, that flaviviruses exploit, is interrupted; c) What different roles do TMDs of NS4A and NS4B play in flavivirus lifecycle. We illustrated how evolutionarily conserved the 2K peptides are for different serotypes of DENV and how the regulation of signalase cleavage at NS4A-2K-NS4B junction affects viral replication and particle release. Besides providing more information on the role of signalase cleavage at NS4A-2K-NS4B junction, this study provided a novel target against flaviviruses for which therapeutics could be designed.

REFERENCES

1.   Fernandez-Garcia MD, Mazzon M, Jacobs M, Amara A. 2009. Pathogenesis of Flavivirus Infections: Using and Abusing the Host Cell. Cell Host Microbe 5:318–328.

2.   Martina BEE, Koraka P, Osterhaus ADME. 2009. Dengue virus pathogenesis: An integrated view. Clin Microbiol Rev 22:564–581.

3.   Schmid MA, Diamond MS, Harris E. 2014. Dendritic cells in dengue virus infection: Targets of virus replication and mediators of immunity. Front Immunol 5:1–10.

4.   Simmonds P, Becher P, Bukh J, Gould EA, Meyers G, Monath T, Muerhoff S, Pletnev A, Rico-hesse R, Smith DB, Stapleton JT, Consortium IR. 2017. ICTV ICTV Virus Taxonomy Profile : Flaviviridae 2–3.

5.   Moureau G, Cook S, Lemey P, Nougairede A, Forrester NL, Khasnatinov M, Charrel RN, Firth AE, Gould EA, De Lamballerie X. 2015. New insights into flavivirus evolution, taxonomy and biogeographic history, extended by analysis of canonical and alternative coding sequences e0117849. PLoS One 10.

6.   Kuno G, Chang GJ, Tsuchiya KR, Karabatsos N, Cropp CB. 1998. Phylogeny of the genus Flavivirus. J Virol 72:73–83.

7.   Bhatt S, Gething PW, Brady OJ, Messina JP, Farlow AW, Moyes CL, Drake JM, Brownstein JS, Hoen AG, Sankoh O, Myers MF, George DB, Jaenisch T, William Wint GR, Simmons CP, Scott TW, Farrar JJ, Hay SI. 2013. The global distribution and burden of dengue. Nature 496:504–507.

8.   Sirohi D, Kuhn RJ. 2017. Can an FDA-approved Alzheimer's drug be repurposed for alleviating neuronal symptoms of zika virus? MBio 8:1–6.

9.   Mazeaud C, Freppel W, Chatel-Chaix L. 2018. The Multiples Fates of the Flavivirus RNA Genome During Pathogenesis. Front Genet 9:1–19.

10.   Ng WC, Soto-Acosta R, Bradrick SS, Garcia-Blanco MA, Ooi EE. 2017. The 5′ and 3′ untranslated regions of the flaviviral genome. Viruses 9:1–14.

11.   Barrows NJ, Campos RK, Liao KC, Prasanth KR, Soto-Acosta R, Yeh SC, Schott-Lerner G, Pompon J, Sessions OM, Bradrick SS, Garcia-Blanco MA. 2018. Biochemistry and Molecular Biology of Flaviviruses. Chem Rev 118:4448–4482.

12.   Garcia-Blanco MA, Vasudevan SG, Bradrick SS, Nicchitta C. 2016. Flavivirus RNA transactions from viral entry to genome replication. Antiviral Res 134:244–249.

13. Polacek C, Friebe P, Harris E. 2009. Poly(A)-binding protein binds to the non-polyadenylated 3′ untranslated region of dengue virus and modulates translation efficiency. J Gen Virol 90:687–692.

14. Selisko B, Wang C, Harris E, Canard B. 2014. Regulation of Flavivirus RNA synthesis and replication. Curr Opin Virol 9:74–83.

15. Selisko B, Potisopon S, Agred R, Priet S, Varlet I, Thillier Y, Sallamand C, Debart F, Vasseur JJ, Canard B. 2012. Molecular Basis for Nucleotide Conservation at the Ends of the Dengue Virus Genome. PLoS Pathog 8.

16. Hodge K, Tunghirun C, Kamkaew M, Limjindaporn T, Yenchitsomanus PT, Chimnaronk S. 2016. Identification of a conserved RNA-dependent RNA polymerase (RdRp)-RNA interface required for flaviviral replication. J Biol Chem 291:17437–17449.

17. Welsch S, Miller S, Romero-Brey I, Merz A, Bleck CKE, Walther P, Fuller SD, Antony C, Krijnse-Locker J, Bartenschlager R. 2009. Composition and three-dimensional architecture of the dengue virus replication and assembly sites. Cell Host Microbe 5:365–75.

18. Byk LA, Gamarnik A V. 2016. Properties and Functions of the Dengue Virus Capsid Protein. Annu Rev Virol 3:263–281.

19. Mukhopadhyay S, Kuhn RJ, Rossmann MG. 2005. A structural perspective of the Flaviviral Life lycle 3.

20. Yost SA, Marcotrigiano J. 2013. Viral precursor polyproteins: Keys of regulation from replication to maturation. Curr Opin Virol 3:137–142.

21. Perera R, Kuhn RJ. 2008. Structural proteomics of dengue virus. Curr Opin Microbiol 11:369–377.

22. Rothan HA, Kumar M. 2019. Role of Endoplasmic Reticulum-Associated Proteins in Flavivirus Replication and Assembly Complexes. Pathogens 8:148.

23. Scaturro P, Stukalov A, Haas DA, Cortese M, Draganova K, Płaszczyca A, Bartenschlager R, Götz M, Pichlmair A. 2018. An orthogonal proteomic survey uncovers novel Zika virus host factors. Nature 561:253–257.

24. Puschnik AS, Marceau CD, Ooi YS, Majzoub K, Rinis N, Contessa JN, Carette JE. 2017. A Small-Molecule Oligosaccharyltransferase Inhibitor with Pan-flaviviral Activity. Cell Rep 21:3032–3039.

25. Aktepe TE, Liebscher S, Prier JE, Simmons CP, Mackenzie JM. 2017. The Host Protein Reticulon 3.1A Is Utilized by Flaviviruses to Facilitate Membrane Remodelling. Cell Rep 21:1639–1654.

26. Lin DL, Inoue T, Chen YJ, Chang A, Tsai B, Tai AW. 2019. The ER Membrane Protein Complex Promotes Biogenesis of Dengue and Zika Virus Non-structural Multi-pass Transmembrane Proteins to Support Infection. Cell Rep 27:1666-1674.e4.

27. Xie X, Zou J, Puttikhunt C, Yuan Z, Shi P-Y. 2015. Two Distinct Sets of NS2A Molecules Are Responsible for Dengue Virus RNA Synthesis and Virion Assembly. J Virol 89:1298–1313.

28. Xie X, Zou J, Xie X, Zou J, Zhang X, Zhou Y, Routh AL, Kang C, Popov VL. 2019. Dengue NS2A Protein Orchestrates Virus Assembly. Cell Host Microbe 26:1–17.

29. Erbel P, Schiering N, D'Arcy A, Renatus M, Kroemer M, Lim SP, Yin Z, Keller TH, Vasudevan SG, Hommel U. 2006. Structural basis for the activation of flaviviral NS3 proteases from dengue and West Nile virus. Nat Struct Mol Biol 13:372–373.

30. Shao S, Hegde RS. Membrane Protein Insertion at the Endoplasmic Reticulum.

31. Rapoport TA, Li L, Park E. 2017. Structural and Mechanistic Insights into Protein Translocation.

32. Grudnik P, Bange G, Sinning I. 2009. Protein targeting by the signal recognition particle. Biol Chem 390:775–782.

33. Chambers TJ, McCourt DW, Rice CM. 1990. Production of yellow fever virus proteins in infected cells: Identification of discrete polyprotein species and analysis of cleavage kinetics using region-specific polyclonal antisera. Virology 177:159–174.

34. Preugschat F, Strauss JH. 1991. Processing of nonstructural proteins NS4A and NS4B of dengue 2 virus in vitro and in vivo. Virology 185:689–697.

35. Cahour A, Falgout B, Lai CJ. 1992. Cleavage of the dengue virus polyprotein at the NS3/NS4A and NS4B/NS5 junctions is mediated by viral protease NS2B-NS3, whereas NS4A/NS4B may be processed by a cellular protease. J Virol 66:1535–42.

36. Płaszczyca A, Scaturroid P, Neufeldtid CJ, Corteseid M, Cerikan B, Ferla S, Brancale A, Pichlmair A, Bartenschlager R. 2019. A novel interaction between dengue virus nonstructural protein 1 and the NS4A-2K-4B precursor is required for viral RNA replication but not for formation of the membranous replication organellePLoS Pathogens.

37. Lobigs M, Lee E. 2004. Inefficient Signalase Cleavage Promotes Efficient Nucleocapsid Incorporation into Budding Flavivirus Membranes. J Virol 78:178–186.

38. Walker SJ, Lively MO. 2013. Signal Peptidase (Eukaryote). Handb Proteolytic Enzym 3:3512–3517.

39. Paetzel M, Karla A, Strynadka NCJ, Dalbey RE. 2002. Signal Peptidases.

40. Klausner RD, Sitia R. 1990. Protein degradation in the endoplasmic reticulum. Cell 62:611–614.

41. Bintintan I, Meyers G. 2010. A new type of signal peptidase cleavage site identified in an RNA virus polyprotein. J Biol Chem 285:8572–8584.

42. York J, Nunberg JH. 2007. Distinct requirements for signal peptidase processing and function in the stable signal peptide subunit of the Junín virus envelope glycoprotein 359:72–81.

43. Zhang R, Miner JJ, Gorman MJ, Rausch K, Ramage H, James P, Zuiani A, Zhang P, Fernandez E, Zhang Q, Dowd KA, Pierson TC, Cherry S, Diamond MS. 2016. pathway required by flaviviruses. Nature 535:164–168.

44. Wolfe MS. 2013. Signal Peptide PeptidaseHandbook of Proteolytic Enzymes. Elsevier Ltd.

45. Voss M, Schröder B, Fluhrer R. 2013. Mechanism, specificity, and physiology of signal peptide peptidase (SPP) and SPP-like proteases. Biochim Biophys Acta - Biomembr 1828:2828–2839.

46. Martoglio B. 1997. Signal peptide fragments of preprolactin and HIV-1 p-gp160 interact with calmodulin. EMBO J 16:6636–6645.

47. Martoglio B, Dobberstein B. 1998. Signal sequences: More than just greasy peptides. Trends Cell Biol 8:410–415.

48. Owji H, Nezafat N, Negahdaripour M, Hajiebrahimi A, Ghasemi Y. 2018. A comprehensive review of signal peptides: Structure, roles, and applications. Eur J Cell Biol 97:422–441.

49. Feldman D, Roniger M, Bar-Sinai A, Braitbard O, Natan C, Love DC, Hanover JA, Hochman J. 2012. The signal peptide of mouse mammary tumor virus-env: A phosphoprotein tumor modulator. Mol Cancer Res 10:1077–1086.

50. Caporale M, Arnaud F, Mura M, Golder M, Murgia C, Palmarini M. 2009. The Signal Peptide of a Simple Retrovirus Envelope Functions as a Posttranscriptional Regulator of Viral Gene Expression. J Virol 83:4591–4604.

51. Griffin S, Clarke D, McCormick C, Rowlands D, Harris M. 2005. Signal Peptide Cleavage and Internal Targeting Signals Direct the Hepatitis C Virus p7 Protein to Distinct Intracellular Membranes. J Virol 79:15525–15536.

52. Rana J, Slon Campos JL, Leccese G, Francolini M, Bestagno M, Poggianella M, Burrone OR. 2018. Role of Capsid Anchor in the Morphogenesis of Zika Virus. J Virol 92:1–15.

53. Lobigs M, Lee E, Ng ML, Pavy M, Lobigs P. 2010. A flavivirus signal peptide balances the catalytic activity of two proteases and thereby facilitates virus morphogenesis. Virology 401:80–89.

54. Miller S, Kastner S, Krijnse-Locker J, Bühler S, Bartenschlager R. 2007. The non-structural protein 4A of dengue virus is an integral membrane protein inducing membrane alterations in a 2K-regulated manner. J Biol Chem 282:8873–8882.

55. Li Y, Lee MY, Loh YR, Kang CB. 2018. Secondary structure and membrane topology of dengue virus NS4A protein in micelles. Biochim Biophys Acta - Biomembr 1860:442–450.

56. Lee CM, Xie X, Zou J, Li S-H, Lee MYQ, Dong H, Qin C-F, Kang C, Shi P-Y. 2015. Determinants of Dengue Virus NS4A Protein Oligomerization. J Virol 89:6171–6183.

57. Paul D, Bartenschlager R. 2015. Flaviviridae Replication Organelles: Oh, What a Tangled Web We Weave. Annu Rev Virol 2:289–310.

58. Hung YF, Schwarten M, Hoffmann S, Willbold D, Sklan EH, Koenig BW. 2015. Amino terminal region of dengue virus NS4A cytosolic domain binds to highly curved liposomes. Viruses 7:4119–4130.

59. Aktepe TE, Liebscher S, Prier JE, Simmons CP, Mackenzie JM. 2017. The Host Protein Reticulon 3.1A Is Utilized by Flaviviruses to Facilitate Membrane Remodelling. Cell Rep 21:1639–1654.

60. Teo CSH, Chu JJH. 2014. Cellular Vimentin Regulates Construction of Dengue Virus Replication Complexes through Interaction with NS4A Protein. J Virol 88:1897–1913.

61. Zhang J, Lan Y, Li MY, Lamers MM, Fusade-Boyer M, Klemm E, Thiele C, Ashour J, Sanyal S. 2018. Flaviviruses Exploit the Lipid Droplet Protein AUP1 to Trigger Lipophagy and Drive Virus Production. Cell Host Microbe 23:819-831.e5.

62. McLean JE, Wudzinska A, Datan E, Quaglino D, Zakeri Z. 2011. Flavivirus NS4A-induced autophagy protects cells against death and enhances virus replication. J Biol Chem 286:22147–22159.

63. Lindenbach BD, Rice CM. 1999. Genetic interaction of flavivirus nonstructural proteins NS1 and NS4A as a determinant of replicase function. J Virol 73:4611–21.

64. Shiryaev SA, Chernov A V., Aleshin AE, Shiryaeva TN, Strongin AY. 2009. NS4A regulates the ATPase activity of the NS3 helicase: A novel cofactor role of the non-structural protein NS4A from West Nile virus. J Gen Virol 90:2081–2085.

65. Zou G, Puig-Basagoiti F, Zhang B, Qing M, Chen L, Pankiewicz KW, Felczak K, Yuan Z, Shi PY. 2009. A single-amino acid substitution in West Nile virus 2K peptide between NS4A and NS4B confers resistance to lycorine, a flavivirus inhibitor. Virology 384:242–252.

66. Campbell CL, Smith DR, Sanchez-Vargas I, Zhang B, Shi PY, Ebel GD. 2014. A positively selected mutation in the WNV 2K peptide confers resistance to superinfection exclusion in vivo. Virology 464–465:228–232.

67. Mertens E, Kajaste-Rudnitski A, Torres S, Funk A, Frenkiel MP, Iteman I, Khromykh AA, Desprès P. 2010. Viral determinants in the NS3 helicase and 2K peptide that promote West Nile virus resistance to antiviral action of 2′,5′-oligoadenylate synthetase 1b. Virology 399:176–185.

68. Lin C, Amberg SM, Chambers TJ, Rice CM. 1993. Cleavage at a novel site in the NS4A region by the yellow fever virus NS2B-3 proteinase is a prerequisite for processing at the downstream 4A/4B signalase site. J Virol 67:2327–35.

69. Lee E, Stocks CE, Amberg SM, Rice CM, Lobigs M. 2000. Mutagenesis of the Signal Sequence of Yellow Fever Virus prM Protein: Enhancement of Signalase Cleavage In Vitro Is Lethal for Virus Production. J Virol 74:24–32.

70. Auclair SM, Bhanu MK, Kendall DA. 2012. Signal peptidase I : Cleaving the way to mature proteins 21:13–25.

71. Munoz-Jordan JL, Laurent-Rolle M, Ashour J, Martinez-Sobrido L, Ashok M, Lipkin WI, Garcia-Sastre A. 2005. Inhibition of Alpha/Beta Interferon Signaling by the NS4B Protein of Flaviviruses. J Virol 79:8004–8013.

72. Roosendaal J, Westaway EG, Khromykh A, Mackenzie JM. 2006. Regulated Cleavages at the West Nile Virus NS4A-2K-NS4B Junctions Play a Major Role in Rearranging Cytoplasmic Membranes and Golgi Trafficking of the NS4A Protein. J Virol 80:4623–4632.

73. Li Y, Kim YM, Zou J, Wang QY, Gayen S, Wong YL, Lee LT, Xie X, Huang Q, Lescar J, Shi PY, Kang C. 2015. Secondary structure and membrane topology of dengue virus NS4B N-terminal 125 amino acids. Biochim Biophys Acta - Biomembr 1848:3150–3157.

74. Li Y, Wong YL, Lee MY, Li Q, Wang QY, Lescar J, Shi PY, Kang CB. 2016. Secondary Structure and Membrane Topology of the Full-Length Dengue Virus NS4B in Micelles. Angew Chemie - Int Ed 55:12068–12072.

75. Miller S, Sparacio S, Bartenschlager R. 2006. Subcellular localization and membrane topology of the Dengue virus type 2 Non-structural protein 4B. J Biol Chem 281:8854–63.

76. Zou J, Xie X, Lee LT, Chandrasekaran R, Reynaud A, Yap L, Wang Q-Y, Dong H, Kang C, Yuan Z, Lescar J, Shi P-Y. 2014. Dimerization of Flavivirus NS4B Protein. J Virol 88:3379–91.

77. Naik NG, Wu H-N. 2015. Mutation of Putative N-Glycosylation Sites on Dengue Virus NS4B Decreases RNA Replication. J Virol 89:6746–6760.

78. Youn S, Li T, McCune BT, Edeling MA, Fremont DH, Cristea IM, Diamond MS. 2012. Evidence for a Genetic and Physical Interaction between Nonstructural Proteins NS1 and NS4B That Modulates Replication of West Nile Virus. J Virol 86:7360–7371.

79. Umareddy I, Chao A, Sampath A, Gu F, Vasudevan SG. 2006. Dengue virus NS4B interacts with NS3 and dissociates it from single-stranded RNA. J Gen Virol 87:2605–2614.

80. Zou J, Lee LT, Wang QY, Xie X, Lu S, Yau YH, Yuan Z, Geifman Shochat S, Kang C, Lescar J, Shi P-Y. 2015. Mapping the Interactions between the NS4B and NS3 Proteins of Dengue Virus. J Virol 89:3471–3483.

81. Chatel-Chaix L, Fischl W, Scaturro P, Cortese M, Kallis S, Bartenschlager M, Fischer B, Bartenschlager R. 2015. A Combined Genetic-Proteomic Approach Identifies Residues within Dengue Virus NS4B Critical for Interaction with NS3 and Viral Replication. J Virol 89:7170–7186.

82. Li XD, Ye HQ, Deng CL, Liu SQ, Zhang HL, Shang B Di, Shi PY, Yuan ZM, Zhang B. 2015. Genetic interaction between NS4A and NS4B for replication of Japanese encephalitis virus. J Gen Virol 96:1264–1275.

83. Zou J, Xie X, Wang Q-Y, Dong H, Lee MY, Kang C, Yuan Z, Shi P-Y. 2015. Characterization of Dengue Virus NS4A and NS4B Protein Interaction. J Virol 89:3455–3470.

84. Khadka S, Vangeloff AD, Zhang C, Siddavatam P, Heaton NS, Wang L, Sengupta R, Sahasrabudhe S, Randall G, Gribskov M, Kuhn RJ, Perera R, LaCount DJ. 2011. A physical interaction network of dengue virus and human proteins. Mol Cell Proteomics 10:1–16.

85. Ishikawa H, Ma Z, Barber GN. 2009. STING regulates intracellular DNA-mediated, type i interferon-dependent innate immunity. Nature 461:788–792.

86. Liang Q, Luo Z, Zeng J, Chen W, Foo SS, Lee SA, Ge J, Wang S, Goldman SA, Zlokovic B V., Zhao Z, Jung JU. 2016. Zika Virus NS4A and NS4B Proteins Deregulate Akt-mTOR Signaling in Human Fetal Neural Stem Cells to Inhibit Neurogenesis and Induce Autophagy. Cell Stem Cell 19:663–671.

87. Ngo AM, Shurtleff MJ, Popova KD, Kulsuptrakul J, Weissman JS, Puschnik AS. 2019. The ER membrane protein complex is required to ensure correct topology and stable expression of flavivirus polyproteins. Elife 8:1–23.

88. Muñoz-Jordán JL, Sánchez-Burgos GG, Laurent-Rolle M, García-Sastre A. 2003. Inhibition of interferon signaling by dengue virus. Proc Natl Acad Sci U S A 100:14333–14338.

89. Umareddy I, Tang KF, Vasudevan SG, Devi S, Hibberd ML, Gu F. 2008. Dengue virus regulates type I interferon signalling in a strain-dependent manner in human cell lines. J Gen Virol 89:3052–3062.

90. Kakumani PK, Ponia SS, S RK, Sood V, Chinnappan M, Banerjea AC, Medigeshi GR, Malhotra P, Mukherjee SK, Bhatnagar RK. 2013. Role of RNA Interference (RNAi) in Dengue Virus Replication and Identification of NS4B as an RNAi Suppressor. J Virol.

91. Davidson AD. 2009. Chapter 2 New Insights into Flavivirus Nonstructural Protein 5Advances in Virus Research, 1st ed. Elsevier Inc.

92. Sahili A El, Lescar J. 2017. Dengue virus non-structural protein 5. Viruses 9:1–20.

93. Lin R-J, Chang B-L, Yu H-P, Liao C-L, Lin Y-L. 2006. Blocking of Interferon-Induced Jak-Stat Signaling by Japanese Encephalitis Virus NS5 through a Protein Tyrosine Phosphatase-Mediated Mechanism. J Virol 80:5908–5918.

94. Best SM, Morris KL, Shannon JG, Robertson SJ, Mitzel DN, Park GS, Boer E, Wolfinbarger JB, Bloom ME. 2005. Inhibition of Interferon-Stimulated JAK-STAT Signaling by a Tick-Borne Flavivirus and Identification of NS5 as an Interferon Antagonist. J Virol 79:12828–12839.

95. De Maio FA, Risso G, Iglesias NG, Shah P, Pozzi B, Gebhard LG, Mammi P, Mancini E, Yanovsky MJ, Andino R, Krogan N, Srebrow A, Gamarnik A V. 2016. The Dengue Virus NS5 Protein Intrudes in the Cellular Spliceosome and Modulates Splicing. PLoS Pathog 12:1–29.

96. Tay MYF, Smith K, Ng IHW, Chan KWK, Zhao Y, Ooi EE, Lescar J, Luo D, Jans DA, Forwood JK, Vasudevan SG. 2016. The C-terminal 18 Amino Acid Region of Dengue Virus NS5 Regulates its Subcellular Localization and Contains a Conserved Arginine Residue Essential for Infectious Virus Production. PLoS Pathog 12:1–34.

97. Zhao B, Yi G, Du F, Chuang YC, Vaughan RC, Sankaran B, Kao CC, Li P. 2017. Structure and function of the Zika virus full-length NS5 protein. Nat Commun 8:1–9.

98. Zhao Y, Soh TS, Lim SP, Chung KY, Swaminathan K, Vasudevan SG, Shi PY, Lescar J, Luo D. 2015. Molecular basis for specific viral RNA recognition and 2'-O-ribose methylation by the dengue virus nonstructural protein 5 (NS5). Proc Natl Acad Sci U S A 112:14834–14839.

99. Klema VJ, Padmanabhan R, Choi KH. 2015. Flaviviral replication complex: Coordination between RNA synthesis and 5'-RNA capping. Viruses 7:4640–4656.

100. Daffis S, Szretter KJ, Schriewer J, Li J, Youn S, Errett J, Lin TY, Schneller S, Zust R, Dong H, Thiel V, Sen GC, Fensterl V, Klimstra WB, Pierson TC, Buller RM, Gale Jr M, Shi PY, Diamond MS. 2010. 2′-O methylation of the viral mRNA cap evades host restriction by IFIT family members. Nature 468:452–456.

101. Lu G, Gong P. 2017. A structural view of the RNA-dependent RNA polymerases from the Flavivirus genus. Virus Res 234:34–43.

102. Best SM. 2017. The Many Faces of the Flavivirus NS5 Protein in Antagonism of Type I Interferon Signaling. J Virol 91:1–14.

103. Yap TL, Xu T, Chen Y-L, Malet H, Egloff M-P, Canard B, Vasudevan SG, Lescar J. 2007. Crystal Structure of the Dengue Virus RNA-Dependent RNA Polymerase Catalytic Domain at 1.85-Angstrom Resolution. J Virol 81:4753–4765.

104. Sampath A, Padmanabhan R. 2009. Molecular targets for flavivirus drug discovery. Antiviral Res 81:6–15.

105. García LL, Padilla L, Castaño JC. 2017. Inhibitors compounds of the flavivirus replication process. Virol J 14:1–12.

106. Byrd CM, Dai D, Grosenbach DW, Berhanu A, Jones KF, Cardwell KB, Schneider C, Wineinger KA, Page JM, Harver C, Stavale E, Tyavanagimatt S, Stone MA, Bartenschlager R, Scaturro P, Hruby DE, Jordan R. 2013. A novel inhibitor of dengue virus replication that targets the capsid protein. Antimicrob Agents Chemother 57:15–25.

107. Lim SP, Wang QY, Noble CG, Chen YL, Dong H, Zou B, Yokokawa F, Nilar S, Smith P, Beer D, Lescar J, Shi PY. 2013. Ten years of dengue drug discovery: Progress and prospects. Antiviral Res 100:500–519.

108. Lim SP, Noble CG, Shi PY. 2015. The dengue virus NS5 protein as a target for drug discovery. Antiviral Res 119:57–67.

109. Tomlinson SM, Watowich SJ. 2008. Substrate inhibition kinetic model for West Nile virus NS2B-NS3 protease. Biochemistry 47:11763–11770.

110. Dong H, Ren S, Zhang B, Zhou Y, Puig-Basagoiti F, Li H, Shi P-Y. 2008. West Nile Virus Methyltransferase Catalyzes Two Methylations of the Viral RNA Cap through a Substrate-Repositioning Mechanism. J Virol 82:4295–4307.

111. Assenberg R, Ren J, Verma A, Walter TS, Alderton D, Hurrelbrink RJ, Fuller SD, Bressanelli S, Owens RJ, Stuart DI, Grimes JM. 2007. Crystal structure of the Murray Valley encephalitis virus NS5 methyltransferase domain in complex with cap analogues. J Gen Virol 88:2228–2236.

112. Bollati M, Milani M, Mastrangelo E, Ricagno S, Tedeschi G, Nonnis S, Decroly E, Selisko B, de Lamballerie X, Coutard B, Canard B, Bolognesi M. 2009. Recognition of RNA Cap in the Wesselsbron Virus NS5 Methyltransferase Domain: Implications for RNA-Capping Mechanisms in Flavivirus. J Mol Biol 385:140–152.

113. Brecher MB, Li Z, Zhang J, Chen H, Lin Q, Liu B, Li H. 2015. Refolding of a fully functional flavivirus methyltransferase revealed that S-adenosyl methionine but not S-adenosyl homocysteine is copurified with flavivirus methyltransferase. Protein Sci 24:117–128.

114. Dong H, Chang DC, Xie X, Toh YX, Chung KY, Zou G, Lescar J, Lim SP, Shi PY. 2010. Biochemical and genetic characterization of dengue virus methyltransferase. Virology 405:568–578.

115. Lim SP, Sonntag LS, Noble C, Nilar SH, Ng RH, Zou G, Monaghan P, Chung KY, Dong H, Liu B, Bodenreider C, Lee G, Ding M, Chan WL, Wang G, Jian YL, Chao AT, Lescar J, Yin Z, Vedananda TR, Keller TH, Shi PY. 2011. Small molecule inhibitors that selectively block dengue virus methyltransferase. J Biol Chem 286:6233–6240.

116. Milani M, Mastrangelo E, Bollati M, Selisko B, Decroly E, Bouvet M, Canard B, Bolognesi M. 2009. Flaviviral methyltransferase/RNA interaction: Structural basis for enzyme inhibition. Antiviral Res 83:28–34.

117. Stahla-Beek HJ, April DG, Saeedi BJ, Hannah AM, Keenan SM, Geiss BJ. 2012. Identification of a Novel Antiviral Inhibitor of the Flavivirus Guanylyltransferase Enzyme. J Virol 86:8730–8739.

118. Iglesias NG, Filomatori C V., Gamarnik A V. 2011. The F1 Motif of Dengue Virus Polymerase NS5 Is Involved in Promoter-Dependent RNA Synthesis. J Virol 85:5745–5756.

119. Najera I. 2013. Resistance to HCV nucleoside analogue inhibitors of hepatitis C virus RNA-dependent RNA polymerase. Curr Opin Virol 3:508–513.

120. Choi SH, Park KJ, Kim SY, Choi DH, Park JM, Hwang SB. 2005. C-terminal domain of hepatitis C virus core protein is essential for secretion. World J Gastroenterol 11:3887–3892.

121. Lobigs M, Zhao HX, Garoff H. 1990. Function of Semliki Forest virus E3 peptide in virus assembly: replacement of E3 with an artificial signal peptide abolishes spike heterodimerization and surface expression of E1. J Virol 64:4346–55.

122. Replication A, Cells M. 2017. crossm Spatial and Temporal Analysis of Alphavirus Replication and Assembly in Mammalian and Mosquito Cells 8:1–16.

123. Roy A, Kucukural A, Zhang Y. 2010. I-TASSER: A unified platform for automated protein structure and function prediction. Nat Protoc 5:725–738.

124. Bendtsen JD, Nielsen H, Von Heijne G, Brunak S. 2004. Improved prediction of signal peptides: SignalP 3.0. J Mol Biol 340:783–795.

125. Sievers F, Wilm A, Dineen D, Gibson TJ, Karplus K, Li W, Lopez R, McWilliam H, Remmert M, Söding J, Thompson JD, Higgins DG. 2011. Fast, scalable generation of high-quality protein multiple sequence alignments using Clustal Omega. Mol Syst Biol 7.

126. Gautier R, Douguet D, Antonny B, Drin G. 2008. HELIQUEST: A web server to screen sequences with specific α-helical properties. Bioinformatics 24:2101–2102.

127. Singh P, Sharma L, Kulothungan SR, Adkar B V., Prajapati RS, Ali PSS, Krishnan B, Varadarajan R. 2013. Effect of Signal Peptide on Stability and Folding of Escherichia coli Thioredoxin. PLoS One 8.

128. Teramoto T, Balasubramanian A, Choi KH, Padmanabhan R. 2017. Serotype-specific interactions among functional domains of dengue virus 2 nonstructural proteins (NS) 5 and NS3 are crucial for viral RNA replication. J Biol Chem 292:9465–9479.

129. Datta R, Waheed A, Shah GN, Sly WS. 2007. Signal sequence mutation in autosomal dominant form of hypoparathyroidism induces apoptosis that is corrected by a chemical chaperone. Proc Natl Acad Sci U S A 104:19989–19994.

130. Snapp EL, McCaul N, Quandte M, Cabartova Z, Bontjer I, Källgren C, Nilsson I, Land A, Von Heijne G, Sanders RW, Braakman I. 2017. Structure and topology around the cleavage site regulate post-translational cleavage of the HIV-1 gp160 signal peptide. Elife 6:1–25.

131. Hegde RS, Bernstein HD. 2006. The surprising complexity of signal sequences. Trends Biochem Sci 31:563–571.

132. Amaya Y, Nakai T, Miura S. 2016. Evolutionary well-conserved region in the signal peptide of parathyroid hormone-related protein is critical for its dual localization through the regulation of ER translocation. J Biochem 159:393–406.

133. Chen CY, Shiu JH, Hsieh YH, Liu YC, Chen YC, Chen YC, Jeng WY, Tang MJ, Lo SJ, Chuang WJ. 2009. Effect of D to E mutation of the RGD motif in rhodostomin on its activity, structure, and dynamics: Importance of the interactions between the D residue and integrin. Proteins Struct Funct Bioinforma 76:808–821.

134. Stocks CE, Lobigs M. 1998. Signal peptidase cleavage at the flavivirus C-prM junction: dependence on the viral NS2B-3 protease for efficient processing requires determinants in C, the signal peptide, and prM. J Virol 72:2141–9.

135. Khromykh AA, Varnavski AN, Sedlak PL, Westaway EG. 2001. Coupling between Replication and Packaging of Flavivirus RNA: Evidence Derived from the Use of DNA-Based Full-Length cDNA Clones of Kunjin Virus. J Virol 75:4633–4640.

136. Pong WL, Huang ZS, Teoh PG, Wang CC, Wu HN. 2011. RNA binding property and RNA chaperone activity of dengue virus core protein and other viral RNA-interacting proteins. FEBS Lett 585:2575–2581.

137. Zhang X, Shi P, Xie X, Xia H, Zou J, Huang L, Popov VL, Chen X. 2019. Zika Virus NS2A-Mediated Virion Assembly. MBio 10:1–21.

138. Scaturro P, Cortese M, Chatel-Chaix L, Fischl W, Bartenschlager R. 2015. Dengue Virus Non-structural Protein 1 Modulates Infectious Particle Production via Interaction with the Structural Proteins. PLoS Pathog 11:1–32.

139. Patkar CG, Kuhn RJ. 2008. Yellow Fever Virus NS3 Plays an Essential Role in Virus Assembly Independent of Its Known Enzymatic Functions. J Virol 82:3342–3352.

140. Kaufusi PH, Kelley JF, Yanagihara R, Nerurkar VR. 2014. Induction of endoplasmic reticulum-derived replication-competent membrane structures by West Nile virus non-structural protein 4B. PLoS One 9.

141. Zou J, Xie X, Lee LT, Chandrasekaran R, Reynaud A, Yap L, Wang Q-Y, Dong H, Kang C, Yuan Z, Lescar J, Shi P-Y. 2014. Dimerization of Flavivirus NS4B Protein. J Virol 88:3379–3391.

142. Youn S, Li T, McCune BT, Edeling M a, Fremont DH, Cristea IM, Diamond MS. 2012. Evidence for a genetic and physical interaction between nonstructural proteins NS1 and NS4B that modulates replication of West Nile virus. J Virol 86:7360–71.

143. Ma Y, Yates J, Liang Y, Lemon SM, Yi M. 2008. NS3 Helicase Domains Involved in Infectious Intracellular Hepatitis C Virus Particle Assembly. J Virol 82:7624–7639.

144. Kümmerer BM, Rice CM. 2002. Mutations in the Yellow Fever Virus Nonstructural Protein NS2A Selectively Block Production of Infectious Particles Mutations in the Yellow Fever Virus Nonstructural Protein NS2A Selectively Block Production of Infectious Particles. J Virol 76:4773–4784.

145. Chatel-Chaix L, Fischl W, Scaturro P, Cortese M, Kallis S, Bartenschlager M, Fischer B, Bartenschlager R. 2015. A Combined Genetic-Proteomic Approach Identifies Residues within Dengue Virus NS4B Critical for Interaction with NS3 and Viral Replication. J Virol 89:7170–7186.

146. Paul D, Bartenschlager R. Flaviviridae Replication Organelles : Oh , What a Tangled Web We Weave.

147. Romero-Brey I, Bartenschlager R. 2016. Endoplasmic reticulum: The favorite intracellular niche for viral replication and assembly. Viruses 8:1–26.

148. Arakawa M, Morita E. 2019. Flavivirus replication organelle biogenesis in the endoplasmic reticulum: Comparison with other single-stranded positive-sense RNA viruses. Int J Mol Sci 20.

149. Li X-D, Deng C-L, Ye H-Q, Zhang H-L, Zhang Q-Y, Chen D-D, Zhang P-T, Shi P-Y, Yuan Z-M, Zhang B. 2016. Transmembrane Domains of NS2B Contribute to both Viral RNA Replication and Particle Formation in Japanese Encephalitis Virus. J Virol 90:5735–5749.

150. Barman S, Adhikary L, Chakrabarti AK, Bernas C, Kawaoka Y, Nayak DP. 2004. Role of Transmembrane Domain and Cytoplasmic Tail Amino Acid Sequences of Influenza A Virus Neuraminidase in Raft Association and Virus Budding. J Virol 78:5258–5269.

151. Xie X, Wang Q-Y, Xu HY, Qing M, Kramer L, Yuan Z, Shi P-Y. 2011. Inhibition of dengue virus by targeting viral NS4B protein. J Virol 85:11183–95.

152. Zmurko J, Neyts J, Dallmeier K. 2015. Flaviviral NS4b, chameleon and jack-in-the-box roles in viral replication and pathogenesis, and a molecular target for antiviral intervention. Rev Med Virol 25:205–223.

153. Teramoto T, Boonyasuppayakorn S, Handley M, Choi KH, Padmanabhan R. 2014. Substitution of NS5 N-terminal domain of dengue virus type 2 RNA with type 4 domain caused impaired replication and emergence of adaptive mutants with enhanced fitness. J Biol Chem 289:22385–22400.

154. Ambrose RL, Mackenzie JM. 2015. Conserved amino acids within the N-terminus of the West Nile virus NS4A protein contribute to virus replication, protein stability and membrane proliferation. Virology 481:95–106.

155. Blaney JE, Manipon GG, Firestone CY, Johnson DH, Hanson CT, Murphy BR, Whitehead SS. 2003. Mutations which enhance the replication of dengue virus type 4 and an antigenic chimeric dengue virus type 2/4 vaccine candidate in Vero cells. Vaccine 21:4317–4327.

156. Lundin M, Monne M, Widell A, von Heijne G, Persson MAA. 2003. Topology of the Membrane-Associated Hepatitis C Virus Protein NS4B. J Virol 77:5428–5438.

157. Escors D, Camafeita E, Ortego J, Laude H, Enjuanes L. 2001. Organization of Two Transmissible Gastroenteritis Coronavirus Membrane Protein Topologies within the Virion and Core. J Virol 75:12228–12240.

158. Diamond MS, Ledgerwood JE, Pierson TC. 2019. Zika Virus Vaccine Development: Progress in the Face of New Challenges. Annu Rev Med 70:annurev-med-040717-051127.

159. Ishikawa T, Yamanaka A, Konishi E. 2014. A review of successful flavivirus vaccines and the problems with those flaviviruses for which vaccines are not yet available. Vaccine 32:1326–1337.

160. Sirohi D, Kuhn RJ. 2017. Can an FDA-Approved Alzheimer's Drug Be Repurposed for Alleviating Neuronal Symptoms of Zika Virus? MBio 8:e00916-17.

161. Bhatt S, Gething PW, Brady OJ, Messina JP, Farlow AW, Moyes CL, Drake JM, Brownstein JS, Hoen AG, Sankoh O, Myers MF, George DB, Jaenisch T, Wint GRW, Simmons CP, Scott TW, Farrar JJ, Hay SI. 2013. The global distribution and burden of dengue. Nature 496:504–7.

162. Mukhopadhyay S, Kuhn RJ, Rossmann MG. 2005. A structural perspective of the flavivirus life cycle. Nat Rev Microbiol 3:13–22.

163. Murray CL, Jones CT, Rice CM. 2008. Architects of assembly: roles of Flaviviridae non-structural proteins in virion morphogenesis. Nat Rev Microbiol 6:699–708.

164. Geiss BJ, Stahla H, Hannah AM, Gari HHH, Keenan SM, Gari AM. 2009. Focus on flaviviruses: current and future drug targets. Future Med Chem 1:1–27.

165. Wang B, Tan X-F, Thurmond S, Zhang Z-M, Lin A, Hai R, Song J. 2017. The structure of Zika virus NS5 reveals a conserved domain conformation. Nat Commun 8:14763.

166. Brecher M, Chen H, Li Z, Banavali NK, Jones SA, Zhang J, Kramer LD, Li H. 2016. Identification and Characterization of Novel Broad-Spectrum Inhibitors of the Flavivirus Methyltransferase. ACS Infect Dis 1:340–349.

167.	Dong H, Liu L, Zou G, Zhao Y, Li Z, Lim SP, Shi PY, Li H. 2010. Structural and functional analyses of a conserved hydrophobic pocket of flavivirus methyltransferase. J Biol Chem 285:32586–32595.

168.	Zhou Y, Ray D, Zhao Y, Dong H, Ren S, Li Z, Guo Y, Bernard KA, Shi P, Li H. 2007. Structure and Function of Flavivirus NS5 Methyltransferase □. J Virol 81:3891–3903.

169.	Chen H, Zhou B, Brecher M, Banavali N, Jones SA, Li Z, Zhang J, Nag D, Kramer LD, Ghosh AK, Li H. 2013. S-Adenosyl-Homocysteine Is a Weakly Bound Inhibitor for a Flaviviral Methyltransferase. PLoS One 8:23–26.

170.	Lim SP, Sonntag LS, Noble C, Nilar SH, Ng RH, Zou G, Monaghan P, Chung KY, Dong H, Liu B, Bodenreider C, Lee G, Ding M, Chan WL, Wang G, Jian YL, Chao AT, Lescar J, Yin Z, Vedananda TR, Keller TH, Shi P. 2011. Small Molecule Inhibitors That Selectively Block Dengue Virus Methyltransferase * □ 286:6233–6240.

171.	Shan C, Xie X, Muruato AE, Rossi SL, Roundy CM, Azar SR, Yang Y, Tesh RB, Bourne N, Barrett AD, Vasilakis N, Weaver SC, Shi PY. 2016. An Infectious cDNA Clone of Zika Virus to Study Viral Virulence, Mosquito Transmission, and Antiviral Inhibitors. Cell Host Microbe 19:891–900.

172.	Pettersen EF, Goddard TD, Huang CC, Couch GS, Greenblatt DM, Meng EC, Ferrin TE. 2004. UCSF Chimera - A visualization system for exploratory research and analysis. J Comput Chem 25:1605–1612.

173.	Allouche A. 2012. Software News and Updates Gabedit — A Graphical User Interface for Computational Chemistry Softwares. J Comput Chem 32:174–182.

174.	Patkar CG, Larsen M, Owston M, Smith JL, Kuhn RJ. 2009. Identification of inhibitors of yellow fever virus replication using a replicon-based high-throughput assay. Antimicrob Agents Chemother 53:4103–14.

175.	Xie X, Zou J, Shan C, Yang Y, Kum DB, Dallmeier K, Neyts J, Shi PY. 2016. Zika Virus Replicons for Drug Discovery. EBioMedicine 12:156–160.

176.	Coutard B, Barral K, Lichière J, Selisko B, Martin B, Aouadi W, Lombardia MO, Debart F, Vasseur J-J, Guillemot JC, Canard B, Decroly E. 2017. Zika Virus Methyltransferase: Structure and Functions for Drug Design Perspectives. J Virol 91:1–15.

177.	Li JQ, Deng CL, Gu D, Li X, Shi L, He J, Zhang QY, Zhang B, Ye HQ. 2018. Development of a replicon cell line-based high throughput antiviral assay for screening inhibitors of Zika virus. Antiviral Res 150:148–154.

178.	Noueiry, Amine O., Olivo, Paul D., ...Diamond MS. 2007. Identification of Novel Small-Molecule Inhibitors of West Nile Virus Infection. J Virol 81:11992–12004.

179.	Shi PY, Tilgner M, Lo MK. 2002. Construction and characterization of subgenomic replicons of New York strain of West Nile virus. Virology 296:219–233.

180.	Prescott J, Hall P, Acuna-Retamar M, Ye C, Wathelet MG, Ebihara H, Feldmann H, Hjelle B. 2010. New world hantaviruses activate IFNλ production in type I IFN-deficient vero E6 cells. PLoS One 5:1–8.

181.	Garg H, Sedano M, Plata G, Punke EB, Joshi A. 2017. Development of Virus like Particle Vaccine and Reporter Assay for Zika Virus. J Virol JVI.00834-17.

182.	Zhang C, Feng T, Cheng J, Li Y, Yin X, Zeng W, Jin X, Li Y, Guo F, Jin T. 2017. Structure of the NS5 methyltransferase from Zika virus and implications in inhibitor design. Biochem Biophys Res Commun 492:624–630.

183.	Weltman JK, Skowron G, Loriot GB. 2007. Influenza A H5N1 hemagglutinin cleavable signal sequence substitutions. Biochem Biophys Res Commun 352:177–180.

184.	Cui J, Chen W, Sun J, Guo H, Madley R, Xiong Y, Pan X, Wang H, Tai AW, Weiss MA, Arvan P, Liu M. 2015. Competitive Inhibition of the Endoplasmic Reticulum Signal Peptidase by Non-cleavable Mutant Preprotein Cargos * 290:28131–28140.

185.	Zou J, Xie X, Wang Q-Y, Dong H, Lee MY, Kang C, Yuan Z, Shi P-Y. 2015. Characterization of Dengue Virus NS4A and NS4B Protein Interaction. J Virol 89:3455–3470.

186.	Campbell RK, Bergert ER, Wang Y, Morris JC, Moyle WR. 1997. Chimeric proteins can exceed the sum of their parts: implications for evolution and protein design. Nat Biotechnol 15:439–443.

187.	Bouslama L, Nasri D, Chollet L, Belguith K, Bourlet T, Aouni M, Pozzetto B, Pillet S. 2007. Natural Recombination Event within the Capsid Genomic Region Leading to a Chimeric Strain of Human Enterovirus B. J Virol 81:8944–8952.

VITA

Shishir was born as an older child to Shyam Krishna Poudel and Janaki Poudel in the outskirts of Kathmandu, Nepal. He finished his undergraduate and masters from Tribhuvan University with a specialization in General Microbiology and Medical Microbiology, respectively. It was during his time as an undergraduate when he developed fascinations for microorganisms and the enigma surrounding them. These fascinations led to his study on multidrug resistance in clinical settings for his master's dissertation. After working as an assistant instructor for Dr. Manoj Thapa, a viral immunologist, in Kathmandu after obtaining the master's degree, he was influenced to get his PhD in virology and joined Purdue University as a graduate student. In the laboratory of Dr. Richard J Kuhn, a prominent flaviviral structural biologist, he studied about dengue and Zika viruses. His research focused on understanding the roles of non-structural proteins 4A and 4B of dengue virus in replication and infectious virion production. He devoted his time on understanding the host cell signalase cleavage of viral polyprotein and how that would affect viral life cycle. During his tenure as a graduate student, he also worked on developing tools to study Zika virus and antiviral compounds. He also worked on developing a prototype biochip that could be used in field to identify whether mosquitoes are carrying flaviviruses or not. He plans to devote his future to virology/immunology.